STUDIES IN PREPARATIVE SCALE

HIGH PRESSURE LIQUID CHROMATOGRAPHY

by

HAZEL M. PYPER, B.Sc.

THESIS SUBMITTED FOR THE DEGREE OF

DOCTOR OF PHILOSOPHY

UNIVERSITY OF EDINBURGH 1984

DECLARATION

This thesis is the original composition of the author's work, unless stated otherwise, and has not been submitted previously for any other degree.

I attended the following post-graduate lecture courses:-

"Intensive HPLC Course" by Professor J.H. Knox, Edinburgh University.

"Computer Course" by Dr. C. Pounder, Edinburgh University.

"Scientific German" by German Department, Edinburgh University.

"Course In Mass Spectrometry" by Professor J.H. Beynon, University College, Swansea.

"Zeolites" by Dr. B. Lowe, Edinburgh University.

"Electronics and Microprocessors" by Mr. A. King, Edinburgh University.

"Molecular Interactions In Industrial Food Research" by Colworth Laboratory, Unilever Research.

Chemistry Department Seminars (1978-82).

This thesis is dedicated to my mother,
who sadly is no longer with us.

I miss you, mum ...

ACKNOWLEDGEMENTS

I would like to express my sincere thanks to Professor John H. Knox for his help, encouragement and understanding during my research for this thesis.

I would also like to thank the following; The Chemistry Department for the use of library and laboratory facilities and for providing me with a post-graduate award, for which thanks are also extended to the Senatus Postgraduate Studies Committee of Edinburgh University;
Unilever Research, Colworth House, for the provision of a CASE award, and in particular to Mr. A.D. Jones;
to members of staff, research students and the staff of the Wolfson Liquid Chromatography Unit for their advice and friendship during the course of this work;
to Mrs. Christian Ranken for typing the text of this thesis;
to Maggy Clover and Sue Croft for typing the diagrams and graphs, and to my father and friends for their support.

Finally my special thanks go to Dr. John I. Evans for all of his help, understanding, encouragement and friendship during the past few years and to whom this thesis is also dedicated.

ABSTRACT

In Chapter 1 a brief history of both analytical and preparative chromatography is given.

Chapter 2 provides some basic parameters and definitions which are used throughout this thesis.

Chapter 3 describes the effect which thermodynamic factors have on column efficiency and resolution. The different modes of liquid chromatography are also described and the basic thermodynamic equations given.

In Chapter 4 the effect which kinetic factors have on column efficiency and resolution are discussed. The development of the various Kinetic Theories is described from the Theoretical Plate Model to the van Deemter Equation, the Random Walk Model and finally the Non-equilibrium Model.

Chapter 5 reviews the equipment and techniques employed in preparative-scale HPLC as well as the various column packing methods. The development of a preparative separation is also discussed.

The effects of increased sample load in preparative liquid chromatography produced both by increased sample volume and by increased sample concentration is discussed in chapter 6. Those factors which affect column loadability and sample throughput are examined along with various methods for improving sample throughput.

Chapter 7 describes the structure, preparation and bonding of silica gels.

A prototype preparative column system is described and

tested in chapter 8. This system is extremely versatile due to the interchangeability of the different units. Results show that the best geometry of column units is that which connects the loading pre-column via the sandwich piece to the main column with no secondary flow through the side-arm. Loading experiments show that sample linear capacity is greater when the sample is loaded via the pre-column.

Chapter 9, describes loading experiments carried out on a set of columns constructed such that the internal diameters were the same but the column lengths were different and which were packed such that the particle diameter, dp, of the stationary phase used was roughly proportional to the column length ie. $dp \propto \ell$, approximately. The term "isochronic" has been coined to describe such a set of packed columns since the elution time of any solute will be the same with all such columns if the pressure drop, Δp, remains the same. The results of the loading experiments showed that, contrary to what was expected, it is better in terms of sample throughput to use the SHORT column (93mm x 7mm id.) packed with SMALL particles (dp = 10.64μm). By comparing results obtained using the prototype preparative column system, it was found that the maximum throughput obtainable for a particular number of plates is greater for the WIDER column. It is therefore concluded that it is best to use short, wide columns packed with small particles in the range 10-20μm.

In the Reserved Chapter, more detail is given as to the actual preparation and bonding of the ODS-silica used in this thesis.

CHAPTER 1

INTRODUCTION AND HISTORY OF CHROMATOGRAPHY

Chapter 1. Introduction And History Of Chromatography

INTRODUCTION AND HISTORY OF CHROMATOGRAPHY

1.1 Introduction

Chromatography, in its most general form, is a separation technique which involves applying a sample to one end of a rigidly held bed of some partitioning or support material and subsequently passing a fluid or mobile phase through the bed which washes the sample down the column and thereby, hopefully, effects a separation of the individual components of the sample. This is achieved if the solutes possess sufficiently different affinities for the stationary and mobile phases.

Most of the research carried out so far has been on the analytical scale, though much of the early classical work was mainly preparative in nature. However, more recently, attention has been turned towards separations on the preparative scale.

The early part of this chapter (1.2) will deal with the general background of analytical chromatography while the latter part (1.3) will deal with the general background of preparative scale chromatography. A more detailed review of preparative scale chromatography will be carried out in a later chapter.

1.2 The History of Chromatography

Although the discovery of chromatography is generally accorded to Michael Tswett, a Russian botanist working at the turn of the century, it has been suggested[1,2] that the earliest observations of paper chromatography date back about 2,000 years when one Pliney The Younger is said to have effected a

separation and detected ferrous sulphate using papyrus impregnated with an extract of gallnut.

More recently, at the end of the 19th century,[3] Runge[4,5] and Schoenbein[6,7] published work carried out on paper chromatography, or Kapillaranalyse as it was called. Their technique was to dip strips of paper into mixtures of dyestuffs which were separated into the individual components by what was basically a frontal separation process.

Thin layer chromatography was first reported by the Dutch biologist Beyerinck,[8] while the very first report on column chromatography came from Reed.[9] Unfortunately, however, these early scientists failed to understand the basic processes involved in the methods which they had used and, as a result, these separation techniques were not developed any further.

Michael Tswett, on the other hand, is generally regarded as the father of chromatography because of the vast contribution which he made to both the practice and the understanding of this technique. He was the first person to fully appreciate the basic processes involved and in 1906[10,11] coined the terms "chromatography" and "chromatogram", which is incidently the year which some authors wrongly give for the discovery of chromatography. His very first observations of the phenomenon had been made in 1899[12,13] whilst working on plant chlorophylls. In his first paper published in 1903,[14] Tswett expanded on these observations announcing[12,14] "the possibility of developing a new method of physical separation of different substances dissolved in organic liquids ... based on the ability of solutes to form physical adsorption compounds with different mineral and organic solids". He also gave birth to the principle of

gradient elution by using a step-wise change in solvent.

By 1910, Tswett[15,16] had essentially developed the theory of dynamic differential migration and foresaw the analogy between paper and thin layer chromatography. Unfortunately, with the death of Tswett in 1919, the technique fell into disuse. Fears had been voiced that there were chemical reactions taking place between the solutes and the support materials. Also many chemists, biologists and biochemists failed to grasp the fundamental processes involved and mistakingly thought it to be merely a type of single stage extraction.

In 1931, however, chromatography was 'rediscovered' by Kuhn, Lederer and Winterstein,[17,18] who essentially used Tswett's methods.

Most of the work had, up till now, been carried out on adsorption chromatography, but in 1941 Martin and Synge[19] published a paper which was to herald the beginning of a new era for chromatography. They achieved a chromatographic separation of neutral amino acids as a result of the difference in the partition coefficients of the various acetylated amino acids between water and an immiscible organic solvent and later[20] showed that the relative positions of the amino acids depended on the solvent used. By drawing analogies between chromatography, fractional distillation and countercurrent extraction, they developed their "theoretical plate" theory[19] for column efficiency. They predicted that in order to obtain improved column efficiency, smaller particles and higher pressures would have to be used. Furthermore, they foresaw the development of gas-liquid chromatography to which they could apply

their plate theory and in 1952 Martin and Synge[21] demonstrated the technique of gas-liquid partition chromatography, the same year in which they were awarded the Nobel Prize in Chemistry.

In 1938, Ismailov and Schraiber[22] described the use of thin layers of adsorbent coated onto glass plates. Modern TLC dates from 1951 and owes much to Kirchner *et al.*[23,24] The credit for its popularisation, however, is generally accorded to Stahl.[25,26] At this stage, both paper and thin layer chromatography were superior in speed and efficiency than classical liquid open column chromatography, with separations of around 30 minutes for the former compared to hours or even days for the latter.

It was unfortunate that, at this point in time, many scientists still failed to grasp fully the physico-chemical processes involved in chromatography, despite the earlier work carried out by Martin and Synge.

By the 1960's gas chromatography (G.C.) had developed into a sophisticated technique. The low viscosity of the carrier gas permits rapid diffusion of the vapourised solute in the column resulting in virtually instantaneous equilibrium between the mobile and stationary phases. Fast elution of solutes from the column could also be achieved since the low viscosity of the carrier gas allows large flow rates. As a result of the greater efficiency of these columns, more sensitive detectors and better data recording systems had to be developed. These chromatographic systems could also be automated for analytical work.

During this time, the fundamental principles and theory were laid down and much of the credit for this is due to van Deemter *et al.*[27]

Gas chromatography had found most of its application at

this stage in the petrochemical industry and, as a chemical engineer, van Deemter was used to dealing with mass transfer problems which helped him in the development of the theory. With liquid chromatography, however, the biologists and organic chemists who used this technique were not so adept in handling such problems and consequently little or no development of liquid chromatographic theory occurred.

Around the same time, ion exchange chromatography was used in the separation of rare earth elements and in the separation of amino acids,[28,31] the latter still being widely used to this day. Hamilton[32-34] contributed much to the development of this technique and used the van Deemter equation to calculate his results.[34] He demonstrated that the time taken for analyses could be shortened by using smaller particle sizes (dp) and larger pressure drops (Δp) across the column. Once again, however, these scientists were way ahead of their time and their work was largely ignored. Had other workers been able to appreciate the work of these people, the development of high pressure liquid chromatography might have occurred years sooner than it did.

Although the development of the theory of liquid chromatography had lagged behind that of gas chromatography, it was realised that the two phenomena were analogous and that much of the theory, knowledge and understanding built up on the latter was applicable to, and could be translated in terms of, liquid chromatography. It was Giddings[35,36] who most clearly pointed this out. He showed that "the inter-relation of particle diameter, pressure drop, mobile phase velocity and column efficiency could be applied equally well to liquid

chromatography if the correct scaling factors were used." These scaling factors are needed because liquids are around a hundred times more viscous than the gases used, resulting in an increase in the operating pressures of the same order. Also, since the rates of diffusion of solutes in liquids is of the order of 10^3 to 10^4 times smaller compared to their diffusion rate in gases, the particle diameter of the support materials have to be reduced by the order of the square root of the above ratio if the mass transfer rates are to be equivalent. Giddings also improved on the 'theoretical plate model' for column efficiency of Martin and Synge, first by introducing the 'random walk model'[35-37] and then the 'relaxation model'.[38] This led to the 'non-equilibrium theory'[35] which describes band broadening in terms of complex kinetic and diffusion processes. One of the conclusions arrived at theoretically[36] was that the optimum particle size (dp) was around 2-20μm and that high pressures would have to be used in liquid chromatography.

The introduction of reduced parameters[39] enabled the direct comparison of results obtained using different columns, packing materials, eluents and solutes.

Horvath *et al.*[40] and Huber[41] also realised that reducing the particle size and operating at high pressures would overcome the higher liquid viscosities and in their papers described the first high pressure liquid chromatographs.

At this time Snyder[42] greatly increased the understanding of the thermodynamics of adsorption chromatography.

As with the case of gas chromatography such an increase in separating efficiency necessitated the development of more

sensitive U.V. detectors capable of detecting down to nanogram levels of absorbing solutes. Also because the liquid chromatographic column had a much smaller optimal geometric size, the design of injector and detector systems were of great importance.

With the advancement in chromatography theory came an improvement in support materials. By 1942, selective surface-active packing materials were in use as well as natural and synthetic zeolites (ion exchange chromatography).

The latter part of the 1960's[43-47] saw the development and utilisation of pellicular packing materials in ion exchange[43, 44] and liquid-liquid partition chromatography.[45-47] These materials consisted of an impervious core coated with a thin layer of porous material which greatly improved the mass transfer properties and resulted in a substantial increase in column efficiency. However Sie and van den Hoed,[48] and Kennedy and Knox,[49] showed that fully porous materials, if well packed, could produce columns as efficient as those packed with pellicular materials of the same size. Apparently the earlier workers had used inferior materials and packing techniques and thus had not produced very efficient columns. On the other hand, the most sophisticated of these pellicular supports, the "controlled surface porosity" materials developed by Kirkland,[47] were better. These were soda glass beads coated with a 1-2μm layer of silica microspheres by a patented process. This was marketed as Zipax^{R}, and was perhaps the most widely used pellicular support material in use in the 1970's. These materials reduced band broadening due to slow mass transfer within the stagnant mobile phase held in the pores of the

packing material. By reducing the depth of the pores, solute molecules rapidly move into and out of the stagnant mobile phase in the pores.

Kirkland[50] also developed a material based on controlled surface porosity supports with covalently bound organic phases with a variety of functional groups and marketed as Permaphase[R].

However, although Kirkland's pellicular materials were able to generate about twice as many theoretical plates as totally porous materials of the same size, they suffered from having a low sample capacity due to their low surface area, and too large a dp.

Another way to reduce the problems of stagnant mobile phase was to reduce the particle size. It has been shown[51] both by theory and practice that a particle size of around 5μm provides a good compromise between efficiency, pressure drop, analysis time and reproducibility of packing. These micro-particles produced columns of greater efficiency than those packed with the larger particles and as a result, pellicular materials became obsolete. The dry packing techniques used for packing the larger particles, for example the rotate-bounce-tap method,[52-55] became inadequate for particles smaller than 20μm, and so slurry packing techniques[56-61] were developed to enable the bed to be packed uniformly, as individual particles are packed against the growing bed.

While adsorption chromatography on silica gel with its polar surface is applicable to the separation of non-polar solutes, it is of little use in the separation of polar and ionic solutes. As a result, these silica gel microparticles were further developed by the bonding of various organic groups

onto the surface, thus enabling the nature of the surface to be made completely non-polar. Such materials are used in what is known as reversed-phase liquid chromatography. Because of the relatively low surface area of the pellicular materials (1-10m^2/g), the bonding of these materials was carried out by depositing polymers within the pores, as carried out by Kirkland.[56] However, the relatively high surface area of the fully porous materials (eg. 200m^2/g) has enabled the organic groups to be bonded onto the surface as a unimolecular layer. The advantage of the latter is that materials so produced have better mass transfer properties.

Several reviews have been published[62-65] which discuss the preparation of such materials and their applications. The most common organic groups employed by commercial manufacturers can be divided into three groups:[66]

(i) Hydrophobic groups, especially octadecyl ($C_{18}H_{37}$) groups but also groups with shorter chain lengths such as C_1, C_2 and C_8.

(ii) Polar groups such as aminopropyl, cyanopropyl ether and glycol.

(iii) Ion-exchange groups such as sulphonic acid, amino and quaternary ammonium groups.

A more detailed account of the preparation of bonded phases will be discussed later in chapter 7.

1.3 The History of Preparative Chromatography

Much of the early work on column liquid chromatography could be regarded as having been preparative in nature and in fact Tswett was the first to develop preparative chromatography.

These early separations were carried out on open glass columns packed with adsorbent material using coloured compounds which enabled the separation to be easily followed. The sample was added to the top of the column and suction was applied to the bottom of the column to effect the separation of the components into a series of bands. These bands were not eluted from the column and the plug of adsorbent material was pushed out of the column. The different bands were then cut out from the plug and the adsorbed component was extracted with a polar solvent. By using dialysis tubing instead of glass, the separation of the bands was made easier by cutting through the tubing. The separation technique was improved by using small quantities of solution and using fresh solvent to elute the bands from the bottom of the column, so enabling solutions of pure component to be collected.

In his second paper,[11] Tswett described the use of large columns, 20mm id., for preparative chromatography and also the practice of applying a slight pressure to the top of the columns.

In the 1930's, particles tended to be small in size (1-10μm)[67] and packed dry with tamping[17,18,68.69] or slurry packed by adding aliquots of material and gradually increasing the vacuum applied to the bottom of the column.[70,71] At this time, silica gel was not in use as an adsorbent and of the materials which were used then, only Al_2O_3 (alumina) and Florosil are found in use today.

Some of the most noteworthy of the early preparative-scale pioneers are to be found in references [17,18,67-74]. The trend in particle size then moved to much coarser particles

with dp of 100-200μm[75-78] whilst present day trends have moved back to smaller particles ranging from 10-75μm. In general, particles larger than 20μm are dry packed or are slurry packed if they are smaller than 20μm.

Two interesting industrial uses of preparative liquid chromatography in the 1940's of pilot plant scale were in a project involved with the development of the atomic bomb[79] and in a project established to determine the constituents of crude petroleum. In the first of these projects, large scale ion exchange chromatography was used to separate rare earths from samples of crude rare-earth salts. Spedding *et al.*[80] published details of a plant which consisted of 24 columns, 10 ft x 4 in with an 8 ft long bed of Amberlite I.R.-100 resin. 100 g samples of the crude rare-earth salts were loaded onto these columns and eluted with 0.5% citrate solution at a flow rate of 0.5 cm/min. The rare-earths were recovered from the individual fractions collected and then further purified before use.

In the second of the projects, the aim was to establish the constituents of crude petroleum. This project was established in 1927 and ran till 1967. The project has been discussed in several articles.[81-86] In the early years only fractional distillation was used but by 1935 fractionation by selective adsorption on silica gel was being used. In 1943 simple adsorption filtration was replaced by true chromatographic separations, and in 1956 gas chromatography was introduced. By 1960 the project had succeeded in isolating 175 hydrocarbons of crude petroleum.

At the end of the 1960's[86,87] industrial ion exchange

chromatography was in use in water de-ionizing units, employing large columns of 50cm-150cm in diameter.

However, the development of preparative scale high pressure liquid chromatography has been somewhat neglected in the past in favour of analytical scale high pressure liquid chromatography and as a result, agreement has not yet been reached as to the optimum dimensions of the column, particle size or sample load. In view of the wide range of practical separation problems to be found in preparative-scale HPLC however, this is not surprising.

REFERENCES

Chapter 1

1. R.J. Block, R. LeStrange, and G.Zweig; "Paper Chromatography: A Laboratory Manual" Academic Press, New York, 1952, page 1.
2. G. Zweig and J. Sherma; J.Chromatog.Sci., 11, (1973), 29.
3. J.G. Kirchner; J.Chromatog.Sci., 13, (1975), 558.
4. F.F. Runge; Ann.Phys.Chem.XVII, 31, (1834), 65.
5. F.F. Runge; Ann.Phys.Chem.XVIII, 32, (1834), 78.
6. C.H. Schoenbein; Poggendorf's Annalen, 42, (1837), 422.
7. C.H. Schoenbein; Verhandel, Naturforsch.Ges.Basel, 3, (1861), 249.
8. M.W. Beyerinck; Z.Physik.Chem., 3, (1889), 110.
9. L. Reed; Proc.Chem.Soc., 9, (1893), 123.
10. M.S. Tswett; Ber.Deut.Bot.Ges., 24, (1906), 316.
11. M.S. Tswett; Ber.Deut.Bot.Ges., 24, (1906), 384.
12. G. Hesse and H. Weil; "Michael Tswett's First Paper On Chromatography" M. Woelm, Eschwege 1954.
13. K. Sakodynskii; J.Chromatogr., 73, (1972), 303.
14. M.S. Tswett; Tr.Protok.Varshav.Obshch.Estestroispyt. Otd.Biol., 14, (1903, publ. 1905), 20.
15. H. Strain; Ind.& Eng.Chem., 14, (1942), 245.
16. M.S. Tswett; Khromofilli v Rastitelnom i Zhivotnom Mire; Izd.Karbasnikov Warsaw 1910.
17. R. Kuhn, E. Lederer,and A.Winterstein Hoppe Seyler's Z. Physiol.Chem., 197 (1931), 147.
18. R. Kuhn and E. Lederer; Ber.Deut.Chem.Ges., 64, (1931), 1349.

19. A.J.P. Martin and R.L.M. Synge; Biochem.J., 35, (1941), 1358.

20. R. Consden, A.H. Gorden and A.J.P. Martin; Biochem.J., 38, (1944), 224.

21. A.J.P. Martin and R.L.M. Synge; Biochem.J., 50, (1952), 679.

22. S. Ismailov and H Schreiber; Adv.In.Chromatog., 3, (1966), 85 (Translation).

23. J.G. Kirchner, J.M. Miller, and G.J. Keller; Anal.Chem., 23, (1951), 420.

24. J.C. Kirchner; J.Chromatog.Sci., 11, (1973), 180.

25. E. Stahl; Chemiker.Ztg., 82, (1958), 323.

26. E. Stahl; 'T.L.C. - A Laboratory Handbook' George Allen & Unwin, London.

27. J.J. van Deemter, F.J. Zuiderweg, and A. Klinkenberg; Chem.Eng.Sci., 5, (1956), 271.

28. S. Moore and W.H. Stein; J.Biol.Chem., 192, (1951), 663.

29. S. Moore and W.H. Stein; J.Biol.Chem., 211 (1954), 893.

30. S. Moore and W.H. Stein; J.Biol.Chem., 211, (1954), 907.

31. S. Moore, D.H. Spackman, and W.H. Stein; Anal.Chem., 30, (1958), 1185.

32. P.B. Hamilton; Anal.Chem., 30, (1958), 914.

33. P.B. Hamilton; Anal.Chem., 32, (1960), 1779.

34. P.B. Hamilton, D.C. Bogue, and R.A. Anderson; Anal.Chem., 32, (1960), 1782.

35. J.C. Giddings; 'Dynamics of Chromatography. Part 1' Marcel Dekker, New York, 1965.

36. J.C. Giddings; Anal.Chem., 35, (1963), 1338.

37. J.C. Giddings; J.Chem.Ed., 35, (1958), 588.

38. J.C. Giddings; J.Chromatog., 2, (1959), 44.

39. J.C. Giddings; J.Chromatog., 13, (1964), 301.

40. C. Horvath, B.A. Preiss, and S.R. Lipsky; Anal.Chem., 39, (1967), 1422.

41. J.F.K. Huber; J.Chromatog.Sci., 7, (1969), 85.

42. L.R. Snyder; "Principles of Adsorption Chromatography" Marcel Dekker, New York (1968).

43. I. Haslaz and C. Horvath; Anal.Chem., 36, (1964), 1178.

44. C.G. Horvath, B.A. Preiss, and S.R. Lipsky; Anal.Chem., 39, (1967), 1423.

45. J.J. Kirkland; J.Chromatog.Sci., 7, (1969), 7.

46. J.J. Kirkland; J.Chromatog.Sci., 7, (1969), 361.

47. J.J. Kirkland; Anal.Chem., 41, (1969), 7.

48. S.T.Sie and N. van den Hoed; J.Chromatog.Sci., 7, (1969), 257.

49. G.J. Kennedy and J.H. Knox; J.Chromatog.Sci., 10, (1972), 549.

50. J.J. Kirkland; J.Chromatog.Sci., 9, (1971), 206.

51. J.H. Knox and M. Saleem; J.Chromatog.Sci., 7, (1969), 614.

52. L.R. Snyder and J.J. Kirkland; "Modern Liquid Chromatography" Wiley Interscience, New York, 1974.

53. J.J. DeStefano and H.C. Beachell; J.Chromatog.Sci., 10, (1972), 654.

54. S.T. Sie and N. van den Hoed; J.Chromatog.Sci., 7, (1969), 257.

55. J.N. Done, J.H. Knox, and J. Loheac; "Applications of HPLC" Wiley, London, 1974.

56. J.J. Kirkland; J.Chromatog.Sci, 9, (1971), 206.

57. J.J. Kirkland; J.Chromatog.Sci., 10, (1972), 593.

58. R.E. Majors; Anal.Chem., 44, (1972), 1722.

59. J. Asshauer and I. Halasz; J.Chromatog.Sci., 12, (1974), 139.

60. T.J.N. Webber and E.H. McKerrell; J.Chromatogr., 122, (1976), 243.

61. P.A. Bristow, P.N. Brittain, C.M. Riley, and B.F. Williamson; J.Chromatogr., 131, (1977), 57.

62. D.C. Locke; J.Chromatog.Sci., 11, (1973), 120.

63. D.C. Locke; J.Chromatog.Sci., 12, (1974), 433.

64. V. Rehak and Smolkova; Chromatographia, 9, (1976), 219.

65. A. Pryde; J.Chromatog.Sci., 12, (1974), 486.

66. J.H. Knox; Editor 'High Performance Liquid Chromatography' Edinburgh University Press.

67. E. Geeraert and M. Verzele; Chromatographia, 11, (1978), 640.

68. H. Strain; J.Biol.Chem., 105, (1934), 523.

69. L. Zechmeister and L.V. Cholnoky; J.Liebig's Ann.Chem., 509, (1934), 269.

70. A. Winterstein and G. Stein; Hoppe-Seyler's Z.Physiol.Chem., 220, (1933), 247.

71. A. Winterstein and K. Schön; Hoppe-Seyler's Z.Physiol. Chem., 230, (1934), 139.

72. P. Karrer and O. Walker; Helv.Chim.Acta, 16, (1933), 641.

73. P. Karrer and F.M. Strong; Helv.Chim.Acta, 19, (1936), 25.

74. L. Zechmeister and L.V. Cholnoky; J.Liebig's Ann.Chem., 509, (1934), 269.

75. J.J. Kirkland; "Modern Practice of Liquid Chromatography" Wiley Interscience, New York, 1971.

76. R.E. Majors; Anal.Chem., 44, (1972), 1722.

77. L.R. Snyder and J.J. Kirkland; "Introduction to Modern L.C." Wiley Interscience Publ. 1974.

78. H. Veering; Critic.Rev.Anal.Chem., 5, (1975), 165.

79. L.S. Ettre; Chromatographia, 5, (1979), 302.

80. F.H. Spedding, E.I. Fulmer, T.A. Butler, E.M. Gladrow, M. Gobush, P.E. Porter, J.E. Powell, and J.M. Wright; J.Am.Chem.Soc., 69, (1947), 2812.

81. F.D. Rossini; J.Chem.Ed., 37, (1960), 554.

82. B.J. Mair and A.L. Gaboriault; Ind.Eng.Chem.Ind.Ed., 39, (1947), 1072.

83. F.D. Rossini, B.J. Mair, and A. Streiff; "Hydrocarbons From Petroleum" Reinhold, New York, 1953.

84. B.J. Mair; Proc.Seventh World Petrol.Congr., 9, (1967), 39.

85. D.L. Camin and A.J. Raymond; J.Chromatog.Sci., 11, (1973), 625.

86. L.S. Ettre and A. Horvath; Anal.Chem., 47, (1975), 422A.

87. R.S. Timmins, L. Mir, and J.M. Ryan; Chem.Eng., 76, (1969), 170.

CHAPTER 2

BASIC PARAMETERS AND DEFINITIONS

Chapter 2. Basic Parameters And Definitions

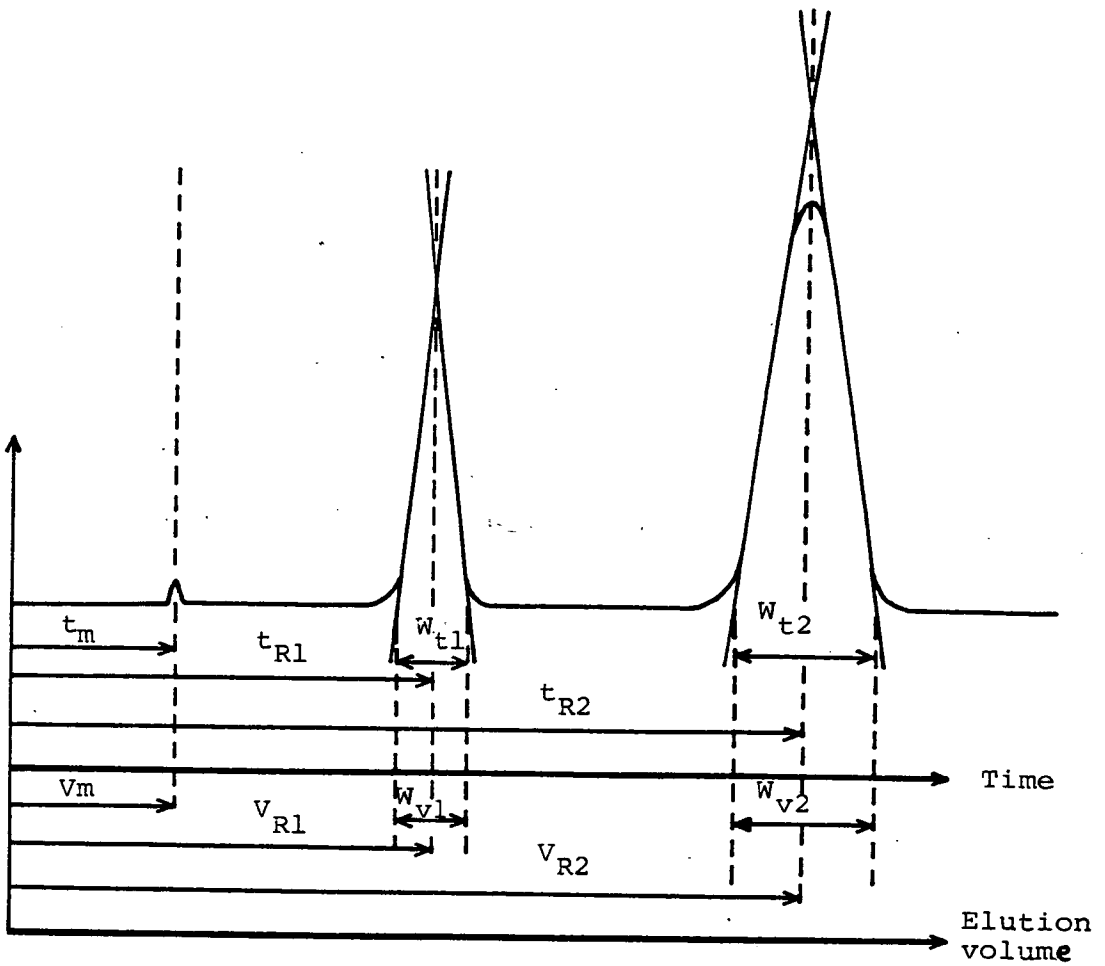

Figure 2.1 Parameters for defining retention and peak width.

BASIC PARAMETERS AND DEFINITIONS

2.1 Introduction

Chromatography involves the separation of different solutes in a mixture due to their differential migration rates as they are eluted through the column. As these bands of solutes migrate down the column bed at their different rates, the bands spread to produce, where the distribution isotherm is linear as it usually is in the case of an analytical injection, a Gaussian concentration profile.

The ultimate goal in HPLC is to minimise the band spreading, to control the rates of migration of these bands and to arrive at the optimum blend of speed of elution, resolution and economic use of both pressure and solvents. "The key to resolution ... is the proper combination of the differential migration of solutes and the control of band spreading."

The differential migration rates of solutes is due to their different affinities for the stationary phase and the migration rate of a solute depends on the equilibrium distribution of individual molecules between the stationary and mobile phases.

Before we consider the thermodynamic theory of chromatography, it is necessary to define some basic parameters. Figure 2.1 helps to illustrate some of these parameters.

2.2 Retention and the Column Capacity Ratio, k'.

The retention time, or elution time, t_R, is the time taken for a small injection volume of a solute to be eluted down the column bed, taken from its point of injection to the time the peak maximum emerges from the bottom of the column.

The volume of eluent which passes through the column during this time is known as the retention volume, or elution volume, V_R, such that

$$V_R = t_R \times f_v \qquad (2\text{-}1)$$

where f_v is the volumetric flow rate.

The time taken for an unretained solute, or the mobile phase, to pass through the column is denoted by t_m. The equivalent elution volume, V_m, corresponds to the volume of eluent in the packed column.

The phase capacity ratio, k', is the basic parameter for describing the degree of retention. Basically, it is the additional time which a band of solute takes to elute through the column compared to the time taken for an unretained solute to elute, divided by the elution time of the unretained solute. This is written as:

$$k' = \frac{t_R - t_m}{t_m} = \frac{V_R - V_m}{V_m} \qquad (2\text{-}2)$$

and by rearranging this equation we can therefore express V_R as:

$$V_R = V_m (1+k') \qquad (2\text{-}3)$$

The linear flow rate, U, is the speed at which the eluent moves through the column and can be found by dividing the length of the column, L, by t_m, the time taken for an unretained or solvent molecule to pass through the column, ie.

$$U = \frac{L}{t_m} \qquad (2\text{-}4)$$

The linear flow rate, or eluent velocity, U, is also connected to the volume flow rate, f_v, via the mean cross-sectional area of the eluent phase, a_m, by the expression:

$$U = \frac{f_v}{a_m} \qquad (2\text{-}5)$$

As a solute band moves through the column bed, its molecules are moving into and out of the mobile phase, and therefore the linear velocity of the solute band, U_{band}, will be less than the linear velocity of the eluent as a result of the time spent by the molecules in the stationary phase where there is no movement.

2.3 The Number of Theoretical Plates, N.

The efficiency of a chromatographic column is measured by the number of theoretical plates, N, to which the column is equivalent. This assumes that the processes are random and that the peaks are Gaussian in shape.

Justification of N will be given later in Chapter 4.

2.4 Resolution

The ultimate goal in chromatography is to achieve an adequate separation between two consecutively eluting solute bands. The resolution of two such compounds, as illustrated in figure 2-1 is defined as:

$$R_s = \frac{\text{Separation of peak maxima}}{\text{mean peak width at base}}$$

ie.
$$R_s = \frac{t_{R2} - t_{R1}}{\frac{1}{2}(W_1 + W_2)} \qquad (2\text{-}6)$$

where t_{R2} and t_{R1} are the retention times of the solute maxima of peaks 2 and 1 respectively, and W is the base width of the corresponding eluted bands in units of time.

Resolution can also be expressed in terms of the retention volumes, V_R.

ie. $$R_s = \frac{V_{R2} - V_{R1}}{\frac{1}{2}(W_1 + W_2)} \qquad (2\text{-}7)$$

Generally speaking, R_s must have a value of greater than around 1.5 to achieve an adequate resolution of base-line separation. A larger value of R_s would result in a better resolution.

To improve resolution, then either the separation of the peaks must be increased while maintaining the same peak width or the peaks must be made narrower whilst maintaining their relative retention. The former can be achieved by changing the relative partition ratios of the solutes between the mobile and stationary phases ie. by changing the eluent composition. This is the easier of the two methods in practice, and the factors which are involved are thermodynamic in nature. The latter method of improving resolution involves increasing the efficiency of the column which is controlled by kinetic considerations.

The separation factor, α, is defined as

$$\alpha = \frac{k'_2}{k'_1} = \frac{K_2}{K_1} \qquad (2\text{-}8)$$

where K_1 and K_2 are the equilibrium distribution coefficients of each solute between the mobile and stationary phases.

The resolution, R_s, can be related to the selectivity, α, the column capacity ratio, k', and to the efficiency of the column, N, by considering the equations for N, t_R, W_t and k'. The resulting expression is given by:

$$R_s = \frac{1}{4} \left[\frac{\alpha-1}{\alpha}\right] \left[\frac{k'_2}{1+k'_2}\right] N^{\frac{1}{2}} \qquad (2\text{-}9)$$

where k'_2 is the phase capacity ratio for solute 2. The first two terms are purely thermodynamic while the last term, $N^{\frac{1}{2}}$, is normally controlled by kinetic factors only.

Equation (2-9) can also be written as

$$R_s = \frac{1}{2} \left[\frac{\alpha-1}{\alpha+1}\right] \left[\frac{\bar{k}'}{1+\bar{k}'}\right] N^{\frac{1}{2}} \qquad (2\text{-}10)$$

(a) (b) (c)

where $\bar{k}' = \frac{1}{2}(k'_1+k'_2)$,

(a) represents the Relative Partition Factor,

(b) represents the Retention Factor,

and (c) represents the Column Efficiency Factor.

The above equation illustrates that for a separation to occur

(1) solutes must be retained to different extents ie $\alpha \neq 1$,

(2) solutes must be retained ie $k' \neq 0$.

and (3) the column must be equivalent to a minimum number of theoretical plates (N).

2.5 Basic Parameters in Exclusion Chromatography

In exclusion chromatography, the pore volume of the supporting matrix is denoted by V_p and the interstitial volume

outside these particles is denoted by V_o. It should be mentioned that the interstitial volume, V_o, will not be the same as the volume of eluent within the column, V_m, since there will be some held within the pores of the support material, ie.

$$V_m = V_o + V_p \qquad (2\text{-}11)$$

The degree of permeation of a solute, or the partition ratio between the stationary and mobile phases, K, is equal to the fraction of the pore volume accessible to that particular solute. The retention volume of the solute can therefore be written as:

$$V_R = V_o + KV_p \qquad (2\text{-}12)$$

From this equation is is clear that K=0 represents the case where solutes are totally excluded while K=1 represents the case where solutes enter all of the pores of the support material.

By combining the above equations, (2-11) and (2-12), with the equation obtained for the retention volume in adsorption chromatography, namely:

$$V_R = V_m (1+k') \qquad (2\text{-}3)$$

we arrive at an expression with respect to the phase volume for the phase capacity ratio, k', ie.

$$k' = (K-1) \frac{V_p}{V_m} \qquad (2\text{-}13)$$

Alternatively, if we consider the volumes of the mobile zone,

the corresponding equation for the retention volume can be written as

$$V_R = V_o (1+k") \qquad (2-14)$$

where k" is the zone capacity ratio.

By combining equations we have

$$k" = K ({}^{V_p}/_{V_o}) \qquad (2-15)$$

From the equation for the phase capacity ratio, k', we see that the value of k' is negative for solutes which are partially excluded, while the value for k" is always positive and is between 0 - $({}^{V_p}/_{V_o})$.

CHAPTER 3

THE THERMODYNAMICS OF CHROMATOGRAPHY

Chapter 3. The Thermodynamics Of Chromatography

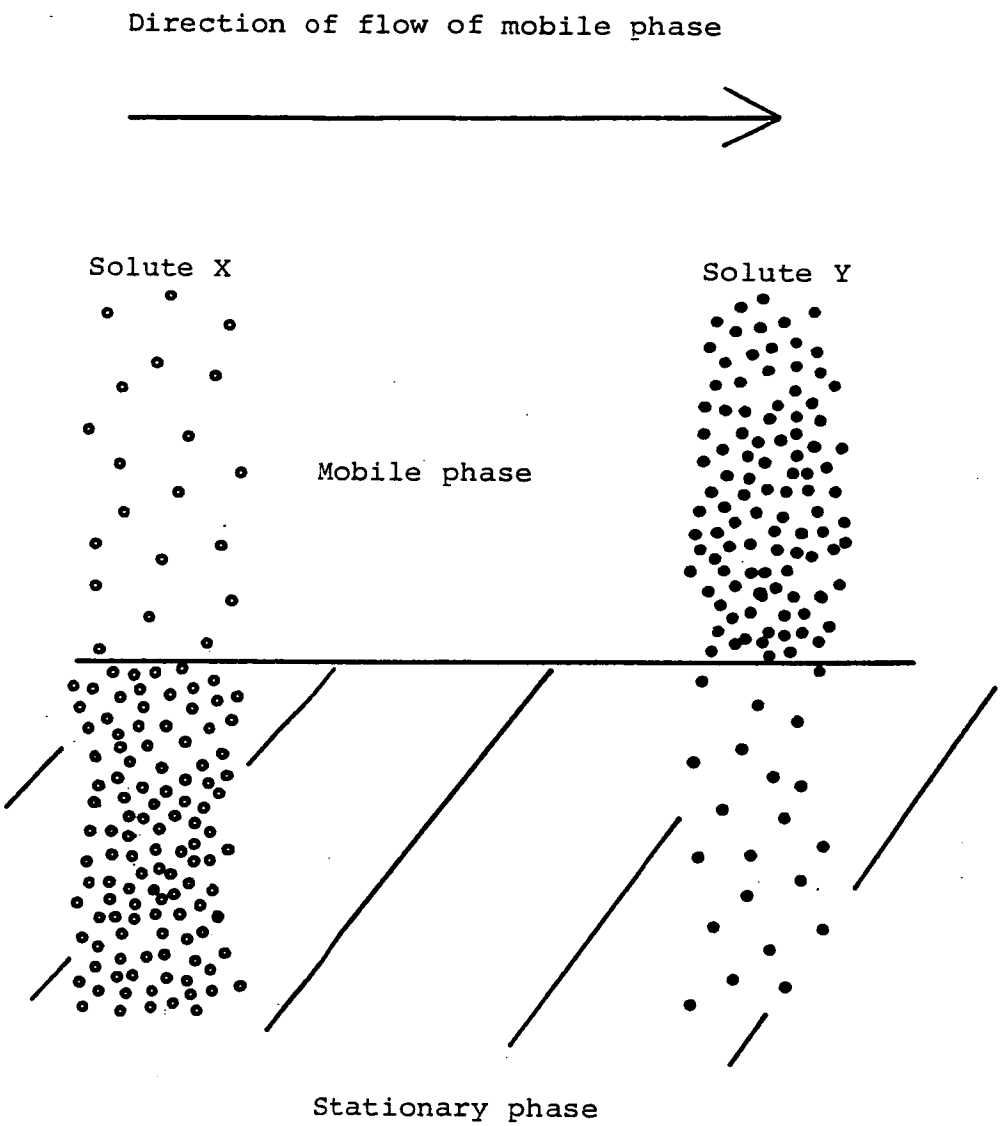

Figure 3.1

The partitioning of two solutes, X and Y, between a stationary and a mobile phase.

THE THERMODYNAMICS OF CHROMATOGRAPHY

3.1 Introduction

The thermodynamics of chromatography are basically concerned with the fundamental aspects of retention as distinct from the kinetic aspects which are basically concerned with band spreading.

As the thermodynamic and kinetic processes are virtually independent of each other, they can fortunately be treated separately.

This chapter will deal with the thermodynamic aspects and the kinetic aspects will be dealt with in the next chapter.

3.2 The Thermodynamics of Chromatography

Consider two different solute molecules, X and Y, whose partitioning between a stationary phase and a mobile phase is as illustrated in figure 3-1.

At equilibrium, solute Y is present mainly in the mobile phase. Since solute molecules will only move down the column when they are in the mobile phase, solute X must move much more slowly through the column than solute Y, assuming that equilibrium is fairly rapidly attained. Thus the speed at which each solute moves through the column depends upon the fraction of molecules of that solute which are present in the mobile phase at any one time.

The equilibrium distribution of molecules between the two phases is influenced by such variables as the column temperature and the compositions of both the mobile and

stationary phases.

As has already been mentioned, equilibration between the mobile and stationary phases is rapid and therefore it follows that the average speed of the molecules in the solute band relative to the speed of the mobile phase can be assumed to be equal to the fraction of time the solute molecules spend in the mobile phase at equilibrium. This can be expressed as:

$$\frac{U_{band}}{U} = \text{fraction of molecules in the mobile phase at equilibrium} \qquad (3\text{-}1)$$

ie.
$$\frac{U_{band}}{U} = \frac{q_m}{q_m+q_s} = \frac{1}{1+\frac{q_s}{q_m}} \qquad (3\text{-}2)$$

where U_{band} and U are the velocities of the band and the eluent respectively, and q_m and q_s are the quantities of solute in the mobile and stationary phases respectively.

It can be seen from equation (2-2) that:

$$k' = \frac{\text{amount of solute in stationary phase}}{\text{amount of solute in mobile phase}}$$

ie.
$$k' = \frac{q_s}{q_m} \qquad (3\text{-}3)$$

Since equilibrium is rapidly attained, we can regard q_s and q_m as equilibrium values, and so they can be expressed as:

$$q_s = C_s.V_s \qquad (3\text{-}4)$$

and
$$q_m = C_m.V_m \qquad (3\text{-}5)$$

where C_s, C_m are the equilibrium concentrations of the solute

in the stationary and mobile phases respectively, and V_s, V_m are the volumes of those phases in the column.

It is obvious that there is an inverse relationship between the linear velocity of a solute band, U_{band}, and its elution time, t_R ie:

$$\frac{U_{band}}{U} = \frac{t_m}{t_R} \qquad (3\text{-}6)$$

By considering equation (3-3) we can express equation (3-2) as:

$$\frac{U_{band}}{U} = \frac{1}{1+k'} \qquad (3\text{-}7)$$

As the individual molecules migrate through the column, they undergo adsorption onto and desorption from the surface of the stationary phase. Equilibrium between the two phases is rapidly achieved and the equilibrium distribution so produced between the mobile phase (m) and the stationary phase (s) of molecules of a solute (X) can be represented as:

$$X_m \rightleftharpoons X_s \qquad (3\text{-}8)$$

The distribution coefficient, K_x, of the above equilibrium is given by:

$$K_x = \frac{C_s}{C_m} \qquad (3\text{-}9)$$

where C_s, C_m are the equilibrium concentrations of X in the stationary and mobile phases respectively.

By combining equations (3-3), (3-4), (3-5) and (3-9), we can express the phase capacity factor, k', in terms of the equilibrium distribution coefficient, K, and the ratio of the

mobile and stationary phase volumes, ie.

$$k' = \frac{C_s V_s}{C_m V_m} \qquad (3\text{-}10)$$

$$\text{therefore} \quad k' = K. \frac{V_s}{V_m} \qquad (3\text{-}11)$$

The standard free energy change, ΔG^{Θ}, for a solute molecule going from the mobile phase into the stationary phase is given by the equation:

$$\Delta G^{\Theta}_{m \to s} = -RT \ell n K_x \qquad (3\text{-}12)$$

By considering equation (3-11) we can write the above as:

$$\Delta G^{\theta}_{m \to s} = -RT \ell n \left[\frac{k'}{(V_s/V_m)} \right] \qquad (3\text{-}13)$$

The corresponding equation describing the standard change in enthalpy ΔH^{Θ}, is given as

$$\Delta H^{\Theta}_{m \to s} = RT^2 \frac{d \ell n K_x}{dT} \qquad (3\text{-}14)$$

In gas chromatography, $\Delta H^{\Theta}_{m \to s}$ is large (approximately ΔH_{vap}) whereas in liquid chromatography $\Delta H^{\Theta}_{m \to s}$ is relatively small so that temperature control is not so important with the latter which accounts for the use of ambient conditions in the great majority of L.C. separations.

3.3 The Effects of Non-linear Isotherms

The theoretical aspects which have been discussed so far have assumed that the distribution isotherm, which is given by

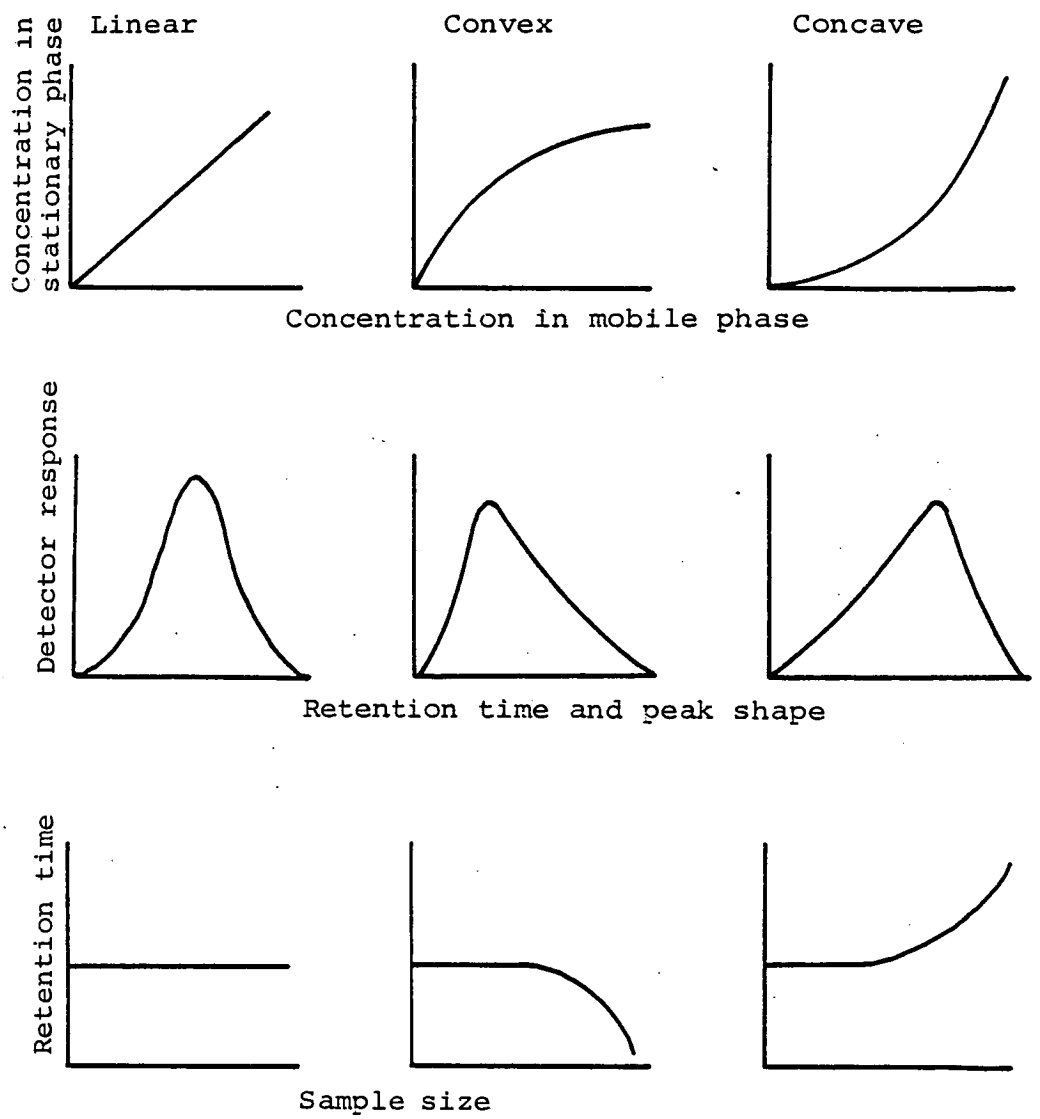

Figure 3.2 The three basic types of distribution isotherm showing the effect of peak shape and retention time.

the plot of the concentration of solute in the stationary phase versus the concentration of solute in the mobile phase, is linear ie. that the distribution coefficient, K, is constant throughout the separation. In practice, however, K often varies with sample concentration and such separations are described as non-linear isotherm separations. There are three basic types of distribution isotherm as illustrated in figure 3-2 and these are:

a) linear, in which K is independent of sample concentration,
b) convex, in which K decreases with increasing sample concentration, and which is the most commonly found type of isotherm in adsorption chromatography, and
c) concave, in which K increases with increasing sample concentration.

Figure 3-2 also illustrates the effect which sample concentration has on band shape and solute retention. In the case of a linear isotherm, the sample bands are symmetrical and peak retention remains constant with respect to sample concentration. With a convex isotherm, K decreases and therefore peak retention decreases with increasing sample concentration. As the rate at which solute molecules migrate through the column depends on the time spent in the mobile phase, the high concentration part of the sample band will move faster through the bed which leads to bands which are tailed. Conversely, for a concave isotherm, K increases and therefore peak retention increases with increasing sample size which produces bands with a pronounced leading edge. In practice, the mass of samples involved in most analytical separations is generally small enough to lie within the linear

range of the distribution isotherm and so isotherm non-linearity is not usually a problem. However, for preparative separations much larger sample masses are loaded onto the column and in such cases isotherm non-linearity is a serious problem as will be discussed more fully in Chapter 6.

3.4 The Different Modes of Liquid Chromatography

The increased understanding of liquid chromatography, which has been greatly assisted by the improvements and developments of equipment such as packing materials, columns and detectors, has shown that the theoretical basis for all types of liquid chromatography is the same. The only differences between the various liquid chromatographic techniques are in the composition, structure and type of stationary phase, and the type of molecular forces which are involved in partitioning the solute molecules between the mobile and stationary phases.

Thus the modern liquid chromatograph can be used to perform all types of liquid chromatography simply by changing the mobile phase and the stationary phase in the column.

The main forms of liquid chromatography are now considered.

3.4.1 Adsorption Chromatography

Adsorption chromatography, or liquid-solid chromatography (LSC) as it is also referred to as, is based on solute molecules adsorbing onto and desorbing from the surface of a polar adsorbent material. The adsorbent is usually porous with the most common adsorbent materials being silica gel and alumina, although the latter is not used to any great extent nowadays. Typical surface areas range from 50-400m^2g^{-1}. A more detailed

discussion of the properties and preparation of silica gel will be given in a later chapter.

The theoretical understanding of adsorption chromatography is more advanced than any other form of liquid chromatographic technique and much of the credit is due to the work of Snyder.[1]

The basic mechanism of retention involves solute molecules adsorbing onto, and thus displacing solvent molecules from, the surface of the stationary phase. The equilibrium which is set up can be illustrated by:

$$X_m + n\ S_{ads} \rightleftharpoons X_{ads} + n\ S_m$$

where X_m and X_{ads} are the solute molecules in the mobile phase and adsorbed onto the stationary phase respectively, S_m and S_{ads} are the solvent molecules in the mobile phase and adsorbed onto the stationary phase respectively, and where n is the number of moles of adsorbed solvent molecules which are displaced.

The free energy change, ΔE, occurring in the above process can be expressed as:

$$\Delta E = E_{x,ads} + nE_{s,m} - nE_{s,ads} - E_{x,m} \qquad (3\text{-}15)$$

where the E's as used by Snyder are in fact dimensionless quantities given by:

$$\Delta E = \frac{-\Delta G}{2.303RT} \qquad (3\text{-}16)$$

Since the energies of adsorption are much greater than the interactions between solute and solvent molecules in the mobile phase, then to a first approximation, we can ignore the contributions to ΔE from the mobile phase, ie.

$$\Delta E = E_{x,ads} - nE_{s,ads} \qquad (3\text{-}17)$$

If we consider the contribution made to the adsorption energy, ΔE, by the individual adsorbed molecules then we can express this in terms of functions, ie:

$$\Delta E_{s,ads} = f(s).\ f(A)$$

$$\text{and} \quad \Delta E_{x,ads} = f(x).\ f(A)$$

where f(A) is a function of the adsorbent surface known as the surface activity function and is the same for all solutes and eluents. f(A) is usually denoted by the symbol α and "is arbitrarily given the value of unity for a thermally activated adsorbent that has not been deactivated. For adsorbents that have been sufficiently deactivated ... α is in the range 0.5 to 0.9."[2]

We can now rewrite equation (3-17) as:

$$\Delta E = \alpha.f(x) - n\alpha.f(s) \qquad (3\text{-}18)$$

When α=1, then S_x^Θ and S_s^Θ are the standard adsorption energies for the solute and solvent molecules respectively, and hence:

$$\Delta E = \alpha(S_x^\Theta - nS_s^\Theta) \qquad (3\text{-}19)$$

The eluent strength parameter, $\varepsilon°$, which is discussed in greater depth later in this chapter, is defined as being the adsorption energy of the solvent per unit area of standard activity surface, ie:

$$\varepsilon^\circ = \frac{S_s^\circ}{A_s} \qquad (3\text{-}20)$$

where S_s° is a dimensionless free energy of adsorption of the solvent onto the surface and A_s is the area occupied by an adsorbed solvent molecule in units of 0.085 nm^2 (which corresponds to the effective area of an aromatic carbon atom).

Since n is the number of solvent molecules displaced by one solute molecule, we can say that:

$$n = \frac{A_x}{A_s} \qquad (3\text{-}21)$$

By substituting the above into equation (3-19) we get:

$$\Delta E = \alpha \left(S_x^\circ - \frac{A_x}{A_s} S_s^\circ\right) \qquad (3\text{-}22)$$

and considering equation (3-20)

$$\Delta E = \alpha \left[S_x^\circ - \left(\frac{A_x}{A_s}\right) \varepsilon^\circ A_s\right] \qquad (3\text{-}23)$$

therefore $$\Delta E = \alpha \left(S_x^\circ - A_x \varepsilon^\circ\right) \qquad (3\text{-}24)$$

The thermodynamic equilibrium constant, K_{th}, for the adsorption of a solute molecule, X, is given by

$$K_{th} = \frac{N_{x,ads}}{N_{x,m}} \qquad (3\text{-}25)$$

where $N_{x,ads}$ and $N_{x,m}$ are the mole fractions of X in the adsorbed and mobile phases respectively.

When dealing with HPLC on an analytical scale, the number

of moles of solvent (n_s) greatly exceeds the number of moles of solute (n_x) in both of the phases and so we can say that:

$$N_{x,ads} \approx \frac{n_{x,ads}}{n_{s,ads}} \qquad (3\text{-}26)$$

$$\text{and} \quad N_{x,m} \approx \frac{n_{x,m}}{n_{s,m}} \qquad (3\text{-}27)$$

By substituting for $N_{x,ads}$ and $N_{x,m}$ into equation (3-25) we have:

$$K_{th} = \frac{n_{x,ads}\, n_{s,m}}{n_{x,m}\, n_{s,ads}} \qquad (3\text{-}28)$$

which can be further expressed as

$$K_{th} = k' \cdot \frac{V_m}{V_s} \qquad (3\text{-}29)$$

where V_m is the volume of the mobile phase and V_s is the volume of an adsorbed monolayer of mobile phase molecules.

The free energy change, ΔE, is also equal to the logarithm of the thermodynamic equilibrium constant, K_{th}, ie:

$$\Delta E = \log K_{th} \qquad (3.30)$$

By considering equations (3.30) and (3.29), we can write

$$\Delta E = \log k' + \log \left(\frac{V_m}{V_s} \right) \qquad (3.31)$$

and by substituting equation (3-24) into equation (3-31) and rearranging the equation in terms of k' we have:

$$\log k' = \underbrace{\log \left(\frac{V_s}{V_m} \right)}_{\text{Phase volume term}} + \underbrace{\alpha \, (S_x^\circ - A_x \varepsilon^\circ)}_{\text{Free energy term}} \qquad (3\text{-}32)$$

where $(S^{\circ}_{x} - A_{x}\varepsilon^{\circ})$ contains the properties of the eluent and solute.

By comparing equation (3-32) with equation (3-11) ie.

$$k' = K \frac{V_s}{V_m} \qquad (3\text{-}11)$$

we can express the distribution coefficient, K, as

$$\log K = \alpha (S^{\circ} - A_{x}\varepsilon^{\circ}) \qquad (3\text{-}33)$$

The Solvent Strength Parameter, ε°.

During the adsorption process, both solute molecules and mobile phase molecules compete for the polar adsorption sites. The weaker the interaction between the mobile phase and the stationary phase the stronger will be the adsorption of the solute molecules and thus k' will be increased. The converse will of course be true ie. the stronger the interaction between the mobile phase and the stationary phase the weaker will be the adsorption of the solute molecules and thus k' will be decreased.

The solvent strength parameter, ε°, has been measured for many solvents and a list of these arranged in order of increasing strength is referred to as an *eluotropic series* and this can be used to find an optimum strength for a particular separation problem. If the initial solvent produces k' values which are too large, ie. the retention time is too long, then the eluent strength is too weak and one must use a stronger solvent. Where the retention time is too short, then a weaker solvent

Table 3-1 Eluotropic series for alumina[3].

Eluent	ε°	UV cut-off (nm)
Pentane	0.00	210
1-pentene	0.08	215
Carbon tetrachloride	0.18	265
2-chloro-2-methyl propane	0.30[a]	225
Methylene chloride	0.42	235
1,2-dichloroethane	0.49	225
Dioxan	0.56	220
Ethyl acetate	0.58	260
Diethylamine	0.63	225
Acetonitrile	0.65	190
Methanol	0.95	205

[a] Assumed the same as for 2-chloropropane

has to be used. This can easily be found, in the case of a single solvent system, by looking up the ε° values in the eluotropic series. In this way a suitable solvent strength can easily be homed in on by this trial-and-error method. An eluotropic series for alumina, which also holds well for other polar adsorbents, is given in table 3-1.[1,3]

Often, mixtures of solvents, and in particular binary solvents,[1,4,5] are used rather than pure solvents. This can be advantageous since the solvent strength changes continuously between the two values for the pure solvents. Another advantage of binary solvents is that, for a particular solvent strength, the composition can be varied to optimize the separation factor, α, (solvent selectivity) for various solute-pairs in the sample. A final advantage is that solvent viscosity can be kept low by selecting a non-viscous solvent as the main component of the mixture.

Optimization of solvent strength, ε°, and solvent selectivity, α, has been recently reviewed by Snyder *et al.*[6]

An important practical consideration in adsorption chromatography, is the partial deactivation of the stationary phase. This is necessary because of the inhomogeneity of the silica gel surface due to the presence of a small number of geminal silanol groups. These are highly active groups which strongly adsorb hydrophilic groups. Their adsorptive capacity, however, is low as they are present in low concentration. This means that overloading of this type of retentive mechanism occurs at low solute concentration and results in peak tailing. To overcome this problem, the groups on the surface should be made to be of equal activity so that only one type of retentive

mechanism is in operation ie. the groups should either be all strongly active or should all be less active. In practice, the concentration of the residual silanol groups is reduced and this partial deactivation of the surface is achieved by the addition of either water, methanol or glycol to the eluent. The topic of deactivation has been covered in depth by Snyder.[1]

3.4.2 Reversed Phase Chromatography

Although adsorption chromatography and liquid-liquid partition chromatography are both powerful and commonly used separation techniques, they are not without their limitations and disadvantages. For example, both adsorption chromatography and liquid-liquid partition chromatography are unsuitable for the separation of highly polar or ionic compounds since they will have a very large affinity for the polar stationary phase and will therefore have very long retention times. This problem can be circumvented by using a non-polar stationary phase and a polar mobile phase. Polar molecules, which have little affinity for the non-polar stationary phase, will not be strongly retained and therefore will be quickly eluted, while non-polar molecules will be more strongly retained. This type of chromatography is known as "reversed-phase" chromatography since the order of elution, ie. polar before non-polar, is the reverse to what it is in normal phase chromatography. The term was first introduced in 1950 by Howard and Martin.[14]

Hydrophobic stationary phases suitable for use in reversed-phase chromatography are generally prepared by the chemical bonding of an organic moiety onto the surface of silica gel.

Such phases were first introduced in 1969 by Halász and Sebastian.[15] Alternatively, stationary phases for use in reversed-phase liquid-liquid chromatography (RP-LLC) can, in principle, be made hydrophobic by coating the support with a non-polar stationary phase, eg. squalane, but in practice, RP-LLC is difficult to carry out. This is because the hydrophobic coating, which is only mechanically held within the pores, tends to be displaced by the hydrophilic part of the mobile phase. An added problem is that, as with normal phase LLC, gradient elution cannot be used with RP-LLC since this would also strip the stationary liquid phase from the support material. Clearly, preparation of a hydrophobic stationary phase by the chemical bonding of organic groups will overcome the aforementioned problems with RP-LLC.

The main problem with chemically bonded stationary phases is that the bonded organic groups can be cleaved off by buffer solutions which are either too acidic or too basic, or which contain oxidising agents. However, the problem of stationary phase stability at very low and very high pH values can be overcome by using carbon as the stationary phase as this is a ready-made non-polar material which is stable at all values of pH. Carbon has been used as a packing material as far back as the 1940's but produced poor column efficiencies and badly tailed peaks. However in recent years several workers,[55-57] and in particular Knox and co-workers,[60] have greatly improved on these earlier carbon materials and it is only a matter of time before carbon is regularly used for reversed-phase

separations. Other advantages over chemically bonded stationary phases include its ability to separate compounds in a homologous series as well as geometrical isomers.

The preparation of hydrophobic packing materials is most commonly achieved by the chemical bonding of octadecyl groups ($C_{18}H_{37}$-) although groups with shorter chain lengths (eg. C_2H_5- and C_8H_{17}-) are also used. The longer the chain length of the bonded moiety, the greater will be the solute retention with a given eluent. The preparation of chemically bonded stationary phases will be discussed more fully in Chapter 7.

It is possible that many of the commercial materials available for reversed-phase chromatography will contain a small number of residual silanol groups[16] and this will result in the retention mechanism being a mixture of adsorption and partition which will cause peak tailing. It is possible to react these active silanol groups with trimethylsilyl groups ($(CH_3)_3Si$-) thus reducing the degree of adsorption of the solutes onto the support material and improving on the peak shape by reducing peak tailing.

The mobile phases which are used with chemically-bonded reversed-phase materials are normally polar solvents or mixtures of polar solvents. For a given set of conditions it is generally found that the eluent strength increases as the polarity of the solvent decreases. Generally speaking, the order of the eluent strength of various solvents used in reversed-phase chromatography is opposite to that found by Snyder[1] for normal-phase chromatography (using alumina as the adsorbent). Table 3-1 lists the properties of some commonly used eluents in order of increasing polarity and therefore of decreasing eluent

strength (for reversed-phase chromatography). By combining any of the solvents with water or an aqueous buffer, eluents of intermediate strength can be obtained.

The retention of ionic or ionisable solutes can be greatly influenced by the pH of the eluent and this is dependent on the dissociation constant of the solutes. For the separation of such solutes it is important to maintain the pH of the eluent by means of a buffer which ensures rapid equilibration of the dissociation of the solutes and thus prevents badly tailed peaks.

As the organic moiety is chemically bonded onto the silica surface it is now possible to use gradient elution to assist in separation of a mixture which contains solutes with a wide range in retention values. This involves a continuous decrease in the polarity of the eluent during the chromatographic run and is usually achieved by a gradual increase in the organic content of the mobile phase e.g. in acetonitrile-water or methanol-water mixtures.

The mechanism of reversed-phase chromatography is not as yet fully understood. Recent ideas on the subject can be found in several papers.[17-26,58] There are two main theories as regards the mechanism which is involved.

a) The "partitioning" model suggests that the non-polar surface of the stationary phase extracts the more hydrophobic component from a binary mobile phase,[17] thus forming an organic-rich liquid layer at the surface, and that the separation occurs by partition of the solute between the mobile phase and this organic-rich layer.

b) The "adsorption" model suggests that retention is due to the adsorption of the solute to the bonded organic layer via hydrophobic interactions.

Results obtained so far suggest that the processes which are involved are complex and that they may depend significantly on the structure of the stationary phase, although even here there is no agreement. For packing materials with the brush-like structure, for example those of Halasz and Sebastian,[27] it is thought that retention is due to adsorption of the solute to the bonded organic layer as well as to the unreacted silanol groups on the surface of the support material. This view is also shared by Horvath[58] though he assumed the structure of the bonded phase to consist of a "molecular fur" of covalently bonded organic groups.

For polymeric bonded phases, Kirkland[17,33] has suggested two models to describe the mechanism. The first is the "partitioning" model while the second suggests a mechanism where dissolution is the main process but where adsorption on the polymer surface[17,21,33] and interphase adsorption of the solute at the stationary phase/support material interface may also occur.[34-38]

While the organic group bonded onto the support material controls the selectivity of the solute functional group, the separation of individual compounds within the same class in reversed-phase chromatography has been correlated to their relative solubilities in the mobile phase.[22] For saturated hydrocarbonaceous bonded phases (eg. $C_{18}H_{37}$-) the elution order for the members of a homologous series is inversely proportional to their solubility in the mobile phase.

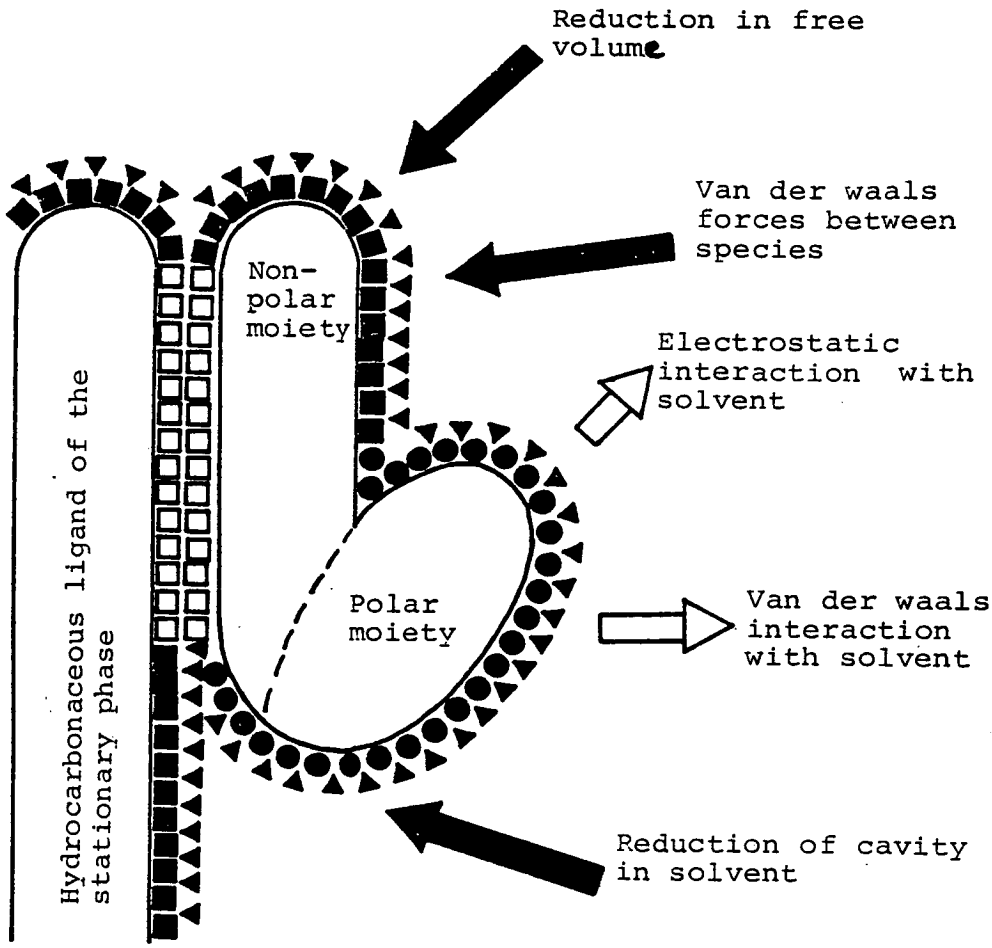

Figure 3.3

Schematic illustration of eluite binding to hydrocarbonaceous ligate at the stationary phase surface brought about by solvophobic effect. The arrows represent the balance of forces whose resultant is the binding force. The open squares represent the amount by which the surface area contacting the solvent has been reduced.
(Reproduced from Reference 59).

3.4.2.1 The Thermodynamics of Reversed-phase Chromatography

The most comprehensive theory on the thermodynamics of reversed-phase chromatography is that produced by Horvath.[58,59] His treatment considers the processes involved in terms of the properties of the solute, namely the surface area and the dipole moment, and the properties of the bulk solvent, namely the surface tension and the dielectric constant. The different forces involved in the reversible association of a solute molecule to the chemically bonded stationary phase, as described by Horvath, are illustrated schematically in figure 3-3. According to the theory, the strength of the interaction between a polar solute molecule and the non-polar stationary phase in the presence of a polar eluent is influenced by the balance of the opposing forces arising from the solvent effect.

The free energy, ΔG°, which describes the reversible association of solutes to the chemically bonded non-polar groups is related to the equilibrium constant, K, for the association by the expression:

$$\Delta G^\circ = -RT\ell nK \qquad (3\text{-}35)$$

It has previously been shown that

$$k' = K \frac{V_s}{V_m} \qquad (3\text{-}36)$$

where k' is the phase capacity ratio and V_s, V_m are the volumes of the stationary and mobile phases respectively. By combining equations (3-35) and (3-36) we can express the phase capacity ratio in terms of the free energy of association as

$$\ell nk' = \ell n \left(\frac{V_s}{V_m}\right) - \left(\frac{\Delta G^\circ}{RT}\right) \qquad (3\text{-}37)$$

3.4.3 Liquid-liquid Partition Chromatography

Liquid-liquid partition chromatography (LLC) involves the distribution of solute molecules between two immiscible liquid phases, one mobile and the other stationary, according to their relative solubilities. The ability of the technique to differentiate between minute differences in solute solubilities means that it is a very useful technique.

This form of chromatography was first introduced by Martin and Synge, and is described in their now classic paper published in 1941.[7]

The stationary phase is mechanically held within the pores of an inert support which can be either porous or pellicular.

The most commonly used technique for coating the support material with the stationary liquid phase is to slurry the support in a solution of the stationary liquid phase in a volatile solvent. The volatile solvent is then slowly evaporated under nitrogen, leaving a uniform coating of the stationary liquid phase on the support material, which can then be dry packed.

An alternative coating method used for microparticles (ie. <25-30μm) is the "in situ" or "dynamic coating" method. This is used because microparticles have to be slurry packed and, unfortunately, many of the stationary liquid phases used are soluble in the slurry solvents and would therefore be stripped from the support material during packing. With this method, the column is first slurry packed and then a solution of the stationary liquid phase is passed through the column, followed by a mobile phase which will cause the stationary phase to be precipitated onto the support material.

To prevent mixing of the two liquid phases, they are required to be of widely different polarities. In normal phase L.L.C., where the stationary phase is polar, the mobile phase will be non-polar. Polar solutes will be more strongly retained, and therefore will be eluted later than non-polar solutes.

Although the stationary and mobile phases are chosen to have little or no mutual solubility, there will never-the-less be some removal of the stationary liquid phase by the mobile phase with time. If this is not prevented, then the nature of the separation mechanism will change to a mixture of partition and adsorption, leading to poor chromatography. This problem can, however, be avoided by pre-saturating the mobile phase with stationary phase prior to it being introduced into the column. This is most easily achieved by passing the mobile phase through a pre-column which is packed with a high surface area support material (eg. silica gel) onto which the stationary phase has been deposited. The mobile phase then becomes saturated with the stationary phase and this prevents any leaching of the stationary phase during the chromatographic process. The pre-column can then be included in the chromatographic system in front of the main column.

The criteria for thermodynamic equilibrium for a solute partitioned between two immiscible phases is that the activity for the solute be the same in both phases, ie:

$$a_s = a_m \qquad (3\text{-}38)$$

where a_s and a_m represent the activity of the solute in the stationary and mobile phases respectively.

The partition coefficient, K, is given by

$$K = \frac{C_s}{C_m} \qquad (3\text{-}39)$$

where C_s and C_m are the concentrations of the solute in the stationary and mobile phases respectively.

This can be expressed in terms of the solute activity coefficients in the stationary and mobile phases, namely γ_s and γ_m, as

$$K = \frac{(a_s/\gamma_s)}{(a_m/\gamma_m)} \qquad (3\text{-}40)$$

By considering equation (3-38), this becomes

$$K = \frac{\gamma_m}{\gamma_s} \qquad (3\text{-}41)$$

Since we have seen that

$$k' = K \frac{V_s}{V_m} \qquad (3\text{-}42)$$

we can re-write equation (3-42) as

$$k' = \frac{V_s}{V_m} \cdot \frac{\gamma_m}{\gamma_s} \qquad (3\text{-}43)$$

In general, LLC separates according to type and sometimes number of substituent groups. Its great advantage over liquid-solid adsorption chromatography (LSC) is that it is a good method for separating members of a homologous series since their activity coefficients vary with their molecular weight.

However, LLC can not be used over such a wide range of retention (k') values as LSC because of the necessity for the stationary and mobile phases to be immiscible whilst at the same time both must be necessarily solvents for the solute. If the solvent strength is increased in order to elute strongly retained compounds, this may well result in the stationary liquid phase becoming more soluble in the mobile liquid phase causing the former to be stripped from the support material. A further disadvantage, therefore, is that gradient elution cannot be performed with L.L.C.

Selection of suitable solvent pairs is still largely empirical but has been made easier by the semi-quantitative classification of solvents with respect to their ability to undergo different types of intermolecular interactions on the basis that "like dissolves like." The polarity of a solvent is indicated by the Hildebrand solubility parameter,[8-10] δ, which is defined as "the energy of vapourisation per millilitre of pure substance." ie.

$$\delta_x = \left(\frac{\Delta H_{vap}}{V_x}\right)^{\frac{1}{2}} \qquad (3\text{-}44)$$

A low value of δ (eg. 7.1 for n-pentane) indicates that the solvent is non-polar while a high value (eg. 21 for water) indicates that the solvent is polar. In normal phase LLC, an increase in the solvent polarity, ie. an increase in the δ value, will result in an increase in the solvent strength and therefore will reduce the k' values of the samples.

Much work has been done in the field of LLC by Huber[11-13] who has developed a special type of partition system which involves a two-phase ternary mixture. This involves stirring

three components together, for example methylene chloride, ethanol and water,[11,12] until equilibrium is reached whereupon the two layers are separated, the aqueous layer being used as the stationary phase and the organic layer as the mobile phase.

3.4.4 Ion Exchange Chromatography

Ion exchange chromatography is a technique used in the separation of ionic or ionizable compounds.

The support material consists of a matrix onto which a charge-bearing group is chemically bonded. Cation exchangers contain negatively charged groups and are used for exchanging cationic species while anionic exchangers contain positively charged groups and are used for exchanging anionic species, eg.

$R\text{-}SO_3^-\ H^+$	Strong cation exchanger
$R\text{-}NR_3^+\ OH^-$	Strong anion exchanger
R-COOH	Weak cation exchanger
$R\text{-}NH_2$	Weak anion exchanger

The mobile phase will contain an associated counter ion whose charge is opposite to that of the surface functional group. Solute ions are therefore in competition with these mobile phase counter-ions for the ionic sites on the ion exchange material, and it is this which forms the basis of retention. This can be represented as:

$$R\text{-}SO_3^-,\ Na^+ + X^+ \rightleftharpoons R\text{-}SO_3^-,\ X^+ + Na^+ \qquad (3\text{-}45)$$

where $R\text{-}SO_3^-,\ Na^+$ represents the ion exchange site with Na^+

being the associated counter-ion present in the mobile phase, X^+ is the solute ion and where $R\text{-}SO_3^-$, X^+ is the ion pair produced when X^+ displaces the counter ion.

With weak ion exchangers, their ability to participate in the exchange process will depend on the pH of the system. For weak cation-exchangers, the pH must be high enough to force the following dissociation equilibrium to the right.

$$HA \rightleftharpoons H^+ + A^-$$

Conversely, for weak anion-exchangers, the pH must be low enough to force the dissociation equilibrium to the right.

$$B + H^+ \rightleftharpoons BH^+$$

When using weak ion exchangers, the eluent has to be buffered to control the position of the acid-base equilibrium, otherwise the proportion of neutral and ionised forms will change throughout the chromatographic band. This would result in serious peak tailing since the neutral and ionised forms would have different degrees of retention.

Retention is also inversely proportional to the ionic strength of the eluent and is inversely proportional to the concentration of the counter ion, and these factors can also be utilised to manipulate retention.

There are several different types of ion exchange materials available. The early materials used in classical chromatography were made by bonding acidic or basic functional groups onto a porous matrix produced by co-polymerisation of styrene and divinyl benzene but were unable to withstand much pressure and tended to swell up in solvents. Modern resins however have more

cross-linking and are used increasingly eg. Dionex.

Pellicular ion exchange materials were introduced in 1967 by Horvath *et al.*[39] and consisted of glass beads coated with a thin film of ion exchange resin. Such materials have been largely superceded by packing materials which consist of porous silica gel with ion exchange functional groups chemically bonded onto the surface.[40,41] These materials are much more efficient due to their excellent mass transfer properties and their ability to withstand pressure.

3.4.4.1 Thermodynamics of Ion Exchange Chromatography

The retention of a solute in ion exchange chromatography depends on the equilibrium established for the displacement of the counter ion, which is present in the eluent, by the solute ion.

$$\begin{aligned} &\text{Cation Exchange} \quad X^+ + R^-Y^+ \rightleftharpoons Y^+ + R^-X^+ \\ &\text{Anion Exchange} \quad X^- + R^+Y^- \rightleftharpoons Y^- + R^+X^- \end{aligned} \qquad (3\text{-}46)$$

where X is the solute ion, Y is the counter ion and R is the resin.

Let us consider a more specific example of cation exchange as given by:

$$X^+ + (R'\text{-}SO_3^-, Na^+) \rightleftharpoons Na^+ + (R'\text{-}SO_3^-, X^+) \qquad (3\text{-}47)$$

where the equilibrium constant K_{eq} is given by:

$$K_{eq} = \frac{[Na^+][R'\text{-}SO_3^-, X^+]}{[X^+][R'\text{-}SO_3^-, Na^+]} \qquad (3\text{-}48)$$

The capacity factor, k', is proportional to the distribution coefficient, K, and the ratio of the concentrations of solute X^+ in the stationary and mobile phases, ie.

$$k' \propto K = \frac{[R'\text{-}SO_3^-, X^+]}{[X^+]} \qquad (3\text{-}49)$$

By comparing equations 3-38, and 3-49, we can write

$$k' \propto K_{eq} \frac{[R'\text{-}SO_3^-, Na^+]}{[Na^+]} \qquad (3\text{-}50)$$

It is obvious that the concentration of the ion exchange sites $[R'\text{-}SO_3^-, Na^+]$ must be constant since this is determined by the structure of the support material. The phase capacity ratio k' therefore is inversely proportional to the counter-ion concentration.

$$\text{ie. } k' \propto \frac{1}{[Na^+]} \qquad (3\text{-}51)$$

The pH of the eluent has an indirect effect on the phase capacity ratio, k', in the case of weakly ionized solutes since the pH will affect the position of the acid-base equilibria which is established. In this way, solute retention can be manipulated by the control of the pH.

For example, if we consider the case of a weak acid, then k' is proportional to the fraction of solute which is ionized, ie.

$$k' \propto \text{fraction ionized} = \frac{[R.COO^-]}{[R.COOH] + [R.COO^-]} \qquad (3\text{-}52)$$

The dissociation constant for a weak acid, K_a, is given by

$$K_a = \frac{[R\text{-}COO^-][H_3O^+]}{[R\text{-}COOH]} \qquad (3\text{-}53)$$

By rearranging equation (3-53) and substituting into equation (3-52) we get

$$k' \propto \frac{\left(\frac{K_a[R\text{-}COOH]}{[H_3O^+]}\right)}{[R\text{-}COOH] + \left(\frac{K_a[R.COOH]}{[H_3O^+)}\right)} \qquad (3\text{-}54)$$

The pH of the eluent however will not affect the k' for strong acids and bases since they are completely ionized.

3.4.5 Ion-pair Chromatography

Ion-pair chromatography (IPC) is a separation technique based on the method of ion-pair extraction[44] in which ionic or ionisable compounds are extracted from an aqueous solvent into an organic solvent by complexing them with ions of the opposite charge, known as pairing ions, which contain a hydrophobic moiety. Much of the early work in developing this extraction method into a chromatographic technique was carried out by Schill and co-workers.[42-45]

3.4.5.1 Normal-phase Ion-pair Chromatography

In normal-phase IPC, the stationary phase is aqueous and the mobile phase is organic. The support material, which is

usually silica gel, is coated with an aqueous buffer, which normally contains the pairing ion, by the "dynamic coating" method which is described in section 3.4.3.

For the separation of bases, an organic acid such as perchloric acid is used as the pairing ion while for the separation of acids a base such as tetraethylammonium hydroxide is used as the pairing ion. It is also possible to use a pairing ion which is U.V. absorbing if the compound to be separated does not itself absorb in the U.V. region.

The problem with using normal-phase IPC is that the eluent is required to be pre-saturated with the aqueous buffer to prevent stripping of the aqueous phase from the support material. Furthermore, the column has to be re-equilibrated each time the pairing ion or its concentration is changed.

3.4.5.2 Reversed-phase Ion-pair Chromatography

In reversed-phase IPC, the stationary phase is organic and the mobile phase is aqueous. A chemically bonded silica, such as ODS-silica, is generally used as the stationary phase and as the organic phase is now bonded onto the support material there are no problems with bleeding. Changes in the pairing ions and in their concentration can therefore be easily made.

One form of reversed-phase IPC is a technique developed by Knox and Laird[51] known as 'soap' chromatography in which the pairing ion, which is present in the aqueous mobile phase, is a detergent. For the separation of acids, a cationic pairing agent, such as cetrimide[51] is used while for the separation of bases an anionic pairing agent[52] is used.

To obtain a separation, the pH is first adjusted so that the solutes are in the ionized form. The mobile phase is then chosen so that the solutes are virtually unretained. If a small amount of ion-pairing agent (eg. 0.01-0.1%) is then added, the solute retention should dramatically increase (for reversed-phase IPC).

Horvath *et al.*[46] and other workers[47-50] have proposed the existence of two different types of retention mechanism for ion-pair chromatography. The first type proposes that the solute molecule forms an ion-pair with the pairing ion in the mobile phase and that this uncharged ion-pair then partitions into the hydrophobic stationary phase. The second proposed mechanism[51-53] suggests that the unpaired pairing ions partition into the hydrophobic stationary phase with the ionic group pointing away from the surface. The ionic solute molecules then migrate towards them to form ion-pairs. This last mechanism is often referred to as the "ion-exchange" mechanism.

The proposal of two different kinetic mechanisms is thought by Knox and Hartwick[54] to have arisen because some workers have incorrectly associated them with two possible thermodynamic equilibria arising from the situation where either a) the support is almost saturated with respect to the adsorption of the pairing ion, or b) there is incomplete saturation of the support by the pairing ion. However, Knox and Hartwick have reminded us that whichever mechanism does occur, it will have no bearing on the actual solute retention since retention is influenced by thermodynamic factors while the kinetic factors affect the peak width only.

Reversed-phase IPC is particularly useful in the separation

of drugs and their metabolites and other biological samples since aqueous eluents are used and samples can be injected neat.

3.4.5.3 Thermodynamics of Ion-pair Chromatography

By analogy with ion-exchange chromatography it can be shown that, for normal-phase IPC

$$k' = \frac{1}{E_{xp}[P^+]_{aq}} \times \frac{V_s}{V_m} \qquad (3.55)$$

where E_{xp} is the ion-pair extraction equilibrium coefficient, $[P^+]_{aq}$ is the concentration of the pairing ion in the aqueous phase and V_s, V_m are the volumes of the stationary and mobile phases respectively. Therefore, for normal-phase IPC, retention is inversely proportional to the concentration of the pairing ion ie.

$$k' \propto \frac{1}{[P^+]_{aq}} \qquad (3\text{-}56)$$

Similarly, for reversed-phase IPC, it can be shown that

$$k' = E_{xp}\,[P^+]_{aq} \times \frac{V_s}{V_m} \qquad (3\text{-}57)$$

and that therefore solute retention is directly proportional to the pairing ion concentration, ie.

$$k' \propto [P^+]_{aq} \qquad (3.58)$$

3.4.6 Exclusion Chromatography

Exclusion chromatography, which is also known as Gel chromatography, is the name given to the technique whereby the separation of compounds is based strictly on the differences in their molecular size, and sometimes on their geometry. Since size is mainly dependent on molecular weight, it is sometimes thought that separation depends primarily on molecular weight.

Gel chromatography encompasses Gel Permeation Chromatography (G.P.C.) where separations are carried out in organic solvents for the separation of non-polar solutes, and Gel Filtration Chromatography (G.F.C.) where separations are carried out in aqueous solutions for the separation of polar solutes.

There are two main types of packing materials, namely soft gels such as cross-linked polystyrenes, or porous inorganic solids such as silica gel or glass. The same silicas used for adsorption can be used for exclusion chromatography. For true exclusion chromatography to take place, the support matrix must be chemically inert ie.no adsorption should take place. Adsorption onto the packing material can be prevented by careful selection of the eluent ie.by choosing a mobile phase of similar constitution to the support matrix in the case of gels eg. a toluene/polystyrene combination. This means that cross-linked polystyrenes are unsuitable for use with aqueous mobile phases. Prevention of adsorption onto silica gel can be achieved by using a strong solvent or by the chemical bonding of protective functional groups onto its surface.

Some of the gels swell in certain solvents, are mechanically

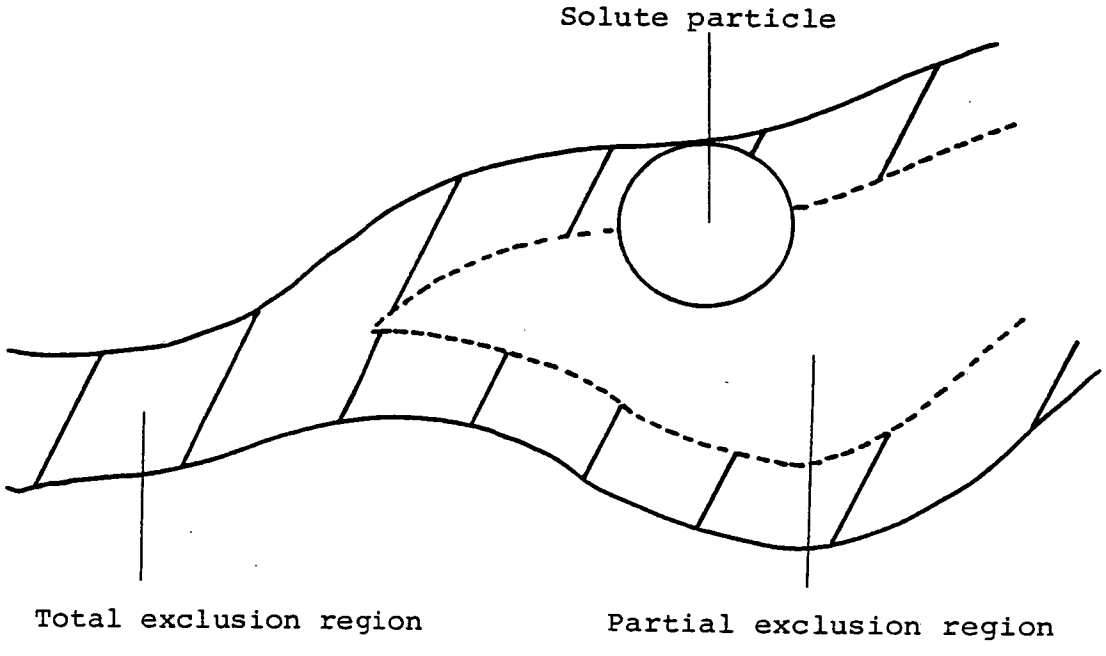

Figure 3.4 Partial and total exclusion regions within the pores of the stationary phase.

unstable and therefore do not withstand pressure (eg. dextrans and agarose). Cross-linked polystyrene beads can withstand moderate pressures but for high pressure liquid chromatographic separations, the rigid porous silica gels or glasses must be used.

The basic principle of exclusion is that the centre of gravity of a large molecule cannot approach closer to any solid surface, for example the pore walls, than its hydrodynamic radius. It is therefore possible to define a region within the pore structure of any material from which the centre of gravity of a molecule is excluded, as illustrated in figure 3-4. In a material containing a range of pore sizes, large molecules can be partially excluded from wide pores and totally excluded from narrow pores. Partial exclusion can also occur with materials in which the pores are perfectly uniform as illustrated in figure 3-4. As the sample band moves down the column, those molecules which are totally excluded will elute first. Intermediate-size molecules which enter some, but not all of the pores will be moderately retained, whilst the smaller molecules which enter most of the pores are more retained. Finally, the solvent molecules which are very small, will permeate through the entire porous matrix and therefore will be eluted last. This means that even with a complex sample, all of the components are eluted in a relatively short time and all before the retention time for the solvent, t_m. This is the opposite to the other forms of liquid chromatography. The separation time for a chromatographic run is easily predicted since it is equal to the retention time of the last peak, ie. the solvent peak, t_m.

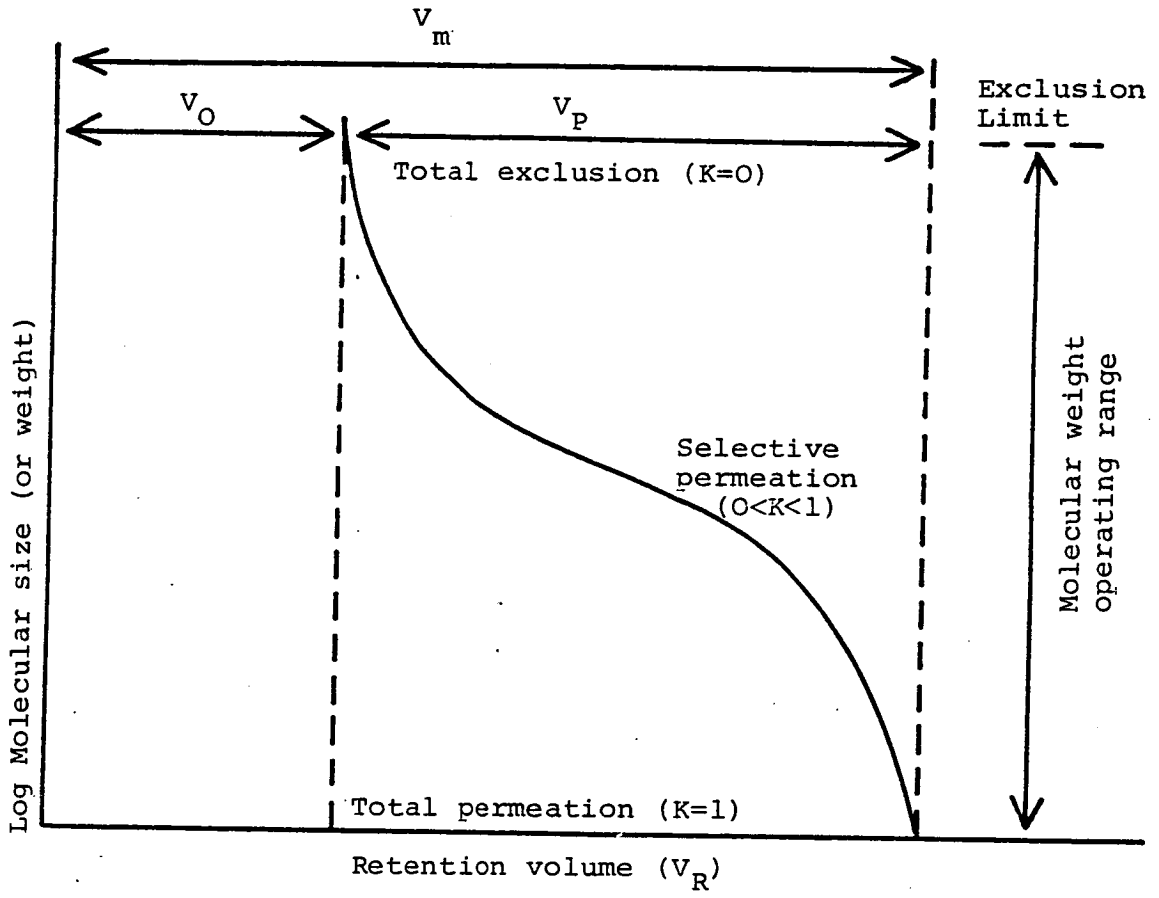

Figure 3.5 Calibration curve for exclusion chromatograghy

Retention times or volumes can be also easily predicted according to molecular weight.

Because the sample bands spend little time in the column, the emerging bands are narrow and are easily detected using refractometer detectors, even though these detectors are relatively insensitive.

Exclusion data is normally plotted in the form of a calibration curve relating the logarithm of the molecular weight to the elution volume, V_R, or the partition coefficient, K. An example of such a calibration curve is shown in figure 3-5.

The identification of discrete compounds is fairly straightforward but for the assignments of molecular weights in polymeric substances a calibration curve must be constructed first if a molecular weight distribution is required preferably using molecules of similar chemical composition.

Exclusion chromatography is particularly useful for the separation of complex biomedical molecules such as proteins and nucleic acids, polymers, organic and inorganic molecules, polar and non-polar materials as well as simple molecules. However, the technique is unable to separate molecules of similar size. Another disadvantage is that, since all the solutes elute before the solvent peak, the column has a limited peak capacity which is limited by the fact that the ratio of the pore volume, V_p, to the column void volume, V_o, ie. $\frac{V_p}{V_o}$ is restricted. Since V_o is usually around 40% of the empty column volume it is difficult to obtain a value of $\frac{V_p}{V_o}$ greater than 1 without making particles of such a high pore volume as to make it impracticable.

The limited peak capacity limits the ability of the technique to resolve complex samples, but this could be overcome by the coupling together of several columns packed with materials of different pore sizes.

REFERENCES

Chapter 3

1. L.R. Snyder; "Principles of Adsorption Chromatography" Marcel Dekker.
2. J.H. Knox (Editor); "High Performance Liquid Chromatography" Edinburgh University Press, 1978.
3. R.E. Majors in "Practical H.P.L.C." p.99. C.F. Simpson (Editor), Heyden 1976.
4. R.E. Majors in "Practical HPLC" p.100. C.F. Simpson (Editor), Heyden 1976.
5. L.R. Snyder and J.J. Kirkland; "Introduction to Modern LC" p.257. Wiley Interscience.
6. L.R. Snyder, J.L. Glajch, and J.J. Kirkland; J.Chromatogr. 218 (1981), 299.
7. A.J.P. Martin and R.L.M. Synge; Biochem.J., 35 (1941), 1358.
8. J.H. Hildebrand and R.L. Scott; "The Solubility of Nonelectrolytes" 3rd ed., Dover, New York, 1964.
9. L.R. Snyder in "Modern Practice of L.C." J.J. Kirkland (ed.), Ch.7, Wiley Interscience, New York, 1971.
10. R.A. Keller, B.L. Karger, and L.R. Snyder in "Gas Chromatography" 1970, Stock & Perry eds. Inst. of Petroleum, London, 1971.
11. J.F.K. Huber, D.A.M. Meijers, and J.A.R.J. Hulsman; Anal.Chem., 44 (1972), 111.
12. J.F.K. Huber, E.T. Alderlieste, H. Harren, and H. Poppe; Anal.Chem., 45 (1973), 1337.
13. J.F.K. Huber, F.F.M. Kolder, and J.M. Miller; Anal.Chem., 44 (1971), 105.

14. G.A. Howard and A.J.P. Martin; Biochem.J., 56 (1950), 532.
15. I. Halasz and I. Sebastian; Angew.Chem., 81 (1969), 464.
16. J.N. Done; J.Chromatogr., 125 (1976), 43.
17. J.J. Kirkland; J.Chromatog.Sci., 9 (1971), 206.
18. J.H. Knox and A. Pryde; J.Chromatogr., 112 (1975), 171.
19. K. Karch, I. Sebastian, I. Halasz, and H. Engelhardt; J.Chromatogr., 122 (1976), 171.
20. J.H. Knox and G. Vasvari; J.Chromatogr., 83 (1973), 181.
21. M.J. Telepchak; Chromatographia, 6 (1973), 234.
22. D.C. Locke; J.Chromatog.Sci., 12 (1974), 433.
23. E.J. Kikta and E. Grushka; Anal.Chem., 48 (1976), 1098.
24. D.F. Horgan and J.N. Little; J.Chromatog.Sci., 10 (1972), 76.
25. B.L. Karger, J.R. Gant, A. Hartkopf, and P.H. Weiner; J.Chromatogr., 128 (1976), 65.
26. K. Karch, I. Sebastian, and I. Halasz; J.Chromatogr., 122 (1976), 3.
27. I. Sebastian and I. Halasz; Chromatographia, 7(8) (1974), 371.
28. M.Uihlein and I. Halasz; J.Chromatogr., 80 (1973), 15.
29. E. Grushka and J. Kikta; Anal.Chem., 46(11) (1974), 1370.
30. I. Halasz and I. Sebastian; J.Chromatog.Sci., 12(4) (1974), 161.
31. B.L. Karger and E. Sibley; Anal.Chem., 45(4) (1973), 740.
32. M. Uihlein and I. Halasz; J.Chromatogr., 80 (1973), 1.
33. J.J. Kirkland; Anal.Chem., 43(12) 36A (1971).
34. M.B. Evans; Chromatographia, 3 (1970), 337.

35. M.B. Evans; Chromatographia, 4 (1971), 441.

36. R.L. Martin; Anal.Chem., 33 (1961), 347.

37. R.L. Martin; Anal.Chem., 35 (1963), 116.

38. D.C. Locke in "Advances in Chromatography" Vol.8, 1969, p.55, J.C. Giddings and Keller, eds. Marcel Dekker.

39. C. Horvath, B.A. Preiss, and S.R. Lipsky; Anal.Chem., 39 (1967), 1422.

40. G.B. Cox, C.R. Loscombe, M.J. Slucutt, and J.A. Upfield; J.Chromatogr., 117 (1976), 269.

41. K.K. Unger and D. Nyamah; Chromatographia, 7 (1974), 63.

42. S. Eksborg and G. Schill; Anal.Chem., 45 (1973), 2092.

43. B. Fransson, K.-G. Wahlund, I.M. Johansson, and G. Schill; J.Chromatogr., 125 (1976), 327.

44. G. Schill in "Ion Exchange and Solvent Extraction" Vol.6, Edited by J.A. Marinsky and Y. Marcus; Marcel Dekker, New York, 1974.

45. G. Schill in "Assay of Drugs and Other Trace Compounds in Biological Fluids" Edited by E. Reid, North Holland Publishing Co., New York, 1976.

46. C.S. Horvath, W. Melander, I. Molnar and P. Molnar; Anal.Chem., 49 (1977), 2295.

47. R.A. Bidlingmeyer, S.N. Deming, W.P. Price, Jr. B. Sachok, and M. Petrusek; J.Chromatogr., 186 (1979), 419.

48. R.P.W. Scott and P. Kucera; J.Chromatogr., 175 (1979), 51.

49. R.S. Deelder, H.A.J. Linssen, A.P. Konijnendijk, and J.L.M. van den Veen; J.Chromatogr., 185 (1979), 241.

50. K. Unger, R. Kern, M.C. Minou, and K.F. Krebs; J.Chromatogr., 99 (1974), 435.

51. J.H. Knox and G.R. Laird; J.Chromatogr., 122 (1976), 17.

52. J.H. Knox and J. Jurand; J.Chromatogr., 125 (1976), 89.

53. J.H. Knox and J. Jurand; J.Chromatogr., 149 (1978), 297.

54. J.H. Knox and R.A. Hartwick; J.Chromatogr., 204 (1981), 3.

55. H. Colin, C. Eon, and G. Guichon; J.Chromatogr., 119 (1976), 41.

56. H. Colin, C. Eon, and G. Guichon; J.Chromatogr., 122 (1976), 223.

57. H. Colin and G. Guichon; J.Chromatog.Sci., 18 (1980), 54.

58. C. Horvath and W. Melander; J.Chromatog.Sci., 15 (1977), 393.

59. C. Horvath in "Techniques in Liquid Chromatography," C.F. Simpson (editor), Wiley 1982, p.267.

60. M.T. Gilbert, J.H. Knox, and B. Kaur; Chromatographia, 16 (1982), 138.

CHAPTER 4

KINETICS OF CHROMATOGRAPHY

Chapter 4. Kinetics Of Chromatography

KINETICS OF CHROMATOGRAPHY

4.1. Introduction

In order to achieve an effective separation, each component in a sample mixture must possess significantly different rates of migration so that their zone centres become disengaged as they move through the column bed.

It has already been said that the control of migration rates is connected to the thermodynamic equilibrium distribution of each solute between the stationary and mobile phases and this has been dealt with in depth in Chapter 3.

The other factor influencing the resolution of solutes is the degree of band spreading which takes place through the column. Obviously, the narrower the band or the less the band dispersion, the greater will be the resolution.

As we have already seen in Chapter 2, the equation for the resolution, R_s, (equation 2-9) is influenced by both thermodynamic considerations (the first 2 factors) and by kinetic considerations (the plate number N), ie.

$$R_s = \frac{1}{4}\left(\frac{\alpha-1}{\alpha}\right)\left(\frac{k'_2}{1+k'_2}\right)N^{\frac{1}{2}} \qquad (2\text{-}9)$$

Obviously improvement in resolution can be achieved by alterations in both the thermodynamic and kinetic parameters. In practice, resolution of mixtures containing a few solutes can be improved by altering k' ie. by adjusting the mobile phase strength and in some cases the type of stationary phase used, or by altering the selectivity, α, by altering the mobile phase composition. Changing the separation temperature can also alter the resolution. Peak tailing is often, though not always,

due to thermodynamic effects and usually increases with retention. Any attempt, therefore, to reduce this tailing in the case of either a single solute with different eluents or of similar solutes in the same eluent, must be attempted by reducing k'. However, the improvement of resolution via thermodynamic considerations, ie. the adjustment of retention, is limited as in the case of the analysis of a complex mixture. In this case, in order to improve resolution the kinetic efficiency of the column has to be improved ie. N has to be increased. It is therefore better all round to start with a highly efficient column. Thus, much effort has been expended on the understanding and improvement of the kinetics of chromatography although the more recent work has perhaps been concentrating more on the thermodynamic aspects of resolution improvement (ie. ion-pair chromatography, soap chromatography etc).

Since the early days of chromatography, the theory dealing with these kinetic processes has advanced greatly and much of the credit is due to Giddings.[1] Although this theory was developed for gas chromatography, it is easily applied to liquid chromatography.[2,3]

We shall consider the development of kinetic theory but restricting attention to those theories which have made the most significant contribution to our understanding of the overall kinetic processes.

However, before we go on to discuss these theories, we shall consider some more basic parameters.

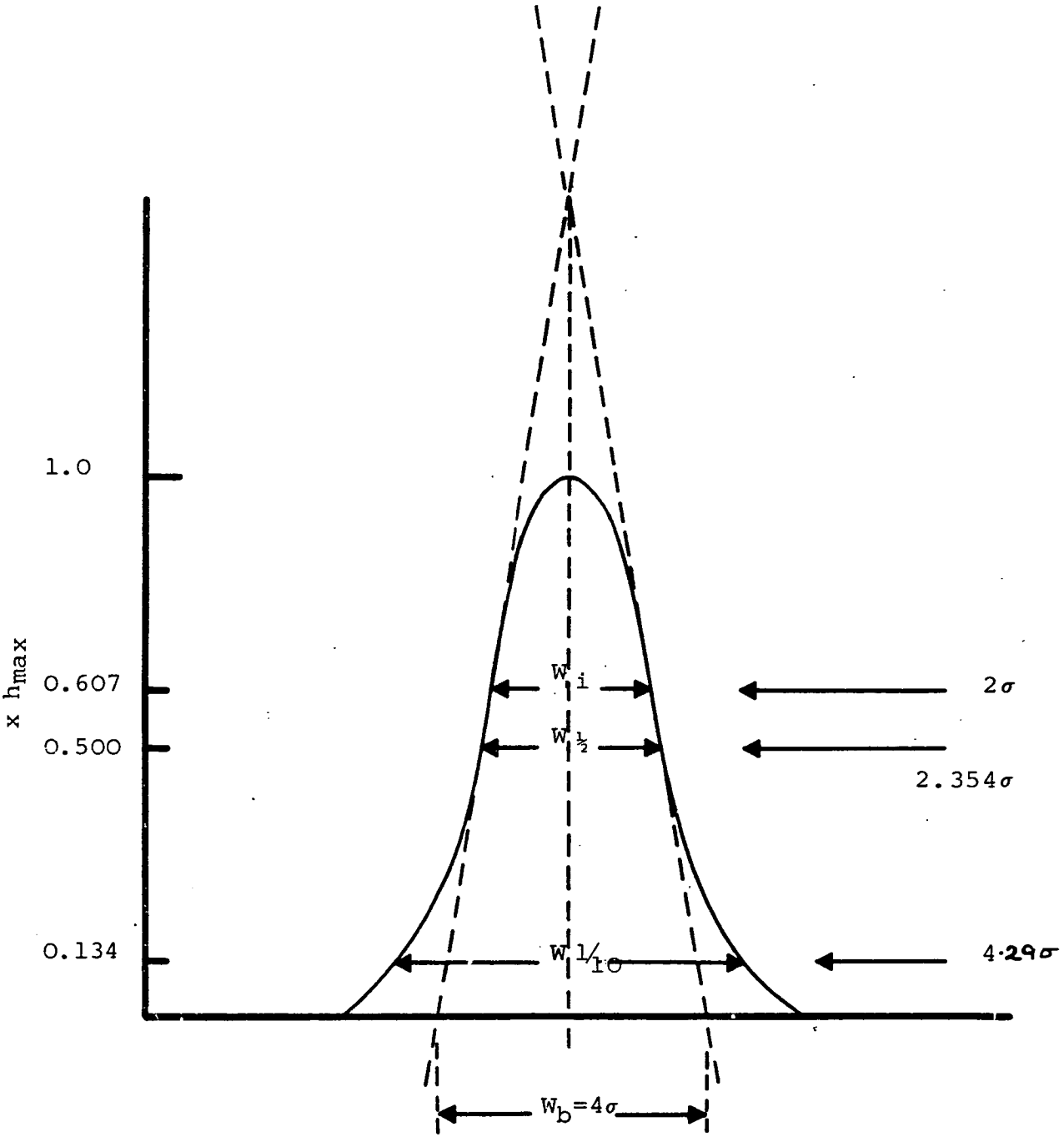

Figure 4.1 Relationship between σ and H for a Gaussian shaped peak.

4.2 The Number of Theoretical Plates and the Plate Height

The plate height theory was introduced by Martin and Synge[4] in 1941 in an attempt to explain peak dispersion in chromatography. Although this theory has been superceded over the years by other theories, the concept of the theoretical plate has remained in use throughout since it is a convenient parameter to use when quantitatively dealing with zone dispersion.

The ideas used in the plate height theory and definitions of the terms used will be given in detail in Section 4.3.

The theoretical plate is thought of as a "slice" of any column which broadly describes an equilibrium region. The height equivalent to a theoretical plate is denoted by HETP, or more usually as H, and is the thickness of such a "slice." The HETP of a column is a measure of its efficiency.

The number of theoretical plates, N, is the total number of plates which make up the column bed, and is defined as:

$$N = \frac{L}{H} \qquad (4\text{-}1)$$

where L is the length of the column bed.

In general, well behaved chromatographic peaks are Gaussian in shape and obey the equation:

$$y = y_o \exp\left[-\Delta x^2/2\sigma^2\right] \qquad (4\text{-}2)$$

where x is the distance (or any convenient width) from the peak centre, σ is called the standard deviation and σ^2 is the variance of the distribution. Figure 4-1 shows the relationship between the standard deviation σ and the height

equivalent to a theoretical plate, H.

The plate height theory, and all subsequent theories, predict that the width of a solute band increases with the square root of the distance, Z, migrated: that is

$$\sigma_Z^2 \propto Z \qquad (4\text{-}3)$$

The plate height, H, can be shown to be equal to the rate of increase of the variance of the Gaussian profile with the distance migrated, ie.

$$H = \frac{d\sigma_Z^2}{dZ} \qquad (4\text{-}4)$$

If we consider this for a uniform column of length L, we can assume that the plate height is constant and we can therefore write

$$H = \frac{\sigma_L^2}{L} \qquad (4\text{-}5)$$

The number of theoretical plates, N, will then be given by

$$N = \frac{L}{H} = \frac{L^2}{\sigma_L^2} \qquad (4\text{-}6)$$

It has been shown that the capacity factor, k', of a solute can be expressed as

$$k' = \frac{V_R - V_m}{V_m} \qquad (4\text{-}7)$$

If we rewrite this in terms of the elution volume, V_R, this gives:

$$V_R = V_m\ (1+k') \qquad (4\text{-}8)$$

Now, V_m corresponds to the volume of eluent in the packed column and can be shown as

$$V_m = L.A \qquad (4-9)$$

where A is the cross-sectional area of the mobile phase in the column.

Substituting equation 4-9 into equation 4-8 gives

$$V_R = L.A \quad (1+k') \qquad (4-10)$$

and rearranging this gives us

$$L = \frac{V_R}{A(1+k')} \qquad (4-11)$$

We can also express this in the form of the variance σ_L^2 ie.

$$\sigma_L^2 = \left[\frac{\sigma_V}{A(1+k')}\right]^2 \qquad (4-12)$$

or $$\sigma_V = \left[\sigma_L.A.(1+k')\right]^2 \qquad (4-13)$$

We have seen that $N = \frac{L}{H} = \frac{L^2}{\sigma_L^2}$ (4-6)

and by substituting equation (4-11) into the above equation (4-6) we can write

$$N = \left[\frac{V_R}{A(1+k')}\right]^2 \frac{1}{\sigma_L^2} \qquad (4-14)$$

But $$\sigma_L^2 = \left[\frac{\sigma_V}{A(1+k')}\right]^2 \qquad (4\text{-}12)$$

therefore $$N = \left[\frac{V_R}{A(1+k')}\right]^2 x \left[\frac{A(1+k')}{\sigma_V}\right]^2$$

therefore $$N = \frac{V_R^2}{\sigma_V^2} \qquad (4\text{-}15)$$

In practice however the concentration profile of the emerging solute is recorded as a function of time. However, as the elution volume is proportional to the elution time, we can re-write the above equation in terms of time ie.

$$N = \frac{t_R^2}{\sigma_t^2} \qquad (4\text{-}16)$$

The width at the base of the peak is measured by drawing tangents to the points of inflection and is taken as the distance between where these lines cross the baseline (see figure 4-1). For a symmetrical (Gaussian) peak, this distance, W_t, is equal to

$$W_t = 4\sigma \qquad (4\text{-}17)$$

By substituting equation (4-17) into equation (4-16) we have

$$N = 16\left(\frac{t_R}{W_t}\right)^2 \qquad (4\text{-}18)$$

Alternatively, the width of the peak at half the peak height ($W_{\frac{1}{2}}$) can be measured. In this case as we can see from figure 4-1 that

$$W_{\frac{1}{2}} = 2.354\sigma \qquad (4\text{-}19)$$

which when substituted into equation 3-16 gives

$$N = 5.54 \left(\frac{t_R}{W_{\frac{1}{2}}} \right)^2 \qquad (4\text{-}20)$$

4.3 Reduced Parameters

Reduced parameters, which are dimensionless, were introduced by Giddings[1,5] as a way of expressing various important chromatographic parameters by relating them to the particle diameters, dp, rather than to the column bed as a whole. The use of reduced parameters has been further expanded upon by Knox.[6,7]

Reduced parameters enable results obtained by different laboratories using different columns, different sizes and types of packing materials and different eluents to be compared on a self consistent basis.

The most commonly used parameters are defined below, but a more complete list of reduced parameters can be found in a review by Bristow and Knox.[8]

The reduced plate height, h, is given by

$$h = \frac{H}{dp} \qquad (4\text{-}21)$$

and is equal to the number of particles to the thickness of a plate.

Since $N = \frac{L}{H}$

and $$N = 5.54 \left(\frac{t_R}{W_{\frac{1}{2}}}\right)^2 \qquad (4\text{-}20)$$

then $$h = \frac{L}{N} \cdot \frac{1}{dp}$$

or $$h = \frac{1}{5.54}\left(\frac{W_{\frac{1}{2}}}{t_R}\right)^2 x \ \frac{L}{dp} \qquad (4.21)$$

The reduced velocity, ν, is given by

$$\nu = \frac{U.dp}{D_m} = \frac{L}{t_m} x \frac{dp}{D_m} \qquad (4\text{-}22)$$

where U is the mean linear velocity of the eluent and D_m is the diffusion coefficient for the solute in the mobile phase. ν is therefore a measure of the rate of flow relative to the rate of diffusion over one particle diameter.

The reduced length, ℓ, is given by

$$\ell = \frac{L}{dp} \qquad (4\text{-}23)$$

and is equal to the number of particles which make up the total length of the bed.

The dimensionless column flow resistance parameter, ϕ, is a measure of the resistance to flow of the packed bed and is given by

$$\phi = \frac{dp^2}{K} \qquad (4\text{-}24)$$

where K is the chromatographic permeability of the column and is expressed as:

$$K = \frac{U\eta L}{\Delta p} \qquad (4\text{-}25)$$

where η is the eluent viscosity, Δp is the pressure drop across the column and L is the column length.

It has been established that for a well-packed, efficient column, h should be between 2-10, ν should be in the range 3-20 and ϕ should be between 500-1,000, depending on the type of packing and the packing technique used. For example, glass beads would have $\phi \sim 500$ whereas for porous silica gel ϕ would be $\sim$1,000. Slurry packing reduces ϕ by around a half to two thirds of these values.

4.4 The Development of the Theories of the Kinetics of Chromatography

The first person to put forward a theory to explain the kinetic processes of chromatography was Wilson. His paper published in 1940[3] produced a sound qualitative description which has provided a useful basis for further theoretical development.

In his treatment, Wilson assumed that the adsorption isotherm for a given solute had a linear relationship with its concentration, that there was instantaneous equilibrium of the solutes between the stationary and mobile phases, and that the effects of diffusion could be neglected. He did, however, acknowledge that because of the last two assumptions, this resulted in producing only an approximate description of the chromatographic processes since diffusion, adsorption and desorption proceed at finite rates. It was also because of

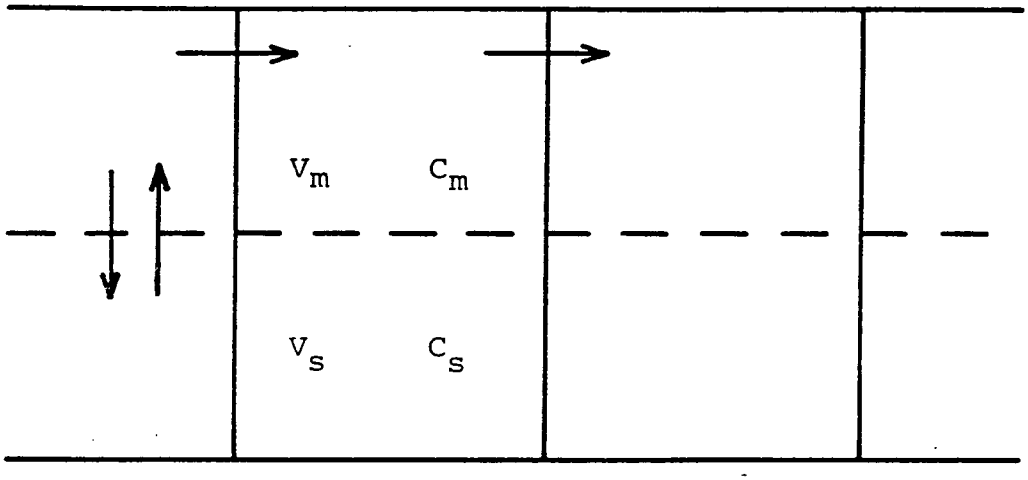

Figure 4.2

A schematic representation of the Plate Model. V_m and V_s are the volumes of the mobile and stationary phases. C_m and C_s are the solute concentrations in the mobile and stationary phases respectively.

these last two assumptions where he made no allowances for diffusion or the lack of equilibrium between the two phases in his theory that his work was largely ignored.

However, his paper did include some important concepts. Wilson stated that excessive band spreading would occur at either very high or very low flow rates, thus indicating the existence of an optimum flow rate to be found between the two extremes. He also reported that "the width of a band may increase because of diffusion, or because the leading edge of the band migrates too rapidly on account of a low rate of adsorption, or because the trailing edge of the band migrates too slowly on account of a low rate of desorption." This description given by Wilson was a forerunner of the non-equilibrium concepts which were later developed by Giddings.[1]

4.4.1 The Theoretical Plate Model

In 1941, Martin and Synge[4] proposed a model to explain the phenomenon of band broadening based on concepts used for distillation. In this model,which is illustrated in figure 4-2, the column was considered to be made up of a number of discrete layers, or "theoretical plates," by analogy with fractional distillation, and "the height equivalent to a theoretical plate" (HETP or H) was defined as being "the thickness of the layer such that the solution issuing from it is in equilibrium with the mean concentration of solute in the non-mobile phase throughout the layer." In order to simplify the model, several assumptions were made:[5]

a) "The chromatographic column is visualized as being divided

into volume elements, or plates.

b) At each plate, the partitioning of the solute between the mobile and stationary phases is assumed to be fast so that it reaches equilibrium before moving onto the next plate or volume element.

c) The partitioning coefficient of the solute is the same in all plates, or throughout the column and is concentration independent.

d) Diffusion of the solute in the axial direction can be neglected, or confined to where the solute is.

e) The flow of the mobile phase is regarded as being discontinuous."

While the assumption (c), ie. that the distribution isotherm is linear, is true for very dilute solutions, the partition coefficient is seldom independent of the concentration at significant concentrations. The effect of non-linear distribution isotherms has already been mentioned in Section 3.2.

The theory proposed by Martin and Synge was the first to describe the development of a zone profile as the band moved through the column bed under the influence of non-equilibrium and under linear isotherm conditions. After a sufficiently long development time ie. when the number of plates becomes very large, the zone profile becomes Gaussian in shape. When averaged over each plate the solute is considered to be in equilibrium between the two phases and therefore "band dispersion results from the flow of eluent to the next plate and the subsequent re-equilibration of the solute."

While the plate theory itself does not provide any conclusions about the factors affecting the "height equivalent to a

theoretical plate", HETP, Martin and Synge stated that "HETP depends upon the factors controlling diffusion and upon the rate of flow of liquid. There is an optimum rate of flow ... since diffusion from plate to plate becomes relatively more important the slower the flow of liquid and tends .... to increase HETP." Also "the HETP is proportional to the rate of flow of liquid and to the square of the particle diameter. Thus the smallest HETP should be obtainable by using very small particles and a high pressure difference across the length of the column."

Many of the conclusions arrived at by Martin and Synge in this paper were far seeing indeed and were not expressed on a firm theoretical foundation until many years later. The main drawback to this model is that it fails to describe the actual kinetic processes involved. The idea of the theoretical plate as defined by Martin and Synge implies a degree of non-equilibrium ie. the concentration issuing from the plate is in equilibrium with the mean concentration throughout the plate, but the concentration is not uniform throughout the plate. They did not, however , link the rate of equilibration with the plate height which Giddings later did.

4.4.2 The van Deemter Equation

The equation derived by van Deemter *et al.*[9] for gas chromatography was the first of its kind which related the height equivalent to a theoretical plate (HETP) to the fluid velocity. The zone dispersion was shown to be influenced by three separate mechanisms which were assumed to contribute

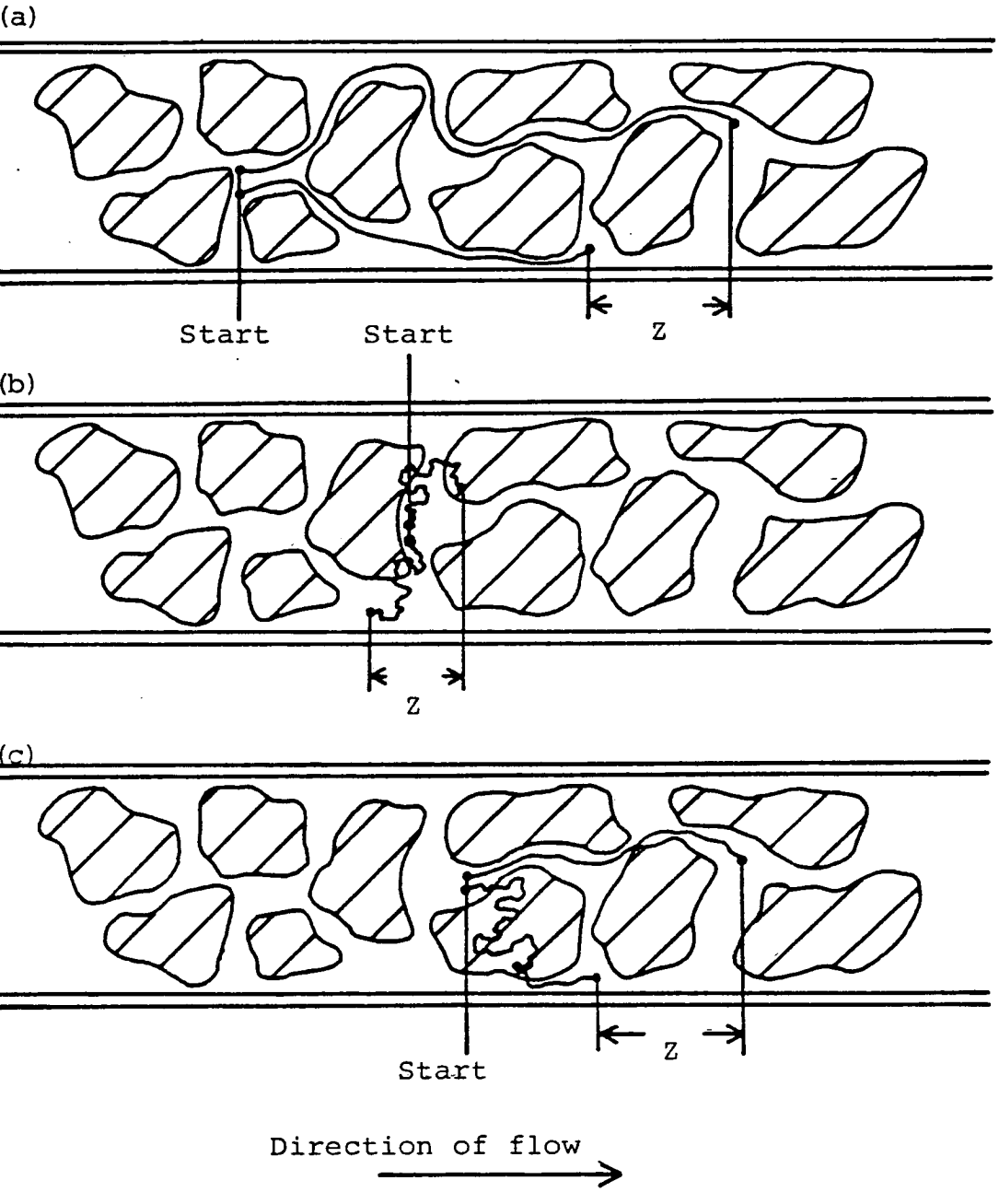

Figure 4.3 Major dispersive mechanisms in chromatography. The diagrams show two molecules initially adjacent and the distance, Z separating them after operation of the dispersion processes.

(a) Dispersion due to tortuous flow in the mobile phase.

(b) Dispersion due to axial diffusion (figure illustrates case where there is no flow).

(c) Dispersion due to slow equilibration between mobile and stationary phases.

independently to the HETP as additive terms. These are:

a) eddy diffusion, or flow anisotropy,

b) longitudinal or axial molecular diffusion,

and c) solute mass transfer,

and these are illustrated schematically in figure 4-3.

a) Eddy Diffusion or Flow Anisotropy

Due to the different tortuous flow paths through the column bed which are available to the individual solute molecules, the total distance travelled by each molecule will vary depending on the route taken through the bed. Also, the velocity of a molecule will vary depending on whether it is in the mainstream of the flow path or in an eddy. Both of those factors result in zone spreading.

The contribution to the overall plate height by eddy diffusion is given by

$$H_{flow} = 2 \lambda dp \qquad (4\text{-}26)$$

where λ is the packing characterisation factor.

b) Longitudinal or Axial Molecular Diffusion

The dispersion of the solute in the mobile phase occurs in the direction of the flow and the contribution which this makes to the overall value of H is given as

$$H_{axial} = \frac{2 D_m \gamma_m}{U} \qquad (4\text{-}27)$$

where D_m is the solute diffusion coefficient in the mobile phase, γ_m is the obstruction factor for diffusion of the mobile

phase through the bed and termed the tortuosity factor, and U is the fluid velocity.

c) Solute Mass Transfer

During the chromatographic process, sorption and desorption occur at unpredictable intervals. When sorbed into the stationary phase, the molecules lag behind the zone centre and when they are desorbed into the mobile phase they move faster than the zone centre. This stop-start process results in band dispersion.

The contribution made by solute mass transfer, for a spherical shell, is given by

$$H_{mass} = \underbrace{\frac{8}{\pi^2}}_{\text{for a spherical shell}} \cdot \frac{k'}{(1+k')^2} \cdot \frac{d_s}{D_s} \cdot U \qquad (4\text{-}28)$$

where d_s is the thickness of the film of stationary phase and D_s is the diffusion coefficient of the solute in the stationary phase.

The Overall Plate Height Equation

The overall plate height, H_{tot}, is expressed as the sum of all of the individual contributions to the dispersion of a band and is given by

$$H_{tot} = H_{flow} + H_{axial} + H_{mass}$$

$$\therefore H_{tot} = [2\lambda d_p] + \left[\frac{2D_m\gamma_m}{U}\right] + \left[\frac{8}{\pi^2} \cdot \frac{k'}{(1+k')^2} \cdot \frac{d_s}{D_s} \cdot U\right] \qquad (4\text{-}29)$$

This equation has been expressed in a more simple form by Keulemans and Kuwantes[10] as:

$$H = A + \frac{B}{U} + C.U. \qquad (4\text{-}30)$$

As a result of the van Deemter equation, the fluid velocity required to produce the minimum plate height can be calculated by differentiating the above equation.

Thus: $$H_{min} = A + 2(B.C.)^{\frac{1}{2}} \qquad (4\text{-}31)$$

which requires that $$U_{min} = \left(\frac{B}{C}\right)^{\frac{1}{2}} \qquad (4\text{-}32)$$

4.4.3 The Random Walk Model

In their paper published in 1955, Giddings and Eyring[11] introduced probability (statistical) concepts to describe the processes of molecular migration in chromatography, which in effect proved to be the forerunner of Giddings' Random Walk Theory.[12,13]

The Random Walk Model considers the movement of individual solute molecules through the column to consist of a series of random and extremely erratic steps. However, although the movements of these individual molecules are random and unpredictable, the consideration of the statistics of a large number of molecules results in the overall process being predictable. In this case the concentration profile will become Gaussian in shape centred around the middle of the moving zone. The base width of the Gaussian profile is equal

to 4σ (see figure 4.1) ie.

$$W = 4\sigma \qquad (4\text{-}33)$$

σ is the standard deviation given by

$$\sigma = \ell\sqrt{n} \qquad (4\text{-}34)$$

where ℓ is the fixed step length and n the number of steps taken. From this basic equation we see that σ is directly proportional to the step length, ℓ, but only increases with the square root of the number of steps, $n^{\frac{1}{2}}$. This is a consequence of the fact that the steps may be forwards or backwards.

It is more usual to use the term "variance" where:

$$\text{Variance} = \sigma^2 = \ell^2 n \qquad (4\text{-}35)$$

where n is the number of random steps taken by a solute molecule and ℓ is the length of such a step.

For a number of independent random processes each of which make a contribution, H_i, to the zone dispersion, then the total zone dispersion is given by:

$$H_{tot} = \Sigma H_i \qquad (4\text{-}36)$$

$$\text{where} \quad H_i = \frac{\sigma_i^2}{L} \qquad (4\text{-}37)$$

Giddings has used his Random Walk Model to produce equations representing the contributions made to the plate height by the different processes affecting zone dispersion.

Longitudinal Molecular Diffusion

The contribution to band spreading due to longitudinal,

or axial molecular diffusion in the mobile phase is given as being:

$$H_{axial} = \frac{2\,\gamma_m D_m}{U} \qquad (4\text{-}38)$$

where D_m is the diffusion coefficient of the solute in the mobile fluid, U is the average mobile phase velocity and where γ_m is an obstructive factor of slightly less than unity due to the molecules having to move round the particles of support material which has an affect of reducing the actual distance diffused.

The ratio of the time spent in the stationary phase to the time spent in the mobile phase is given by

$$\frac{t_s}{t_m} = k' \qquad (4\text{-}39)$$

We can also write a similar expression for axial molecular diffusion in the stationary phase, ie.

$$H_{axial} = \frac{2\gamma_s D_s k'}{U} \qquad (4\text{-}40)$$

where D_s is the diffusion coefficient of the solute in the stationary phase, γ_s is also an obstructive factor which again causes a reduction in the actual distance diffused since "diffusion in the stationary phase cannot take place in a direct unobstructed path."

The total contribution to the overall band dispersion by longitudinal or axial molecular diffusion is therefore:

$$H_{axial} = \frac{2(\gamma_m D_m + \gamma_s D_s k')}{U} \qquad (4\text{-}41)$$

ie. $$H_{axial} = \frac{B}{U} \qquad (4\text{-}42)$$

Diffusion Due to Mass Transfer (Adsorption-Desorption Kinetics)

The process of sorption-desorption is influenced by two different mechanisms or by some combination of both. These are (1) the molecular sorption-desorption processes onto or from the stationary phase surface which will occur only if there is at least a certain energy (activation energy) and (2) adsorption-desorption kinetics caused by molecules diffusing into and out of localized regions (diffusion controlled kinetics).

The Random Walk Model treats the complex sorption-desorption kinetics in a simple way in that the sorption-desorption process follows the laws of first order kinetics with the rate of sorption-desorption being proportional to the number of molecules available to react. Within the chromatographic column, let the fraction of molecules in the mobile phase be R and the fraction of molecules in the stationary phase be (1-R).

ie. R = fraction of molecules in mobile phase

(1-R) = fraction of molecules in stationary phase.

When a molecule is adsorbed, it ceases to migrate down the column since its velocity is now zero, while the rest of the zone continues to migrate down the column. When it is desorbed, it moves back into the mainstream of the mobile phase and its velocity becomes greater than that of the zone centre. The overall effect is that the zone broadens and moves as a whole

at a fraction of the mobile phase velocity. The velocity of the centre of the solute zone is proportional to the fraction of the solute molecules, R, in the mobile phase and is given by

$$\text{Velocity of zone centre} = R.U. \qquad (4\text{-}43)$$

where U is the mobile phase velocity.

The fraction of solute molecules in the mobile phase can also be expressed as:

$$R = \frac{1}{(1+k')} \qquad (4\text{-}44)$$

where k' is the phase capacity ratio.

In the random walk model, the length of a step, ℓ, is taken as the difference between the distance moved by a solute molecule and the distance moved by the zone during one step and is given by:

$$\ell = t_a U - R t_a U \qquad (4\text{-}45)$$

where t_a is the time spent in the mobile phase during one step.

The number of steps, n, will be equal to the column length, L, divided by the length of each step, ℓ, multiplied by 2 since both the adsorption and desorption steps must be taken into consideration.

$$\text{ie.} \quad n = 2 \times \frac{L}{\ell} \qquad (4\text{-}46)$$

By considering equations (4-35), (4-37) and (4-45) we can write

$$H = \frac{(t_a U - RUt_a)^2 \times 2L}{(t_a U - RUt_a) \times L}$$

$$\therefore \quad H = 2\, t_a . U\,(1-R) \tag{4-47}$$

The fraction of molecules in the mobile phase, R, can also be expressed as:

$$R = \frac{t_a}{1-t_a} = \frac{t_a}{t_d} \tag{4-48}$$

where t_a is the time spent in the mobile phase and t_d is the time spent in the stationary phase. By combining equations (4-47), (4-48) and (4-44) we can write:

$$H = 2\, t_d U R(1-R)$$

$$\text{ie. } H = \frac{2\, t_d U k'}{(1+k')^2} \tag{4-49}$$

If we assume that the stationary phase is uniformly distributed throughout a spherical particle, then the time of desorption, t_d, is proportional to $\frac{dp^2}{D_s}$ ie.

$$t_d \propto \frac{dp^2}{D_s} \tag{4-50}$$

then we can treat this diffusion controlled kinetics in the same way as adsorption-desorption kinetics when considering the random walk model. In this case we have

$$H = \frac{2 U dp^2 k'}{D_s (1+k')^2}$$

$$\text{or} \quad H = \frac{q . U dp^2 k'}{D_s (1+k')^2} \tag{4-51}$$

where D_s is the diffusion coefficient of the solute in the stationary phase and q is a configuration factor which takes into account the precise shape of the stationary phase pools and which for a uniform sphere is equal to $\frac{1}{30}$.

Eddy Diffusion and the Coupling Theory of Eddy Diffusion

With classical eddy diffusion, the only contribution to band spreading arises from the variations in the velocity of the individual molecules caused by the fluctuations in the fluid velocity as it passes through the bed. Where the passages between the particles are very narrow the fluid velocity will be small whereas large unrestricted passages will result in a large fluid velocity.

However, when considering the contribution made to zone dispersion by the inequalities of the flow velocity of the mobile phase, one must also take into account the fact that the time spent by a molecule in a region of a given flow path may be reduced either by eddy diffusion or by molecular diffusion across a channel where it may diffuse quite quickly into regions of the mobile phase where there is an entirely different downstream velocity. This would result in there being more displacement steps, n, of a shorter length, ℓ.

The effect on the plate height, H, of the coupling of the flow and the diffusion contributions is that H is reduced since it is proportional to ℓ^2 while only being proportional to n ie:

$$H \propto \ell^2 n \qquad (4\text{-}52)$$

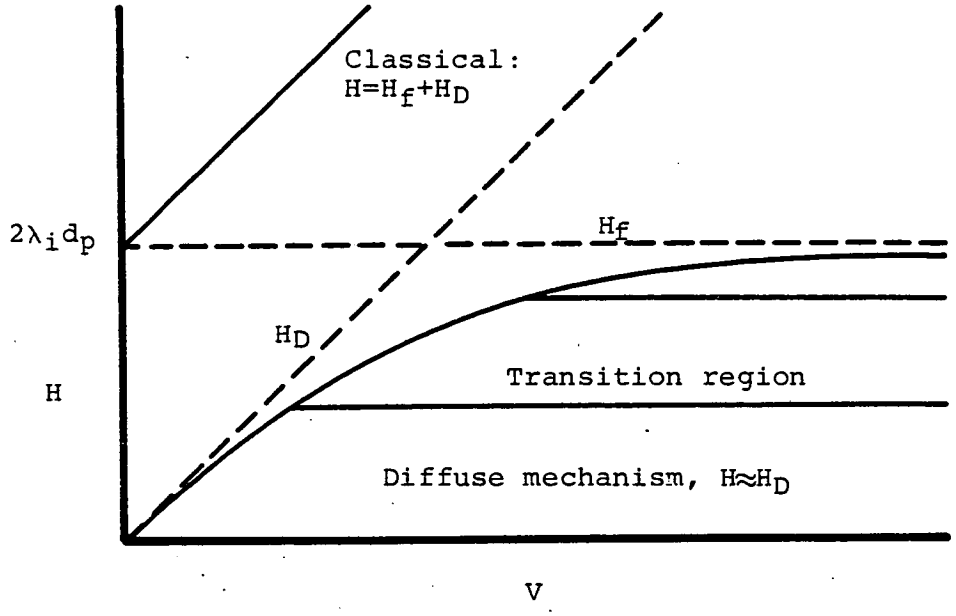

Figure 4.4

Contrast between coupling and classical expressions for plate height as a function of velocity. The coupling H is always less than H_f and H_D, while the classical H is always greater than either of these. Similar curves would be found if the sum of all velocity-inequality effects were considered, with the exception that the transition region would be considerably extended.
(Reproduced from reference 1)

The contribution to the overall plate height given by the coupling of eddy diffusion and molecular diffusion is

$$H = \frac{1}{1/H_f + 1/H_d} \qquad (4\text{-}53)$$

where H_f is the contribution due to the flow mechanism alone and H_d is the contribution due to the transverse diffusive mechanism alone.

We can therefore write:

$$H = \sum_i \frac{1}{1/(2\lambda_i dp) + D_m/(W_i U dp^2)} \qquad (4\text{-}54)$$

The above equation differs greatly with the corresponding classical form of the equation where

$$H = H_f + H_d \qquad (4\text{-}55)$$

Figure 4-4 clearly shows that the value of H obtained from the coupling theory is less than H_f or H_d and that it approaches the smaller of the two terms below ie. H approaches H_d at low velocities and approaches H_f at high velocities.

By considering equations (4-41), (4-51) and (4-54) obtained using Giddings Random Walk model, the van Deemter equation can be re-written as

$$H = \underbrace{\frac{2(\gamma_m D_m + \gamma_s D_s k')}{U}}_{(a)} + \underbrace{\sum_i \frac{1}{1/2\lambda_i dp + D_m/W_i U dp^2}}_{(b)} + \underbrace{\frac{qUdp^2 k'}{(1+k')^2 D_s}}_{(c)} \qquad (4\text{-}56)$$

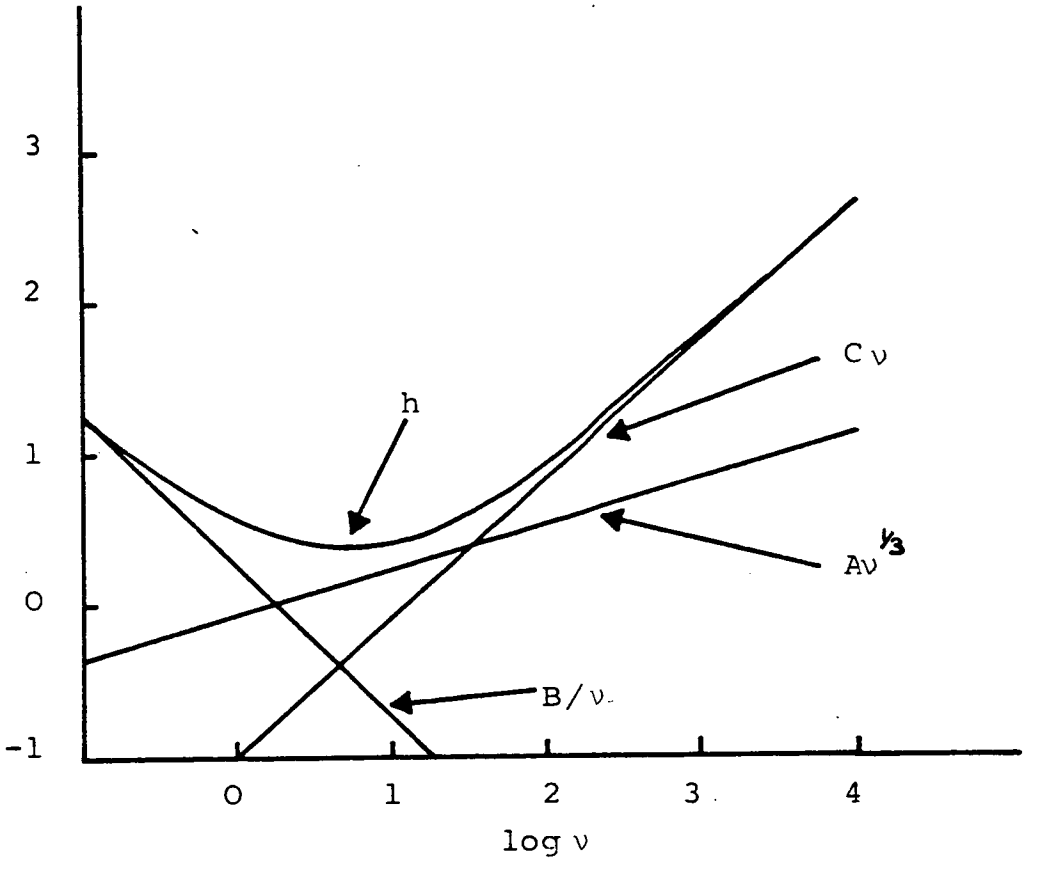

Figure 4.5

Logarithmic plot of reduced plate height h against reduced velocity, ν, according to the equation $h=A\nu^{1}/_{3}+B/\nu+C\nu$ showing the velocity dependence and contributions of the individual terms (A=1, B=2, C=0.1).

where (a) represents longitudinal molecular diffusion,

(b) represents the coupling of molecular diffusion and eddy diffusion,

and (c) represents the mass transfer in the stationary phase.

Experiments[14] have shown that neither equation (4-54) or equation (4-56) accurately reflects the velocity dependence of the coupling of molecular diffusion and eddy diffusion. However this can be shown by experiment[14] to be fitted reasonably well by (constant x $U^{1/3}$).

The general equation (4-56) can be simplified by using reduced parameters and introducing constants to give:

$$h = \frac{B}{\nu} + A\nu^{1/3} + C.\nu \qquad (4\text{-}57)$$

The A-term is a measure of the "goodness of packing" of a column and is around 1 for a well packed column. The B-term is a constant related to the diffusivity of the solute. The C-term is determined by the efficiency of mass transfer between the flowing and static regions of the column.

These constants are dimensionless, and for a good column have the approximate values

$$A < 1, \quad B \sim 2, \quad C < 0.1$$

A typical h,ν plot is shown in figure 4-5.

At high velocities, the dispersion caused by axial or longitudinal dispersion, $\frac{B}{\nu}$, is low while the dispersion caused by mass transfer, $C\nu$, and the coupling of molecular and eddy diffusion, $A\nu$, are high. At low velocities dispersion caused

by $C\nu$ and $A\nu^{\frac{1}{3}}$ are low while the dispersion due to axial diffusion $\frac{B}{\nu}$ is high.

4.4.4. The Non-equilibrium Theory

The Non-Equilibrium Model which was developed by Giddings[1] is based, not on single molecular considerations as in the case of the Random Walk Model, but on consideration of the movement of a concentration pulse through the column as a whole.

Although the concept of non-equilibrium is easy to understand, the mathematics are more complicated and will not be dealt with here. This theory does however provide rigorous expressions for contributions to H from mass transfer effects, that is those giving rise to the C-term, as well as providing the mathematical justification for the configurational factor of $q = \frac{1}{30}$ in the C-term for spherical particles mentioned earlier.

As the chromatographic zone moves through the column, the concentration of the solute in both the mobile and stationary phases increases until it reaches a maximum and then decreases. A finite amount of time is required for the sorption-desorption processes to bring the stationary phase concentration into equilibrium with the mobile phase concentration. However, as the zone is continuously moving, equilibrium is never quite reached and the concentration of solute in the stationary phase therefore lags behind that in the mobile phase.

At the front of the zone, the concentration of solute in the mobile phase will be the greater, while on the trailing edge of the zone the concentration in the stationary phase will be the greater.

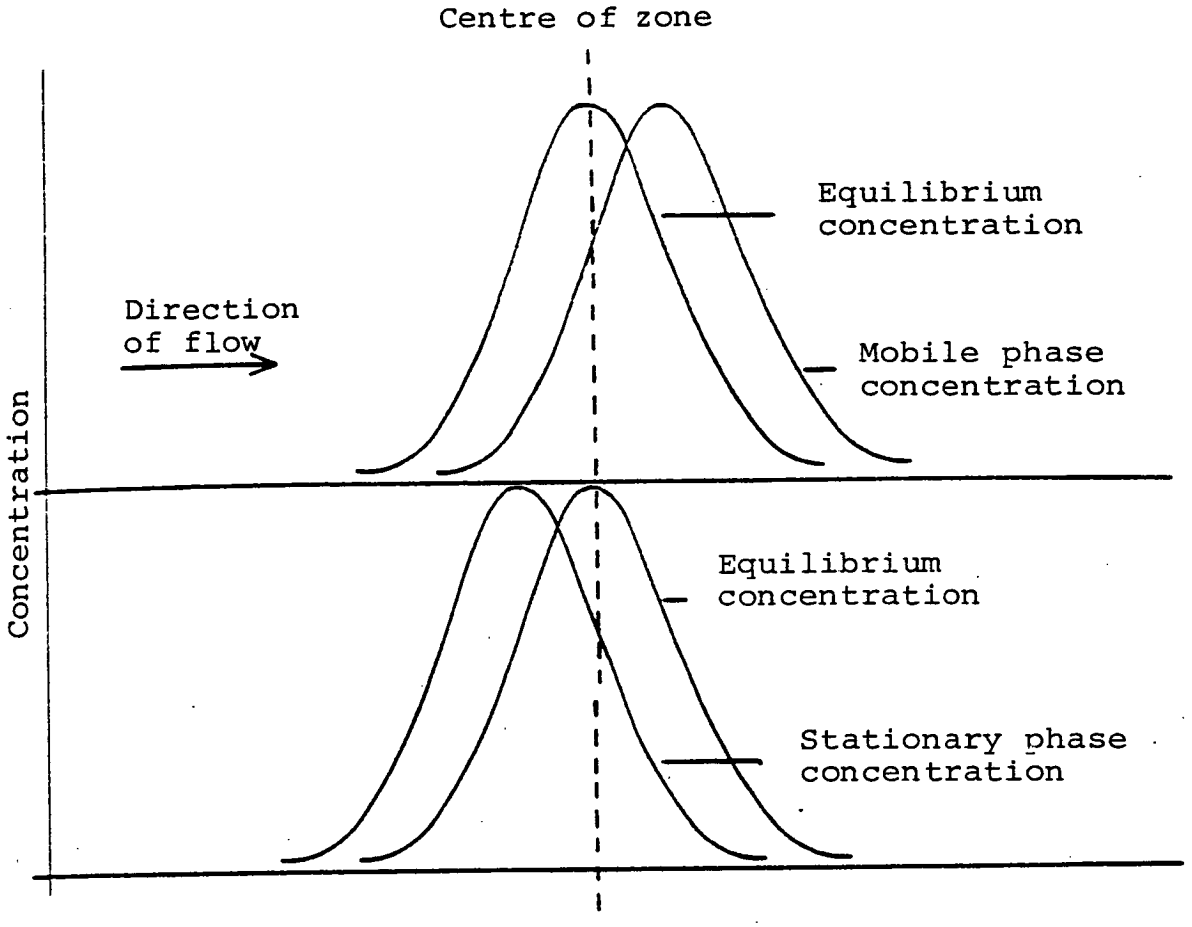

Figure 4.6 Schematic diagram of the non-equilibrium theory showing that the actual concentration profile for the stationary phase lags behind that which would exist at equilibrium (ie. with an infinite exchange rate between phases). The diagram also shows that the actual mobile phase concentration is displaced ahead of the equilibrium value.

True equilibrium between the stationary and mobile phases only occurs at the maximum of the zone profile. The above model is clearly illustrated in figure 4-6. The distance separating the two concentration curves, ie. the "real" and the equilibrium curves, for either phase is a measure of the degree of non-equilibrium which is in turn an important factor in determining the amount of band spreading. The smaller this distance is, the more efficient the system will be. This is achieved when the zone moves slowly through the column so preventing rapid concentration changes, or when the rate of the sorption-desorption processes is high.

It has been mentioned in Chapter 3, that the speed of migration is directly proportional to the fraction of molecules in the mobile phase. Consequently, the front of the zone must move faster than the zone centre since the actual fraction of molecules in the mobile phase is greater than the fraction in the mobile phase at equilibrium. The converse is true for the rear of the zone which will therefore move more slowly than the zone centre. Thus as the zone moves down the column it continually broadens.

REFERENCES

Chapter 4

1. J.C. Giddings, "Dynamics of Chromatography" Part I, Marcel Dekker, New York, 1965.
2. J.C. Giddings; Anal.Chem., 35 (1963), 2215.
3. J.N. Wilson; J.Am.Chem.Soc., 62 (1940), 1583.
4. A.J.P. Martin and R.L.N. Synge; Biochem.J., 34 (1941) 1358.
5. J.C. Giddings; J.Chromatogr., 13 (1964), 301.
6. J.H. Knox; Ann.Rev.Phys.Chem., 24 (1973), 29.
7. J.H. Knox and M. Saleem; J.Chromatog.Sci., 7 (1969), 614.
8. J.H. Knox and P. Bristow; Chromatographia, 10 (1977), 6.
9. J.J. van Deemter, F.J. Zuiderweg, and A. Klinkenberg; Chem.Eng.Sci., 5 (1956), 271.
10. A. Keulemans and A. Kuwantes, "Vapour Phase Chromatogr.," Desty Ed., Butterworths, London, p.15 (1956).

or A. Keulemans in Gas Chromatography 1961, Reinhold, New York.

11. J.C. Giddings and H. Eyring; J.PHys.Chem., 59 (1955), 416.
12. J.C. Giddings; J.Chem.Ed., 35 (1958), 588.
13. J.C. Giddings in "Chromatography" E. Heftmann (Ed.), Reinhold, New York.
14. G.J. Kennedy and J.H. Knox; J.Chromatog.Sci., 10 (1972), 549.

CHAPTER 5

PREPARATIVE HIGH PRESSURE LIQUID CHROMATOGRAPHY

Chapter 5. Preparative High Pressure Liquid Chromatography

PREPARATIVE HIGH PRESSURE LIQUID CHROMATOGRAPHY

5.1 Introduction

The most general definition of the term "preparative high pressure liquid chromatography" is one which covers all cases where the separated components of a mixture are collected for further use in some subsequent procedure. However, most workers regard preparative HPLC as referring specifically to those separations involving relatively large columns operating under overload or near-overload conditions, that is conditions where the solute concentration in the bands is high enough such that the concentration no longer lies in the linear part of the distribution isotherm. This corresponds roughly to a sample load of 1 mg sample/g of packing material, whereas most analytical separations are carried out with loads of below 0.1 mg/g packing material and often down to the nanogram/g level. Under such conditions of overload, both column efficiency[1] and the phase capacity ratio, k', are lower than when the column is operating under analytical conditions.

Using the general definition, preparative HPLC can, in principle, involve the separation of materials ranging from nanogram to kilogram quantities. The separation of kilogram amounts of material falls into the category of industrial-scale chromatography and will not be dealt with in this thesis. Laboratory scale preparative HPLC with which we are concerned with can involve the isolation of a few milligrams of material or of gram quantities of material depending upon what the collected material is to be used for. For example, only a few milligrams (1-100 mg) are required for positive identification

Category	Preparative Column Type	Resolution N	Application	Required amount of pure sample (mg)	Stationary Phase Present (g)	Column ID (mm)	MACS[a] (mg)
1	Analytical	High	Mass Spectrometry	0.001	0.2-3.2	1-5	0.2-3.2
2	Analytical	High	Infra-red Spectroscopy	0.1	0.2-3.2	1-5	0.2-3.2
3	Wide-bore Analytical	Moderate	N.M.R.[b]	0.1-10	3-12	6-11	3-12
4	Wide-bore Analytical	Moderate	Elemental Analysis	1-25	7-25	6-11	7-25
5	Long,narrow	Moderate	Synthesis	10^2-10^3	25-100	10-30	20-10^3
6	Short,thick	Low	Large Scale	10^3-10^5	10^2-10^3	20-100	10^3-10^5
7	Industrial	Low	Commercial	10^4-10^6	10^3-10^5	10^2-10^3	10^4-10^6

Table 5-1 Maximum allowable compound size (MACS) with respect to stationary phase loading and column dimensions (adapted from Reference 2)

[a] These values of MACS can vary and are controlled by the separation factor, α.

[b] Nuclear Magnetic Resonance.

by instrumental and chemical techniques while larger amounts of material (>100 mg) are required for use as analytical standards or as compounds for further organic synthetic work. Preparative HPLC can also be used for sample clean-up prior to analytical HPLC or GC, to prepare pure samples for biological testing (mg-gram quantities) or in the commercial preparation of rare chemicals or biological compounds.

In order to cover such a wide range of preparative separations a wide variety of equipment is required and this is illustrated in table 5-1. We will be concerned with categories 3, 4 and 5 in this thesis as categories 1 and 2 are not strictly preparative scale separations while categories 6 and 7 require industrial scale equipment.

The normal analytical scale equipment is often adequate for the separation of small quantities of material (eg. 1-100 mg). However, where larger amounts are required, specially designed equipment is necessary and this will be discussed in more depth in the next section.

In the past preparative separations have very often been carried out along similar lines to analytical separations simply by increasing the sample load. This is often accompanied by an increase in column diameter and hence an increase in the amount of stationary phase. Unfortunately, the full preparative potential of the chromatographic columns were often not exploited.

With analytical HPLC, the objective is to obtain a specific resolution in the shortest possible time. Sample capacity is not normally a problem in this case since the amounts injected are small. The aim therefore is to achieve optimisation of

both resolution and speed of separation. However, with preparative HPLC, the aim is to achieve optimisation of the amount of material separated per unit time, ie. the sample throughput, of a given purity under certain conditions as set by the size of equipment, cost of packing material and cost of solvents. Therefore, in preparative HPLC, sample capacity is an equally important factor which has to be taken into consideration along with resolution and the speed of separation. Unfortunately these three factors are mutually incompatible as illustrated in the following diagram.

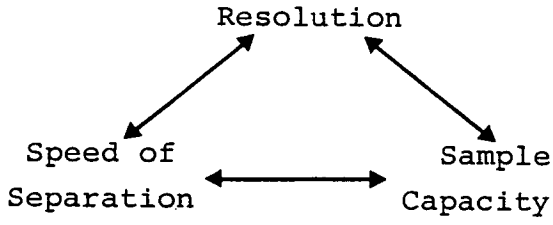

This means that one factor cannot be maximised without sacrificing one or both of the other factors and a compromise has to be reached, the nature of which depends on the particular separation problem. For example, if a high sample capacity is desired, this may be achieved only at the expense of either the resolution, or the separation speed, or both.

There are various factors which can affect the maximum sample throughput obtainable. The original composition of the sample and the nature of the separation ie. whether the compound of interest is a trace component, a single major component or one of two closely eluting components, are important along with the yield and purity that is required. These factors will naturally depend on the specific problem at hand. The

parameters of the phase system used, for example the selectivity factor and distribution isotherm displayed by the individual components in the phase system are also important and will depend on both the original sample and the phase system chosen. More general factors which have to be considered include column dimensions, particle size, injection mode and eluent velocity.

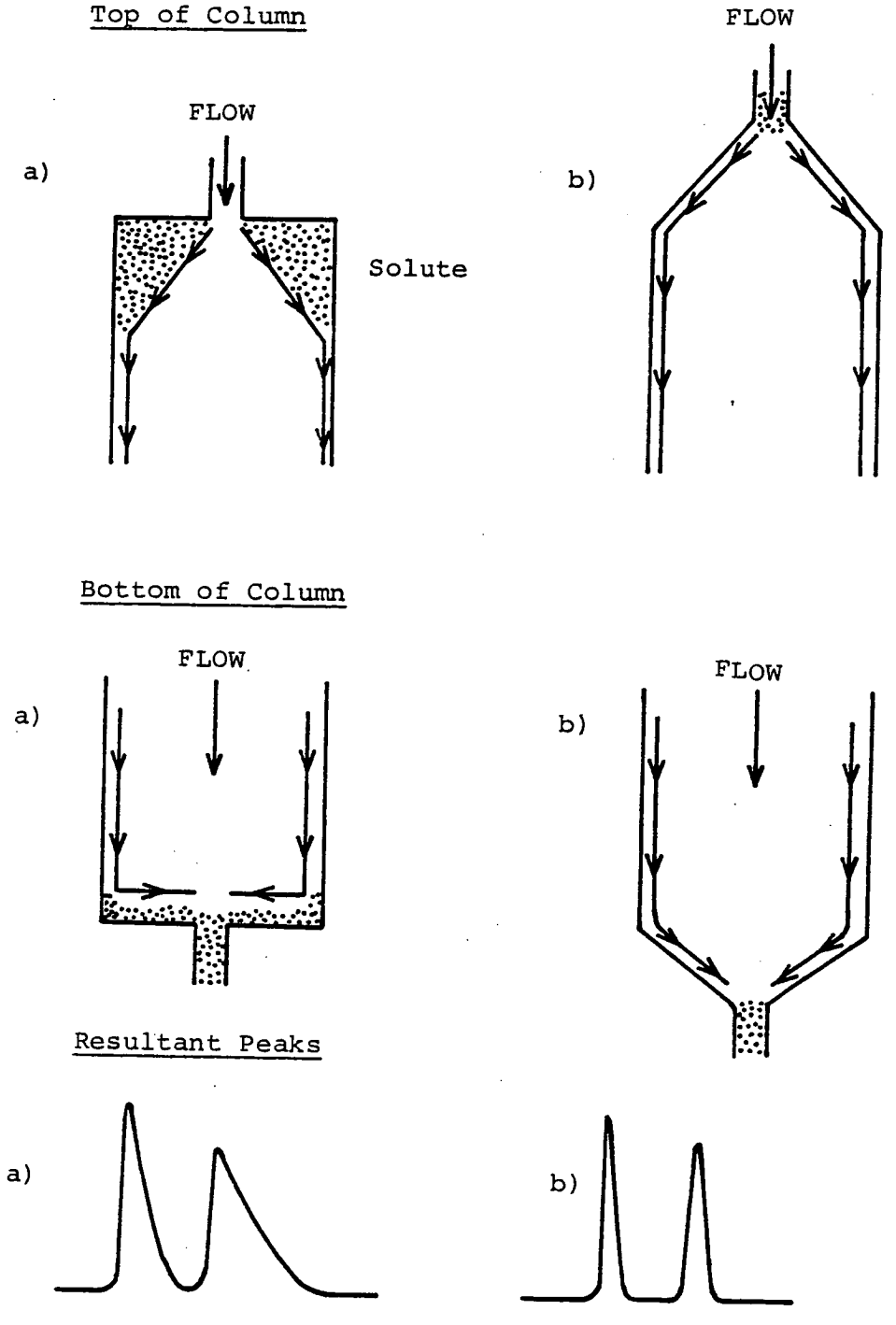

Figure 5.1 Different designs of both top and bottom end fittings.

a) With sharp, unswept corners (90° angle).

b) With coned, cleanly swept corners (120° angle).

5.2 Equipment for Preparative HPLC

5.2.1 Columns

Larger diameter columns are normally used in preparative scale separations since they allow for a higher sample capacity of the column. Increased sample capacity can be achieved by increasing the column length but this leads to increased pressure requirements or increased separation times, and so is less favoured.

A number of workers have studied the effect of column diameter on efficiency for preparative columns used with analytical size samples but the conclusions arrived at appear to differ. Wolf[1] for example has claimed that for columns of 50 cm in length and ranging from 0.77-2.36 cm in diameter, efficiencies were as much as a factor of four more than when compared to a column of narrow bore dimensions (50 cm x 2.1 mm id). Furthermore, he found that column efficiency increased with increasing column diameter. However this was not substantiated by Wehrli[3], De Jong *et al.*[4] and De Stefano and Beachell[5] who found that column efficiency was not dependent on the column diameter used.

One problem which can occur with wider columns as a result of a poor inlet system and/or column-top design is that "dead" areas may exist at the top of the bed which are unswept by the mobile phase, as illustrated in figure 5-1.a. Any solute molecule entering this area must diffuse back into the mainstream before it can continue migrating down through the column resulting in extra band-spreading, peak asymmetry and tailing. It is obvious that the greater the mobile phase velocity[6] the less

able are these molecules to diffuse out of these unswept areas. In the design of large scale columns, therefore, careful consideration has to be given to the design of the top of the column, and also as to how the sample is taken off at the bottom. The problem of unswept areas can be prevented by designing the columns so that both the top and bottom are coned to an angle of around 120° as shown in figure 5-1.b. Various column top terminators have been used and these will be discussed in more depth in section 5.2.2.

Apart from preparative columns which are more or less scaled up versions of analytical columns, ie. made of stainless steel but wider and/or longer, two different types of designs have emerged in recent years which have been used with some success; these are the radially compressed columns[7,8] of Waters and the axially compressed columns[9-11] of Jobin-Yvon with the second type being the more successful.

5.2.1.1 Axially Compressed Column (Jobin-Yvon)

Godbille and Devaux have used axially compressed columns of 8 cm[9] and 18 mm[10] internal diameter in which the bottom of the stainless steel column acts as a piston. To pack the column, a slurry of the mobile phase is poured into the column and is compressed by the piston with the excess solvent passing out through the top of the column. They concluded that the good efficiencies and column capacities achieved with these columns were due to the constant axial pressure acting on the packed bed which is maintained throughout the analyses. Another advantage of this type of design is that the amount of stationary phase used, and hence the length of the column bed, can be

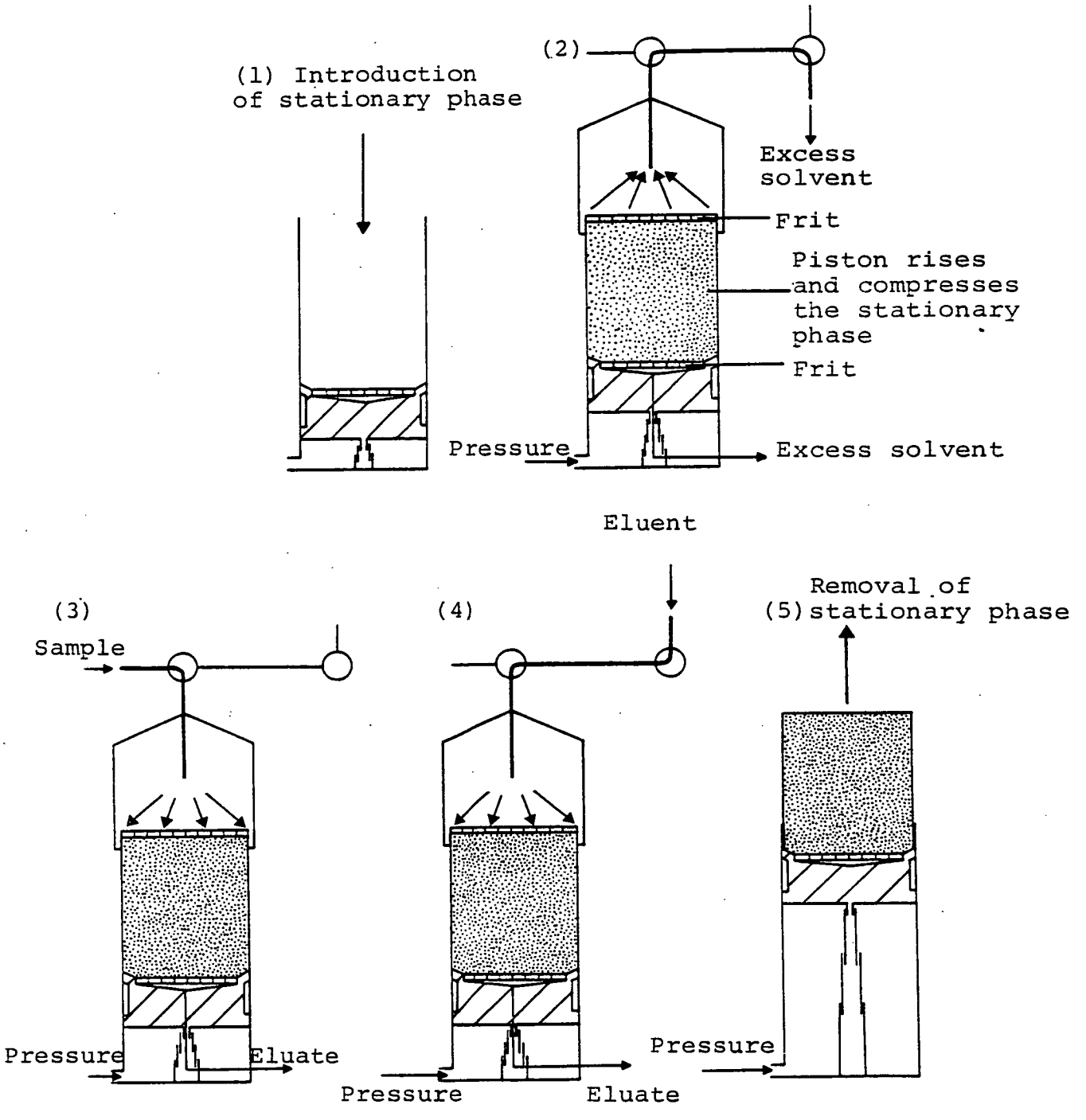

Figure 5.2 The operation of an axial compression column. (1) and (2) show the preparation of the column, (3) shows the loading of the sample onto the column, (4) shows the elution of the sample and (5) the removal of the support.
(Reproduced from reference 12).

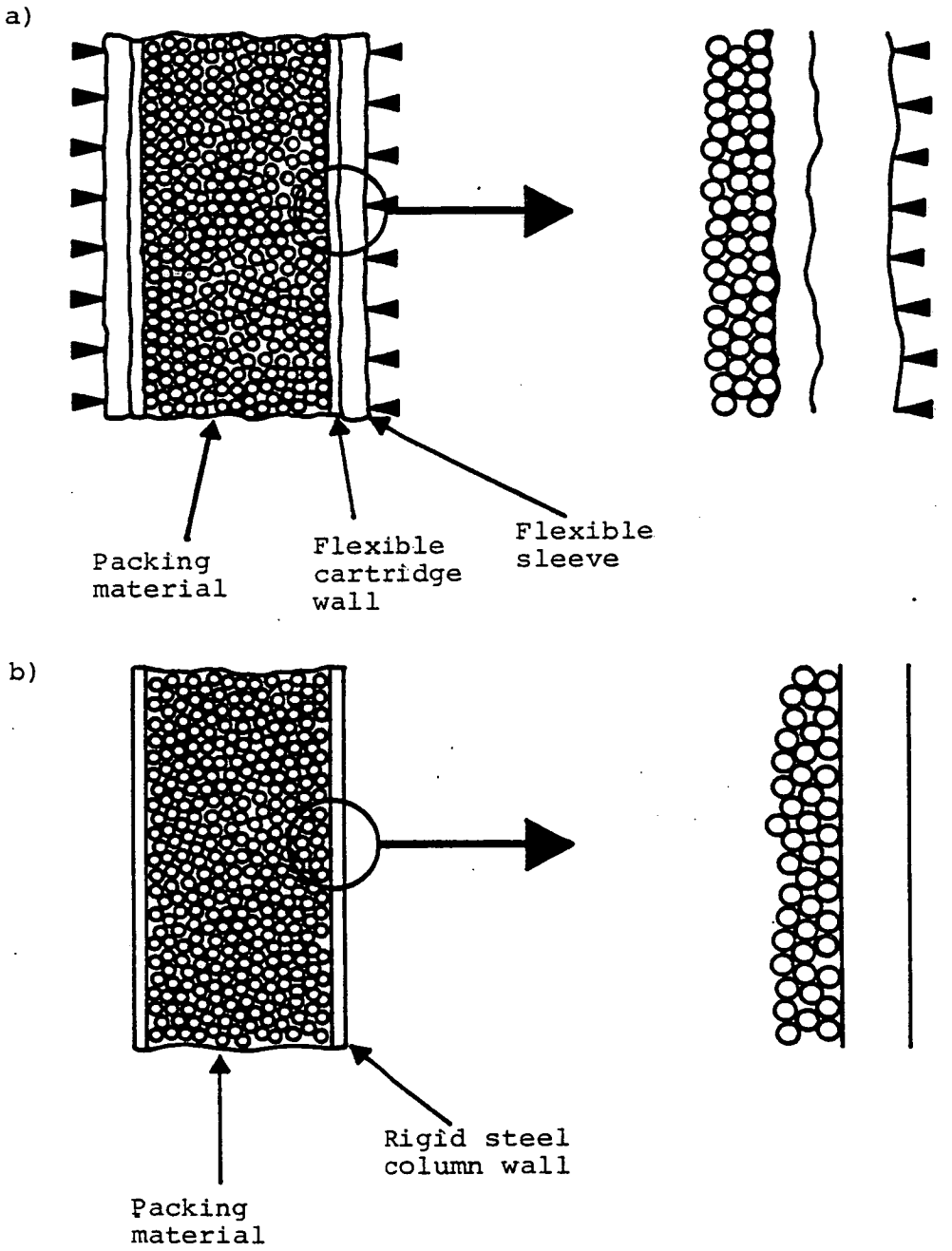

Figure 5.3 Schematic representation of (a) a radially compressed column, and (b) a rigid wall steel column.
(Reproduced from reference 12).

varied as desired. A diagram illustrating this type of column is given in figure 5-2.[12]

However, because the compression of the bed is by gas pressure acting on the piston, this pressure is limited to around 30-50 atm for safety reasons and this therefore restricts the pressure at which the liquid chromatographic system can be operated resulting in a low maximum operation pressure.

5.2.1.2 Radially Compressed Columns (Waters Associates)

Little *et al.*[7] and Eon[8] have described the use of radially compressed columns which have also been used by other workers.[13-16]

These are flexible walled cartridges, usually made of PTFE, which are enclosed in an outer stainless steel jacket and pressurized with nitrogen. The pressure is maintained throughout the chromatographic run at 50 bar above the operating pressure of the column. This ensures that the walls of the cartridge are compressed against the packing material and this is believed to reduce the irregularity of the packing area next to the column wall. Figure 5-3 illustrates the salient features of the radially compressed columns. Sample capacity is good as these cartridges are fairly large.

However, the same type of problem exists with this type of column as with the axially compressed column, namely the gas pressure used to compress the column limits the maximum operating pressure of the chromatographic system. This leads to larger particle sizes being used and therefore produces lower efficiencies than with steel walled columns but for preparative separations this may not be such a serious drawback. For optimum HPLC, columns are required to be packed with small particles and to

be operated at high pressures.

Eon[8] has carried out a study of the difference of band broadening between large diameter columns of the regular (ie. stainless steel walled) and of the radially compressed type. By using different injectors and comparing the column efficiencies he found that, when working within the "infinite diameter" mode and using a central injection, there were no differences between the two types of column. However, in those cases where the sample did reach the column wall area, the efficiency of the radially compressed column was still maintained whereas that of the ordinary type dropped off showing that there is some advantage of radially compressed columns.

Little *et al.*[7] have used radially compressed columns to achieve multigram separations in a matter of minutes using a 30 x 5.7 cm id cartridge. Although there was no mention of the efficiency of such a column, it is not likely to be very high. They also demonstrated how resolution could be improved by coupling 2 and 4 columns in series, as well as by employing recycle down one column.

5.2.2 Sample Introduction Systems

Possibly the most important feature of a preparative HPLC system is how the sample is introduced onto the column.

In analytical separations, samples are either introduced using a valve injector or by direct injection. Many workers have shown[17,18] that there is a particular ratio of the column diameter to the particle diameter above which a sample, introduced centrally to the top of the column bed, never reaches

the area of disturbed packing next to the column walls by means of lateral diffusion before it is eluted from the column. This is given by the Knox-Parcher[17] equation as

$$d_c > (2.4 \times d_p \times L)^{\frac{1}{2}}$$

where d_c is the internal diameter of the column, d_p is the particle size diameter and L is the column length. It has been shown that columns operating in this so-called "infinite diameter" mode are more efficient since the flow profile of the solute across the part of the bed which is used is more uniform and therefore band spreading is less than if the solute actually reached the column wall area. Column efficiency can be further improved by injecting the sample into a curtain flow of eluent. However, if columns were packed uniformly across the entire cross-sectional area of the bed, there would be no need for such measures.

A second problem with the method of sample introduction used is the dispersive effect of the injection itself, as mentioned by Coq, Cretier and Rocca.[19] In their paper, they have shown, for analytical scale chromatography, the importance of the mode of injection and have proposed an injection factor, θ, such that

$$V_L = \theta V_i$$

where V_L is the effective width of the sample plug placed on the column and V_i is the actual injection volume. V_L can be measured either by placing a detector immediately after the injection device or it can be determined from the peak width of an unretained solute. The maximum allowable injection

volume, $V_{i,max}$, is greater when θ is smaller ie. $V_{i,max}$ is inversely proportional to θ. The quality of the injection device therefore has a marked effect on the band broadening and thus on both the peak resolution and the maximum sample load which can be placed on the column.

A third problem is that of overloading the stationary phase. With preparative-scale separations, much larger sample masses are loaded onto the column. In this case the sample is best loaded onto the column by covering the entire cross-sectional area of the bed since central injection would cause localized overloading of the stationary phase. This would result in additional band spreading and produce a lower column efficiency. Also, with central injection column loadability would be lower since only a fraction of the total bed is used by the sample. Sample introduction through a curtain flow of eluent also limits the area of the bed which can be loaded with sample, and for well packed columns may make little difference to column efficiency.

The loadability of the column is therefore significantly affected by the mode of sample introduction, and as the sample is best introduced over the entire cross-sectional area of the stationary phase, this means that such columns would not be operating in the infinite diameter mode.

It is clear that the three recomendations for the method of sample introduction, namely

a) the infinite-diameter mode of the column, which suggests that a central injection of sample is preferred,

b) the overloading effect, which suggests sample injection over a wide area of the bed,

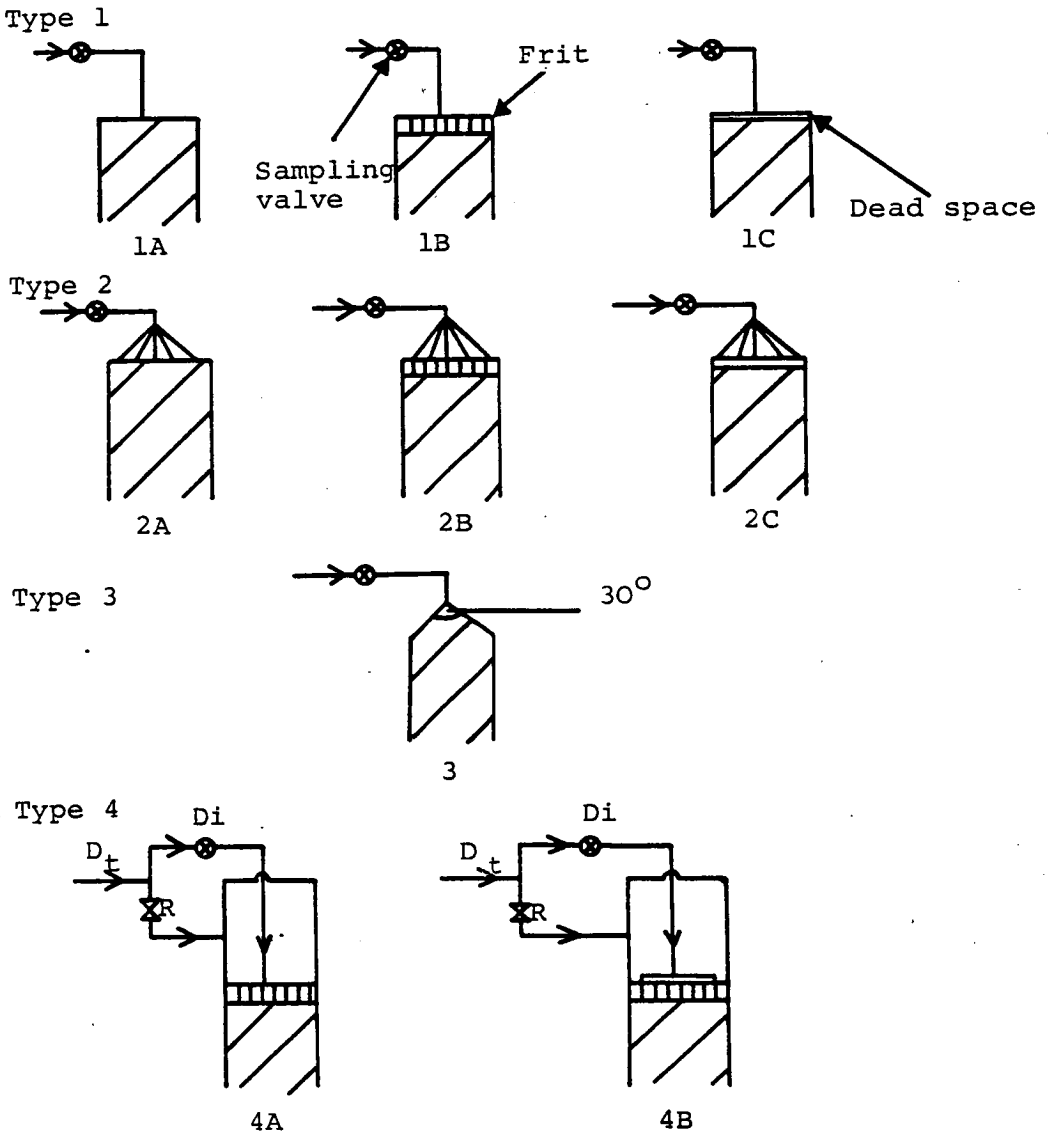

Figure 5.4 Schematic respresentation of various injection devices [19]

Type 1: Injection valve is directly connected to the column. Sample is introduced at one point of the cross-section of the bed.

Type 2: Sample is introduced at 5 points of the cross-section of the bed.

Type 3: A conical column top, filled with stationary phase, is fitted between the column bed and the injection valve.

Type 4: Injection valve used with a split-flow arrangement.

4A is comparable to syringe injection with a curtain flow

4B is a curtain flow system combined with a sprinkler.

and c) the width of the sample plug, which suggests keeping the sample plug to a minimum and if possible no wider than the sample volume itself,

contradict each other, especially a) and b), and that therefore some compromise is required. For example, for large sample loads, the increase in band spreading caused by the irregularly packed area near the column wall is less serious a problem than that caused by localized stationary phase overloading.

Many devices are used in order to achieve an optimum compromise. Various column top terminators have been used in conjunction with syringe injectors, variable volume loop injectors,[10,20] sample vessels[9,21] where the sample is pumped onto the column and also loading pre-columns.[22] In some cases a second pump has been used to pump the sample onto the column although the eluent pump can be used using a series of switching valves. Some of these devices will now be discussed in more depth.

5.2.2.1 Various Column Top Terminators

Coq *et al.*[19] have tested four types of injection method along with different column top terminators as described in figure 5-4, and which were used in conjunction with a sample valve. Results showed that the curtain-flow or split stream injector, type 4, produced the best peak symmetry and consequently the best column efficiency due to the elimination of stagnant eluent areas and the fact that the curtain flow helps to keep the solute away from the wall areas. In particular, injector 4B, which combines the curtain flow with a sprinkler and frit, was found to be superior to 4A which did not contain the sprinkler,

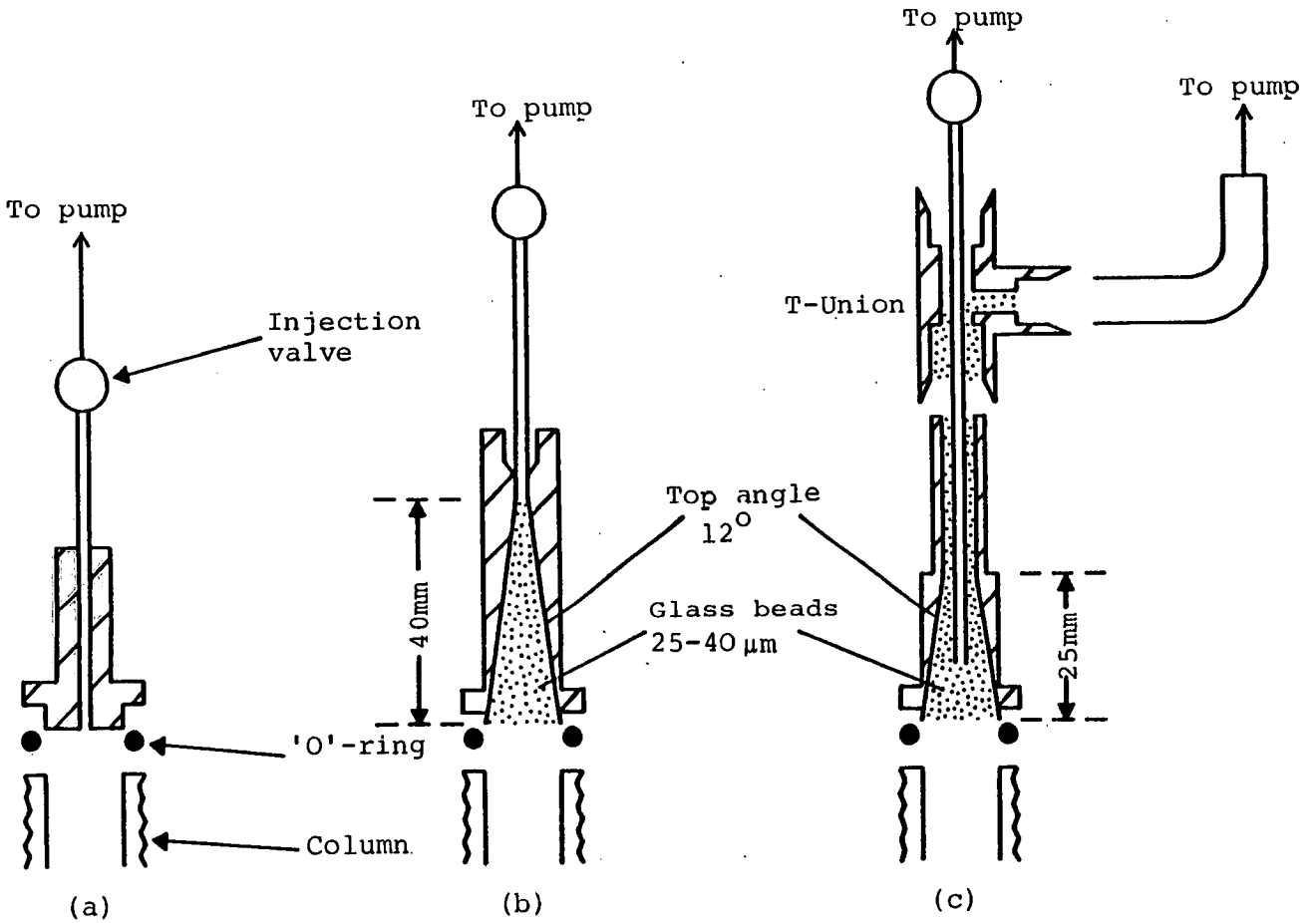

Figure 5.5 Schematic representation of three column-top terminators

(a) Spot injection in the middle of the cross-section of the bed.

(b) A conical column top, filled with glass beads, installed between the column packing and injection valve.

(c) A flow-surrounded injection system together with a conical top, filled with glass beads.

(Reproduced from reference 4).

since larger volumes and concentrations can be introduced before localized overloading occurs. This illustrates the fact that it is better to introduce the sample over a wide area than at one point. It was found that, for injector type 4A, overloading occurred at 3 mg/ml while for type 4B this occurred at 100 mg/ml.

De Jong *et al.*[4] have described the use of two conical dispersers and have compared them to one which introduced the sample centrally to the top of the bed. These three devices are illustrated in figure 5-5.[34] Using analytical size sample loads, they found that the peak asymmetry, as measured at 0.1 of the peak height, increased in the order c<b<a, and also with increasing mobile phase velocity, which they suggested showed the existence of unswept stagnant areas. The curtain-flow conical disperser (c) produced less peak asymmetry than with the ordinary conical disperser due to the fact that, with the former, the sample plug tends to follow flow lines which tend to keep the solute away from the irregularly packed area next to the wall. This encourages the sample to remain within the central uniformly packed core of the column leading to high efficiency. However, when considering the efficiency of the column as calculated at 0.607 of the peak height, the loadability of the column, which they considered as being "the maximum amount of sample that produces no change in N" was 2-3 times smaller when using the curtain-flow disperser (c) than with the ordinary conical disperser (b) due to the smaller amount of packing which is effectively used by the sample. However, due to the fact that the curtain-flow disperser produces less

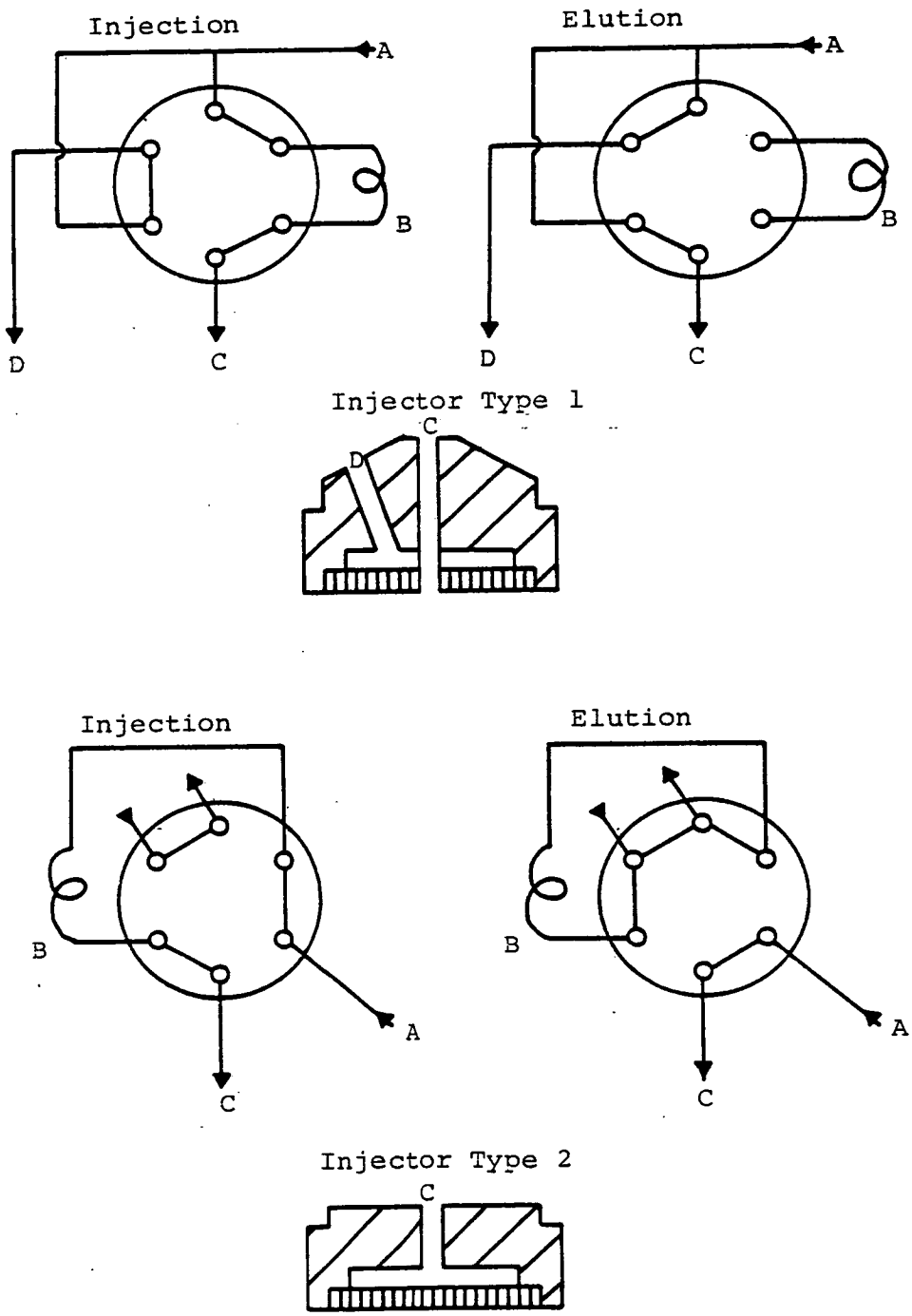

Figure 5.6 Schematic representation of injectors for use with variable volume loop valves. Type 1 is an "on-column" injector while Type 2 is a "swept" injector. A, from solvent reservoir; B, sample loop; C, to the injector; D, mobile phase.
(Reproduced from reference 10).

peak tailing, calculations of the column efficiency at 0.1 of the peak height show that the loadability was significantly better than with the other devices, but only up to a certain load†, after which it dropped to below that of the others. Unfortunately, it was not made clear what sample concentrations or sample volumes these results corresponded to. All this indicates is that a careful balance is required which limits the amount of overloading and at the same time ensures that not too much sample reaches the column walls.

Godbille and Devaux[10] have used two types of injectors in conjunction with variable volume loop valves as illustrated in figure 5-6. The "on column injector" directly injected the sample into the centre of the column bed while the "swept injector" introduced the sample over the entire cross-sectional area of the bed. They found that while the "on column injector" was more efficient for low volume injections (ie. up to 0.5 ml), it was less efficient for large injection volumes (0.5-2 ml). It was suggested that the extra band spreading with the "on-column injector" was a result of the increase in flow velocity at the column inlet when larger volumes were injected. However, a more likely explanation is that when the sample volume is low, no localized overloading occurs, but when a large volume is injected, the sample is concentrated at the centre of the top of the bed and this produces localized overloading.

Variable volume loop injectors and syringe injectors can be used up to around 2 ml in volume. For volumes greater than this, the valve injector can give rise to poorer efficiency, while for the syringe injector, problems are encountered when

---

† This load was approximately 1 mg on a 25 cm x 1 cm id column.

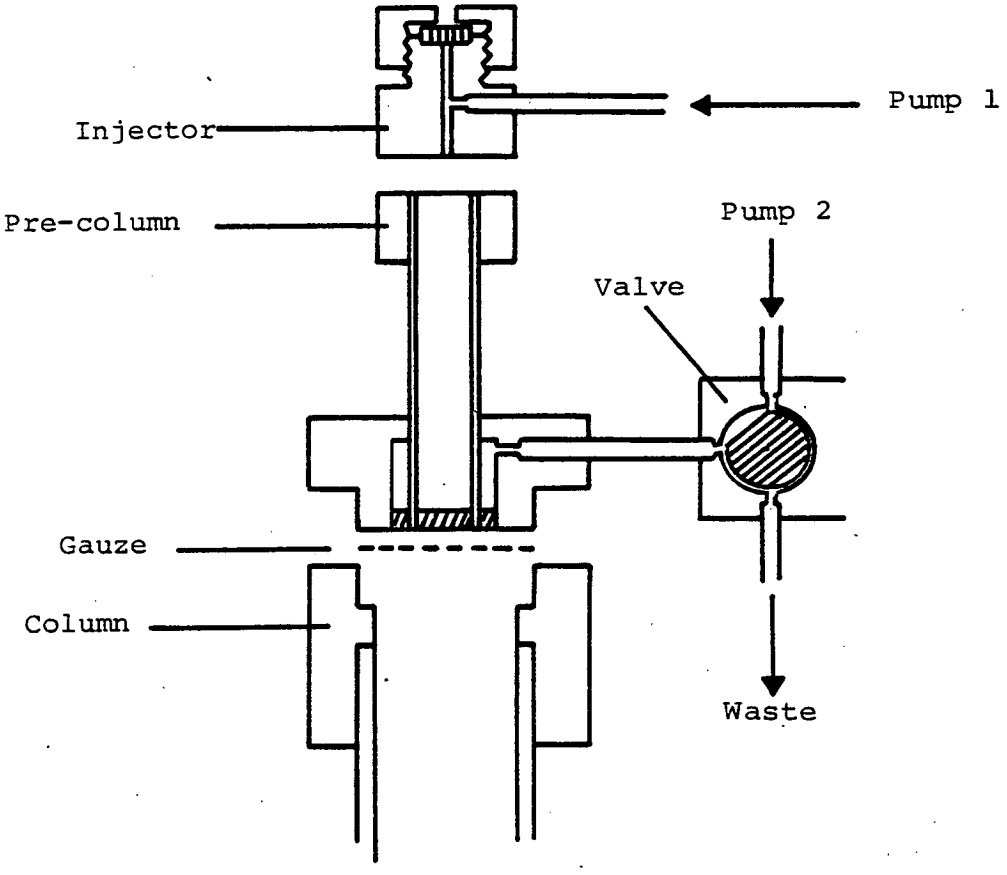

Figure 5.7 Curtain flow pre-column/column assembly (Reproduced from reference 22).

trying to inject large volumes against the high back pressure produced. These problems can be overcome by pumping the sample onto the column either using the eluent pump and a series of valves or alternatively a pump which is used solely for injection purposes.

5.2.2.2 Loading Pre-columns

Another injection system which has been used successfully in this work, and also by Wall,[22] involves the use of a loading pre-column, and a diagram of the pre-column/column assembly is given in figure 8-3. The pre-column was filled with glass beads ($d_p \sim 175$ μm) by a rotate-tap method, and was separated from the main column by a sandwich piece which consisted of a frit and an annular outlet/inlet port connected to a 2-way valve. A septum injector system was then connected to the top of the pre-column. Injections could then be carried out in several ways depending on the injection volume. For analytical size samples, injections were carried out in the on-stream mode. The injection of larger volumes, up to the holding volume of the pre-column, were carried out in the stop-flow mode with the pre-column outlet valve open, thus displacing an equivalent volume of eluent in the process. The great advantage of this method is that the injections are not carried out against the back pressure of the main column. The outlet valve is then closed before opening the valve to the pump to commence the run. Using this arrangement, it is also possible to pump the sample onto the column using a second pump by disconnecting the injector from the main pump and connecting it to the second sample pump. This method is very useful in preparative

separations where it is necessary to concentrate the sample at the top of the column and this technique is discussed more fully in Chapter 10.

Alternatively, by using a second eluent pump connected to the side-arm in conjunction with the main pump, a 'curtain flow' effect can be produced. However experiments carried out to establish whether or not this had any effect on the shape of the peaks produced, and which are described in detail in Chapter 8, showed that, with the equipment designed and used in this thesis, there is no difference in the peak shape produced with or without the 'curtain flow'. It should be pointed out that, in these experiments, the internal diameter of the pre-column is the same as the internal diameter at the top of the coned section of the main column and that therefore no unswept areas should exist at the top of the packed bed.

Wall[22] also stated that "direct injection into an equal diameter pre-column/column system gave the expected good results even when the annular second inlet was incorporated (but not used)." However, he did find that when a pre-column was used which had a different internal diameter to that of the main column the peaks became badly skewed when the curtain flow effect was not in operation, but that the peak shape improved considerably when the curtain flow was in operation. The ratio of the flow between the main column and the second annular inlet used was proportional to the ratio of the cross-sectional areas of [pre-column]:[column-pre-column].

There are three basic differences between the pre-column/column assembly unit used by Wall,[22] as illustrated in figure 5-7, and the one used in this thesis, which is illustrated in the figures 8-3 to 8-7. In the former, the annular outlet/inlet is incorporated into the pre-column itself rather

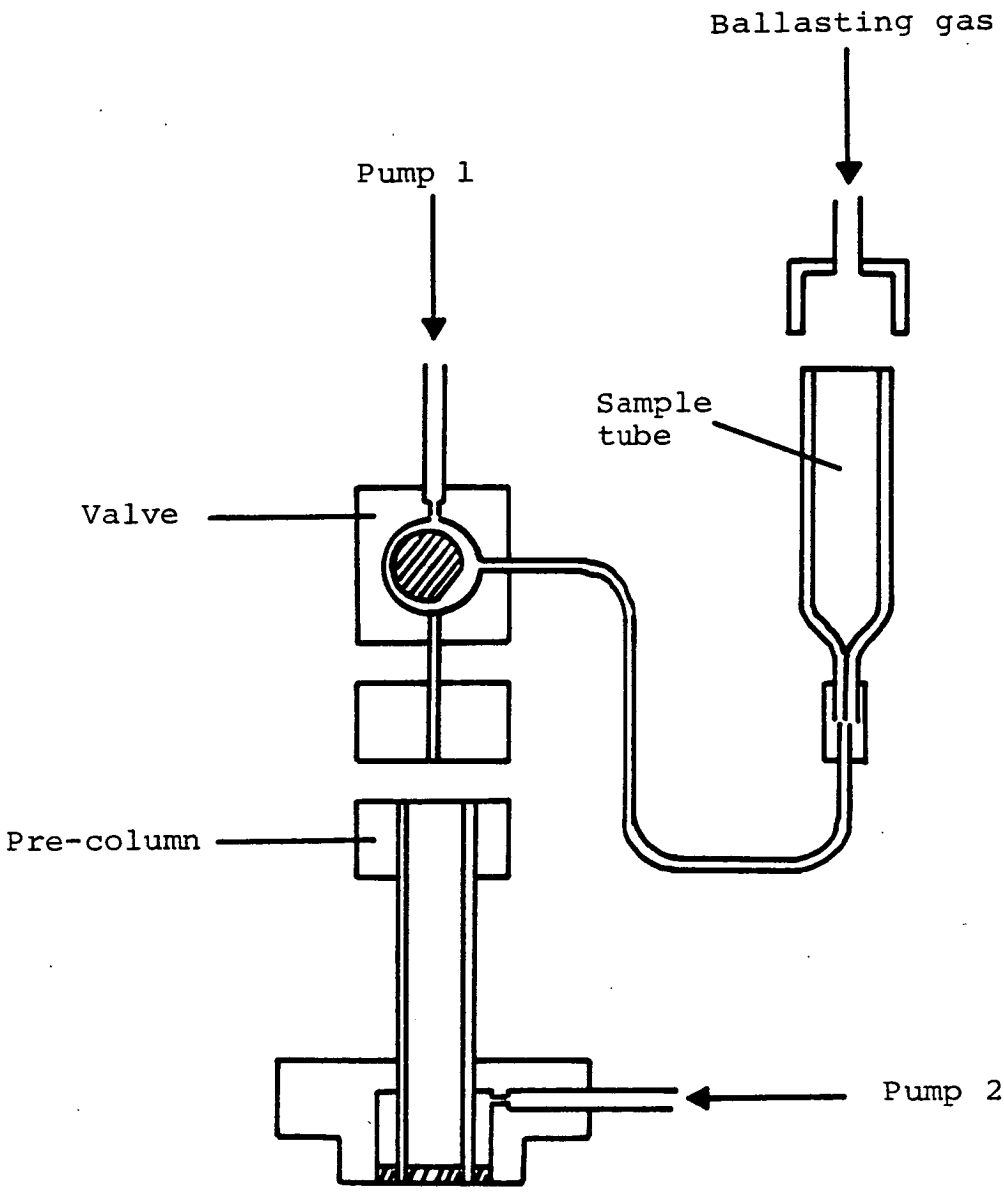

Figure 5.8 Gas-pressurised loading tube attachment.
(Reproduced from reference 22).

than in a separated sandwich piece, which means that the system is less versatile, and the two beds are separated only by a thin stainless steel mesh disc rather than by a frit. Also the top of the main column is not coned and therefore when the internal diameter of the precolumn is not the same as that of the main column, unswept areas of the packed bed exist at the top of the column. This explains why badly tailed peaks are produced and why the curtain facility improves peak shape in such cases.

Wall has also described a gas-pressurised loading tube attachment, as shown in figure 5-8, which aids the loading of large sample volumes. It appears that the pre-columns used were packed with silica gel (∿40μm) and that injection of more than 1 ml of sample caused leakage in the glass-syringe used. However, this problem was not encountered in this work since the pre-column was packed with glass beads of around 175 μm.

5.2.3 Detectors

In preparative HPLC, the detectors used must be able to cope with the larger flow rates often used, and also the large range of concentrations which pass through. To cope with the large flow rates, either the cell volume must be larger than that normally used for analytical separations (8 μl), or alternatively a flow splitter must be introduced into the system so that only a fraction of the eluent passes through the cell. The ratio of the volume of the eluent flowing through the cell and through the splitter can be either fixed or variable. The flow then either rejoins the main flow before collection or is collected separately.

There are two main types of detectors which can be used

in both analytical and preparative separations: universal or bulk detectors, eg. refractive index detectors, which detect all solutes eluting from the column, and selective detectors which detect certain properties of the solutes not found in the eluent eg. fluorescence or U.V. absorbance.

The Refractive Index detector depends on the difference between the refractive index of the eluent and the combined refractive index of the solute in the eluent. The signal produced will vary depending on the eluent used and will be weak where the refractive index values of the eluent and solute are similar. This type of detector is unsuitable for gradient or step-wise elution. However, as this is one of the less sensitive detection methods, it is very suitable for preparative separations.

Another detector often used in preparative HPLC is the U.V. Absorbance Detector, and in particular those with variable wavelength control. This enables the user to "back-off" from the absorbance maximum to a wavelength at which the U.V. absorbance of the solute is lower. In this way, high solute concentrations, which might otherwise overload the detector, can be observed within the detection range. Particular care is required when using selective detectors that the solute of interest is not contaminated with any solute which is undetected by the selective detector used and so bulk property detectors might therefore be more useful especially if the solute concentration is sufficiently large.

Other detectors, such as the electrochemical detector can be used in some instances, but as it is a destructive type, a flow splitter would be required.

5.2.4 Pumps

The type of pump used largely depends on the size of the preparative system being used. For analytical size columns which can be used for separations up to 100 mg, an ordinary analytical pump either of the constant pressure type eg. air driven pressure intensifier pump or of the constant flow type eg. reciprocating pump can be used, with the latter requiring the use of a pulse dampner in the system. The maximum flow rates generated by these reciprocating pumps generally range from 10 ml/min to 30 ml/min. These pumps can also be used to load the sample onto the column prior to separation and for recycling the eluate back onto the column again.

A popular pump used with preparative columns is the pneumatic amplifier pump. This is an air driven constant pressure pump which has the advantage of being able to deliver large volumes of solvent at high pressures and can deliver solvent up to 1 ℓ/min. It can also double as a pump for slurry packing columns when required. One disadvantage however, is that this type of pump is unsuitable for recycling the eluent back through the column.

5.2.5 Fraction Collection

The collection of fractions at the end of a separation can either be carried out manually or can be done using an automated fraction collector, the latter being particularly useful where a large number of runs are to be carried out. These automatic fraction collectors work either by collecting samples of a fixed volume or over a fixed period of time before moving on

to collect the next fraction. An alternative type of fraction collector starts collecting fractions when the system detects a peak beginning to come off. This is determined either by the signal exceeding a certain pre-determined level and/or when it detects the rate of change of the signal increasing above a preset value. However, most automatic fraction collectors are controlled by microprocessors which are able to operate in any of these modes.

5.3 Packing Techniques

Methods for the packing of both analytical and preparative columns can be classified as either dry-packing or wet-packing techniques. The choice of method depends on the size of the particles to be packed and the general opinion is that particles down to 20 μm in size can be dry packed to produce efficient columns. Smaller particles (<20 μm) cannot be dry packed since this produces agglomeration and bridging between particles due to electrostatic charges present on their surface, resulting in packing irregularities and poor efficiency. Also these micro-particles are so light that it is difficult to consolidate the bed. The problems of packing these microparticles can be over-come by employing a wet-packing technique where they are first slurried in a liquid and then forced into the column under pressure so that the particles are filtered onto the growing column bed.

The different packing techniques have been reviewed in several papers,[23-31] and are briefly discussed below.

5.3.1 Dry Packing Methods

Particles with large diameters (>20 μm) are often used in preparative HPLC since large columns packed with microparticulate material would prove very costly. These large particles are easily dry packed and several different methods have been used by different workers. Basically, they all involve the addition of small increments of packing material which is ideally distri-buted uniformly over the entire cross-sectional area of the column[32] followed by consolidation of the bed. These methods

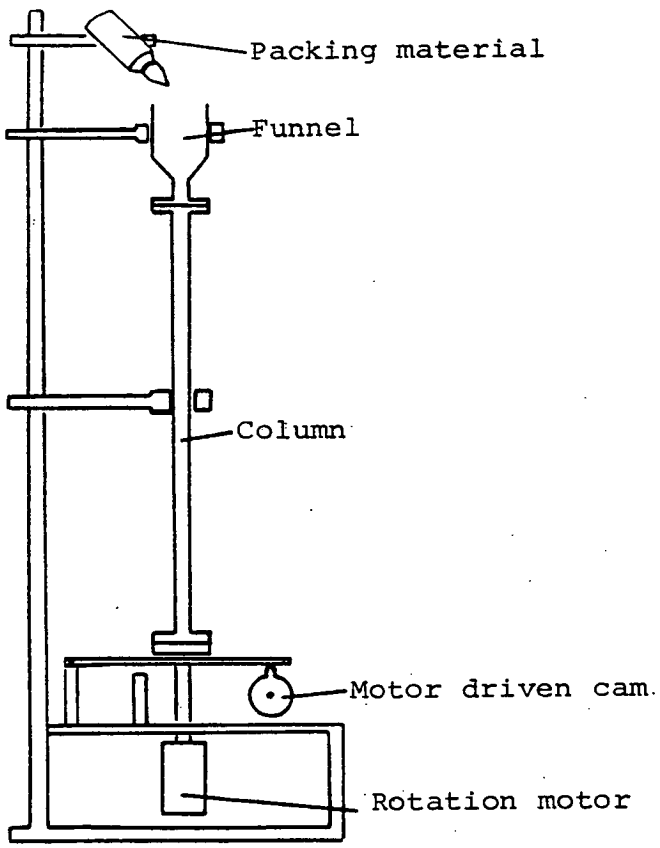

Figure 5.9 Schematic representation of a Rotate - Bounce dry-packing machine.

include the tap-fill[33] method, where the column is bounced gently on a hard base to induce vertical vibrations, and the bounce-tap method[1,6,34-37] which consists of gentle vertical bouncing with simultaneous light tapping on the column wall at the level of the bed to induce lateral vibration followed by gentle bouncing only. It is thought[35] that this light tapping promotes the rapid formation of a dense, stable and homogeneous bed without undue sizing. A less frequently used method involves rotating the column around its vertical axis while tapping the column on the side. A combination of the last two methods is the rotate-bounce-tap method[6] where the column is simultaneously bounced, rotated and tapped on the side at the height of the bed, followed by a period of bouncing only. It is possible to perform this type of packing method mechanically using a machine similar to that which is described in figure 5-9. Another method of dry packing columns has involved tamping[38] the material into the column with a rod to which a perforated disc has been attached. The problem here is that smaller particles tend to pass back through the holes in the disc and are disturbed by the extraction of the rod. Mechanical devices[39-41] have also been developed to automate the procedures.

The problem with all of the afore-mentioned methods is that their description is somewhat ambiguous. The height from which the column is dropped and the force used to vibrate the columns appear to have been chosen arbitrarily. However, a detailed investigation of the various dry-packing method for preparative columns has been carried out by Klawiter *et al.*[42] to establish the relationship between the packing method and the efficiency achieved. Columns of 2-52 mm in diameter and 10-50 cm in length

were packed by tamping which was achieved using a specially constructed device. The silica gel was fed into the column continually during packing from a container fixed to the top of the column. The rate of gel feeding was altered as required by changing the metal gauze at the bottom of the container to one with either larger or smaller holes. They concluded that "the efficiency of the columns packed by the tap-fill method depends essentially on the rate of gel feeding" and that there is an optimum feeding rate, which is governed by the particle size and the column diameter. They found that this optimum packing velocity increased with particle size and column diameter until eventually for the 52 mm i.d. column packed with particles of 124 μm in diameter, there was no optimum packing velocity. They also observed that, while the plate number increased proportionally with column length, the reproducibility of the column efficiency decreased.

Although tapping the column vertically and/or on the side during filling can result in improved column efficiency it can also lead, in some cases, to a deterioration in efficiency. This is because tapping can cause smaller particles to move to the centre of the column while the larger particles move out to the walls of the column.[32,42,43] The inhomogeneity of the bed which this produces results in a distorted flow profile across the column causing greater band spreading due to the faster carrier flow near the walls compared to the centre of the bed. This non-uniformity is reduced if a narrower particle size range is used.

Klawiter *et al.*[42] have described three basic solute zone

shapes, which they attribute to different silica gel feeding velocities, as follows:

1) where the silica feeding velocity was greater than the optimum feeding velocity it was found that the solute zones within the column were curved in the direction of the eluent flow,
2) where the silica feeding velocity was less than the optimum the zones were curved in the direction opposite to that of the eluent flow, and
3) where the silica feeding velocity was approximately the same as the optimum the solute zones were nearly flat or were curved slightly in the direction of the eluent flow.

The different solute zone shapes which are produced indicate that the effect of unevenly packed beds is less for wider columns than for narrower columns. It was also observed that the actual width of the solute zone did not differ greatly whether packed under optimum or non-optimum conditions. The conclusion arrived at by Klawiter *et al.*[42] was that column efficiency is a result of both zone width and zone shape.

Another effect of particle size non-uniformity, which has been observed both in preparative[9,44] and analytical[41,45,46] columns is the formation of peak doublets, although this is perhaps more usually seen as humps on the sides of the peaks or peak tailing and may be mistaken for impurities, although all peaks will show the same effect.

5.3.2 Wet Packing Techniques

The advent of slurry-packing methods has helped towards the realisation of the optimal performance of columns packed with

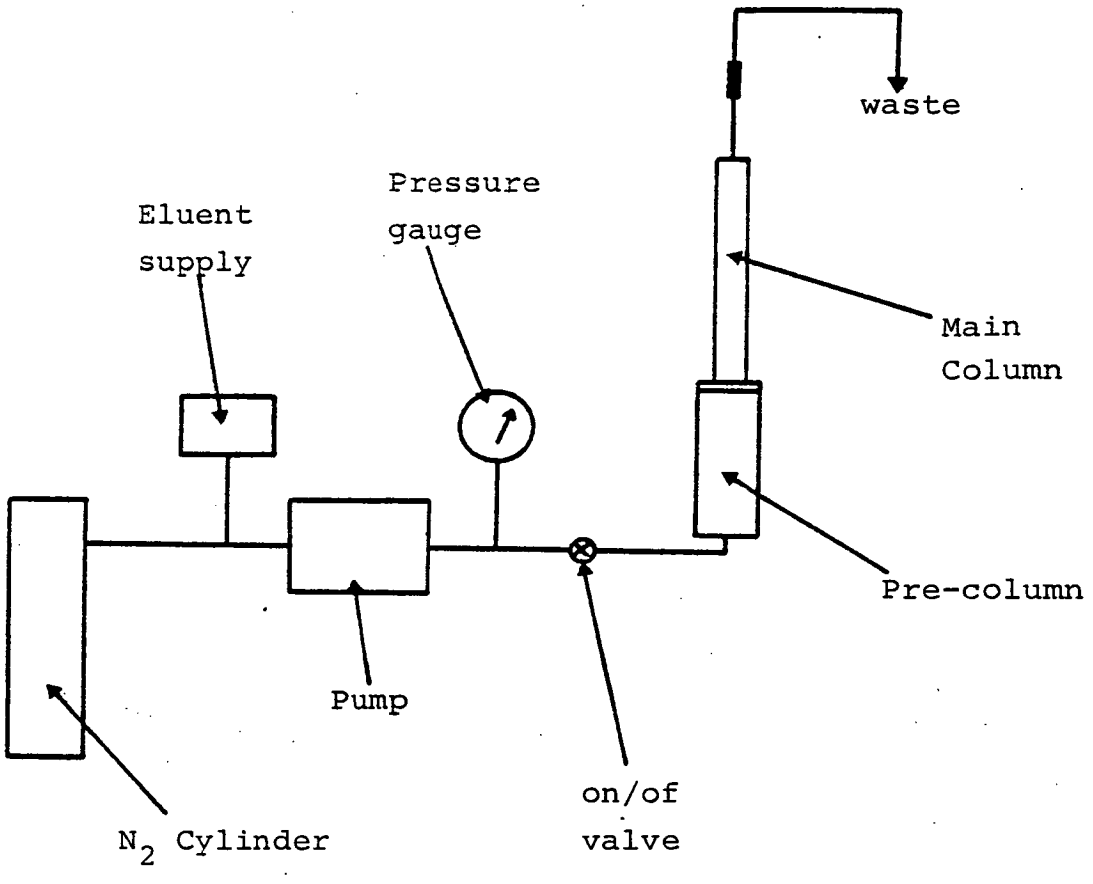

Figure 5.10 Apparatus for the slurry packing of columns (upward mode shown)

microparticulate materials. Higher efficiencies[36,37,47] have been consistently obtained with high-pressure slurry-packing techniques, using apparatus similar to that outlined in figure 5-10, than with dry packing techniques.

There are several different slurry-packing techniques currently in use with no agreement as to which is the best method. The main differences between the various methods lies in the choice of liquid to keep the particles in suspension in the slurry.

The balanced density method[4,9,45,47-62] has been used effectively by several workers. This involves slurrying the stationary phase in a solvent and adding a pre-determined volume of a dispersing agent such as tetrabromoethane or tetrachloroethane so that the resulting solvent mixture has the same density as the stationary phase and the particles do not settle. The main drawback to this method is that highly halogenated solvents are very toxic. These solvents also strongly adsorb onto silica gel and must be washed thoroughly from the column.

To avoid these problems, some workers have used a high viscosity packing method[29,45-63] which involves slurrying the stationary phase in a liquid with a high viscosity which prevents coagulation of the particles since according to Stokes Law, the sedimentation velocity, υ, of a particle is proportional to the square of its diameter, ie. $\upsilon \propto dp^2$, and inversely proportional to the viscosity, η, of the liquid ie. $\upsilon \propto \frac{1}{\eta}$. One problem with this method is the high pressure drop produced across the column during packing. However, the method is advantageous if chemically bonded phases are used, or if the adsorption of the tetrabromoethane is to be avoided.

Mechanical stirring methods[64-67] have also been used where

the stationary phase is kept in suspension by constant stirring in a vessel prior to rapid high pressure packing.

Other workers have preferred to slurry the stationary phase in low viscosity[20,24-27,32,47,48,68-70] liquids, and in some cases in the mobile phase[71,72] itself. Although particles fall out of suspension quickly, they can be packed rapidly and so produce efficient columns. It is felt by some workers[26,27,66,70,73] that by packing upwards rather than downwards, the effect of sedimentation is eliminated.

Other methods used to prevent particle agglomeration include the use of an aqueous ammonium suspension[52,74] for silica and the use of organic acids as slurry agents,[38] the former method minimizing agglomeration by creating repulsion between the particles while the latter decreases the attraction between them.

Where columns are of the axially compressed type,[9,10] packing is achieved by compression of the slurry into the column using the column bottom as a piston.

In addition to packing the bed all in one go, packing has also been carried out in sections[19,22,25] by a downward slurry method.

5.4 The Development of Preparative Separations

The first step in the development of a preparative-scale separation is to achieve a good analytical separation on an analytical column, preferably using a column packed with the same material that is to be used in the preparative column. Thought should be given at this stage as to the type of stationary phase and choice of solvents used since the material has to be recovered from the eluent at the end of the preparative separation. Adsorption chromatography enables the solutes to be easily recovered by the evaporation of the organic solvents and is also much cheaper than bonded phase material, which is an important consideration where large columns are to be used.

The advantages of doing all of the ground work on an analytical scale before moving on to the preparative scale are that it is cheaper since smaller volumes of eluent are used, it uses up less of the original material which may be of importance if it is of limited supply, and the various adjustments to the method can be carried out more easily and the optimum conditions arrived at more quickly.

Once an analytical separation has been achieved, the conditions must be adjusted to obtain maximum resolution of the peaks to allow for the increase in peak width which will result from column overloading.

If we consider the equation for resolution, R_s, ie.

$$R_s = \frac{1}{2} \frac{(\alpha-1)}{(\alpha+1)} \cdot \frac{\bar{k}'}{(1+\bar{k}')} \times N^{\frac{1}{2}}$$

(i) Selectivity — (ii) Peak Capacity — (iii) Column Efficiency

we see that resolution depends on selectivity, peak capacity

and column efficiency. Increasing the resolution by any of these means will enable a larger amount of sample to be loaded onto the column before serious overlapping of the peaks occurs.

The first requirement for adequate separation between the peaks is to ensure that the retention of the peaks is sufficient to give k' of between 1 and 10, and this is achieved by altering the strength of the mobile phase. The increase in solute retention also means that the peak volume increases and that therefore the concentration of the peak maximum decreases which, according to De Jong *et al.*[4] allows for a further increase in column loadability. It should be pointed out that the fraction of the material present in the stationary phase is equal to $\frac{k'}{1+k'}$, of the total amount in the column and that this fraction changes little when k' exceeds ∿2. As the overload in the stationary phase is more than in the mobile phase, where the fraction of material present is equal to $\frac{1}{1+k'}$, , the conclusion reached by De Jong *et al.*[4] seems unlikely to be true. This topic will be considered more fully in Chapter 6.

An even greater separation effect can be achieved by adjusting the selectivity (α) of the eluent through altering the composition of the mobile phase while keeping the eluent strength the same.

Finally, resolution can be improved by increasing the efficiency (N) of the column by increasing the column length, by coupling several columns together in series or by using recycle. Such techniques will be discussed in more detail in the next section. In practice, however, the increased cost either in money, time or pressure requirements may make this a less attractive proposition and it is usually only resorted to if

(i) Analytical separation

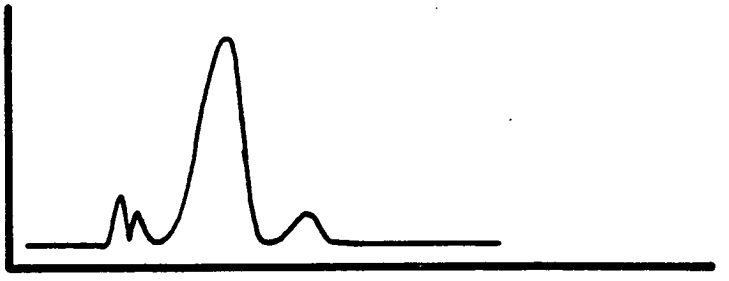

(ii) Increased resolution

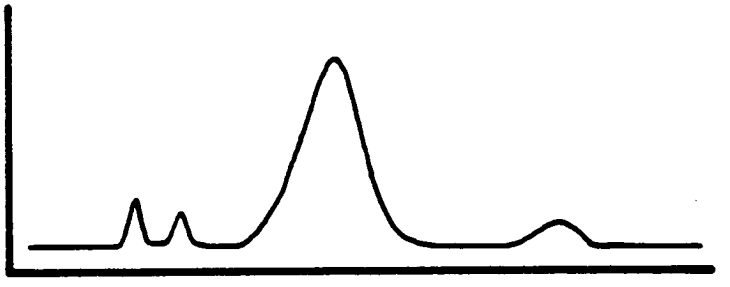

(iii) Loading limit

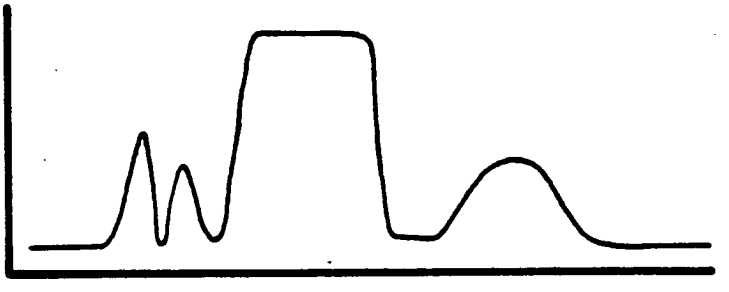

(iv) Overload for yield

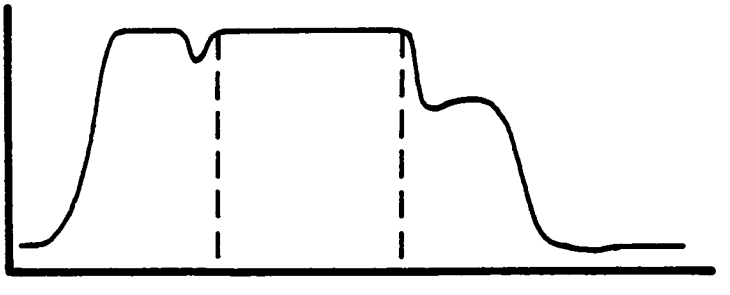

Figure 5.11 A schematic representation showing the various stages of a preparative scale-up for a single major component.

both retention (k') and selectivity (α) have already been optimised and an increase in resolution is still required.

Once the resolution between the peaks has been sufficiently increased, the next stage is to determine the loading limit of the column which is determined as being the point at which the overloaded peaks threaten to merge or overlap. It is generally agreed that this is best carried out by increasing the volume of a dilute solution of the sample (∿1% w/v) rather than by increasing the concentration of the solution since the latter leads to localized overloading of the stationary phase. Ideally, the sample should be made up in the mobile phase but where sample solubility is low, this may not be possible. Where low solubility is a problem, it may be possible to dissolve the sample in another solvent of identical chromatographic strength but with different solvating power[75] thus increasing sample solubility. Samples should not be made up in solvent stronger than the mobile phase since large injection volumes would affect the equilibration of the column and cause severe loss of resolution.

If a greater yield of product is required, then the column can be overloaded beyond the loading limit thus increasing the amount of isolated material collected per unit time, otherwise known as the throughput. Although the peaks overlap, a centre-cut of a major peak can be collected which is of quite high purity. The various stages in the optimisation of a preparative separation are illustrated in figure 5-11.

Having established the maximum overload for the analytical column, the next step is to move onto a preparative column,

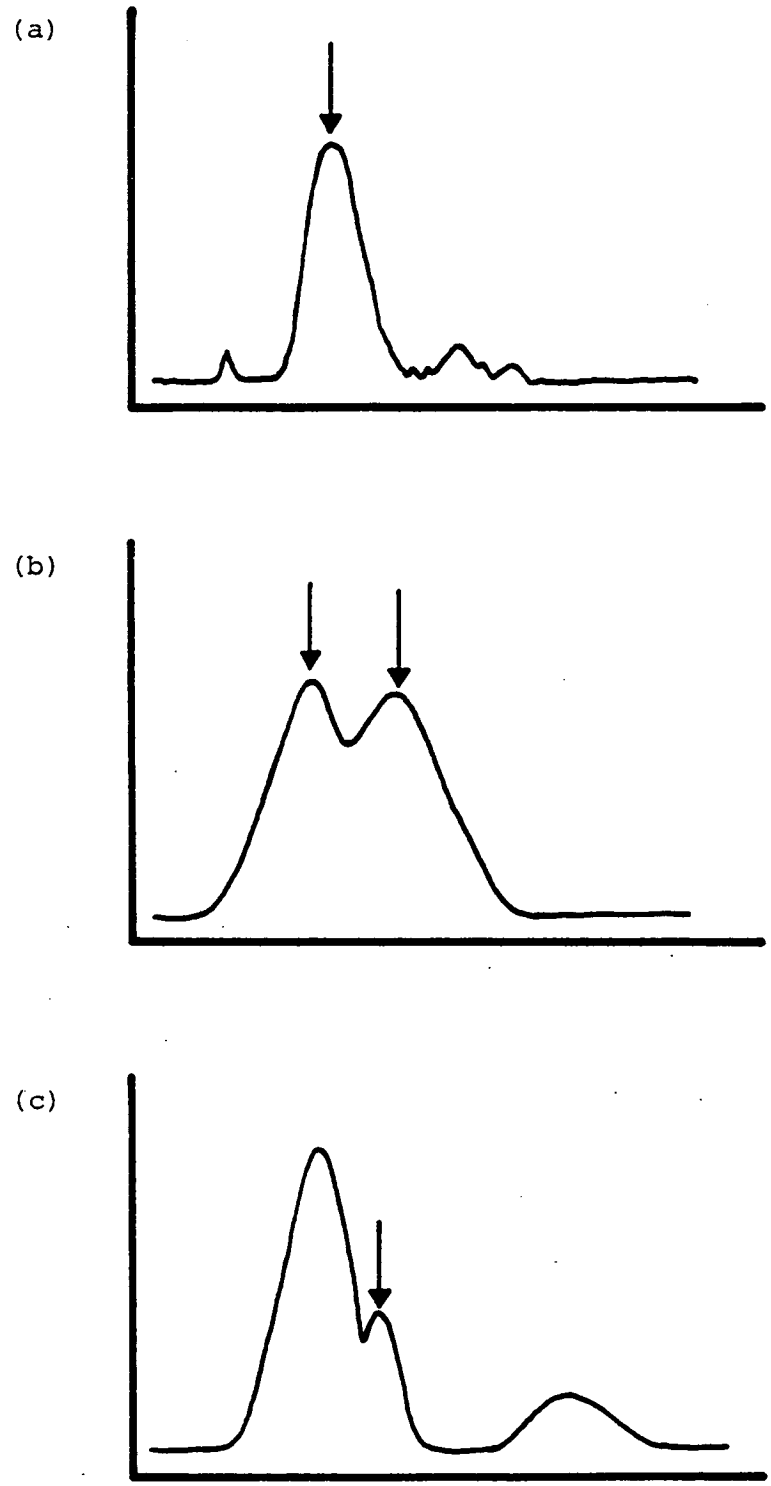

Figure 5.12 Schematic representation showing the various types of preparative - scale problems. (a) The desired component is present as a single major peak. (b) Two or more major components present. (c) The minor component is the desired component.

though in some cases the amounts separated on the analytical column may suffice. Choice of the preparative column used will depend on the problem at hand and the amount of isolated material required. If a separation requires high resolution and high sample capacity, then a longer column may be required although this will increase the separation time. In many cases it is sufficient to increase the diameter of the column only, thus increasing the sample throughput ie. the amount separated per unit time. Since the retention time of a solute is dependent on the linear velocity of the eluent where the flow rate is given by

flow rate = linear velocity x cross-sectional area

then in order to achieve the same mobile phase linear velocity and hence the same retention time when scaling up from an analytical to a preparative column of the same length, an increase in the volumetric flow rate proportional to the square of the column radius (r^2) is required.

Each chromatographic problem can be classified as being of one of three basic types as illustrated in figure 5-12 where either

a) the desired component is a single major component,

b) the desired component is a trace or minor component, or

c) the desired component is one or both of two closely eluting major peaks.

Each of these above situations requires a slightly different approach.

Where the desired material is a single major component,

(i) Loading limit

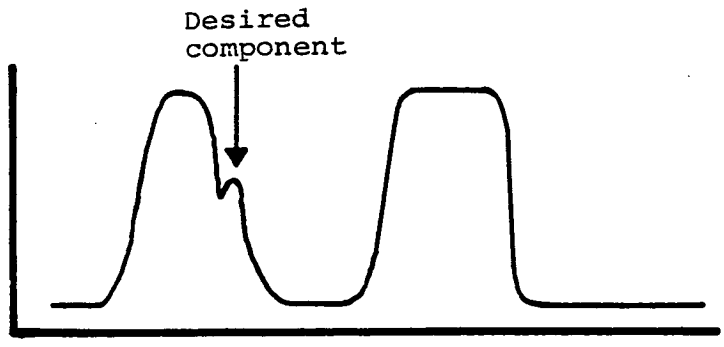

(ii) Overload for yield

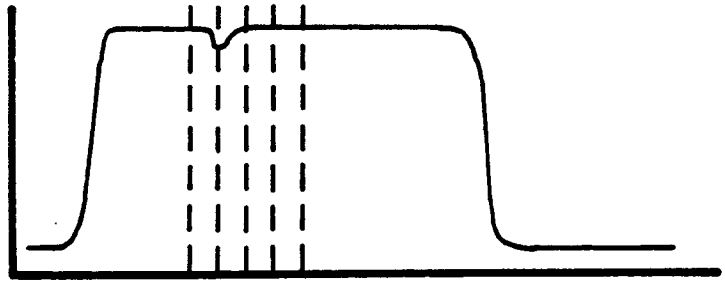

(iii) Selected fractions pooled and concentrated

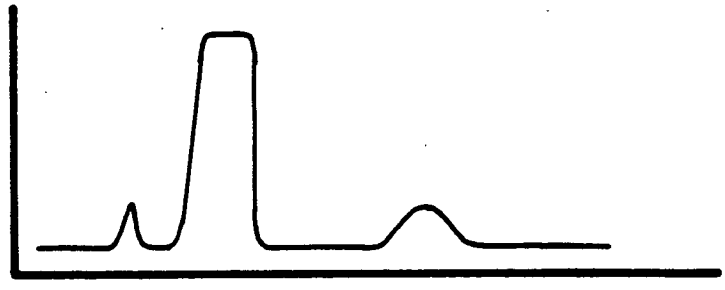

Figure 5.13 The stages involved in the preparative scale-up for a minor component.

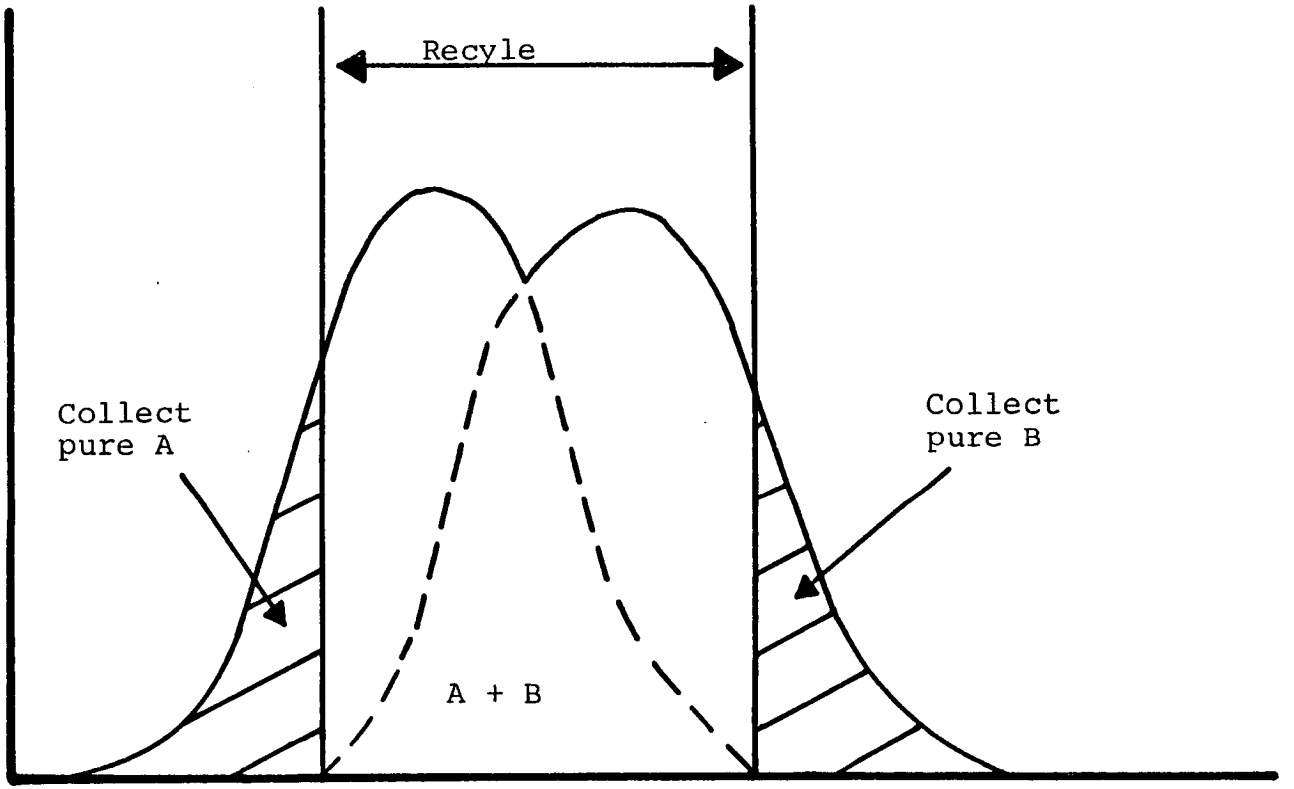

Figure 5.14 Recovery of two incompletely resolved components.

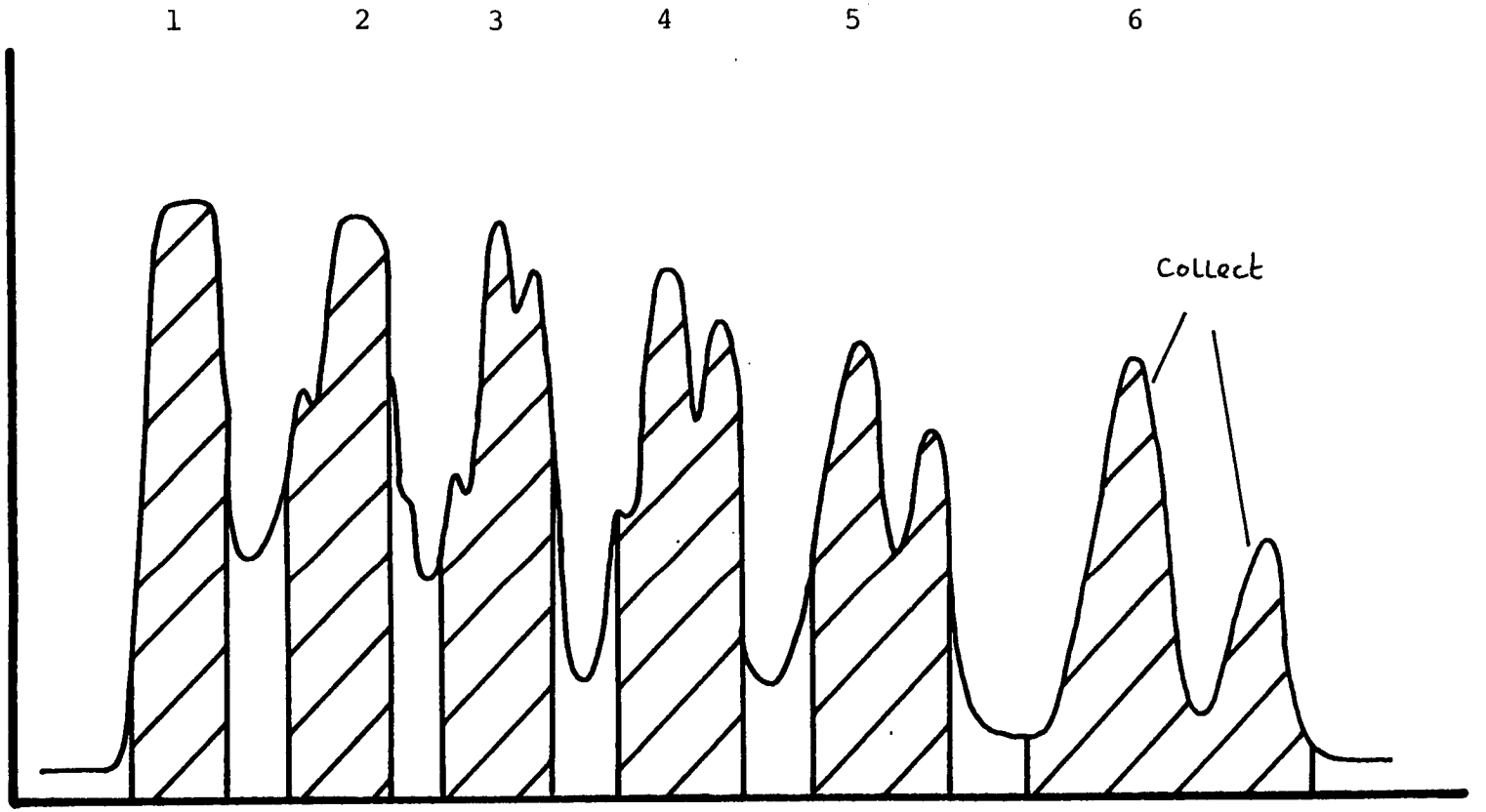

Figure 5.15 Schematic representation of the recycle technique for separating two incompletely resolved peaks. The shaded area is collected and reclycled down the column, except for the two resolved peaks at the end which are collected.

resolution is increased as described previously and the loading limit is established. At this stage, collection of the desired material can be made if the separation produces the required amount of material. Alternatively, if more material is required, the column can be further overloaded so that the peaks overlap and a centre-cut made (see Figure 5-11) which will still produce material of high purity and will result in greater throughput.

Where a minor or trace material is the desired component, as shown in figure 5-13, the first stage involves an enriching step. The loading of the column is first taken up to the loading limit and is then overloaded to increase throughput and yield. A centre-cut is then taken around the elution time as established from the loading limit. If more than one run is carried out, the collected fractions are pooled and then concentrated prior to being passed down the column again. The desired material is now a major component and is now treated in the same way as the first example.

The separation of two major, closely eluting components presents a different problem. In this case, increasing the amount of sample loaded onto the column will result in serious overlapping of the two peaks as shown in figure 5-14. However, shaving off the front and tail areas of the peaks will yield small amounts of pure components and if more material is required, the centre portion of the peaks can be recycled back through the column again as illustrated in figure 5-15. This procedure can be repeated until enough material has been collected. Because the effective column length and therefore the number

of plates which are produced has been increased, recycle increases the resolution between the peaks. Also, the fact that some of the component is removed at the end of each pass also helps increase resolution.

5.5 Techniques in Preparative Chromatography

There are various techniques which can be employed to increase the resolution and hence the throughput of a preparative separation. If in the development of the preparative separation resolution has been increased by the optimisation of eluent strength (k') and the eluent composition (α), then further improvement in resolution can only be brought about by an increase in the effective column length by either recycling the eluate back down the same column, by connecting a number of columns in series or by column switching.

5.5.1 Recycle

The technique of recycle involves taking all or part of the eluent as it leaves the detector and passing it back down the column again. This step can be repeated as often as required and the progress of the separation is monitored each time it passes through the detector. In this way high sample throughput can be achieved since the column can be severely overloaded, while keeping solvent consumption, column length, pressure requirements and cost to a minimum.

The recycle of partially resolved components can either be carried out using a secondary pump or using an automatic switching valve system.

Recycle chromatography requires that the extra band broadening, especially that caused by the switching valve or secondary pumping system, should be kept to a minimum and should be small relative to the band spreading caused by the column itself. Fortunately, since preparative separations give rise to quite large peak

volumes this is not difficult to achieve. Where a secondary pumping system is being used, this should be a small volume reciprocating pump so as to avoid any remixing of the components which are being recycled.

Exclusion chromatography[76] is well suited to the recycle technique since all of the components elute within a fixed volume, which is determined by the column void volume, V_o. Here the maximum attainable K value is 1 where

$$V_R = V_o + K V_p$$
$$= V_o (1+k")$$

where V_R is the retention volume, V_o is the void volume ie. the total volume of the mobile phase, K is the distribution coefficient and V_p is the total volume of the stationary phase ie. solvent within the porous packing. The phase capacity ratio k" is different to k' in other forms of chromatography.
In sorption chromatography, automatic recycle, where all of the eluent is recycled, can only be achieved if the individual solutes have low k' values (<2). This is because there is an increase in band broadening during each recycle step and eventually the volume of eluent required to elute the components is greater than the column void volume. At this stage, the beginning of one cycle starts to overlap with the end of the previous cycle and cross-contamination of the components occurs thus defeating the whole object of the technique. This problem can, however, be overcome by shaving off the extreme front and back areas of the partially resolved peaks which contain the pure components and then recycling the centre-cut section (see

figure 5-15). This reduces the overall increase in band spreading and allows for more recycle steps before the cycles start to overlap.

By careful use of overloading, fraction cutting and recycle therefore, throughput can be increased considerably[77,78] and examples of this technique can be found in several papers.[7,79]

5.5.2 Column Switching

Column switching, or multidimensional chromatography as it is also known as, is a very useful technique to enhance the separation of multicomponent samples, and an excellent review of this technique has been given by Majors.[80] The technique involves transferring selected fractions as they elute from one column to one or more secondary columns thus improving the resolution and increasing the loadability of the original column. As well as coupling two or more liquid chromatographic columns together (LC/LC), it is also possible to combine liquid chromatography with gas chromatography (LC/GC), although the latter is not very useful for preparative separations. When using LC/LC it is possible to combine different modes of liquid chromatography to improve the separation eg. exclusion chromatography followed by adsorption or reversed-phase chromatography, or to use columns operating in the same mode but using eluents of different strength and selectivity.

However, in all cases of LC/LC and LC/GC care must be taken that the solvents used are miscible and that the eluent from the first column is not stronger than the eluent used in the second column otherwise in either situation, additional band spreading will occur and resolution will be reduced.

The problem of solvent incompatibility can be overcome when employing "off-line" column switching which involves the collection of fractions either manually or automatically as they emerge from the detector of the first column followed by re-injection into the second column. If the two eluents are incompatible then the eluent can be removed from the fractions collected after the first column by evaporation and the material redissolved in an eluent suitable for the second column. Alternatively, the sample can be extracted into an immiscible solvent.

Column switching can also be performed in an 'on-line' mode where the columns are connected via a pneumatically operated switching valve which directs selected fractions either onto another column or to waste.

There are advantages and disadvantages in both the off-line and on-line methods. From a preparative point of view, it is easier to increase sample throughput with the on-line method since it is much quicker to use and can be automated although it does require more complicated switching valves. The off-line method is much easier to do and it is possible to concentrate trace or minor solutes from large volumes before reinjection onto the next column. Large volumes containing trace solutes can also be dealt with using an on-line column switching technique which involves on-column concentration where the solvent used in column 1 is weaker than that used in column 2.

A novel form of column switching technique called Boxcar Chromatography has been introduced by Snyder *et al.*[37] This technique is useful for increasing the sample throughput for repetitive separations or for situations where the desired

component is present in a complex mixture. Basically the technique involves continuous multiple injection of the sample on a short first column at predetermined intervals. The eluent is allowed to flow to waste via a switching valve until the desired peak, or peaks, begin to come off whereupon the eluent is directed to a second and much longer column. Once the desired peaks have been redirected in this way, the remainder of the solutes which are not desired are removed to waste. The injection is then repeated and more of the desired components are directed onto the second column. As column 2 is much longer than column 1, the first band of the material will not have moved very far through the second column compared to its elution through the first. In this way several separate sample loads can be separated on the second column simultaneously thus increasing the throughput of the column system considerably.

REFERENCES

Chapter 5

1. J.P. Wolf; Anal.Chem., 45 (1973), 1248.
2. C.E. Reese in "Techniques in Liquid Chromatography", C.F. Simpson (Editor), Wiley Heyden 1976, p.98.
3. A. Wehrli; Z.Anal.Chem., 277 (1975), 289.
4. A.W.J. De Jong, H. Poppe and J.C. Kraak; J.Chromatogr., 148 (1978), 127.
5. J.J. De Stefano and H.C. Beachell; J.Chromatog.Sci., 8 (1970), 435.
6. L.R. Snyder; Anal.Chem., 39 (1967), 698.
7. J.N. Little, R.L. Cotter, J.A. Prendergast, and P.D. McDonald; J.Chromatogr.,126 (1976), 439.
8. C.H. Eon; J.Chromatogr., 149 (1978), 29.
9. E. Godbille and P. Devaux; J.Chromatog.Sci., 12 (1974), 564.
10. E. Godbille and P. Devaux; J.Chromatogr., 122 (1976), 317.
11. F. Gasparinni,S. Cacchi, L. Gaglioti, D. Misiti, and M. Giovannoli; J.Chromatogr., 194 (1980), 239.
12. C.E. Reese in "Techniques in Liquid Chromatography", C.F. Simpson (Editor), Wiley Heyden 1982, p.99.
13. M.J. Pettei, F.G. Pilkiewicz, and K. Nakanishi; Tetrahedron Lett., (1977), 2083.
14. M.A. Adams and K. Nakanishi; J.Liq.Chromatog., 2 (1979), 1097.
15. S.S. Singer and G.M. Singer; J.Liq.Chromatog., 2 (1979), 1219.
16. W.M. Waddel, P.M. Dawson, D.L. Hopkins, K.L. Rach, M. Uemura, and J.L. West; J.Liq.Chromatog., 2 (1979), 1205.

17. J.H. Knox and J.F. Parcher; Anal.Chem., 41 (1969), 1599.

18. J.C. Sternberg and R.E. Poulson; Anal.Chem., 36 (1964), 1492.

19. B. Coq, G. Cretier, and J.L. Rocca; J.Chromatogr., 186 (1979), 485.

20. A.W.J. De Jong, H. Poppe, and J.C. Kraak; J.Chromatogr., 148 (1978), 127.

21. M. Brezina, L. Vodicka, J. Triska, and J. Kriz; J.Chromatogr., 219 (1981), 179.

22. R.A. Wall; J.Liq.Chromatog., 2 (1979), 775.

23. M. Martin and G. Guichon; Chromatographia 10 (1977), 194.

24. H. Elgass, H. Engelhardt, and I. Halasz; Z.Anal.Chem., 294 (1979), 97.

25. R.M. Cassidy, D.S. LeGay, and R.W. Frei; Anal.Chem., 46 (1974), 340.

26. T.J.N. Webber and E.M. McKerrell; J.Chromatogr., 122 (1976), 243.

27. P.A. Bristow, P.N. Brittain, C.M. Rilley, and B.F. Williamson; J.Chromatogr., 131 (1977), 57.

28. M. Broquaire; J.Chromatogr., 170 (1979), 43.

29. D. Bar, M. Caude and R. Rosset; Analusis 4 (1976) 108.

30. M. Kaminski, J. Klawiter, and J.S. Kowalczyk; J.Chromatogr., 243 (1982), 225.

31. R.E. Majors: J.Ass.Offic.Anal.Chem., 60 (1977), 186.

32. S.T. Sie and N. van den Hoed; J.Chromatog.Sci., 7 (1969), 257.

33. J. Kirkland; J.Chromatog.Sci., 10 (1972), 129.

34. H. Beachell and J.J. De Stefano; J.Chromatog.Sci., 10 (1972), 481.

35. J. Klawiter, M. Kaminski, and J.S. Kowalczyk; J.Chromatogr., 243 (1982), 207.

36. J.J. De Stefano and J.C. Beachell; J.Chromatog.Sci., 10 (1972), 654.

37. L.R. Snyder and J.J. Kirkland, 'Modern Liquid Chromatography' Wiley Interscience, New York, 1974.

38. J.J. Kirkland; J.Chromatog.Sci., 7 (1969), 7.

39. K. Prusiewicz, M. Kaminski, and J. Klawiter; J.Chromatogr., 238 (1982), 232.

40. R.P.W. Scott and P. Kucera; J.Chromatogr., 119 (1976), 467.

41. J.J. Kirkland, W.W. Yau, H.J. Stoklosa, and C.H. Dilks; J.Chromatog.Sci., 15 (1977), 303.

42. J. Klawiter, M. Kaminski, and J.S. Kowalczyk; J.Chromatogr., 243 (1982), 207.

43. J.C. Giddings and E.N. Fuller; J.Chromatogr.,7 (1962), 255.

44. E. Geeraert and M. Verzele; Chromatographia, 12 (1979), 50.

45. J. Asshauer and I. Halasz; J.Chromatog.Sci., 12 (1974), 139.

46. B. Coq, C. Gonnet, and J.L. Rocca; J.Chromatogr., 106 (1975), 249.

47. J.J. Kirkland; J.Chromatog.Sci., 9 (1971), 206.

48. R.G. Berg and H.M. McNair; J.Chromatogr., 131 (1977), 185.

49. I. Halasz, R. Endele, and J. Asshauer; J.Chromatogr., 112 (1975), 37.

50. R.P.W. Scott and P. Kucera; J.Chromatog.Sci., 12 (1974), 473.

51. K.K. Unger, R. Kern, M.C. Ninon, and K.F. Krebs; J. Chromatogr.,99 (1974), 435.

52. W. Strubert; Chromatographia, 6 (1973), 50.

53. R.E. Majors; Anal.Chem., 44 (1972), 1772.

54. J.J. Kirkland; J.Chromatog.Sci., 10 (1972), 593.

55. A.W.J. De Jong, H. Poppe, and J.C. Kraak; J.Chromatogr., 209 (1981), 432.

56. L.R. Snyder "Modern Practice of Liquid Chromatography" (J.J. Kirkland, Ed.), Wiley Interscience, New York 1971, p.205.

57. J.J. Kirkland; J.Chromatog.Sci., 10 (1972), 129.

58. R.E. Majors; J.Chromatog.Sci., 11 (1973), 88.

59. R. Endele, I. Halasz, and K. Unger; J.Chromatogr., 99 (1974), 377.

60. H. Englehardt, J. Asshauer, U. Neue, and N. Weigand; Anal.Chem., 46 (1974), 336.

61. J.C. Kraak, H. Poppe, and F. Smedes; J.Chromatogr., 122 (1976), 147.

62. R.E. Majors "Advances in Chromatography" 1973, A. Zlatkis, Editor, Toronto Symposium.

63. C.J. Little, Dale, Ord and Martin; Anal.Chem., 49 (1977), 1311.

64. M. Broquaire; J.Chromatogr.,170 (1979), 43.

65. D. Bar, M. Cande, and R. Rosset; Analusis, 4 (1976), 118.

66. H.P. Keller, F. Erni, H.R. Linder, and R.W. Frei; Anal.Chem., 49 (1977), 1958.

67. H.R. Linder, H.P. Keller, and R.W. Frei; J.Chromatog.Sci., 14 (1976), 234.

68. J.J. Kirkland; J.Chromatog.Sci.,7 (1969), 361.

69. J.C. Liao and J.L. Ponzo; J.Chromatog.Sci., 20 (1982), 14.

70. P. Bristow; J.Chromatogr., 149 (1978), 13.

71. D. Bar, M. Caude, and R. Rosset; Analusis, 4 (1976), 108.

72. B. Coq, C. Gonnet, and J.L. Rocca; J.Chromatogr., 106 (1975), 249.

73. G.E. Berendsen, R. Regouw, and L. De Galan; Anal.Chem., 51 (1979), 1091.

74. M. Caude, Le X. Phan, B. Terlain, and J.P. Thomas; J.Chromatog.Sci., 13 (1975), 249.

75. L.R. Snyder; J.Chromatogr., 92 (1974), 223.

76. K.E. Conroe; Chromatographia, 8 (1975), 119.

77. K.F. Bombaugh and R.F. Levangie; J.Chromatog.Sci., 8 (1970), 560.

78. J.R. Conder and M.K. Shinkgari; J.Chromatog.Sci., 11 (1973), 525.

79. T. Yoshida, C.K. Shu, and E.T. Theimer; J.Chromatogr., 137 (1977), 461.

80. R.E. Majors; J. Chromatog.Sci., 18 (1980), 571.

CHAPTER 6

THE EFFECT OF INCREASED SAMPLE LOADING IN PREPARATIVE LIQUID CHROMATOGRAPHY

Chapter 6. The Effect Of Increased Sample Loading In Preparative Liquid Chromatography

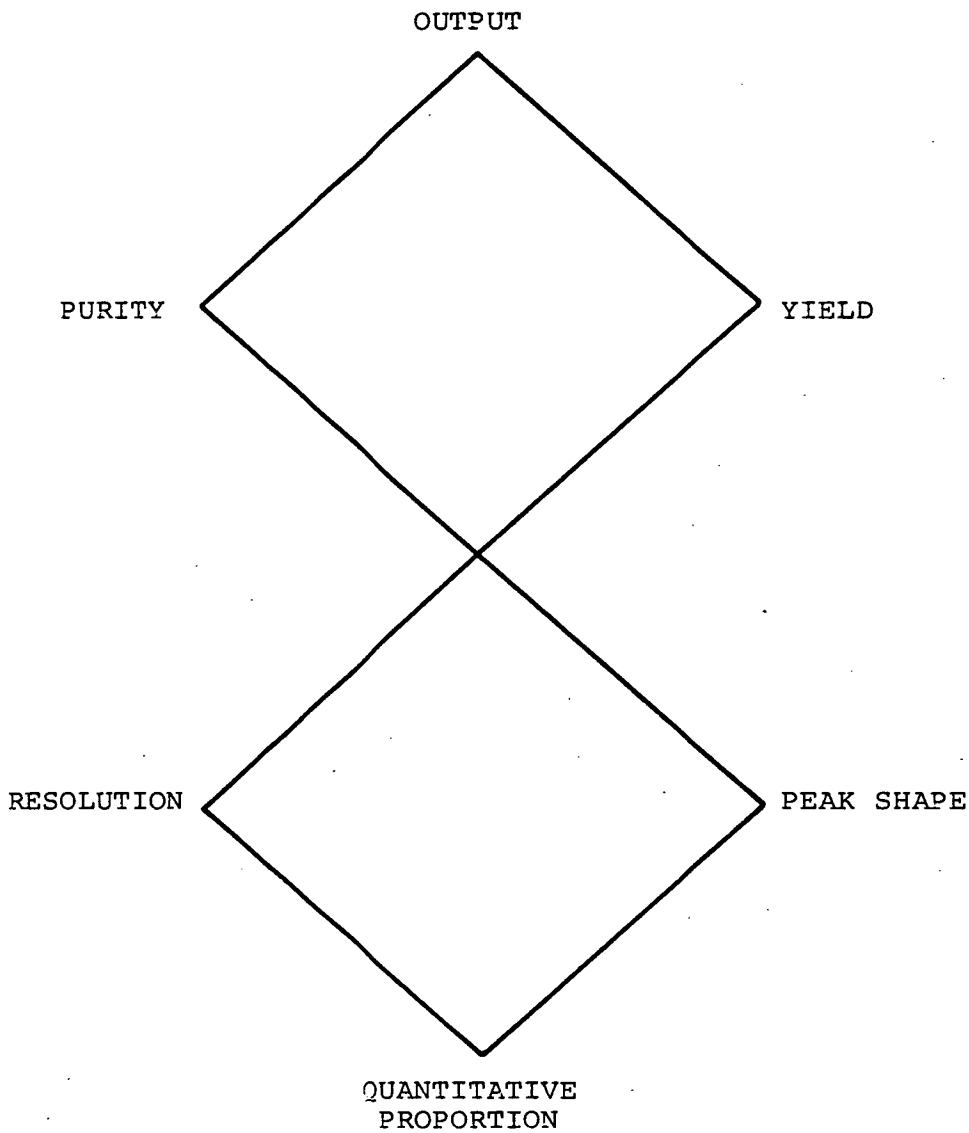

Figure 6.1 The salient features involved in a preparative separation (Reproduced from reference 1).

THE EFFECT OF INCREASED SAMPLE LOADING IN PREPARATIVE LIQUID CHROMATOGRAPHY

6.1 Introduction

A chromatographic column behaves differently under overload conditions compared to when it is operating under non-overload conditions and these factors should be exploited to make the most efficient use of the preparative system.

Wehrli *et al.*[1] have described the salient features involved in a preparative separation as shown in figure 6.1. This illustrates the dependence of *output*, *purity* and *yield*, which are the major *product* characteristics, on *resolution*, *peak shape* and *quantitative proportion*, which are the major *process* characteristics.

The quantitative proportion is the relative amounts of desired components present in the original sample. For a given value of resolution, R_s, band overlap becomes more serious when one of the components is present in much larger quantity than the other. Therefore, in such a case, the resolution required to achieve a specific purity and yield is greater than if the components were present in similar quantities.

The various aspects important in preparative liquid chromatography will now be discussed.

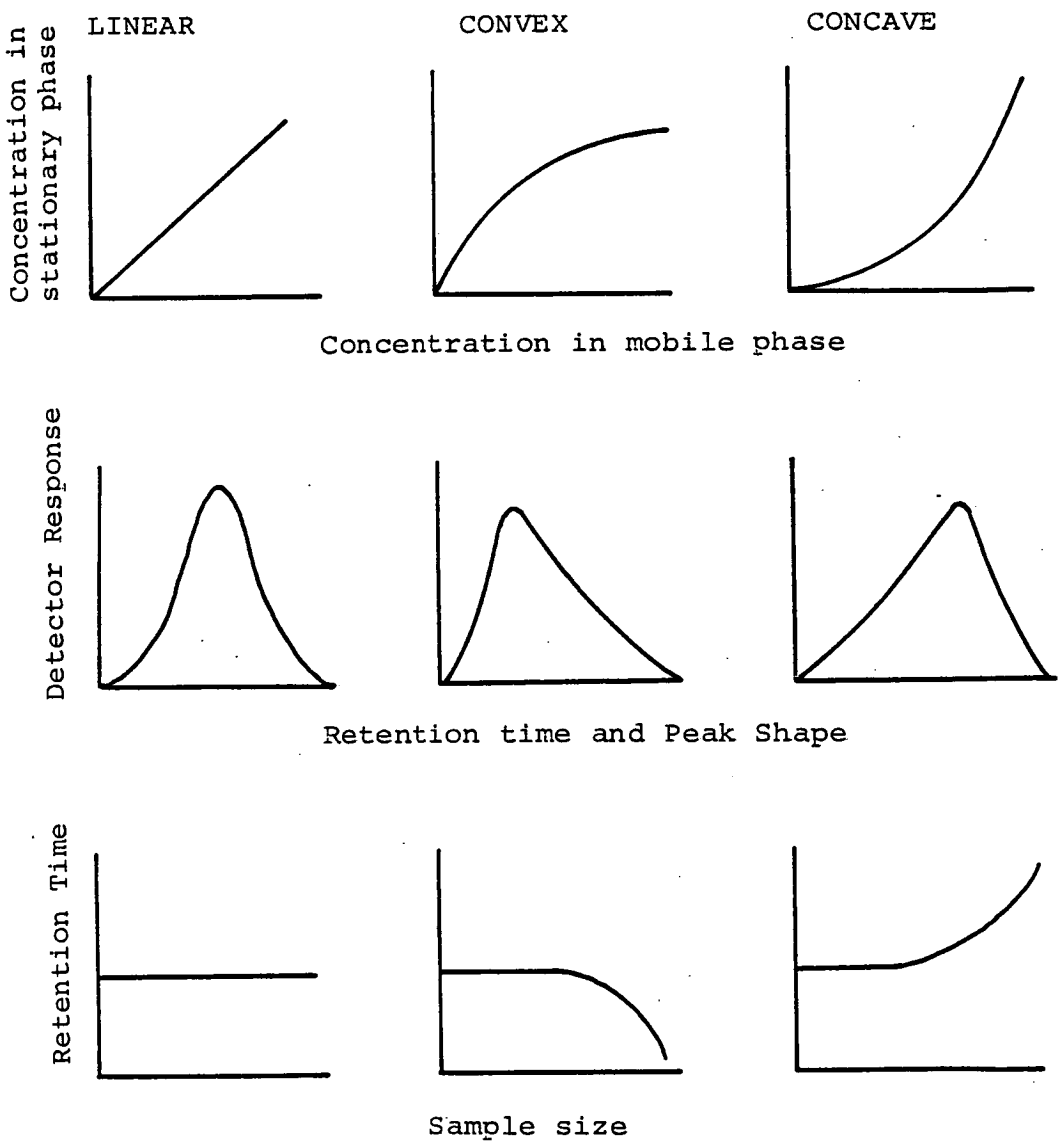

Figure 6.2 Three basic types of distribution isotherm showing the effect on peak shape and retention time. (Reproduced from reference 2).

6.2 Isotherm Non-linearity

The shape of the distribution isotherm of solutes, and in particular the linear range of the isotherm, plays an important part in determining the maximum amount of sample which can be loaded onto the column for a particular separation. In general,[2] the isotherm is usually either convex or concave in shape and is seldom linear. Figure 6.2 illustrates the shape of the chromatographic peaks produced by the different distribution isotherms, and also the effect of the sample size on the peak retention.

The availability of very sensitive detectors has meant that, for analytical-scale separations, samples of low concentration and low volume can be injected onto the columns. Such low sample loads almost always fall in the linear part of the distribution isotherm.

In preparative scale liquid chromatography, however, much larger amounts of sample are loaded onto the column. Since the linear range of the distribution isotherm is limited and does not usually extend into high solute concentrations in the mobile phase, such large sample loads generally fall into the non-linear part of the distribution isotherm.

As the amount of sample loaded onto the column is gradually increased from very low loadings, while still remaining in the linear range of the distribution isotherm, the column efficiency, N, the retention volume, V_R and the phase capacity factor, k', will all remain constant. Within the linear range of the distribution isotherm, peak broadening is due entirely to kinetic considerations (see Chapter 4). As the sample loading is further increased such that the distribution isotherm starts

to deviate from linearity, column efficiency begins to drop and, in the case of a convex distribution isotherm, the retention volume and the phase capacity ratio start to decrease. Eventually, as the loading is further increased, a point is reached where the column efficiency, N, begins to drop increasingly rapidly with load as does V_R and k'. This corresponds to the point at which the column ceases to be operating under non-overload conditions. Such overloading conditions correspond to working in the non-linear part of the distribution isotherm where peak broadening is due to a complex mixture of both kinetic and thermodynamic effects. It is because of this, and the fact that the linear range of the distribution isotherm depends on the solutes in question as well as on the stationary and mobile phase systems chosen that makes it impossible to lay down exact general rules for devising an optimum preparative separation. This problem becomes even more complex when the column is overloaded with more than one component where these materials travel together down the first part of the column and then gradually separate.

The extra peak dispersion caused by thermodynamic effects, as opposed to the usual band broadening caused by kinetic effects, produces asymmetric peaks which are usually tailed. As a result of isotherm non-linearity, the phase capacity ratio, k', is also a function of the concentration.

Under conditions of overload, the definition of HETP, or H, is no longer valid since the peaks are not gaussian in shape. However, as we shall see in Section 6.6.3, N is still useful as a measure of peak width even if N is no longer proportional to the column length, ℓ.

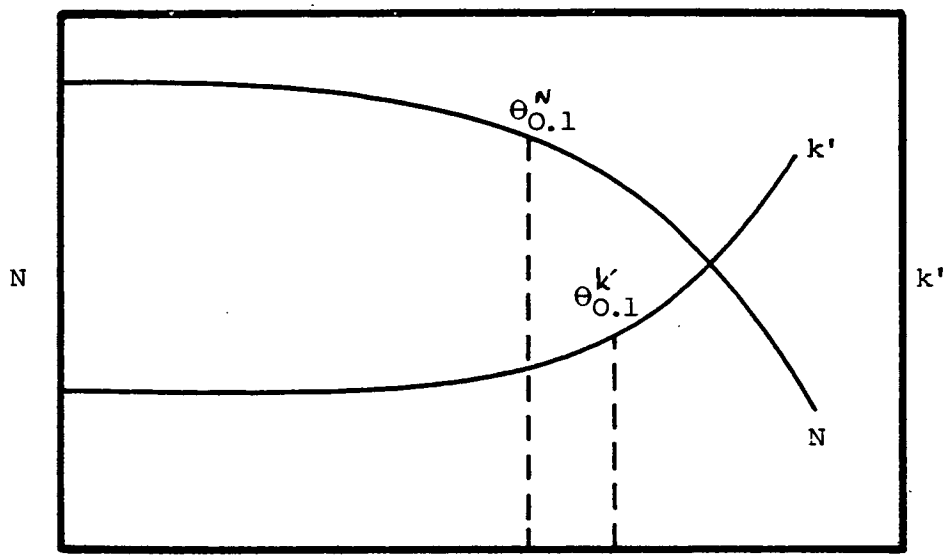

Figure 6.3 The dependence of N and k' on sample load.

The extra band broadening due to column overloading affects the resolution between adjacent peaks and therefore affects both the amount of sample which can be loaded onto the column ie. the loadability of the column and the sample throughput. With difficult separations where adjacent peaks are closely eluting ie. where the selectivity factor α is low, the problem due to operating in the non-linear part of the isotherm is more acute than if the two peaks were well separated since the latter situation is more able to accommodate additional peak broadening before serious peak overlapping occurs.

6.3 Linear Capacity of the Stationary Phase

The sample capacity of a column is described by the linear capacity limit, $\theta^{k'}_{0.1}$, of the stationary phase which is defined by Snyder[3] as being that *weight of sample per gram of stationary phase which causes a 10% decrease in the phase capacity ratio, k'*, from its original constant value at low loading. Alternatively, the linear capacity limit, $\theta^{N}_{0.1}$, can be defined as being that *weight of sample per gram of stationary phase which causes a 10% decrease in the plate number, N*, obtained at low load levels. The values obtained using these two definitions, ie. $\theta^{k'}_{0.1}$ and $\theta^{N}_{0.1}$ are generally not the same, as illustrated in figure 6.3, since N nearly always starts to decrease at much lower loading levels than k' does. For efficient columns, $\theta^{N}_{0.1}$ is less than $\theta^{k'}_{0.1}$. Only for very low efficiency columns is $\theta^{N}_{0.1}$ equal to or greater than $\theta^{k'}_{0.1}$. Either parameter can be used, but when considering the loss of resolution caused by column overloading, the linear capacity defined in terms of N, ie. $\theta^{N}_{0.1}$, is the more relevant. However, a disadvantage of

using $\theta^{N}_{0.1}$ is that, unlike $\theta^{k'}_{0.1}$, it will depend upon the number of plates, N, to which the column is equivalent and possibly also on the particle size, dp.

In general, $\theta^{N}_{0.1}$ has been found to be around a few hundred micrograms per gram of adsorbent while Majors[4] found a value for $\theta^{k'}_{0.1}$ of 1.4 mg/g stationary phase, a factor of ten times more than $\theta^{N}_{0.1}$.

De Jong *et al.*[5] have shown that differences in the linear range of the distribution isotherm can occur for different silica gel adsorbents. Particle size was found to have little influence on the linear capacity limit while materials with larger surface areas had larger linear capacity limits and hence greater sample capacities. Different materials with similar surface areas were found to have similar linear capacities. It appears therefore that, to a first approximation, it is the linear range capacity per unit surface area which is constant rather than the linear range capacity per gram of adsorbent.

In the case of chemically bonded materials, only slight differences in the linear capacity were found for different materials of the same chain length. However it was found that the linear capacity range decreased with increasing chain length which is contrary to what might be expected for a separation process based on the partition of solutes between the mobile and stationary phases.

De Jong *et al.*[5,6] found that the linear capacity, or the specific loadability as they called it, was dependent on the column plate number, N, and not on the amount of the stationary phase present. They reported that identical tubes packed with the same amount of stationary phase but with different particle sizes to produce different numbers of plates, N, resulted in

columns with different linear capacity values, $\theta^{N}_{0.1}$. They also observed that for tubes of different sizes packed with different particle sizes but with similar efficiencies the linear sample capacity values, $\theta^{N}_{0.1}$, were similar. It is worth noting that in the latter situation where similar linear capacities were produced, the reduced column length as given by L/dp was almost the same for each column while in the former situation the reduced length was different. De Jong *et al.* concluded that it is the concentration of a solute *i* in the mobile phase that is the crucial factor in determining column overloading, and that for low plate numbers more solute can be placed on the column before $C^{max}_{i,m}$ is reached, where $C^{max}_{i,m}$ is the maximum concentration of a solute *i* in the mobile phase at the column outlet above which the column is said to be overloaded. This line of argument, which does not appear to be sound, is discussed more fully in section 6.6.3.

It has been suggested by Done[13] that reversed phase materials have a greater linear capacity and are less affected by mass overload than adsorbent materials, but this has not been substantiated by Wall[19] who found no difference in the linear capacity between the two types of material over a narrow range of eluent velocities.

6.4 Factors Affecting Column Loadability and Sample Throughput

The loadability, or loading capacity, of a column is defined as the *maximum amount of sample which can be loaded onto a column at any one time while still maintaining a specified resolution of particular solutes under the chosen chromatographic conditions.*

Sample throughput is defined as being the *amount of material of specified purity collected per unit time.*

The main objective in preparative liquid chromatography therefore is to optimize the column loadability in order to produce the maximum sample throughput for a given resolution and purity specifications, and at minimum cost.

Scott and Kucera[12] have derived an equation for columns which are not overloaded, ie. which are operating in the linear region of the distribution isotherm, which shows the effect which various parameters have on the maximum amount of sample, $M_{i,max}$, that can be loaded onto a column without losing any efficiency. Their argument is based on the fact that $M_{i,max}$ is directly proportional to the plate volume and to the square root of the efficiency ie.

$$M_{i,max} = A \sqrt{n} \ (v_m + Ka_s) \qquad (6-1)$$

where A = constant,

n = column efficiency,

v_m = volume of mobile phase per plate,

K = distribution coefficient of the solute,

and a_s = surface area of the adsorbent per plate.

The retention volume, V_R, of a solute can be expressed as

$$V_R = n \ (v_m + Ka_s) \qquad (6-2)$$

By substituting equation (6-2) into equation (6-1) we have

$$M_{i,max} = \frac{A.V_R}{\sqrt{n}} \qquad (6-3)$$

Scott and Kucera then considered the case of a well-retained solute where $v_m << Ka_s$, ie.

$$V_R \rightarrow nKa_s$$

By considering V_R over the whole of the column length, then

$$V_R \rightarrow K\, dV\, A_s = Kd\ \ \pi r^2 \ell\, A_s \qquad (6\text{-}4)$$

Equation (6-3) can therefore be expressed as

$$M_{i,max} = \frac{A\ K\ d\ \pi r^2\ \ell\ A_s}{\sqrt{n}} \qquad (6\text{-}5)$$

where d = packing density of the adsorbent ($g.ml^{-1}$),

V = column volume,

r = column radius,

ℓ = column length,

and A_s = surface area of the adsorbent (m^2g^{-1})

This represents the maximum mass of sample which can be loaded onto a column such that the minimum resolution required between two solutes is achieved.

By making the assumption that peak dispersion for well retained peaks at a constant flow rate is influenced mainly by the resistance to mass transfer, ie.

$$H \approx \alpha dp^2$$

where α is a constant and dp is the particle diameter, and considering the general equation for HETP, ie.

$$H = \frac{\ell}{n}$$

then equation (6-5) was expressed as

$$M_{i,max} = A\ K\ d\ \pi r^2 \ell\ A_s \left(\frac{\alpha dp^2}{\ell}\right)^{\frac{1}{2}} \qquad (6\text{-}6)$$

In the more general situation where overloading of the column may take place, the maximum throughput which can be obtained for a particular separation problem will depend upon the following different factors.[9]

(i) Geometric and kinetic factors, such as column dimensions, particle size, injection mode and eluent velocity, and which are general parameters.

(ii) Factors of the chosen phase system, such as the selectivity factor, α, the phase capacity ratio, k', and the linear range of the distribution isotherm, which are unique to that particular phase system and to the compounds in the mixture.

(iii) Factors specific to the separation problem at hand, which include the composition of the sample mixture and the yield and purity requirements of the product.

Loadability and sample throughput are closely inter-related and both can be increased in a number of ways.

6.4.1 Geometric and Kinetic Parameters

6.4.1.1 Column Diamter

Column loadability,[9,18,12] and hence throughput, increases directly with the cross-sectional area of the column, or with the square of the column radius. Providing that the volumetric flow rate is also proportionally increased so that the same eluent linear velocity is maintained, the retention time of the solutes will not change on going to a column with a wider diameter, nor will the solvent consumption per mass of solute separated.

6.4.1.2 Column Length

The column length can be increased either by using a longer column, or by coupling several columns together to increase the effective column length.[10,11]

Scott and Kucera[12] have shown (see above) that, for columns which are *not* overloaded, the maximum sample load of a solute, *i*, $M_{i,max}$, which can be placed on a column without losing resolution, when using columns of different lengths but with the same HETP, increases with the square root of the column length, $\sqrt{L}$. The solvent consumption per unit mass also increases with $\sqrt{L}$ since sample dilution, σ_{vol}, in the non-overload region is proportional to $\sqrt{N}$, and since N is proportional to L, ie.

$$M_{i,max} \text{ (linear region)} \propto \sqrt{L}$$

$$\sigma_{vol} \text{ (linear region)} \propto \sqrt{N}$$

$$\text{Solvent consumption per mass of solute} \propto \sqrt{N}$$

$$\propto \sqrt{L}$$

However, although the solvent consumption may increase, the loading capacity of the column may increase more rapidly so that the solvent consumption per mass of solute separated may not be affected.

De Jong *et al.*[6,9] have reported that, for columns of different lengths but with equivalent efficiencies operating in the overload region, the maximum sample load which can be loaded onto the column without loss of resolution increases proportionally with the length, L. This is true where the peak spreading is mainly due to thermodynamic effects, as it

is in the overload region, or non-linear part of the distribution isotherm. The solvent consumption per unit mass of solute is then independent of L since, in the overload region, the sample dilution, σ_{vol}, increases proportionally with N, ie.

$$M_{i,max} \text{ (overload region)} \alpha L$$

$$\sigma_{vol} \text{ (overload region)} \alpha N$$

and solvent consumption per mass of solute (overload region) is constant.

6.4.1.3 Particle Size, dp.

Scott and Kucera[12] have shown that the loading capacity of the column will increase as the square root of the column length, $\sqrt{L}$, if dp is constant (see previous section). However, if dp is increased, then in order to maintain the same column efficiency the column length must also be increased such that $\frac{dp^2}{L}$ is kept constant.[12] The loading capacity should then increase for the longer columns packed with larger particles in proportion to L, a conclusion similar to that reached by De Jong *et al.*[9] for overloaded columns. Under these conditions the solvent consumption per gram will be constant but the separation times will increase when both L and dp are increased, giving some increase in throughput but not a proportional increase.

It is worth noting that in the latter situation where similar linear capacities were produced, the reduced column length as given by $\frac{L}{dp}$ was almost the same for each column while in the former situation the reduced length was different.

6.4.1.4 Mode of Sample Introduction

Wehrli[8] and others[9] have shown that column loadability is greatly affected by the mode of sample introduction and is increased when the sample is introduced over the cross-sectional area of the column. Sample introduction systems have been covered more fully in chapter 5.

6.4.2 Phase System Parameters

6.4.2.1 Resolution, R_s

The loadability and sample throughput can both be increased by increasing the resolution between adjacent peaks. As resolution is given by

$$R_s = \frac{1}{2}\frac{(\alpha-1)}{(\alpha+1)}\left(\frac{\bar{k}'}{1+\bar{k}'}\right).N^{\frac{1}{2}} \qquad (6.7)$$

This can be achieved by increasing the peak retention, ie. increasing k', through decreasing the eluent strength and/or optimizing the selectivity factor, α, by altering the composition of the eluent while maintaining the same solvent strength. However, while the loading capacity of the column may well be increased in this way, the throughput is not necessarily increased.

6.4.2.1.1 Phase Capacity Ratio, k'

An increase in solute retention, ie. in the phase capacity ratio, k', may result in an increase[7] in both the loadability and the sample throughput since the resolution between adjacent peaks will be increased as illustrated by equation 6-7. This increased spacing between the peaks allows for the introduction of a larger sample load before the peaks start to overlap. The increase in k' has the added effect of reducing the maximum concentration of the solute in the eluent, which according to De Jong *et al.*[5] also contributes to an increase in column loadability. Although loadability can be improved in this way, the retention time for the last eluted peak will also increase and so throughput may not be improved. Solvent consumption per mass of solute should remain constant as both loadability and sample dilution increase proportionally with k'.[12]

While Bombaugh and Almquist[7] considered the decrease in resolution, R_s, between two adjacent components as the criterion for the influence of k' on column loadability, both Wherli[8] and De Jong *et al.*[9] considered the decrease in column efficiency, N, for a single solute and stated that an increase in k' does not lead to improved throughput.

6.4.2.1.2 Selectivity, α

One of the best ways to improve loadability and sample throughput through increased resolution is to increase the selectivity coefficient, α. It has been found that "for constant resolution, the maximum allowable sample load increases with increasing selectivity coefficient",[1] and that throughput

can be considerably improved when selectivity is optimised.

However, where the sample contains more than two components, improvement in the selectivity factor for one pair of components may well be at the expense of the selectivity factor for another pair. In such cases throughput may not be increased.

6.4.2.1.3 Number of Plates, N

Resolution can also be improved by increasing the number of plates, N, either by using a more efficient column or by increasing the column length, although the latter is not often used. In order to maintain the time taken for the last peak to elute, an increase in column length would require an increase in the volumetric flow rate and hence an increase in pressure and therefore N is not normally increased by much. Increasing the column length will also reduce the solute peak concentration and produce additional peak spreading. The column linear capacity, $\theta_{0.1}$, and therefore the loadability will also increase, but because t_m is likely to be increased, ie. where the flow rate remains unchanged, there may be little change in throughput.

6.5 Methods of Improving Sample Throughput

The various methods, which can be used to increase the amount of pure material collected per unit time, are given as follows.

6.5.1 Increasing the Eluent Flow Rate

It can be shown experimentally, as illustrated in figure

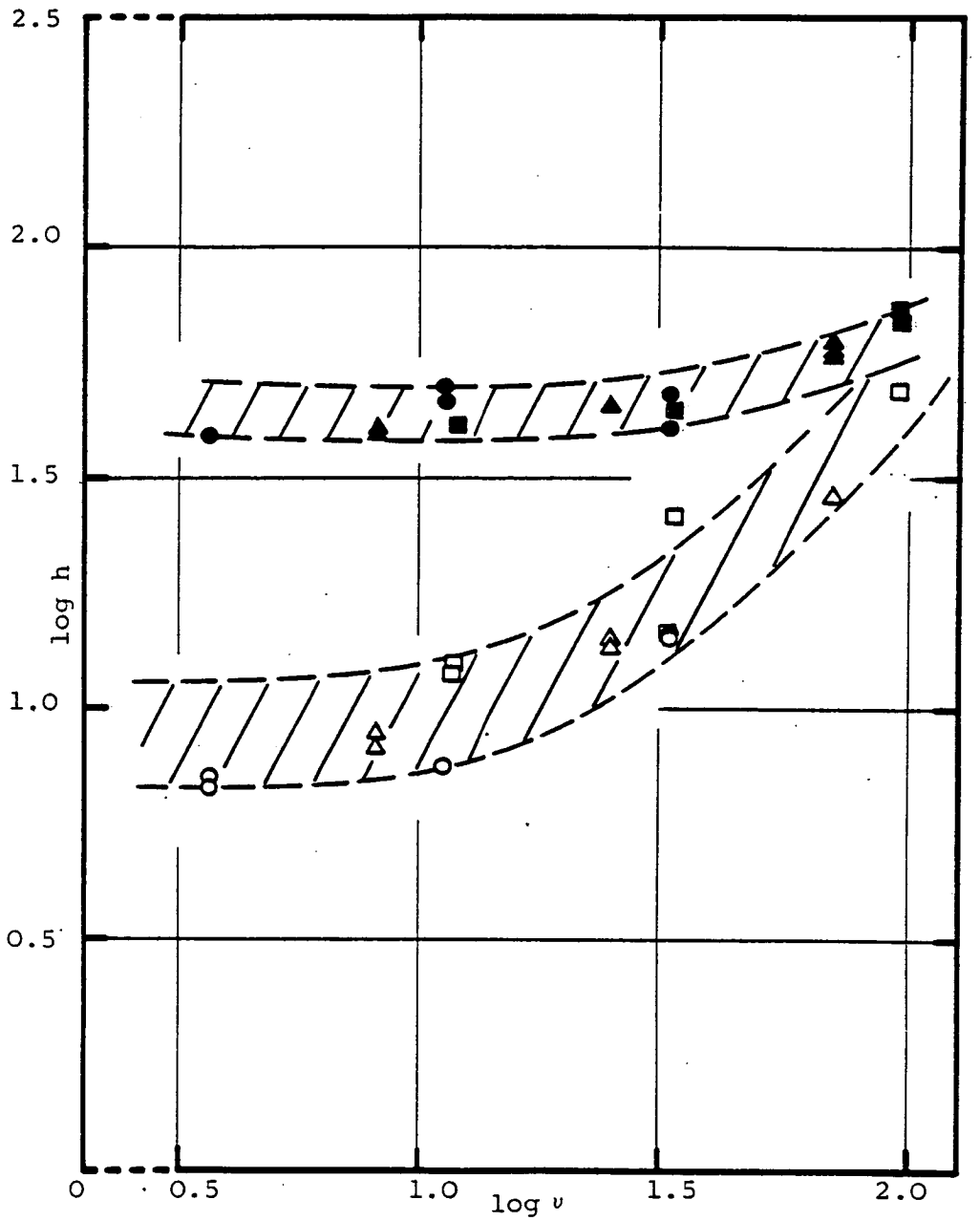

Figure 6.4 The dependence of column efficiency on the eluent flow rate at low and high sample loads.

○ △ □ 10^2µg acetophenone using 93mmx7mm id, 134mmx 7mm id and 247mmx7mm id columns respectively.

● ▲ ■ 10^4µg acetophenone using 93mmx7mm id, 134mmx 7mm id and 247mmx7mm id columns respectively.

6.4, that, for the introduction of a very small load, the efficiency (N) of the column decreases rapidly with increasing eluent velocity (u). Since resolution is proportional to $\sqrt{N}$, the resolution also decreases with increasing eluent velocity. At such a low load level, which would be within the linear range of the distribution isotherm, both the phase capacity factor (k') and the selectivity factor (α) will remain virtually constant throughout the increase in eluent velocity.

As the sample load is increased, column efficiency is lower at low eluent velocities than for low sample loads, but the increase in eluent velocity has less of an effect on the column efficiency and on the resolution, and the H,ν curve flattens out.

At sample loadings above the linear capacity ($\theta_{0.1}$) of the stationary phase, which is discussed earlier in this chapter, where the column is operating in the non-linear part of the distribution isotherm or overload region, both k' and α may be significantly decreased, but the effect of the eluent velocity on the column efficiency and resolution is almost negligible. This means that once adequate resolution for a preparative separation has been established, sample throughput can be increased by operating in the non-linear part of the distribution isotherm and at a high flow rate.[7,9,13,19]

Furthermore, De Jong *et al.*[9] have derived an equation which shows that, once the column and phase system have been chosen and optimised for a particular separation problem, throughput can be increased in proportion to $(\nu/h)^{\frac{1}{2}}$.

6.5.2 Step-wise Flow Programming

Another way to increase sample throughput is to introduce

flow programming[7] where the flow is increased in steps during the chromatographic run. This reduces the time taken for a complex preparative separation where the later peaks are widely spaced, without sacrificing the resolution of the earlier peaks.

Flow programming can cater for sequential injections and therefore has a greater throughput potential than solvent programming.

6.5.3 Step-wise Solvent Programming

A step-wise solvent gradient can also be used to improve sample throughput for widely spaced peaks but it is less desirable than flow programming since the column equilibrium is disturbed and the column has to be regenerated before it is used again.

6.5.4 Recycle

The technique of recycle, which has already been discussed in chapter 5, can also be used to increase sample throughput. This method enables the column to handle substantial loads and also improves the resolving capability of the system, without the expense or inconvenience of using long columns. This method is especially effective when fraction cutting is employed.

6.5.5 Column Coupling

Column coupling has also been mentioned in chapter 5. Basically, the effective number of plates is increased by the coupling together of two or more columns, but this leads to extra pressure requirements of the system.

6.6 The Effects of Increased Sample Mass on Resolution and Column Efficiency

6.6.1 Introduction

Since overloading the column with sample alters the equilibrium to such a degree that the commonly accepted concepts of rate theory no longer apply, a complete theory of band broadening under overload conditions does not yet exist. The amount of sample which can be loaded onto a column can be increased either by increasing the sample volume or by increasing the sample concentration. The effects which each of these methods have on resolution, loadability and sample throughput are discussed now.

6.6.2 Band Broadening Due to Volume Overloading

In analytical-scale chromatography, small injection volumes of low sample concentration are injected onto the column such that chromatography operates in the linear part of the distribution isotherm. When dealing with preparative-scale chromatography however, the chromatography generally falls in the non-linear part of the distribution isotherm and thus additional band spreading occurs. Under conditions of volume overloading, the band broadening, ΔV_{band}, is linear with respect to the injection volume ie. a plot of ΔV_{band} against V_{inj} is linear.

The total volume variance of a chromatographic peak as it emerges from the column outlet is given by

$$\sigma^2_{tot} = \sigma^2_{col} + \sigma^2_{inj} \qquad (6\text{-}8)$$

a) Impulse

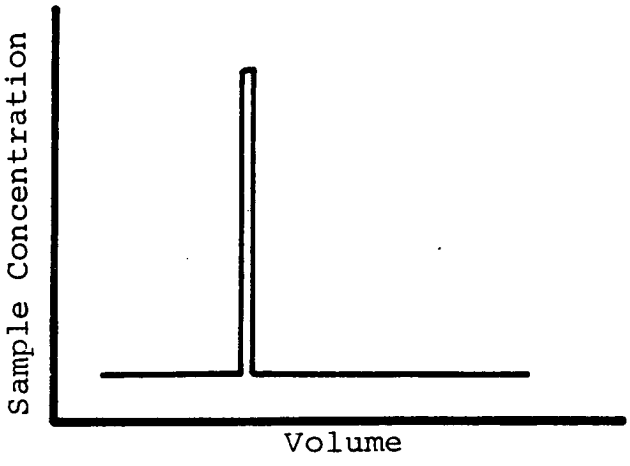

b) Sample plug or double step input

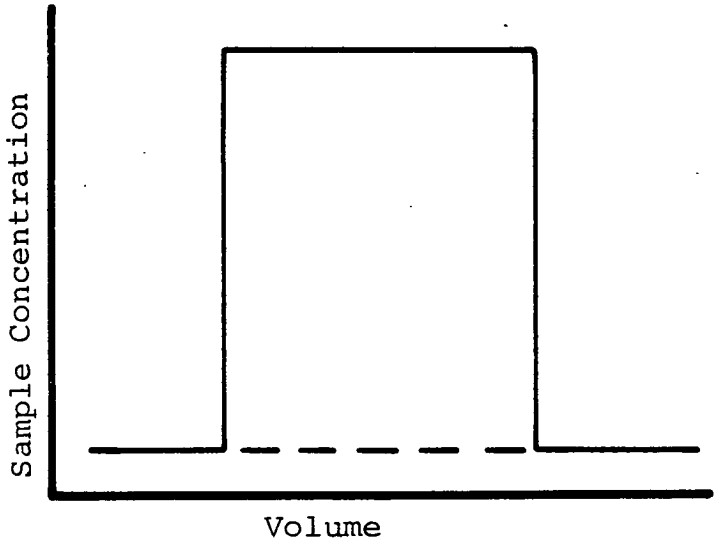

Figure 6.5 Two types of injection profile.

where σ^2_{tot} = volume variance of the distribution function of the component at the column outlet ie. the output profile;

σ^2_{col} = the volume variance due to the chromatographic process;

and σ^2_{inj} = the volume variance of the distribution function of the component at the column inlet ie. the inlet profile, and which depends on the volume of sample introduced.

It is clear from equation 6.8 that the shape of the chromatographic peak, ie. the output profile, is dependent on the shape of the input profile.

Two types of injection profile which are of interest are illustrated in figure 6.5.[14] Figure 6.5(b) is a double step input and represents the injection of a sample plug, while figure 6.5(a), which is also a type of double step input, represents the ideal case of impulse chromatography or a point injection. Such a small injection volume would correspond to operating in the linear part of the distribution isotherm and the resultant chromatographic peak is Gaussian in shape. The general form of the Gaussian error curve,[20] is given by

$$y = y_o \exp(-x^2/2\sigma^2) \qquad (6\text{-}9)$$

where σ is the standard deviation and is equal to half of the peak width at the points of inflection ie. at $y = y_o e^{-\frac{1}{2}}$.

Providing the column is operating in the linear part of the distribution isotherm, then the injection profile for larger injection volumes can, in principle, be considered as being

made up of a number of successive narrow plugs each of which produce a Gaussian shaped elution profile with each of these Gaussian output profiles combining to produce the resultant chromatographic peak. Under such circumstances therefore, it is possible to predict the shape of the output profile by considering the response of the individual narrow plugs.

Reilley *et al.*[14] have derived various mathematical equations to describe the output profile resulting from a large sample input volume. In deriving these equations they made the assumption that the chromatography fell within the linear range of the distribution isotherm.

For a single solute introduced as an ideal impulse profile (point injection), the response function, R_t, of the output profile was given as

$$R_t = \frac{C_i'}{\sqrt{2\pi}\ \sigma_i} \exp - \left(\frac{t-t_{Ri}}{\sqrt{2}\ \sigma_i}\right)^2 \qquad (6\text{-}10)$$

where C_i' is equal to $\int C_i\ dt$, C_i is the concentration of solute i in the feed solution and σ is the standard deviation of a Gaussian curve and is equal to one quarter of the volume between the intersections of the tangents to the inflection points with the axis.

The response function of such an impulse input is more generally described by

$$N = \frac{t_R^2}{\sigma^2} \qquad (6\text{-}11)$$

where N is the column efficiency for a particular solute.

In the case of the introduction of a large volume of sample

with a double step input profile, ie. a sample plug, Reilly *et al.*[14] have shown that the output response function, R_t, can be described by

$$R_{t,i} = \frac{\sum C_i}{2} \text{ erf} \left(\frac{t-t_{R,i}}{\sigma\sqrt{2}} \right) - \frac{\sum C_i}{2} \text{ erf} \left(\frac{t-t_2-t_{R,i}}{\sigma\sqrt{2}} \right) \qquad (6\text{-}12)$$

This has been rearranged by Coq *et al.*[15] to give

$$C = \frac{C_i}{2} \left[\text{erf} \left(\frac{V-V_R}{\sigma\sqrt{2}} \right) - \text{erf} \left(\frac{V-V_R-V_L}{\sigma\sqrt{2}} \right) \right] \qquad (6\text{-}13)$$

where C is the solute concentration of the output profile at output volume, V, C_i is the sample concentration in the feed solution, V_R is the retention volume, σ is the standard deviation of a Gaussian curve and where V_L is the width of the input profile or sample plug. The width of the sample plug, V_L, is related to the injection volume V_i by the expression

$$V_L = \theta \, V_i \qquad (6\text{-}14)$$

where θ is a factor which depends on the efficiency of the sample introduction system.

Coq *et al.*[15] have established an expression for the maximum injection volume, V_i, for a system using the equation which describes the output profile caused by a large sample input volume based on a chromatographic peak which is symmetrical but with a flat top and the following arguments.

For very large injection volumes such that the width of the sample plug V_L is greater than or equal to 8σ, the concentration at the peak maximum $C_{i,m}^{max}$ is the same as the sample

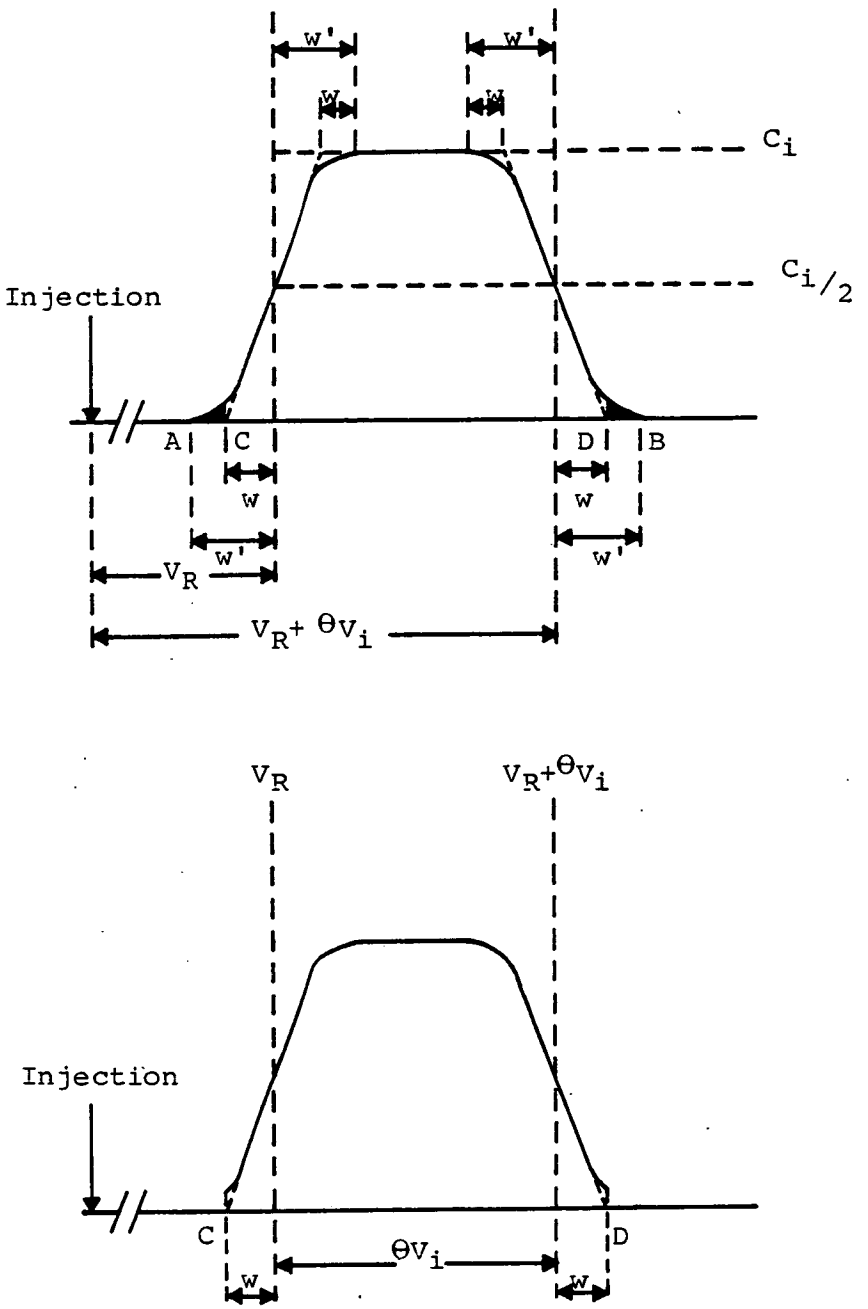

Figure 6.6 Theoretical chromatographic peak for large sample volume (Reproduced from reference 15).

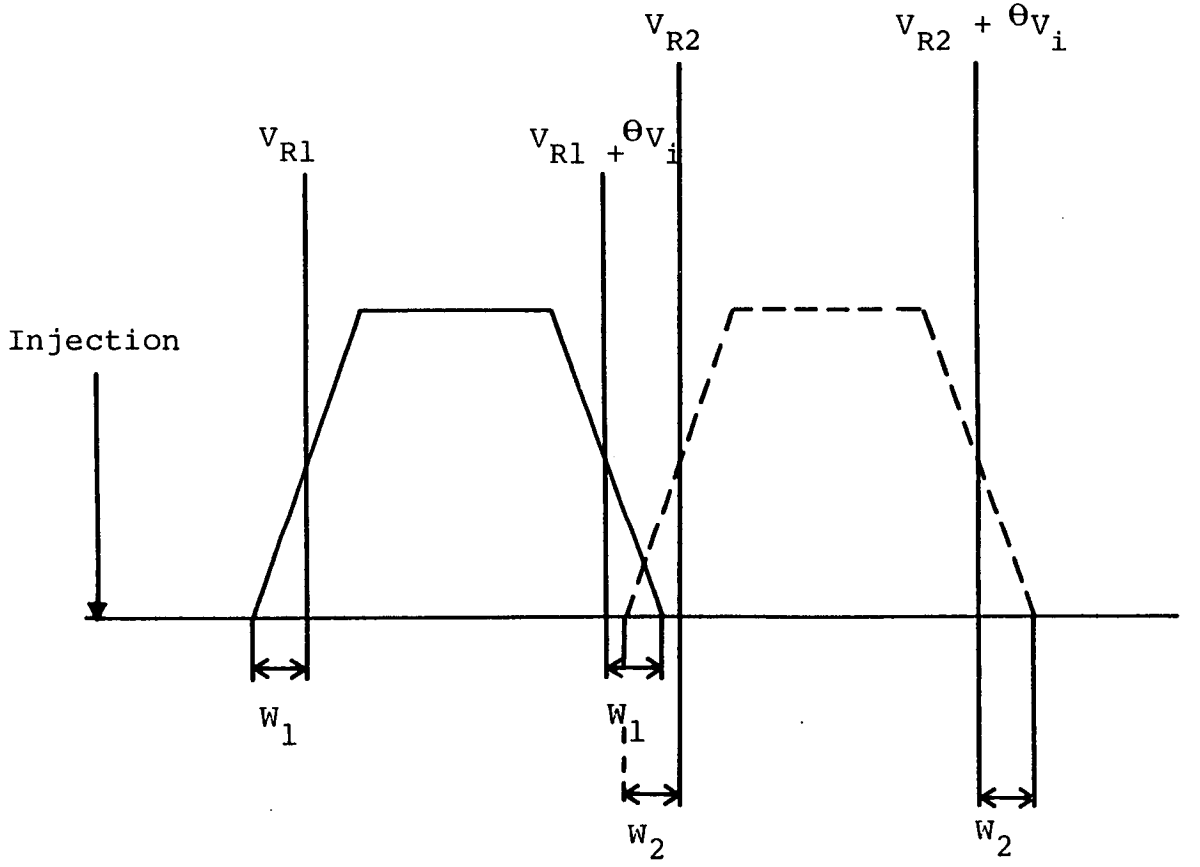

Figure 6.7 Theoretical chromatogram for volume overload. (Reproduced from reference 15).

concentration of the feed solution injected, C_i, ie. there is no dilution of sample as it passes down the chromatographic column. Such a situation is illustrated in figure 6-6. The shaded areas correspond to a mass of solute which is less than 1% of the initial injection sample and was neglected when considering their derivation of an equation describing the maximum injection volume which will produce a certain minimum resolution. Their calculations were therefore based on the theoretical chromatogram of figure 6-7.

The standard equation for the resolution of two solutes, 1 and 2, is

$$R_s = \frac{V_{R,2}-V_{R,1}}{\frac{1}{2}(W_1+W_2)} \qquad (6\text{-}15)$$

This can be expressed in terms of figures 6-6.B and 6-7 as

$$R_s = \frac{V_{R,2}-V_{R,1}}{\theta V_i+W_1+W_2} \qquad (6\text{-}16)$$

Considering the following equations, namely

$$V_{R,1} = V_m+K_1A_s \qquad (6\text{-}17)$$

where V_m is the retention volume of an unretained solute, K_1 is the equilibrium constant and A_s is the surface area of the adsorbent,

$$k_1' = \frac{V_1-V_m}{V_m} \qquad (6\text{-}18)$$

where k' is the phase capacity ratio,

and $$\alpha = \frac{K_1}{K_2} \qquad (6\text{-}19)$$

where α is the selectivity factor, and substituting them into equation (6-16) we can write

$$R_s = \frac{(\alpha-1)\ k'\ V_m}{\theta V_i + W_1 + W_2} \qquad (6\text{-}20)$$

Here θ is the injection factor of the injection device used, V_i is the injection volume and V_m is the column dead volume.

In their derivation, Coq *et al.*[15] assumed a value of 1.25σ for W, and therefore since

$$N = \left[\frac{V_{R,1}}{\sigma_1}\right]^2 \qquad (6\text{-}21)$$

we can write

$$W = 1.25 \left[\frac{V_{R,1}}{\sqrt{N}}\right] \qquad (6\text{-}22)$$

Substituting equation 6-22 into equation 6-20 produces the equation

$$R_s = \frac{(\alpha-1)\ k_1'\ V_m}{\theta V_i + \frac{1.25}{\sqrt{N}}\ [V_{R_1} + V_{R_2}]} \qquad (6\text{-}23)$$

Further substitution of equations 6-17, 6-18 and 6-19 gives

$$R_s = \frac{(\alpha-1)\ k_1' \cdot V_m}{\theta V_i + \frac{1.25}{\sqrt{N}}\ V_m(2+k_1'+\alpha k_1')} \qquad (6\text{-}24)$$

which upon rearranging to express in terms of V_i gives

$$V_i = \frac{V_m}{\theta}\left[\frac{(\alpha-1)\ k_1'}{R_s} - \frac{1.25}{\sqrt{N}}\ (2+k_1'+\alpha k_1')\right] \qquad (6\text{-}25)$$

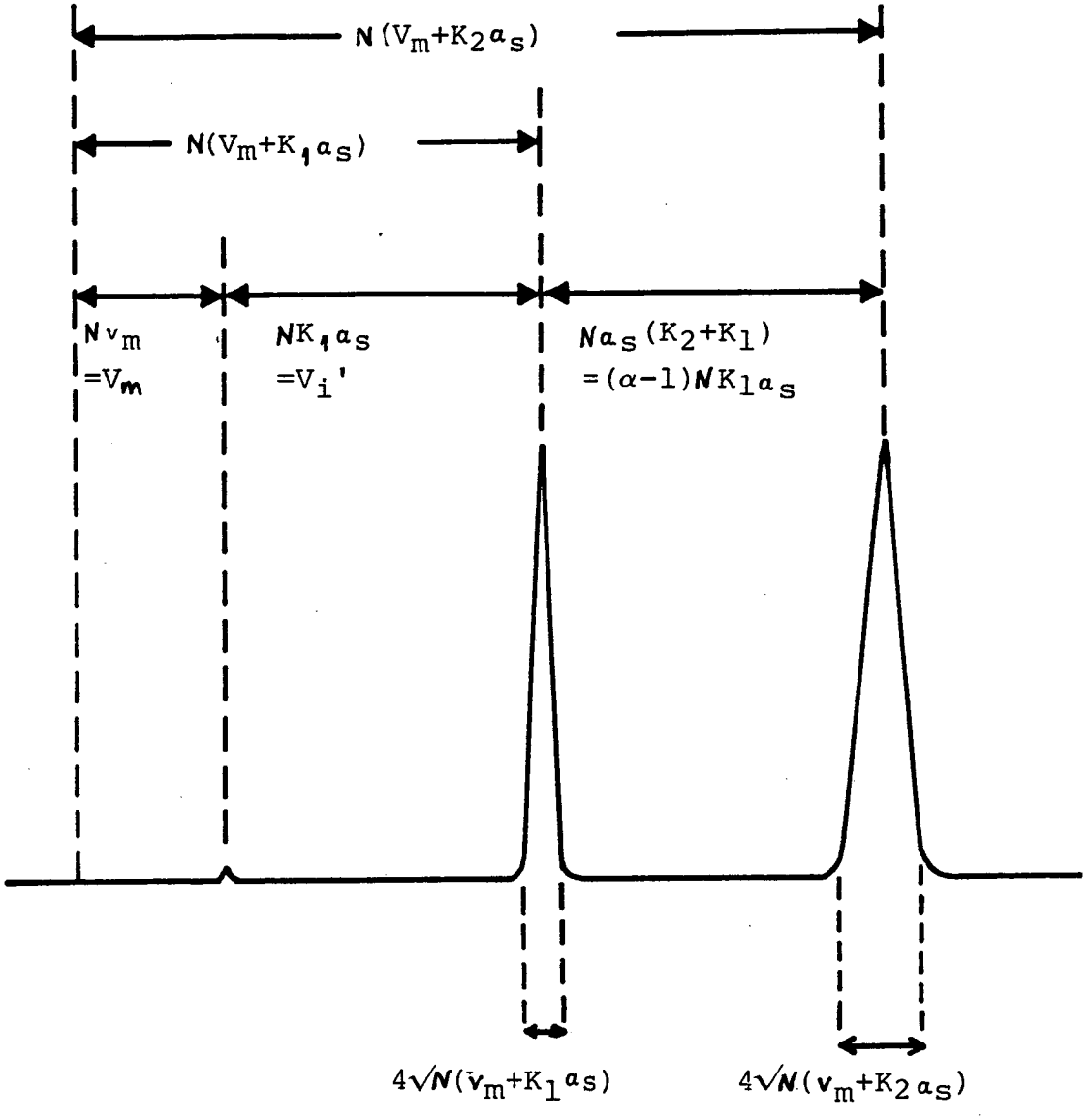

Figure 6.8 Theoretical diagram for volume overload.
(Reproduced from reference 12)

For a preparative separation where there is a minimum resolution which will just meet the requirements of purity, then the maximum injection volume which can be applied to the column is given as

$$V_{i,max} = \frac{V_m}{\theta}\left[\frac{(\alpha-1)\ k'_1}{R_{s,min}} - \frac{1.25}{\sqrt{N}}\ (2+k'_1+\alpha k'_1)\right] \qquad (6\text{-}26)$$

Scott and Kucera[12] have produced a similar expression for the maximum injection volume based on the theoretical diagram shown in figure 6-8. However, they made the assumption that, at very large sample volumes, the peak broadening due to the volume overloading is equivalent, to a first approximation, to the sample injection volume, ie.

$$V_{R2}-V_{R1} = V_i+\tfrac{1}{2}\ (W_1+W_2) \qquad (6\text{-}27)$$

Here $W = 4\sigma$

and since $N = \left[\frac{V_{R,i}}{\sigma_i}\right]^2$

then $W = 4.\ \frac{V_{r,i}}{\sqrt{N}}$ (6-28)

By assuming that both peaks had the same efficiency. they combined equations 6-17, 6-19 and 6-21 to give

$$(\alpha-1)\ K_1A_s = V_i+\frac{2}{\sqrt{N}}(V_m+K_1A_s)+\frac{2}{\sqrt{N}}(V_m+K_2A_s) \qquad (6\text{-}29)$$

This equation can be rearranged to give

$$V_i = (\alpha-1)\ K_1A_s - \frac{2}{\sqrt{N}}\ (V_m+K_1A_s) - \frac{2}{\sqrt{N}}\ (V_m+K_2A_s) \qquad (6\text{-}30)$$

Substituting equations 6-17, 6-18 and 6-19 into equation 6-30 then gives

$$V_i = V_m \left[(\alpha-1)\ k_1' - \frac{2}{\sqrt{N}} (2+k_1'+\alpha k_1') \right] \qquad (6\text{-}31)$$

The main difference between the two equations for the maximum injection volume is that the equation derived by Coq *et al.*[15] (6-26) also contains an injection factor term, θ, which depends on the type of injector and also the resolution term, R_s, with $V_{i,max}$ being inversely proportional to both θ and R_s. This means that the smaller the injection factor, θ, and the smaller the required minimum resolution, $R_{s,min}$, the greater will be the maximum injection volume. The effect of the different types of injection systems has been discussed elsewhere.

The validity of these maximum injection volume equations was tested by both Coq *et al.*[15] and Scott and Kucera,[12] and results obtained were in good agreement with the maximum injection volume as calculated by their respective equations.

Unfortunately, both treatments apply when solute concentration is low and the distribution isotherm is linear. In nearly all practical cases of preparative HPLC, concentration overloading occurs. Nevertheless, these treatments do emphasize that there is significant potential for the use of large injection volumes if the α-values are also large.

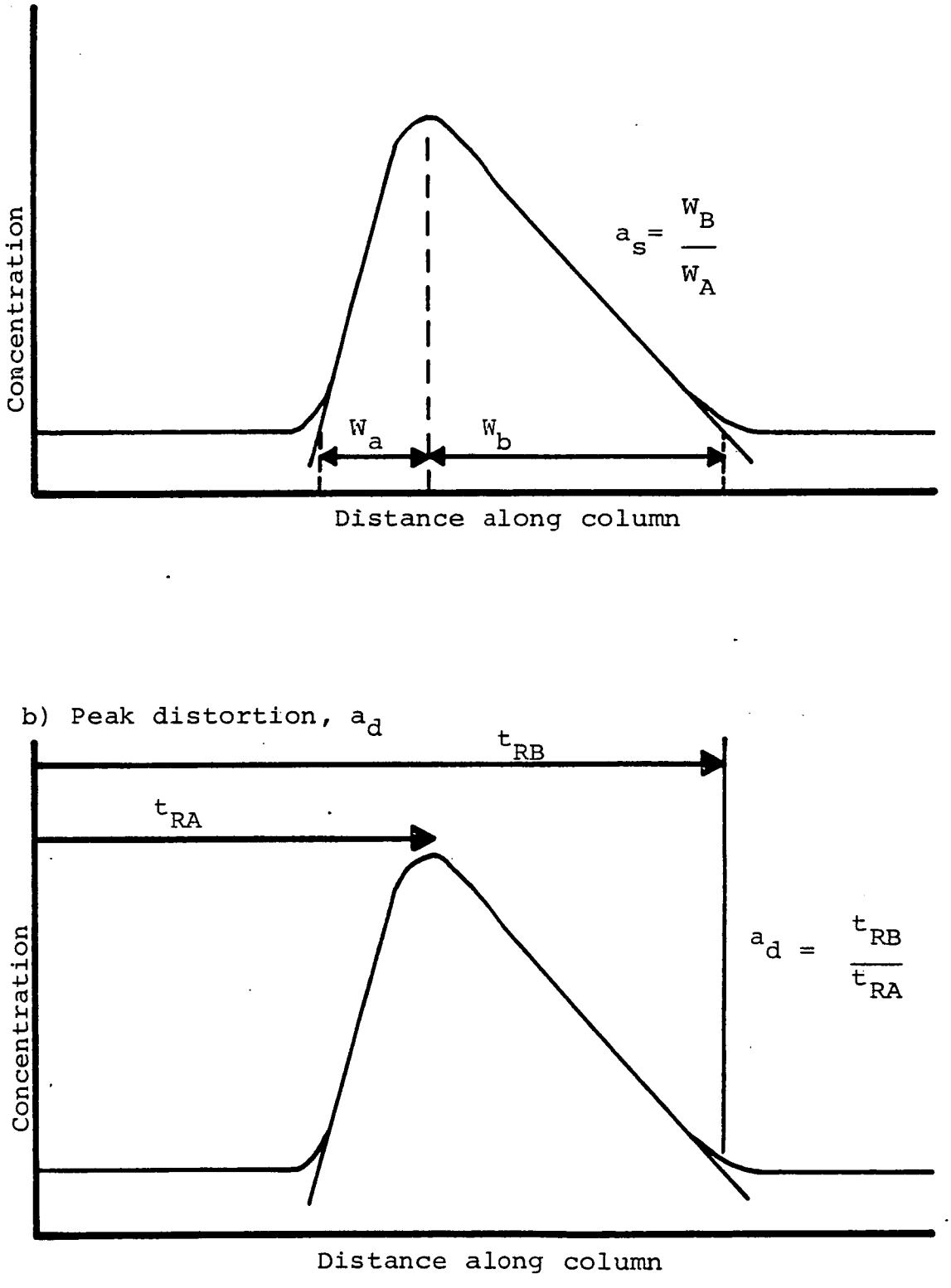

Figure 6.9 Schematic representation showing the difference between a) peak asymmetry and b) peak distortion.

6.6.3 Band Broadening Due To Concentration Overloading

Band broadening due to the thermodynamic effects caused by concentration overloading is difficult to quantify since the broadening increases with the column length, ℓ, in a way which is difficult to predict but which is probably proportional to between $\ell^{\frac{1}{2}}$ and ℓ. This can be explained qualitatively as follows. As the peak moves down the column, not only does the peak width increase but the concentration decreases as it moves down the column. Therefore, the *peak distortion*, as defined in figure 6-9 as

$$a_d = \frac{t_{Rb}}{t_{Ra}} ,$$

which is not to be confused with *peak asymmetry* which is defined as

$$a_s = \frac{W_b}{W_a} ,$$

will gradually decrease, and the nature of this decrease will depend on the distribution isotherm and thus cannot be predicted in advance. When this peak distortion from the thermodynamic effects combines with the peak spreading from the kinetic effects, then the situation becomes rather complicated.

In considering the problem of thermodynamic band broadening when comparing different solutes under overload conditions, there are two possible hypotheses which can be put forward.

1) Column overloading of a particular solute, i, occurs when the solute concentration in the *stationary phase* at the column outlet reaches a certain critical value, $C_{i,s}^{max}$.

2) Column overloading of a particular solute, i, occurs when

the solute concentration in the *mobile phase* reaches a certain critical value, $C_{i,m}^{max}$.

Huber and Gerritse,[16] and indeed most other workers,[1,5,9] have taken the view that column overloading occurs at a particular concentration of a particular solute, *i*, in the mobile phase at the column outlet. This assumption does not seem to be entirely satisfactory, since for significant k' values, the concentration of a solute in the stationary phase is much greater than that in the mobile phase due to the fact that the volume of stationary phase is less than that of the mobile phase. Therefore, we believe that it is more useful to consider overload as occurring when a solute reaches a particular concentration in the stationary phase. It may be, however, that the critical factor in determining column overload involves some combination of these two factors, ie. a fixed solute concentration in both the stationary and in the mobile phase.

Whichever definition is used for overload, it is likely that the critical concentration will depend on the nature of the solute ie. on its distribution isotherm.

Taking all of this into consideration, it is probably best to regard overload as occurring when a particular ratio of mass of solute/mass of packing is reached.

A theoretical analysis of thermodynamic band broadening has been given by Huber and Gerritse[16] for adsorption chromatography. Having made the basic assumption that overloading occurs when a fixed concentration of solute in the eluent at the column outlet is reached, ie. that the maximum solute concentration is fixed, Huber and Gerritsefurther simplified the case for a non-

a) Linear distribution isotherm

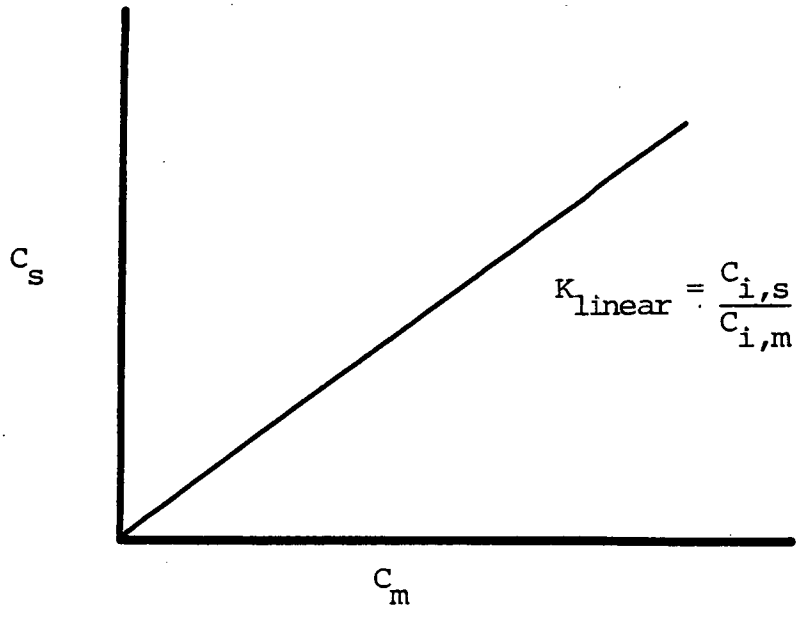

b) Non-linear distribution isotherm

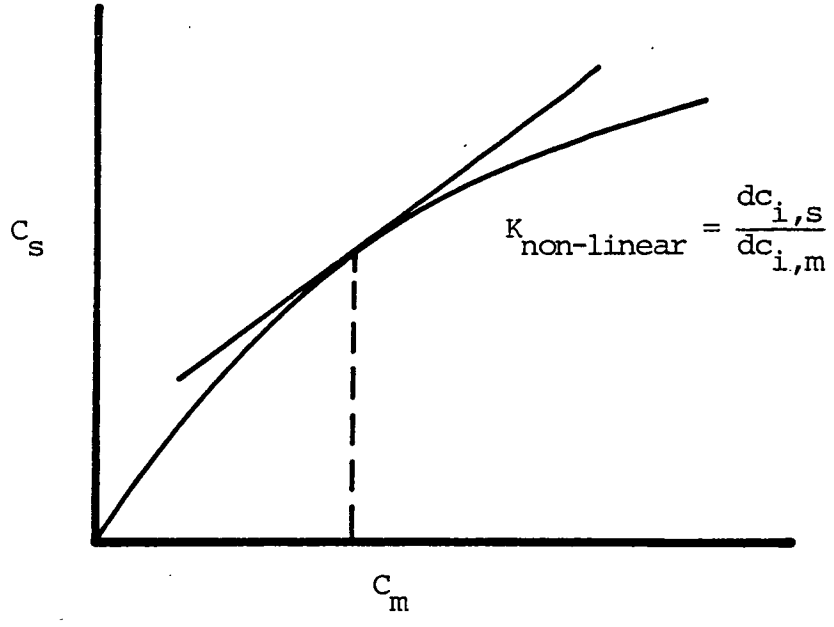

Figure 6.10 The distribution coefficients for
a) a linear distribution isotherm and
b) a non-linear distribution isotherm.

linear distribution isotherm by assuming that the dispersion coefficient for a solute i in the mobile phase, $D_{i,m}$ was zero, which is the same as considering the column to have an infinite number of plates, and also by assuming the fluid velocity averaged over the cross-sectional area to be constant. For such ideal chromatography the maximum solute concentration allowed in the eluent was shown to be given by the equation:

$$t_{R,i}(C_{i,m}) = \frac{L}{U_{av}} \left(1 + \frac{(1-\varepsilon_m)}{\varepsilon_m} \cdot \frac{dC_{i,s}}{dC_{i,m}} \right) \qquad (6\text{-}32)$$

where

L = the column length,

$t_{R,i}(C_{i,m})$ = the retention time of the concentration $C_{i,m}$ for solute i,

U_{av} = the velocity averaged over the cross-sectional area,

ε_m = the fraction of the cross-sectional area occupied by the fluid stream,

$1-\varepsilon_m$ = the fraction of the cross-sectional area occupied by the stationary phase,

$\frac{dc_{i,s}}{dC_{i,m}}$ = the derivative of the distribution isotherm at the mobile phase concentration, $C_{i,m}$.

Equation (6-32) can be rewritten as

$$t_{R,i}(C_{i,m}) = t_m \left(1 + q \frac{dC_{i,s}}{dC_{i,m}} \right) \qquad (6\text{-}33)$$

where t_m = the retention time of an unretained solute,

and q = the phase volume ratio.

It should be mentioned at this stage that for a linear distribution isotherm, the distribution coefficient K is equal to the gradient of the line as shown in figure 6-10a ie.

$$K_{linear} = \frac{dC_{i,s}}{dC_{i,m}} = \frac{C_{i,s}}{C_{i,m}}$$

The retention time is now the same for each concentration value, $C_{i,m}$, and therefore equation 6-33 can be rewritten to give

$$t_{R,i} = t_m(1+qK_i)$$
$$= t_m(1+k'_i) \qquad (6-34)$$

where k'_i is the phase capacity factor of solute *i*.
By contrast, for a non-linear distribution isotherm, K for the migration of a given concentration within a peak is equal to the gradient of the tangent at a particular point on the isotherm as illustrated in figure 6-10b ie.

$$K_{non-linear} = \frac{dC_{i,s}}{dC_{i,m}}$$

Thus the different $C_{i,m}$ values will produce different $t_{R,i}$ values which means that the total mass of solute is spread over a range of $t_{R,i}$ values, whose upper and lower limits are given by equation 6-33 as

$$t_m \left\{ 1 + q \left(\frac{dC_{i,s}}{dC_{i,m}}\right)_{C_{i,m \to o}} \right\}$$

$$\text{and} \quad t_m \left\{ 1 + q \left(\frac{dC_{i,s}}{dC_{i,m}}\right)_{C_{i,m}^{max}} \right\} \qquad (6-35)$$

where $C_{i,m}^{max}$ is the maximum concentration of *i* in the mobile phase *at the column outlet.*

a) Convex

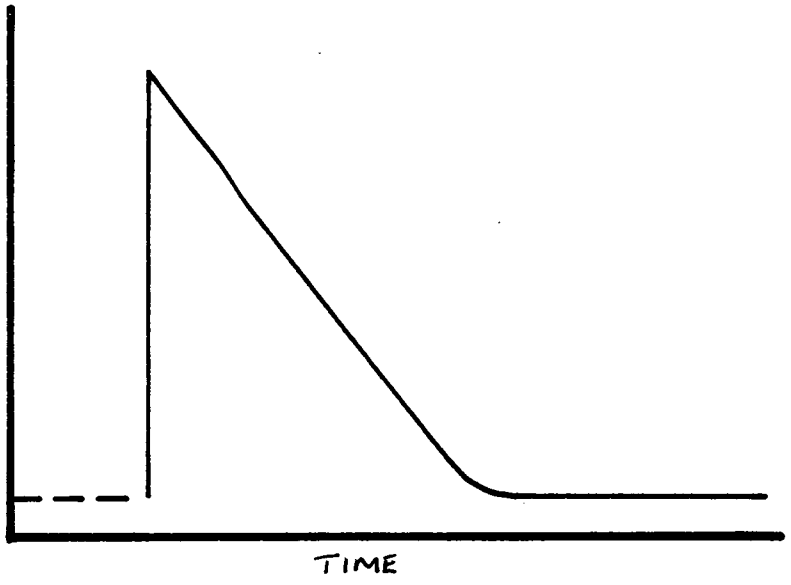

b) Concave

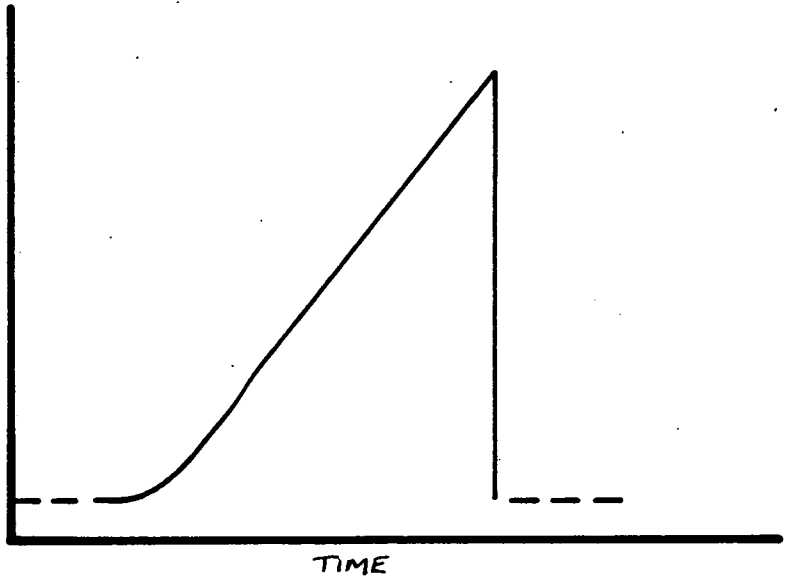

Figure 6.11 The shape of the elution profile of non-linear distribution isotherms for ideal chromatography (no dispersion, infinite pla e number).

Huber[17] has also shown that

$$\int_0^{(C_{i,m})_L^{max}} (C_{i,m})_L \, dt = \frac{Q_i}{W} \qquad (6\text{-}36)$$

where $(C_{i,m})_L^{max}$ = maximum concentration of component i in the mobile phase at the column outlet,

Q_i = the amount of component i loaded onto the column

and W = flow rate.

Equation 6-33 predicts[16] that, for the case of a convex non-linear distribution isotherm for ideal chromatography, the shape of the elution profile is as shown in figure 6-11a, that is the front of the peak is a vertical rise ending in a sharp top and the back of the peak has a slope which is determined by equation 6-33 and hence by the distribution isotherm. Conversely, for a concave non-linear distribution isotherm, an elution profile is predicted which has a sloping front which is determined by equation 6-33 ending in a sharp top with a vertical back as illustrated in figure 6-11a. The maximum concentration of solute *i* in the mobile phase at the column outlet, $C_{i,m}^{max}$, is responsible for the shape of the elution profile and this has been supported both experimentally and by computer simulation.[21] $C_{i,m}^{max}$ is itself determined by the shape of the distribution isotherm, as well as by the solute or solutes of interest and the properties of the column system chosen, and is constant for each component for a column producing a certain number of plates.

Huber and Gerritse[16] have concluded that the maximum amount

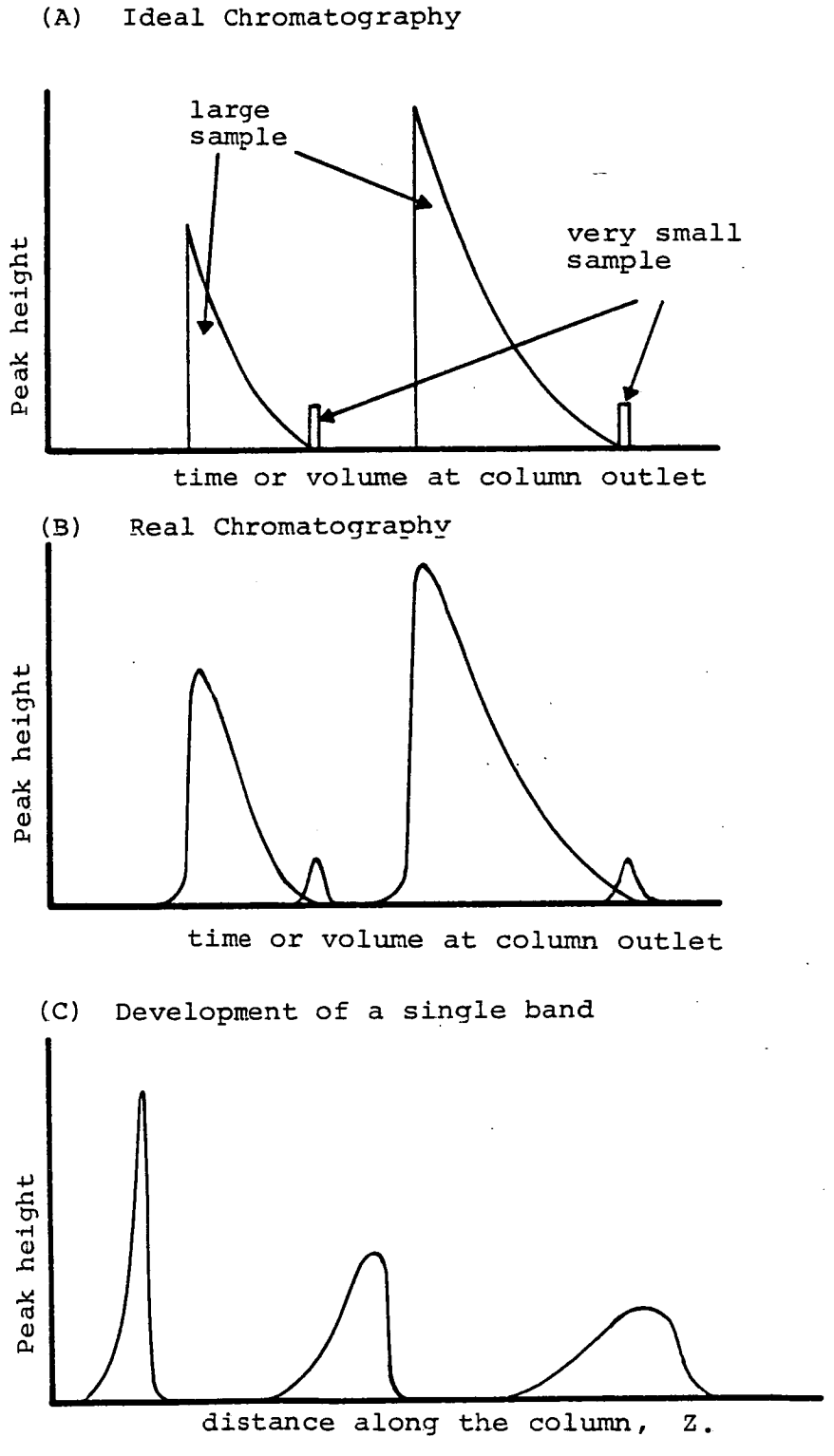

Figure 6.12 Peak broadening and loss of resolution due to isotherm non-linearity at low and high solute loads for (A) Ideal Chromatography (i.e. no dispersion, infinite plate number) and (B) Real Chromatography (i.e. finite plate number), (C) Shows the development of a single band as it moves down the column.

of sample that can be loaded onto a column for a particular separation under selected conditions and with specific requirements for resolution, purity and yield is determined by $C_{i,m}^{max}$. Where this maximum concentration is exceeded, the resolution, purity and yield requirements for a given separation problem cannot be fulfilled. For those cases where there is more than one component of interest, the lower $C_{i,m}^{max}$ value would determine the maximum amount of sample which could be loaded onto the column.

In the ideal case of dispersionless chromatography, a concentration of solute i present at the column outlet equal to $(C_{i,m}^{max})_{ideal}$ would result in the purity and yield achieved being exactly as specified. However in real chromatography where peak dispersion due to kinetic processes does occur, the maximum allowable concentration of the solute at the column outlet which meets the purity, yield and resolution requirements is less than $(C_{i,m}^{max})_{ideal}$ as illustrated in figure 6-12, and is in fact equal to $\alpha(C_{i,m}^{max})_{ideal}$ where α is a proportionality constant of between 0 and 1. For columns with very high plate numbers, α will be close to 1. As the number of plates decreases, $\alpha(C_{i,m}^{max})_{ideal}$ tends towards the maximum concentration limit as determined by the linear range of the distribution isotherm.

The argument presented by Huber and Gerritse[16] is sound once their basic assumptions have been made. However, they have wrongly assumed, like so many other people, that because the eluent profile is determined by $C_{i,m}^{max}$ then overloading must also be determined by $C_{i,m}^{max}$.

Using the same argument as put forward by Huber and

Gerritse, De Jong *et al.*[6] have stated that for a column with a lower plate number, the concentration of the peak maximum is less than for a column with a higher plate number and that therefore a larger amount of sample can be loaded onto the column in the case of a less efficient column before this $C_{i,m}^{max}$ value is reached.

It has already been mentioned that one of the main problems in trying to describe peak broadening due to concentration overloading is that the band becomes more dilute as it passes down the column. Peak distortion will therefore be greatest when the band is most concentrated and the extent of this distortion will decrease with the distance migrated through the column. The concentration may even move out of the non-linear part of the distribution isotherm into the linear part of the isotherm.

The way in which a band moves down a column is fairly involved since each concentration moves down at its own speed, and hence with its own k' value. The peak concentration and hence the peak shape changes, although the peak area remains constant.

As the band moves down the column, the peak distortion, a_d, decreases due to the thermodynamic effect already mentioned ie. the reduction in peak concentration with distance migrated. Eventually column dispersion, or the kinetic effect, takes over and the peaks tend to become symmetrical. This can be illustrated by considering the following simple model. Let us suppose that a sample is injected as a rectangular plug and that it moves down the column as a triangular solute band with a vertical front and a sloping trailing edge (see section 6.6.3). Let us further assume that there is no spreading due to kinetic effects,

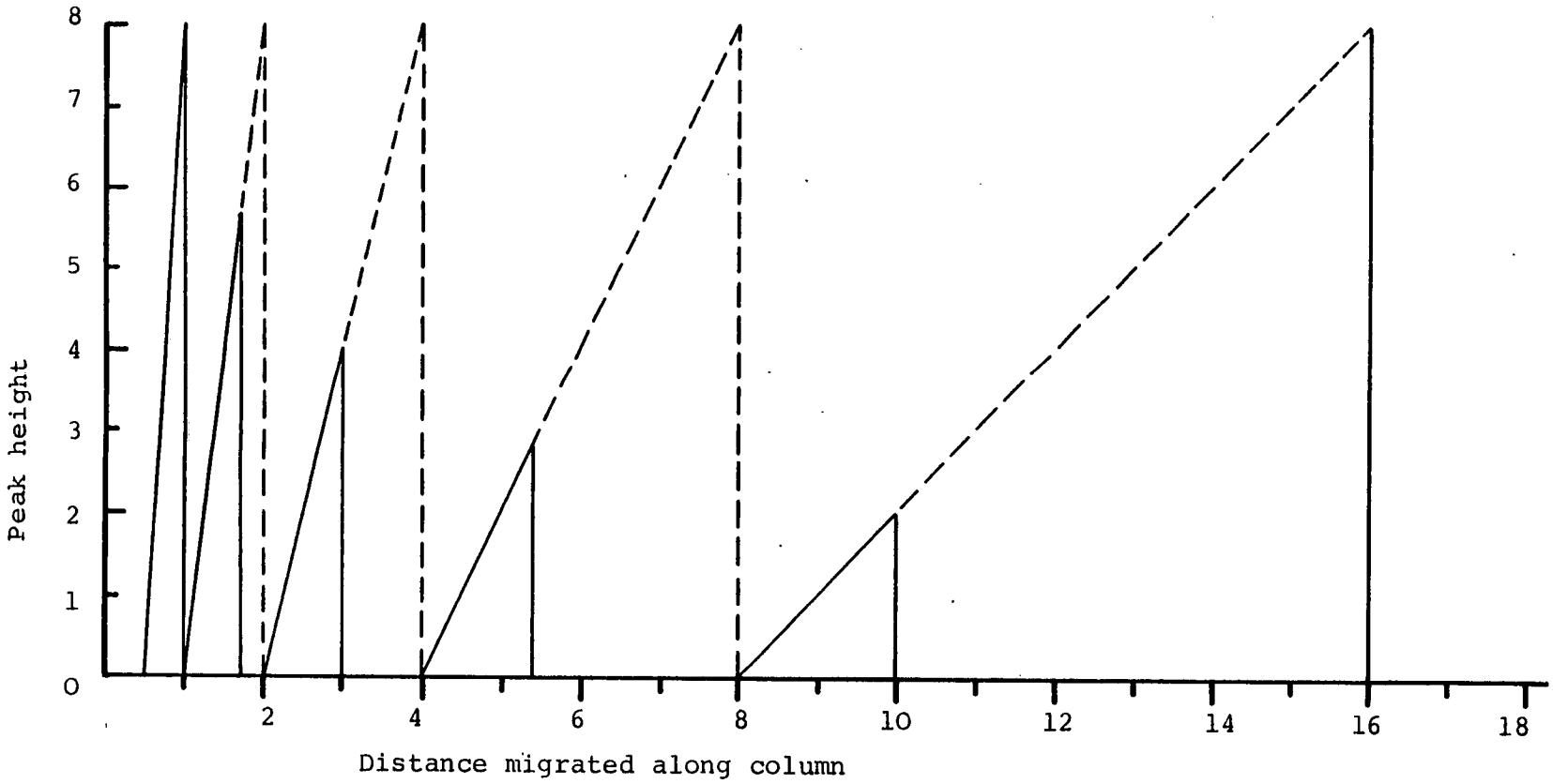

Figure 6.13 The schematic representation of the propagation of a triangular solute band resulting from the injection of a rectangular plug, where there is a variation of 50% between the k' of the maximum concentration and the zero concentration at the column inlet.

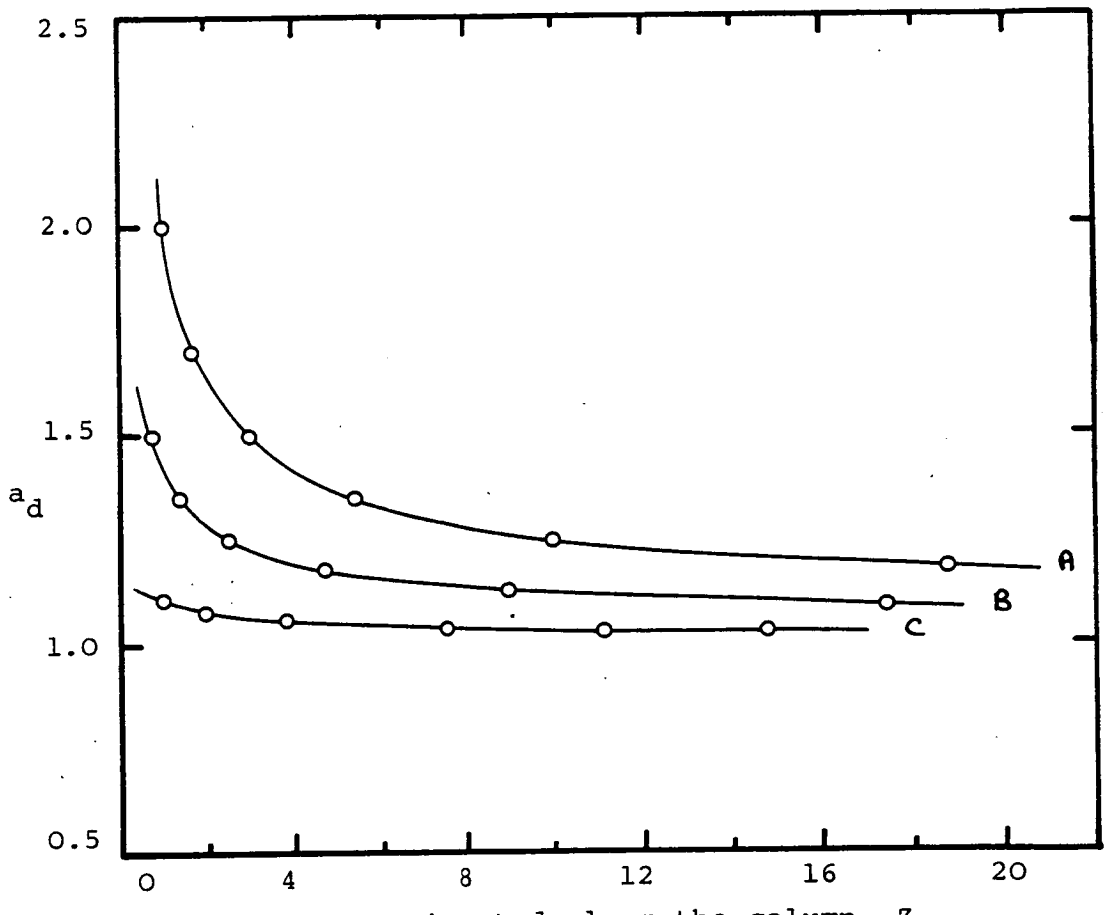

Figure 6.14 Dependence of the peak distortion factor, a_d, with the distance migrated along the column, Z; for A) a 50% variation in k' between the maximum concentration and zero concentration at the column inlet, B) a 50% variation in k' but where the load is 1/4 that of A), and C) a 10% variation in k' with the same load as for B).

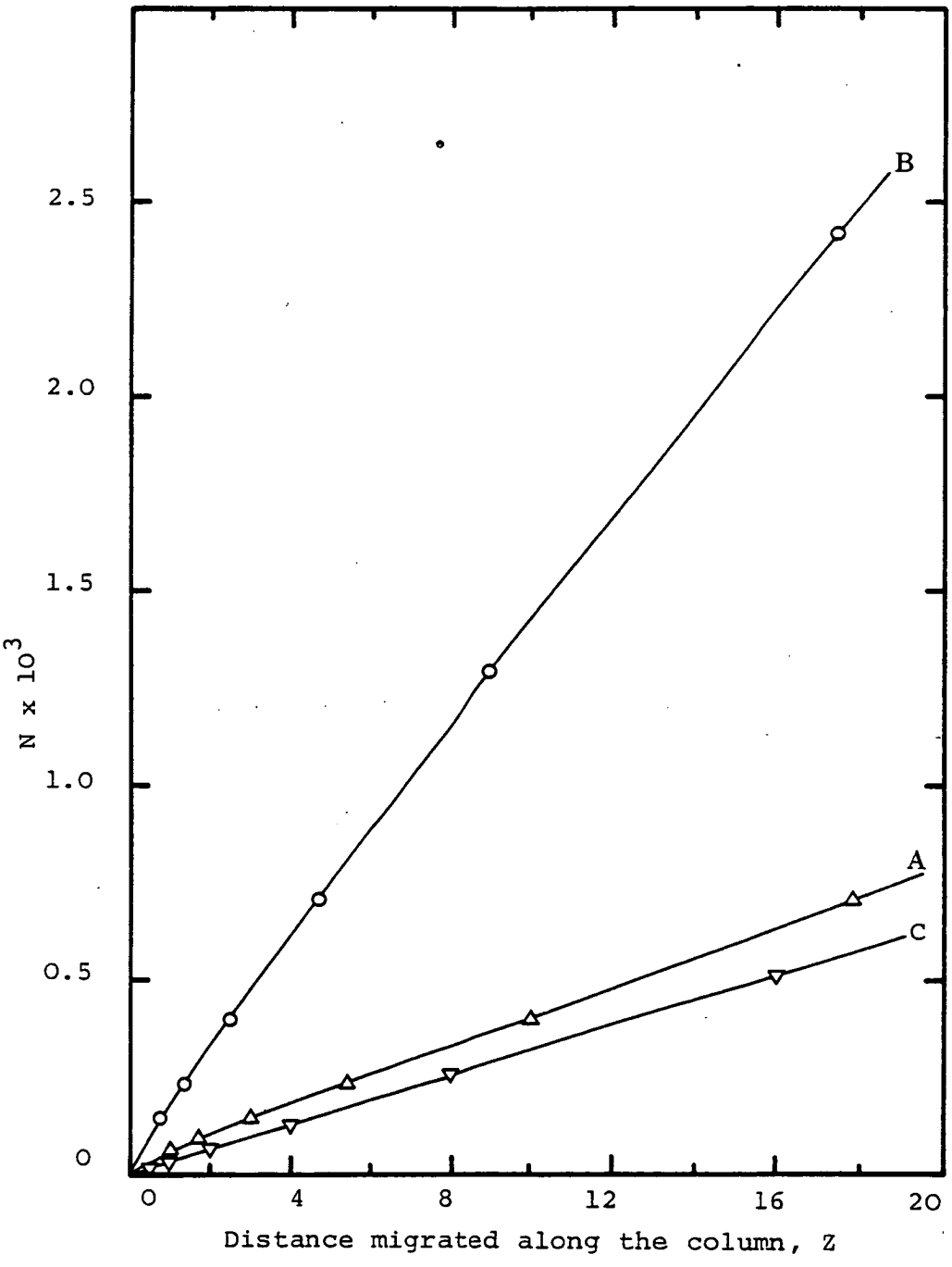

Figure 6.15 Dependence of N with the distance migrated along the column for a 50% variation in k' between the maximum concentration and zero concentration;

A) as measured at the front of the peak (high concentration), where $N \alpha Z^{0.80}$

B) as for (A) but with 1/4 of the load, where $N \alpha Z^{0.95}$, and

C) as for (A) but measured at the rear of the peak (low concentration), where $N \alpha Z$.

ie. that the chromatography is ideal. Each concentration will have its own k' value as it moves through the column and for the example illustrated in figure 6-13, it is assumed that the rate at which the maximum concentration moves through the column is twice that of the minimum, or zero, concentration ie. there is a 50% variation in their respective k' values. It can be seen that from figure 6-13 that as the band moves down the column it becomes wider and lower in order to retain a constant peak area so that the mass of solute remains constant. As a result, the concentration of the peak maximum moves down the distribution isotherm and the peak distortion factor, a_d, defined as

$$a_d = \frac{\text{distance of leading edge from origin}}{\text{distance of trailing edge from origin}}$$

becomes less. In the case illustrated by figure 6-13 a_d is reduced from 2 to 1.25, as shown in figure 6-14.

It is also possible to calculate the number of theoretical plates, N, to which the column is equivalent by using the equation

$$N = 16 \left(\frac{L}{W_z}\right)^2 \qquad (6\text{-}37)$$

where L is the distance travelled along the column and W_z is the width of the peak at the base. It can be seen from figure 6-15 that, as a result of the thermodynamic effects, N increases somewhat less than linearly as the band moves down the column. The way in which N increases with the distance along the column, L, can be evaluated as follows. Assuming that

$$N \propto L^{\beta}, \qquad (6\text{-}38)$$

the exponent β is readily found by plotting log N against log L and finding the slope, β, since

$$\log N \propto \beta \log L,$$

or using two values of N and L and substituting into the equation

$$\log \left(\frac{N_2}{N_1}\right) \propto \beta \log \left(\frac{L_2}{L_1}\right) \qquad (6\text{-}39)$$

Considering figure 6-13 we have

$$\log \left(\frac{400}{64}\right) = \beta \log \left(\frac{10}{1}\right)$$

therefore $\log 6.25 = \beta \log 10$

which gives $\beta = 0.80.$

Therefore, in this case, N increases as $L^{0.80}$, ie.

$$N \propto L^{0.80}$$

If band spreading was entirely determined by kinetic factors then N would increase linearly with the distance migrated since

$$N = \frac{L}{H}$$

It is worth noting that if N is calculated on the basis of the distance travelled by the low concentration end of the peak, ie. the tail end, then N increases exactly linearly with the distance migrated as shown in figure 6-15 ie.

$$N \propto L$$

This simple model indicates that even when band spreading occurs entirely as a result of thermodynamic effects, the band width, W_z, *may* still increase more or less in proportion to $L^{\frac{1}{2}}$, ie. where

$$W_z = (16H)^{\frac{1}{2}} L^{\frac{1}{2}}$$

since $$H = \frac{1}{16} \left(\frac{W_z^2}{L}\right)$$

From this, two conclusions may be drawn.

(1) If one could measure the peak width as a function of the distance travelled along the column then, even if the peak was fairly unsymmetrical, it would be impossible to distinguish between band spreading arising from kinetic effects and from spreading arising from thermodynamic effects if the peak width was proportional to $Z^{\frac{1}{2}}$.

(2) Up until now, the general opinion has been that the concept of HETP cannot be used for unsymmetrical peaks and that under overload conditions one cannot predict the effect that increasing the column length, L, will have on the peak distortion, a_d, and on the number of plates, N, to which the column is equivalent. However, this simple model shows that even when band spreading is caused mainly by a non-linear isotherm, it is still useful to consider the band spreading in terms of N and that the use of the concept of HETP under overload conditions is still justified providing that one does not attempt to interpret HETP in terms of kinetic contributions as one can under non-overload conditions through the equation

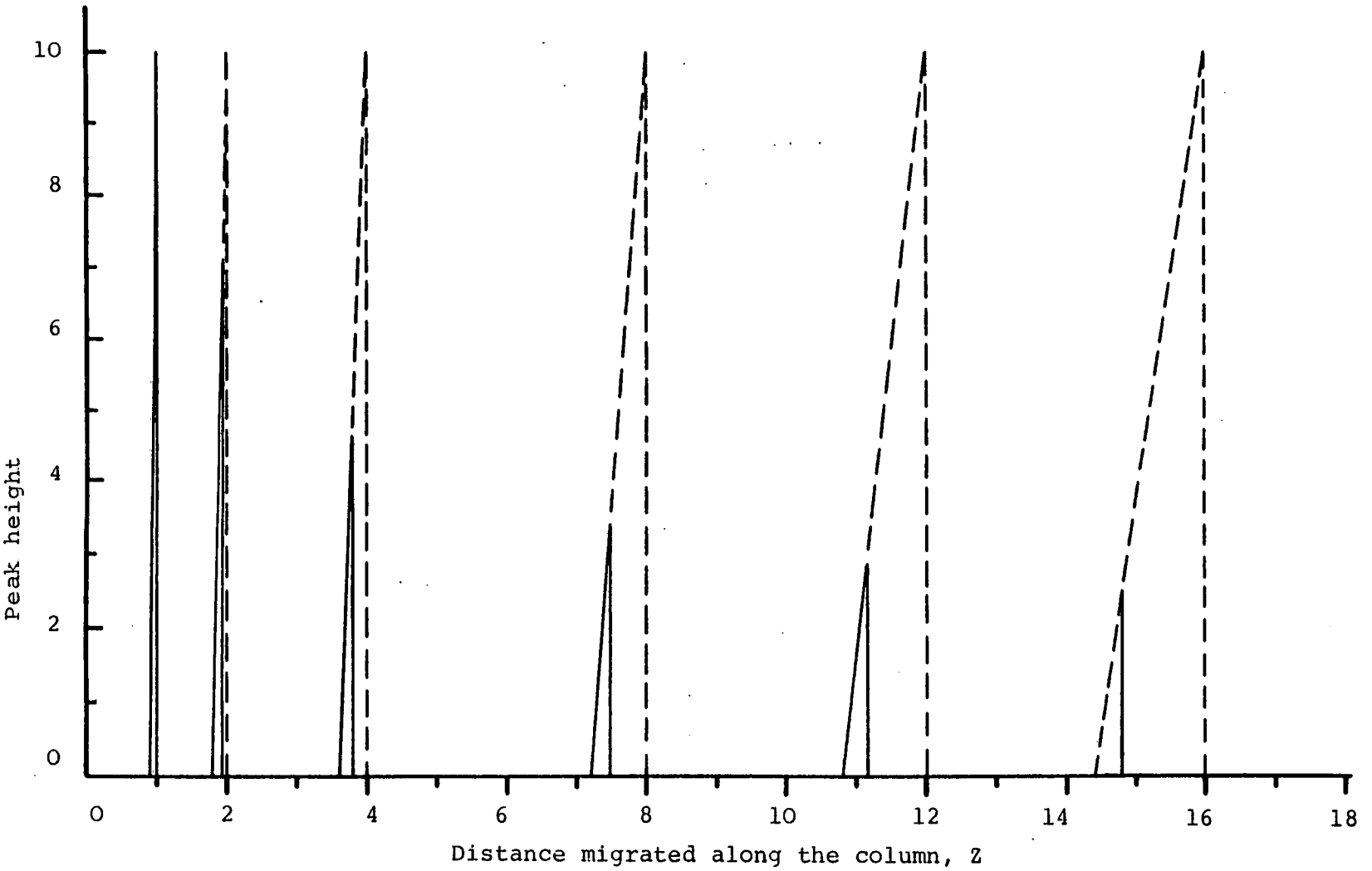

Figure 6.16 The schematic representation of the propagation of a triangular solute band resulting from the injection of a rectangular plug where there is a 10% variation between the k' valves of the maximum concentration and the zero concentration at the column inlet.

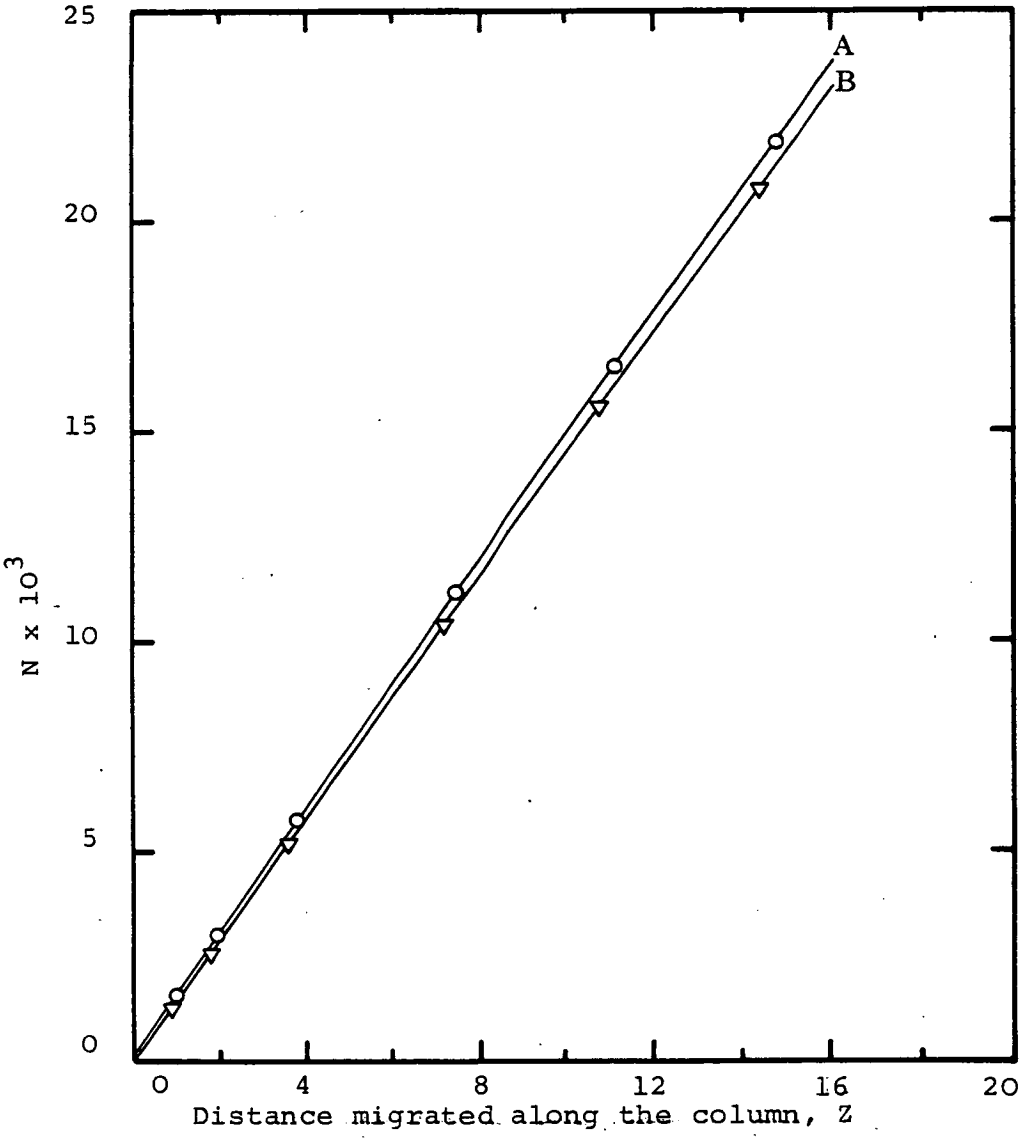

Figure 6.17 Dependence of N with the distance migrated along the column for a 10% variation in k' between the maximum concentration and the zero concentration at the column inlet; (A) as measured at the front of the peak (high concentration), where $N \alpha Z^{0.97}$ and (B) as measured at the rear of the peak (low concentration), where $N \alpha Z$.

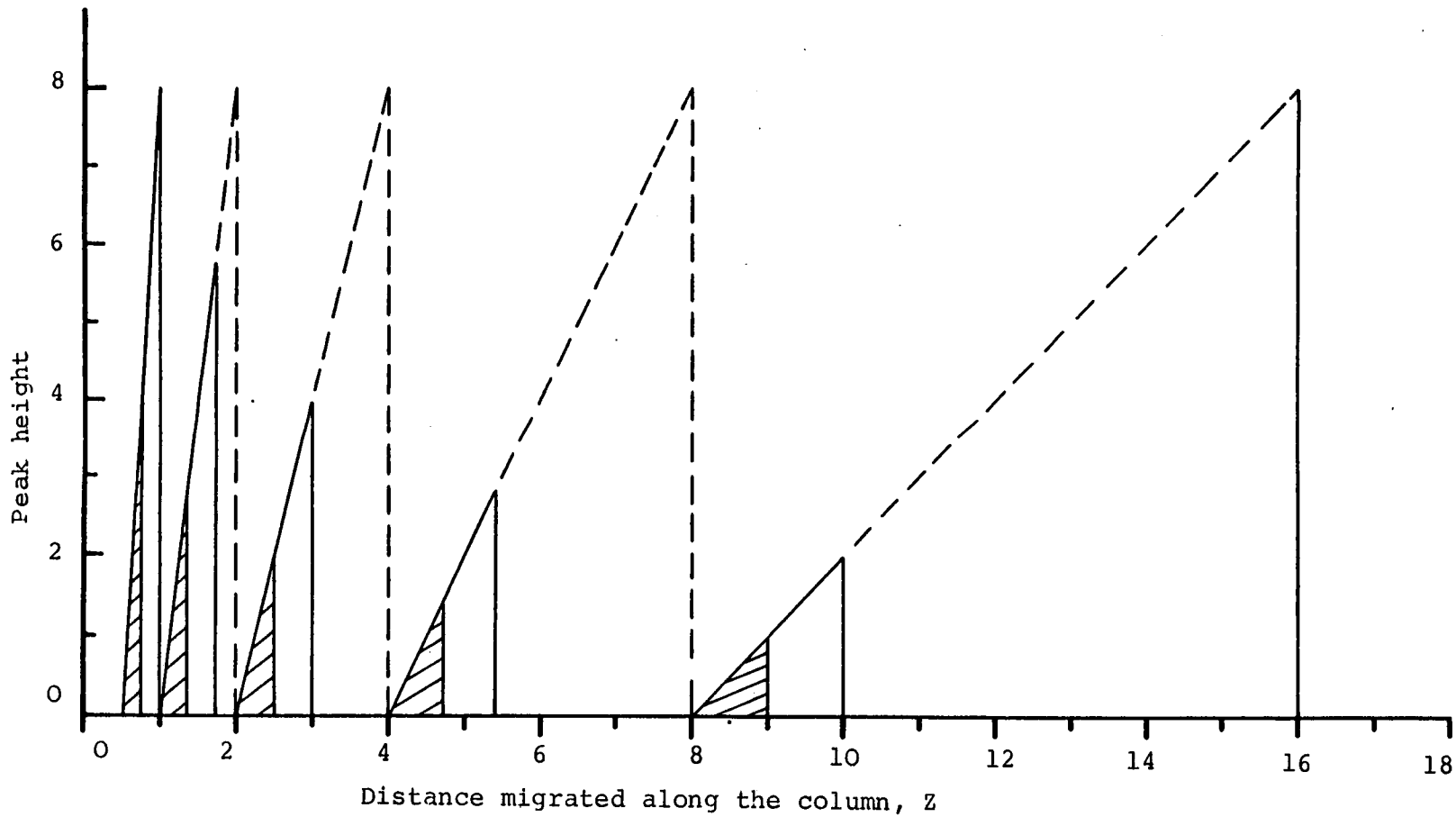

Figure 6.18 A schematic representation illustrating the difference in the propagation of a triangular solute band when the sample size is reduced to ¼ of the original size as given in figure 6.13 (i.e. for a 50% variation between the k' of the maximum concentration and the zero concentration at the column inlet).

$$h = A\nu^{1/3} + \frac{B}{\nu} + C\nu$$

as described in Chapter 4. Therefore, using this model one can predict what will happen to N and a_d as L is increased.

Where the distribution isotherm is only slightly non-linear, with say a 10% variation in the k' values of the maximum concentration and zero concentration points in the solute zone, the bands produced are much narrower and are more symmetrical, as illustrated by figure 6-16. In this case, N, as determined at the maximum concentration point in the zone, is found to increase almost linearly with L as illustrated in figure 6-17, since it is found that

$$N \propto L^{0.97}$$

As with the previous situation, N is found to increase exactly linearly when the low concentration end of the peak is considered.

Peak distortion also decreases with the distance migrated as illustrated in figure 6-14 and is found to be less than at the corresponding distance along the column when there is a larger variation in the k' values.

This model can also be used to find out what happens to the peak width, the plate number, N, and the peak distortion, a_d, when the sample size is reduced, for example to 1/4 of the original sample size, as illustrated in figure 6-18. It can be seen from the diagram in figure 6-18 that the peaks are now narrower and more symmetrical, as

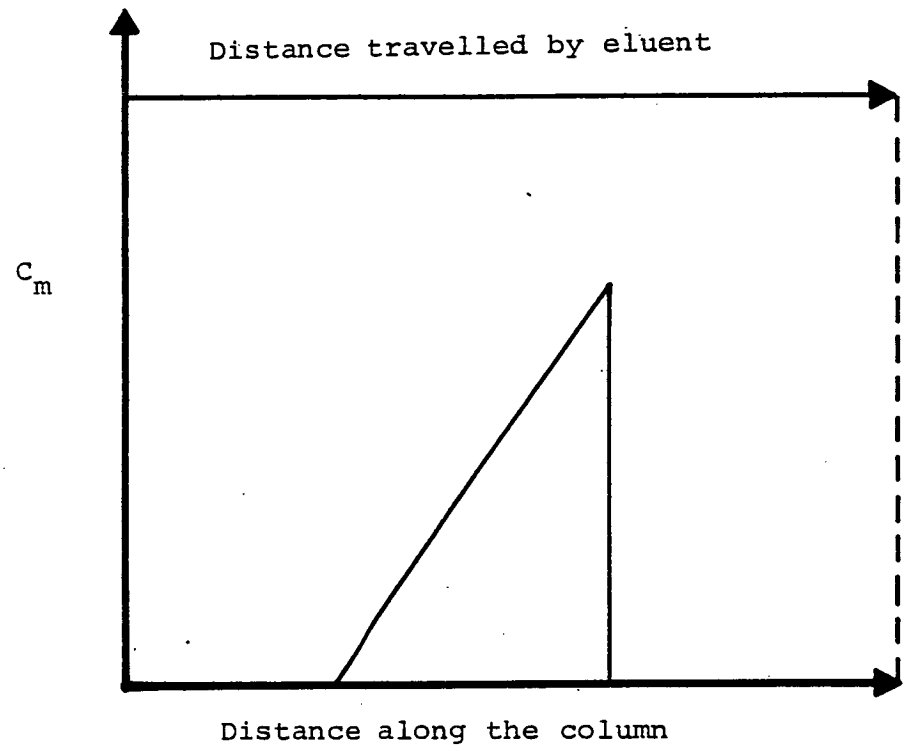

Figure 6.19 Schematic representation of a triangular solute band.

illustrated in figure 6-14. The number of plates N, to which the column is equivalent is also greater, as illustrated in figure 6-15 and it is found that N increases with $L^{0.95}$ ie.

$$N \propto L^{0.95}$$

and therefore increases almost linearly suggesting that band broadening is virtually due entirely to kinetic factors.

The isotherm which describes the model represented schematically in figure 6-13 can be established as follows.

In general, for a non-linear isotherm of the type illustrated in figure 6-10b we can write

$$k'_{Cm} = \frac{V_s}{V_m} \left(\frac{dC_s}{dC_m}\right) \qquad (6\text{-}40)$$

where V_s/V_m is the phase ratio and C_s, C_m are the concentrations of a solute in the stationary and mobile phases respectively.

For the situation which produces a chromatogram of the form illustrated in figure 6-19, then for any concentration, C_m, we have

$$R_{F(C_m)} = R_{F(0)} + \alpha C_m \qquad (6\text{-}41)$$

where $R_{F(C_m)}$ is the rate of movement of a concentration, C_m, $R_{F(0)}$ is the rate of movement of zero concentration and α is a proportionality factor (note that R_F lies between 0 and 1 and can never exceed unity).

In general, R_F can be expressed as

$$R_F = \frac{C_m V_m}{C_s V_s + C_m V_m} = \frac{1}{1+k'}$$

therefore $$k'_{(C_m)} = \frac{1-R_{F(C_m)}}{R_{F(C_m)}} \qquad (6\text{-}42)$$

Combining equations (6-41) and (6-42) we have

$$k'_{(C_m)} = \frac{1-R_{F(O)}^{-\alpha C_m}}{R_{F(O)}^{+\alpha C_m}} \qquad (6\text{-}43)$$

Bu substituting equation (6-40) into equation (6-43) we can write

$$\left(\frac{V_s}{V_m}\right)\left(\frac{dC_s}{dC_m}\right) = \frac{1-R_{F(O)}^{-\alpha C_m}}{R_{F(O)}^{+\alpha C_m}}$$

$$= \frac{1}{R_{F(O)}^{+\alpha C_m}} - 1 \qquad (6.44)$$

Since $C_s = \int_o^{C_s} dC_s$, then

$$\int_o^{C_s} dC_s = \frac{V_m}{V_s}\left\{\frac{1}{R_{F(O)}^{+\alpha C_m}} - 1\right\} dC_m$$

$$= \frac{V_m}{V_s}\left\{\frac{1}{\alpha} \ln \left[\frac{R_{F(O)}^{+\alpha C_m}}{R_{F(O)}}\right] - C_m\right\}$$

therefore $$C_s = \frac{V_m}{V_s}\left\{\frac{1}{\alpha} \ln\left[1 + \frac{\alpha C_m}{R_{F(O)}}\right] - C_m\right\} \qquad (6\text{-}45)$$

If, for the purposes of illustration, we assume $V_m/V_s = 1$, $\alpha = 0.1$, $R_{F(O)} = 0.5$, then equation (6-45) takes the form of

$$C_s = 10 \ln (1 + 0.2C_m) - C_m \qquad (6\text{-}46)$$

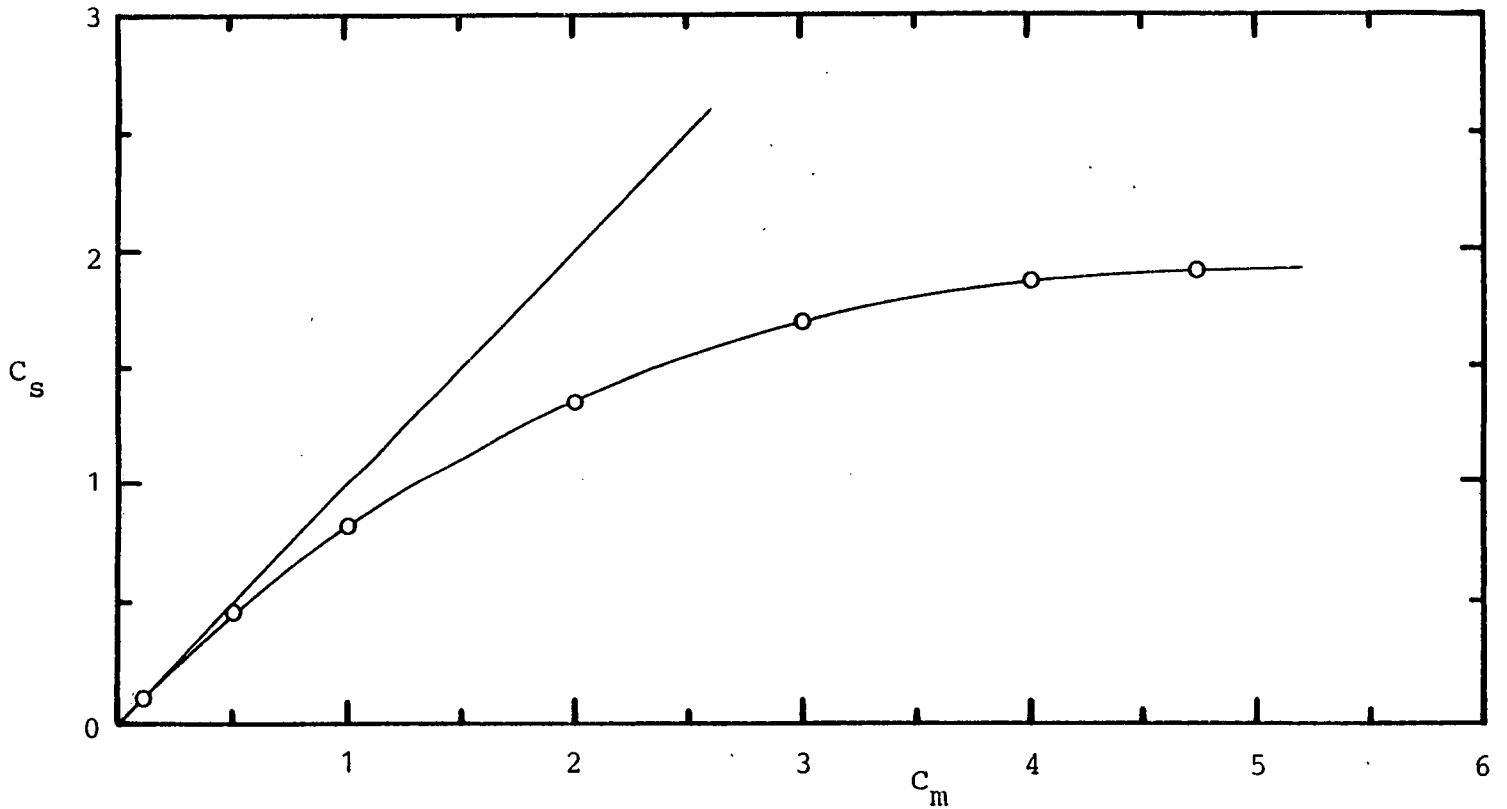

Figure 6.20 C_s versus C_m showing the curve produced by the isotherm as given by equation (6-46) for a chromatogram of the form illustrated in figure (6-19).

The isotherm produced by this equation, and illustrated in figure 6-20, is non-linear with a curve which is reasonably close to the Langmuir isotherm, which is given by

$$C_s = \frac{V_m}{V_s}\left\{\frac{\beta C_m}{1+\gamma C_m}\right\} \qquad (6\text{-}47)$$

References

Chapter 6

1. A. Wehrli, U. Hermann and J.F.K. Huber, J.Chromatogr; 125 (1976) 59.
2. C.F. Simpson in 'Practical Liquid Chromatography', C.F. Simpson (Editor) Heyden 1976, p.5.
3. L.R. Snyder in "Principles of Adsorption Chromatography" Marcel Dekker, New York, 1968.
4. R.E. Majors; Anal.Chem. 44 (1972) 1722.
5. A.W.J. De Jong, J.C. Kraak, H. Poppe and F. Nootigedacht; J.Chromatog. 193 (1980) 181.
6. A.W.J. De Jong, H. Poppe and J.C. Kraak; J.Chromatog. 209 (1981) 432.
7. K.J. Bombaugh and P.W. Almquist; Chromatographia 8 (1975) 109.
8. A. Wehrli; Z.Anal.Chem. 277 (1975) 289.
9. A.W.J. De Jong, H. Poppe and J.C. Kraak; J.Chromatogr. 148 (1978) 127.
10. J.C. Kraak, H. Poppe and F. Smedes; J.Chromatogr. 122 (1976) 147.
11. J.J. Kirkland, W.W. Yau, H.J. Stoklosa and C.H. Dilks; J.Chromatog.Sci. 15 (1977) 303.
12. R.P.W. Scott and P. Kucera; J.Chromatogr. 119 (1976) 467.
13. J.N. Done; J.Chromatogr. 125 (1976) 43.
14. C.N. Reilley, G.P. Hildebrand and J.W. Ashley Jnr.; Anal.Chem. 341 (1962) 1198.
15. B. Coq, G. Cretier and J.L. Rocca; J.Chromatog. 186 (1979) 485.

16. J.F.K. Huber and R.G. Gœritse; J.Chromatogr. 58 (1971) 137.

17. J.F.K. Huber in "Gas Chromatography" M. van Swaay (Editor) Butterworths, London 1962, p.26.

18. J.J. DeStefano and J.J. Kirkland; Anal.Chem. 47 (1975) 1103A.

19. R.A. Wall; J.Liq.Chromatog. 2 (1979) 775.

20. J.H. Knox in "Practical High Performance Liquid Chromatography" C.F. Simpson (Editor), Heyden 1976, p.43.

21. J.C. Smit, H.C. Smit and E.M. de Jager; Anal.Chim.Acta Comput.Tech.Optim.; 122 (1980) 151.

CHAPTER 7

THE STRUCTURE, PREPARATION AND BONDING OF SILICA GELS

Chapter 7. The Structure, Preparation And Bonding Of Silica Gels

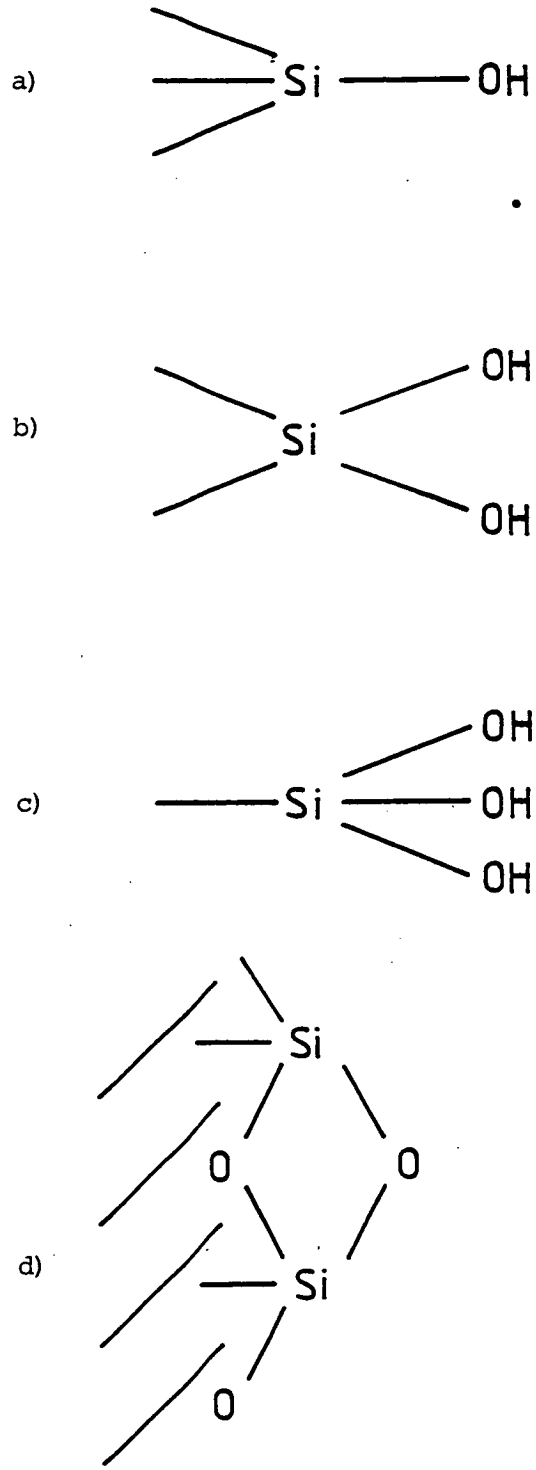

Figure 7.1 The four types of surface groups found on silica gel.

THE STRUCTURE, PREPARATION AND BONDING OF SILICA GELS

7.1 The Structure of Silica

The formation of silica gel by hydrolysis of sodium silicate solution has been outlined in the following reaction scheme.

1st Stage:

Hydrolysis to $Si(OH)_4$ $\xrightarrow{\text{Polymerisation}}$ Colloidal particles of SiO_2

2nd Stage:

a) Dilute solution $\xrightarrow{\text{Aggregation}}$ Weak gel or precipitate.

b) Concentrated solution $\xrightarrow{\text{Aggregation}}$ Strong, firm gel.

Each colloidal particle is a 3-dimensional network of interlinked SiO_4 tetrahedra with hydroxyl groups attached to the surface to complete the tetrahedral co-ordination. The final silica gel is a random aggregation of these colloidal particles. The surface of such a silica gel, after gentle drying, is covered with OH-groups and with physically adsorbed water.

The surface of the silica gel contains four types of surface group[1] as illustrated in figure 7.1. The first three are silanol groups which are either hydrogen bonded to the oxygen atom of an adjacent silanol group or are free groups and the other type are siloxane bridges which are formed by the condensation reaction of two adjacent silanol groups.

The active sites on the silica are the OH-groups and it

is believed[2] that there are two types of active sites, type A and type B. The A-sites consist of a single hydroxyl group whilst the B-sites consist of paired hydroxyl groups, as illustrated in figure 7.2.

At ambient temperatures, the surface of "fully" hydroxylated silicas contain approximately 4.6 hydroxyl groups per 100Å^2 of total surface area,[2] which is equivalent to 8μmole m^{-2}. Of these 1.4±0.1 hydroxyl groups exist as single non-hydrogen-bonded species (1.4 A-type sites per 100Å^2) and the remaining 3.2 hydroxyls exist as pairs (1.6±0.1 type B sites per 100Å^2). Dehydroxylation by heating at 500±50°C results in the complete removal of type B sites to form siloxane bridges, ie.

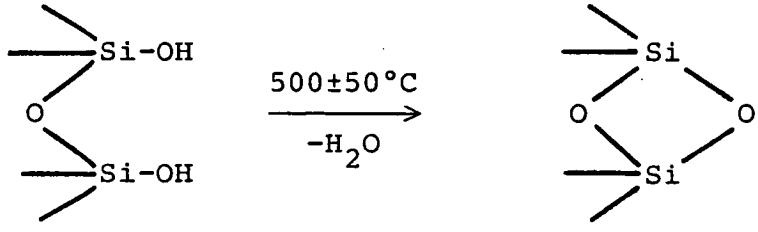

Using thermogravimetric methods, De Boer[3] found that silicas approached a limiting surface concentration of 4.6 hydroxyls per 100Å^2 of surface after they had been repeatedly rehydroxylated and annealed at 450°C. They concluded that such a surface closely resembled the rhombohedral face of β-tridymite in which each of the 4.6 surface silicon atoms per 100Å^2 carried one hydroxyl.

But Tyler *et al.*[4] showed that silicas in general are composed of small primary crystallites possessing hydroxylated surfaces of the order of tens of Å in diameter aggregated into larger spheroidal particles of the order of hundreds of Å in diameter. The assumption was then made that crystallites of

low symmetry such as β-tridymite or β-crystabolite cannot exhibit identical surface planes over all of their exterior surfaces and that therefore a number of crystal planes exist in the surface of silica.

As has already been stated, the number of hydroxyl groups per 100Å^2 of surface area (n_{OH}) assumes a limiting maximum value of $(4.6\pm0.2)/100\text{Å}^2$. This figure is taken as representing a smooth amorphous silica surface where each Si atom carries one OH-group. The decrease of n_{OH} by heating is ascribed to the disappearance of surface irregularities and surface arrangements containing more than one OH-group per surface Si atom. Not all particles of silica which have not been heated to high enough temperatures will be bound via oxygen bridges to three other Si atoms inside the particles. There may be some Si atoms which are only anchored with two or even one Si-O-Si bond to the inside of the particle and such silicon atoms will carry more than one hydroxyl group.

The heating procedure therefore leads to a relatively small decrease of surface area and of pore volume, to an annealing and smoothening process, and to the 'sticking together' of particles at certain points by the formation of Si-O-Si bonds.

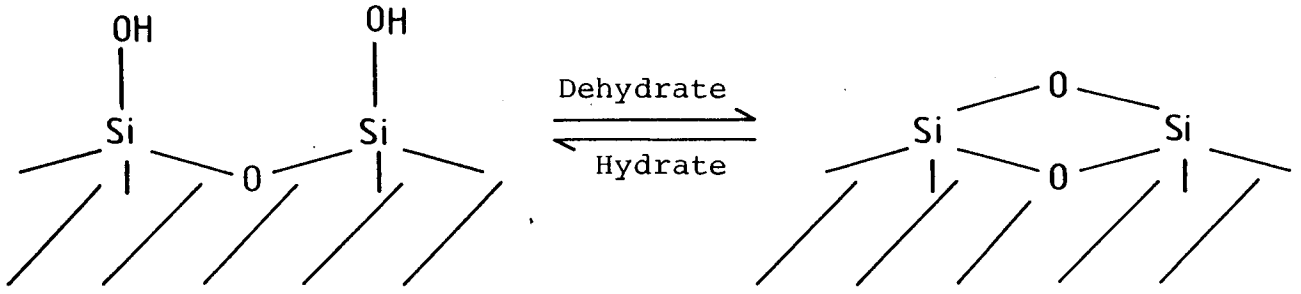

Figure 7.3 Wide pore silica

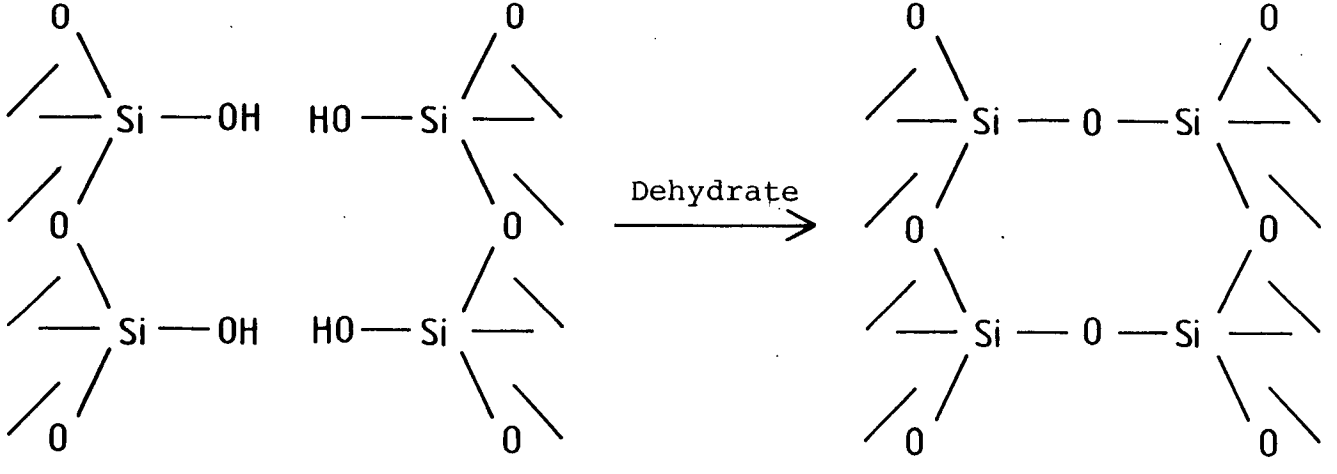

Figure 7.4 Narrow pore silica

7.2 Thermal Modification of Silica

As has already been mentioned, the active sites for adsorption on silica are the surface hydroxyl groups, either isolated or hydrogen-bonded. Amorphous silica does not have such an ordered arrangement of hydroxyl groups as crystalline silica and hydrogen-bonding between neighbouring groups can occur.[5] With narrow pore silicas, the surfaces are covered with many hydrogen-bonded hydroxyl groups while wide pore silicas consist mainly of isolated hydroxyl groups.

De Boer and his co-workers[3,6-8] discovered that physically adsorbed water was removed from the surface by heating at 120°C and that heating at temperatures above this progressively removed chemisorbed water from surface hydroxyl groups. The thermal treatment of silica above 200°C is found to change the surface structure by removing water to produce strained siloxane bridges which are weak adsorbent sites.

With wide pore silicas, the loss of water is from two adjacent hydroxyl groups on the same surface. This reaction can be reversed by boiling in water as illustrated in figure 7.3.

With narrow pore silicas, condensation can occur between hydroxyl groups on different surfaces. In this case, the loss of water is permanent and the siloxane groups so formed cannot be broken by heating in water to regenerate the hydroxyl groups as illustrated in figure 7.4. This can lead to a decrease of surface area and some loss of pore volume. Silica heated to above ∿650°C starts to sinter and does so fairly rapidly as the temperature is raised above this. Sintering causes the surface area and pore volume to decrease dramatically and there is substantial migration of the silica itself. The

temperature at which the sintering becomes significant depends largely upon the impurity content of the silica. Thus pure silica will not sinter below 1000°C, whereas silica containing salts, especially sodium oxide, will sinter at much lower temperatures eg. 700°C. The temperature will also depend on the structure of the silica ie. high surface area materials will sinter at lower temperatures than low surface area materials.

During the thermal treatment, any hydroxyl groups located within the bulk of the solid are removed and very few are regenerated during the rehydroxylation process.[2]

The two types of active sites, the isolated hydroxyl group (type A) and the hydrogen-bonded hydroxyl group (type B), have different adsorption strengths. The latter[9] tends not to lead to good chromatography as they are stronger adsorption sites for anything but monofunctional solutes. The silica is therefore deactivated by adding small amounts of polar compounds (eg. water, methanol) to the eluent to remove these stronger sites so that adsorption can occur at the isolated hydroxyl groups thus forming a relatively uniform adsorption surface. Failure to deactivate these strongly adsorbing sites will produce peak tailing since these sites will hold onto solute molecules more strongly than will the other weaker A-type sites. When performing chromatography, it is essential that the processes involved are all of the same type and not a mixture of two different types.

7.3 Rehydration of Thermally Modified Silica[10]

For silicas which have been thermally treated up to temperatures of 350°C, the amount of water re-adsorbed by the modified silica is of the same order as by un-modified silica. For silicas thermally modified at temperatures of between 350-450°C there is a rapid decrease in the amount of water re-adsorbed. This is because of the condensation between surface hydroxyl groups, which are responsible for the molecular water adsorption, to give siloxane groups. Where siloxane groups have been formed from adjacent hydroxyl groups, as in the case of wide pores, rehydration will break the siloxane group to regenerate two hydroxyl groups. However, where siloxane groups have been formed from hydroxyl groups on different surfaces, as in the case of the narrow pores, rehydration will not break these groups and so the siloxane bridges remain.

Above 700°C the amount of water re-adsorbed decreases significantly as a result of the decrease in the surface area due to sintering.

7.4 Chemically Bonded Silica Gels

The ability to chemically bond different organic groups onto the surface of silica gel, was first mentioned in 1950 by Howard and Martin[11] who used dimethyldichlorosilane to prepare a reversed-phase material to separate C_{12}-C_{18} fatty acids. However, chemically bonded materials fell into disuse until re-introduced in 1969 by Halasz and Sebastian.[12] This has led to the production of a wide variety of novel stationary phases which are suitable for different modes of chromatography. While silica gel can only be used for normal-phase adsorption chromatography, bonded phases can be used for reversed-phase separations, ion exchange separations or even normal phase separations depending on the organic moiety bonded onto the siliceous support and the choice of mobile phase system. Bonded phases are more stable than those used for liquid-liquid partition chromatography (LLC) since the organic moieties are chemically bonded rather than coated onto the silica surface, as in the case of LLC, and therefore they afford greater chromatographic reproducibility.

Chemically bonded stationary phases have been reviewed in several papers.[13-20] Basically the preparation of these phases involves the reaction of an organic moiety with the surface hydroxyl groups, or silanols, of the support. This can be carried out in a number of different ways as described below.

(i) The surface hydroxyl groups can be reacted with an alcohol to produce a silicate ester, ie.

$$\geqslant Si\text{-}OH + R\text{-}OH \longrightarrow \geqslant Si\text{-}OR$$

However, the Si-O-C linkages produced are hydrolysed in the

presence of water.

(2) The surface silanol groups can be first converted to chlorides using thionyl chloride and then either reacted with a primary or secondary amine to produce an aminosilane, ie.

(i) $\geqslant Si\text{-}OH + SOCl_2 \longrightarrow \geqslant Si\text{-}Cl$

(ii) $\geqslant Si\text{-}Cl + R_2NH \longrightarrow \geqslant Si\text{-}NR_2$

or alternatively, reacted with a Grignard reagent or organolithium to produce an organic group directly bonded onto the surface silicon atoms, ie.

(iii) $\geqslant Si\text{-}Cl + R\text{-}Li \longrightarrow \geqslant Si\text{-}R$

Both the Si-N-C and the Si-C linkages formed are stable to hydrolysis and also within the pH range 3-8.

(3) The final and most popular of all of the bonding methods is the reaction of the surface silanol groups with an organochlorosilane, or an alkoxysilane, to produce linkages of the type

$$\geqslant Si\text{-}OH + R_3SiCl \longrightarrow \geqslant Si\text{-}O\text{-}SiR_3$$

where the Si-O-Si-C linkage is stable to hydrolysis and within the pH range 1-8. Above pH 8, the silica itself starts to dissolve and all bonded phases are hydrolysed.

The length of the hydrocarbon chain can vary from C_1 to C_6, C_8, C_{18} and C_{22}, with C_8 and C_{18} being the most popular.

Reversed phases produced by this third method can be prepared in basically two forms; the "brush"- or "bristle"-type material and the "polymeric"- or "fur"-type material.

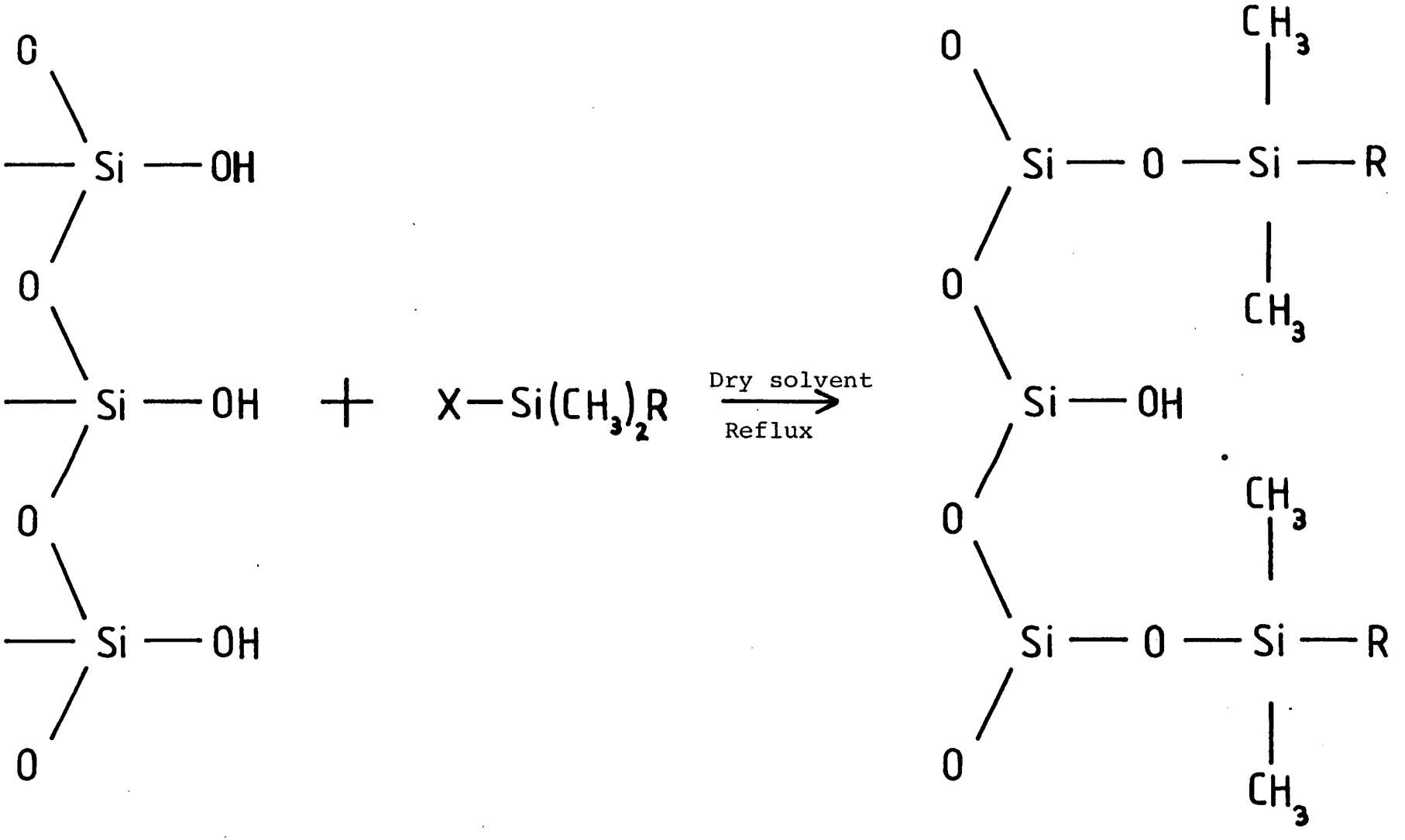

Figure 7.5 Formation of a monomer by reaction with a mono-substituted organosilane

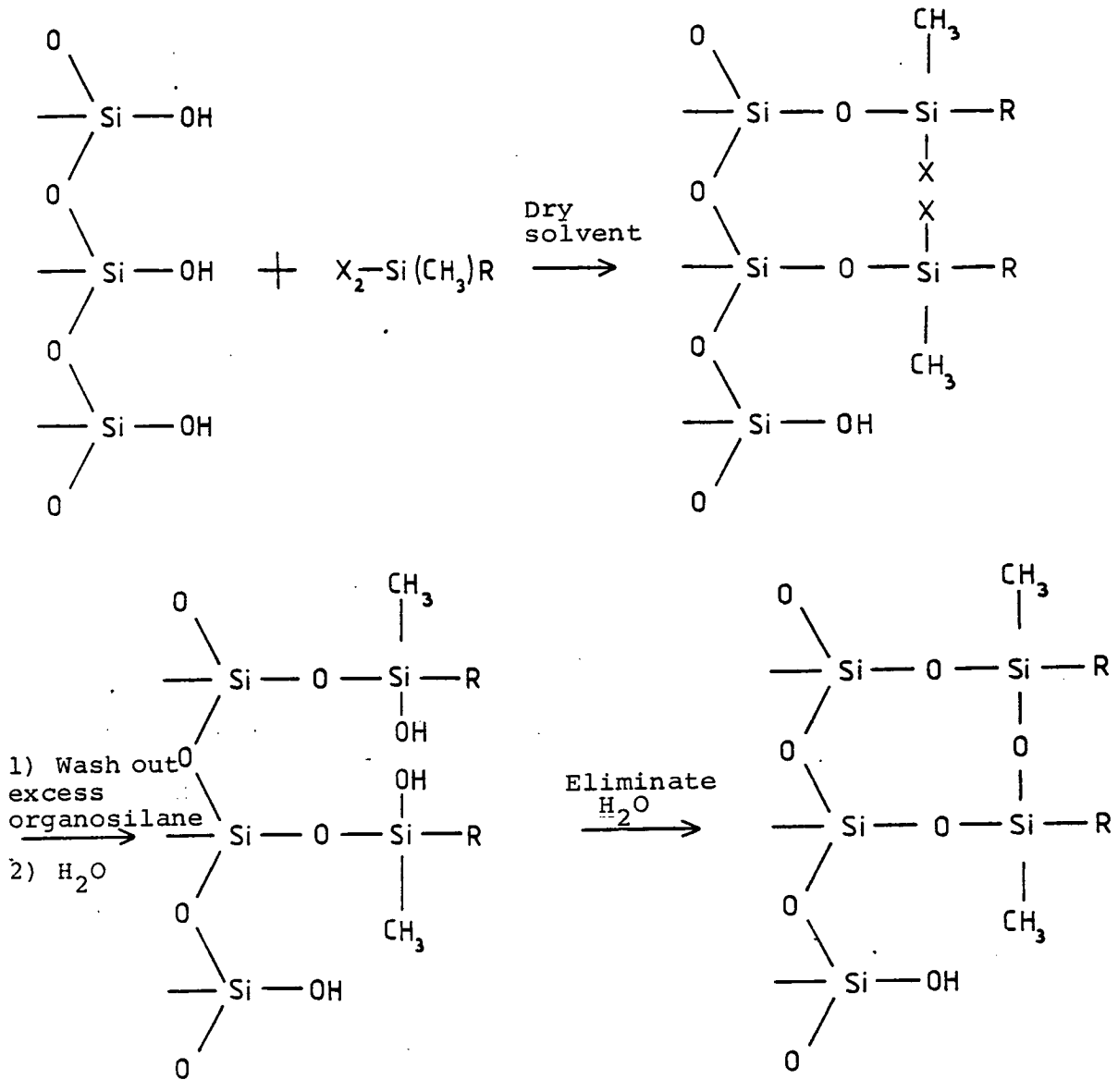

Figure 7.6 The formation of a 2 - dimensional dimer by reaction with a di-substituted organosilane.

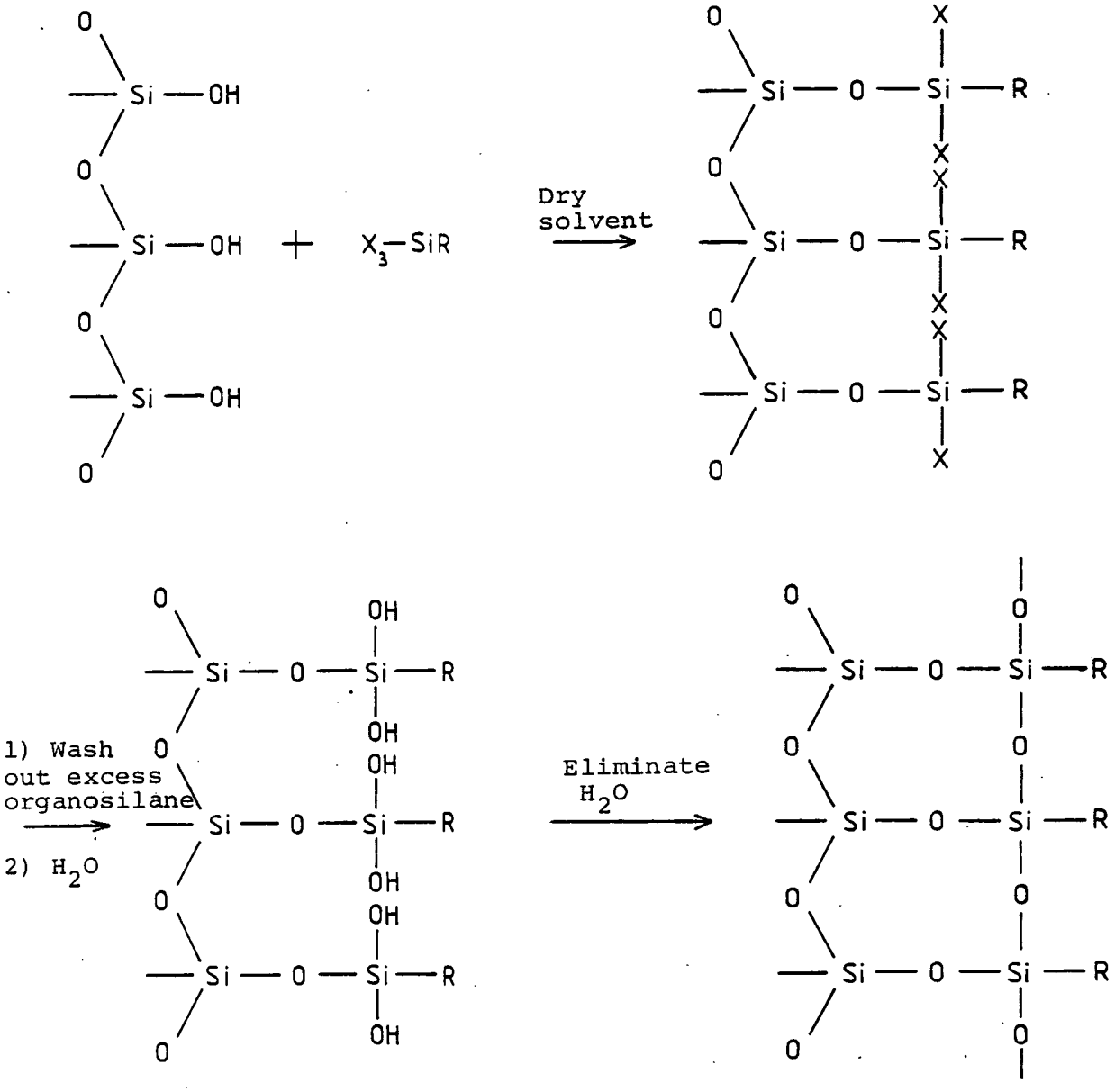

Figure 7.7 The formation of a linear bonded 2-dimensional polymer.

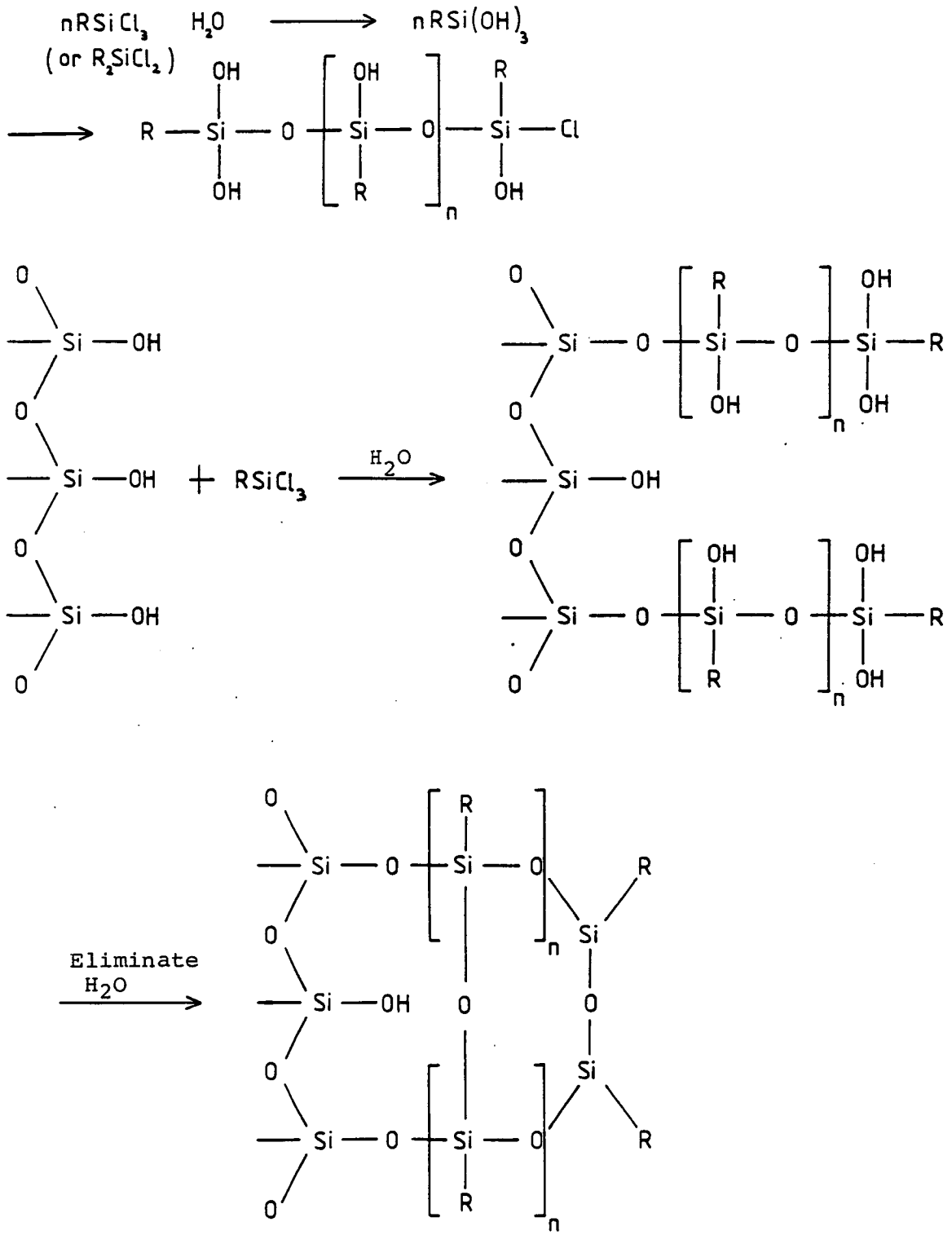

Figure 7.8 The formation of a three-dimensional polymer (e.g. Zipax) where water is added either initially or after anhydrous bonding, but before the excess organosilane has been washed out.

The "brush"-type materials are prepared by reacting the surface silanol groups with a monochlorosilane, such as octadecyldimethylchlorosilane ($C_{18}H_{37}(Me)_2SiCl$), ie.

$$\geqslant Si\text{-}OH + Cl\text{-}Si(Me)_2\text{-}R \xrightarrow[\text{Reflux}]{\text{Dry solvent}} \geqslant Si\text{-}O\text{-}Si(Me)_2\text{-}R + HCl$$

The organosilane molecule in this case reacts with one silanol group to produce a hydrocarbon chain which is attached only at one end to the siliceous surface via an Si-O-Si bond, with the free-moving hydrocarbon chains resembling the bristles on a brush, as illustrated in figures 7-5 and 7-10.

Di- and tri-halogenated organosilanes can also be used. In these cases, since steric effects prevent the formation of more than two bonds between the surface silanol groups and the organosilane, there exists the possibility of the formation of a polymeric phase material, especially if there is any water present during the reaction. When a di-halogenated organosilane is reacted with the silica gel in dry solvent, with the excess organosilane being removed before water is added, then a 2-dimensional dimer is formed as illustrated in figure 7-6. If a tri-halogenated organosilane is used under the same reaction conditions then a linear bonded 2-dimensional polymer is formed as illustrated in figure 7-7. However, if either a di- or a tri-substituted organosilane is reacted with the silica in the presence of water or if water is added after anhydrous bonding but before the excess organosilane is washed out then a true 3-dimensional polymer is formed as illustrated in figure 7-8. In such cases, polymerisation occurs in the organic solvent

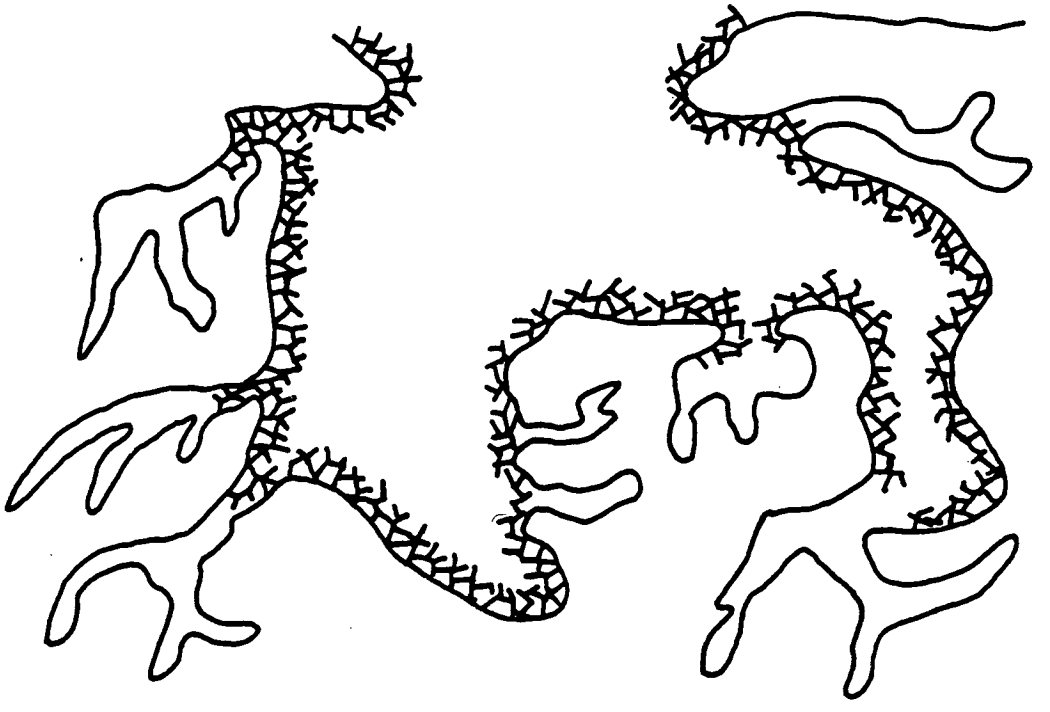

Figure 7.9 Schematic representation of polymeric coating on walls of a silica gel pore. (Reproduced from reference 20).

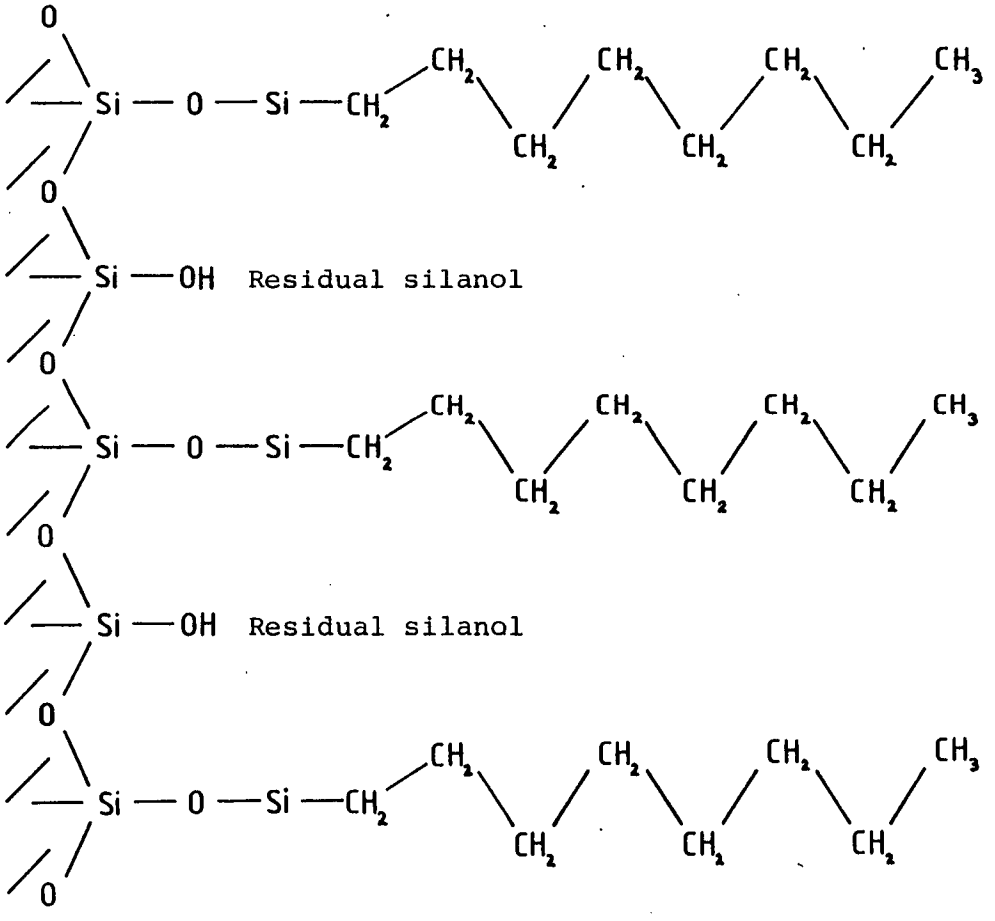

Figure 7.10 A schematic representation illustrating a brush-type material (C_8) and residual silanol groups.

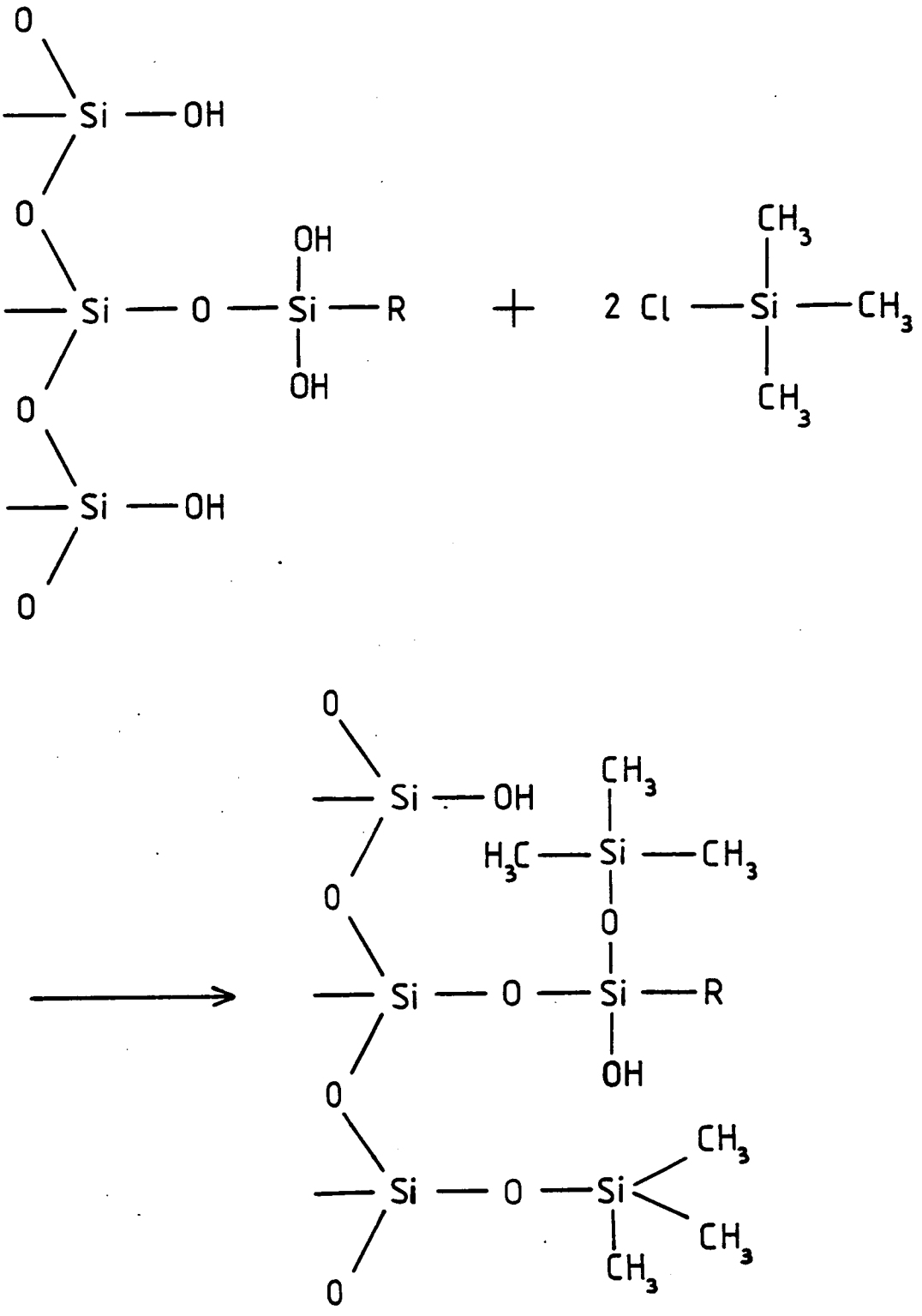

Figure 7.11 Schematic representation of "capping" of residual silanol groups with trimethyl chloro silane.

Table 7.1 Types of Bonded Phases

Function	Type of Separation
Long chain hydrocarbon	Reversed phase
Short chain hydrocarbon	Reversed phase
Aromatic hydrocarbon	Reversed phase
Fluorinated ether	Reversed and normal phase
Ether	
Ester	Normal phase
Cyano	Normal phase
Nitro	Normal phase
Amino	Normal phase, ion exchange
Hydroxyl	Normal phase
Carboxylic acid	Ion exchange
Sulphonic acid	Ion exchange
Quaternary ammonium	Ion exchange

itself, whereupon the polymer then bonds onto the surface of the silica. An illustration of the polymeric coating on the walls of a silica gel pore is given in figure 7-9.

Highly cross-linked polymeric phases are undesirable since this leads to slow solute diffusion and slow mass transfer and therefore poorer column efficiency. Such chemically bonded phases are therefore not as useful for performing reversed-phase chromatography as the "monomeric" or "brush"-type materials.

It should be pointed out that, even after these bonding reactions have taken place, about 50% of the material will still contain residual surface hydroxyl groups, either as a result of steric factors of the reagent or, in the case of di- and tri-substituted organosilanes, due to the formation of new hydroxyl groups by hydrolysis (see figure 7-10). If these residual silanol groups are hydrated, then the rate of mass transfer between the mobile and stationary phases can be increased and therefore lead to improved efficiency. However, if the silanol groups react with a more polar part of the solute molecule then the retention mechanism will be a mixture of both partition and adsorption which may cause tailed peaks, poor peak symmetry or unpredictable retention. This can be prevented by "capping" any accessible residual silanol groups with a monofunctional organosilane such as trimethyl-chlorosilane (Me_3SiCl), as illustrated in figure 7-11.

By using one of the aforementioned types of synthesis, with in some cases a secondary reaction required,[17] it is possible therefore to not only vary the length of the hydro-carbon groups introduced, but also to introduce a wide range of functional groups. Table 7.1 lists some of the functional

groups which can be introduced, and the type of chromatography which can be performed. An extensive review has been published by Majors[16] on both the silica gel and chemically bonded phases which are commercially available.

Retention in reversed-phase chromatography is found to increase with increased carbon loading ie. carbon number, and therefore to increase with increasing chain length[20,21] since both are related. Retention also increases with surface coverage of silica gel and it is found to be greater for "monomeric" or "brush"-type materials. Coverage is less for "polymeric"-type phases since the reagent, and therefore the solutes, are unable to penetrate the small pores. The chemical nature of the bonded moiety also affects the retention as does the concentration of residual silanols which are accessible to the solute molecules. Finally the nature of the silica gel used ie. its porosity, surface area and pore size will also influence the retention properties of the bonded phase so produced.

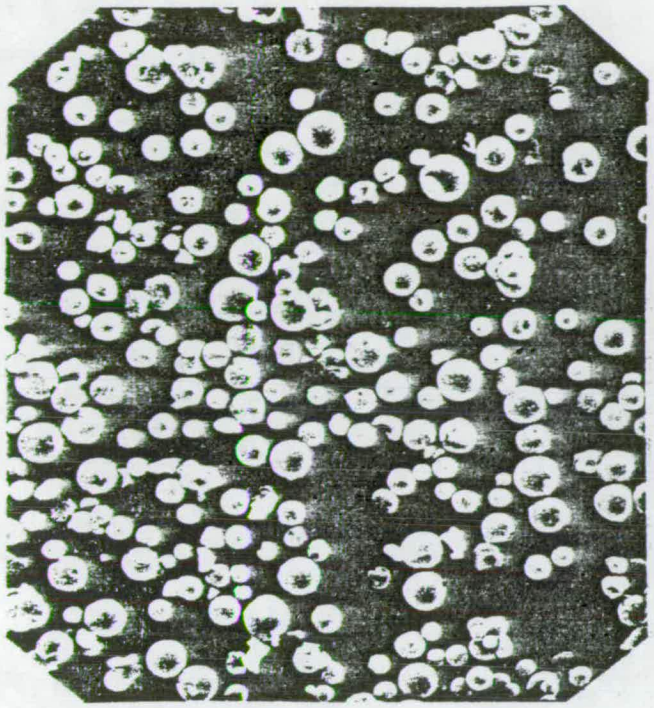

x400

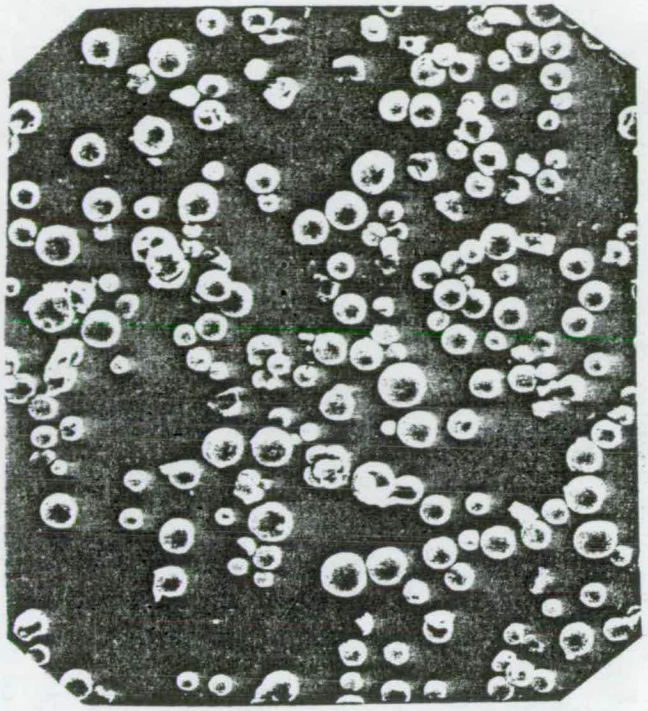

x400

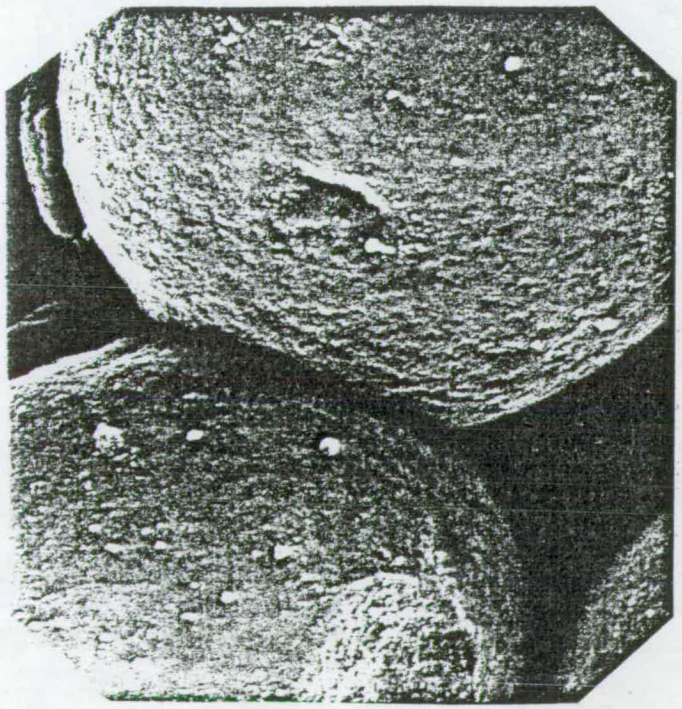

x10,000

Figure 7.13 ODS-silica (5-15μm nominal) prepared as outlined in section R.3.1(iv) of the Reserved Chapter as seen under an electron microscope.

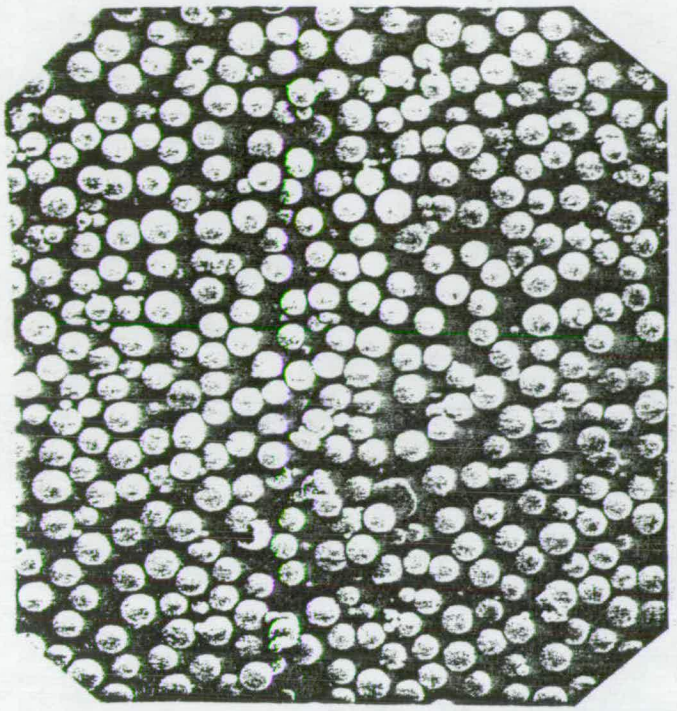

x100

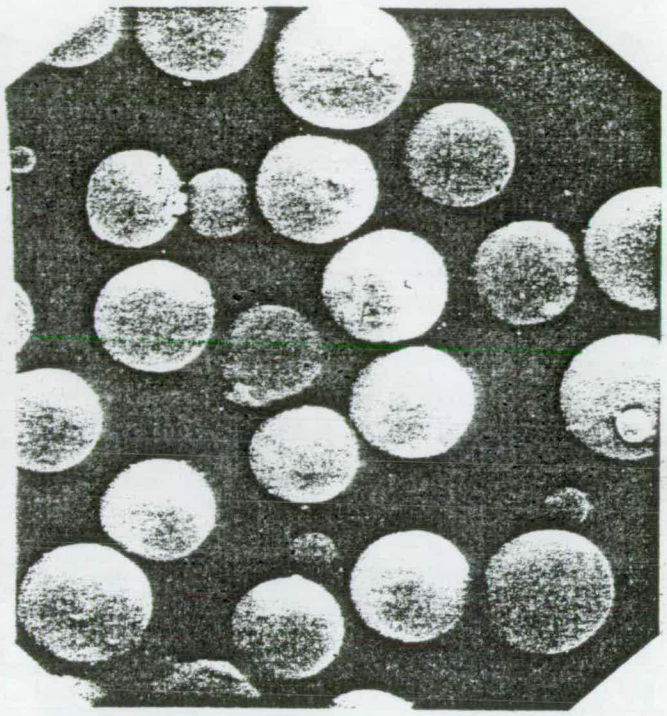

x400

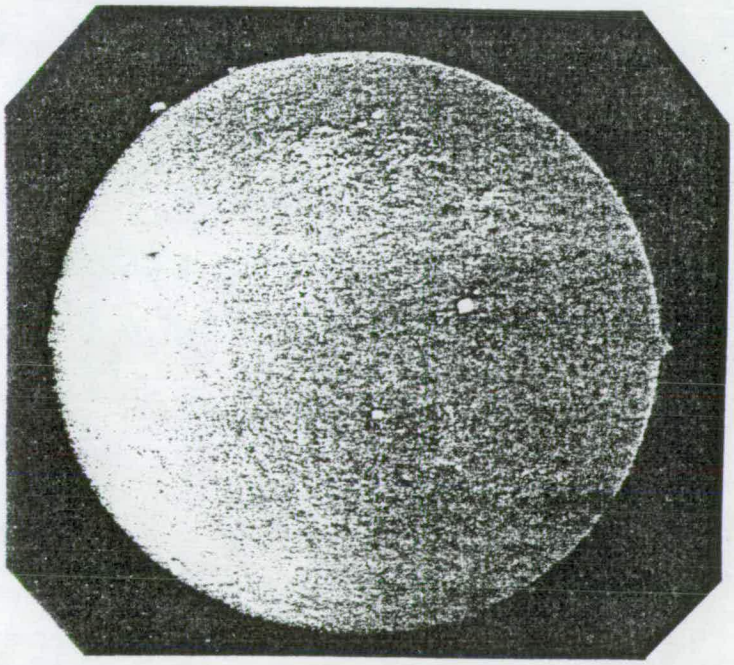

x2,000

Figure 7.12 ODS-silica (sample 6, 48-44μm nominal) prepared as outlined in section R.2.3 of the Reserved Chapter as seen under an electron microscope.

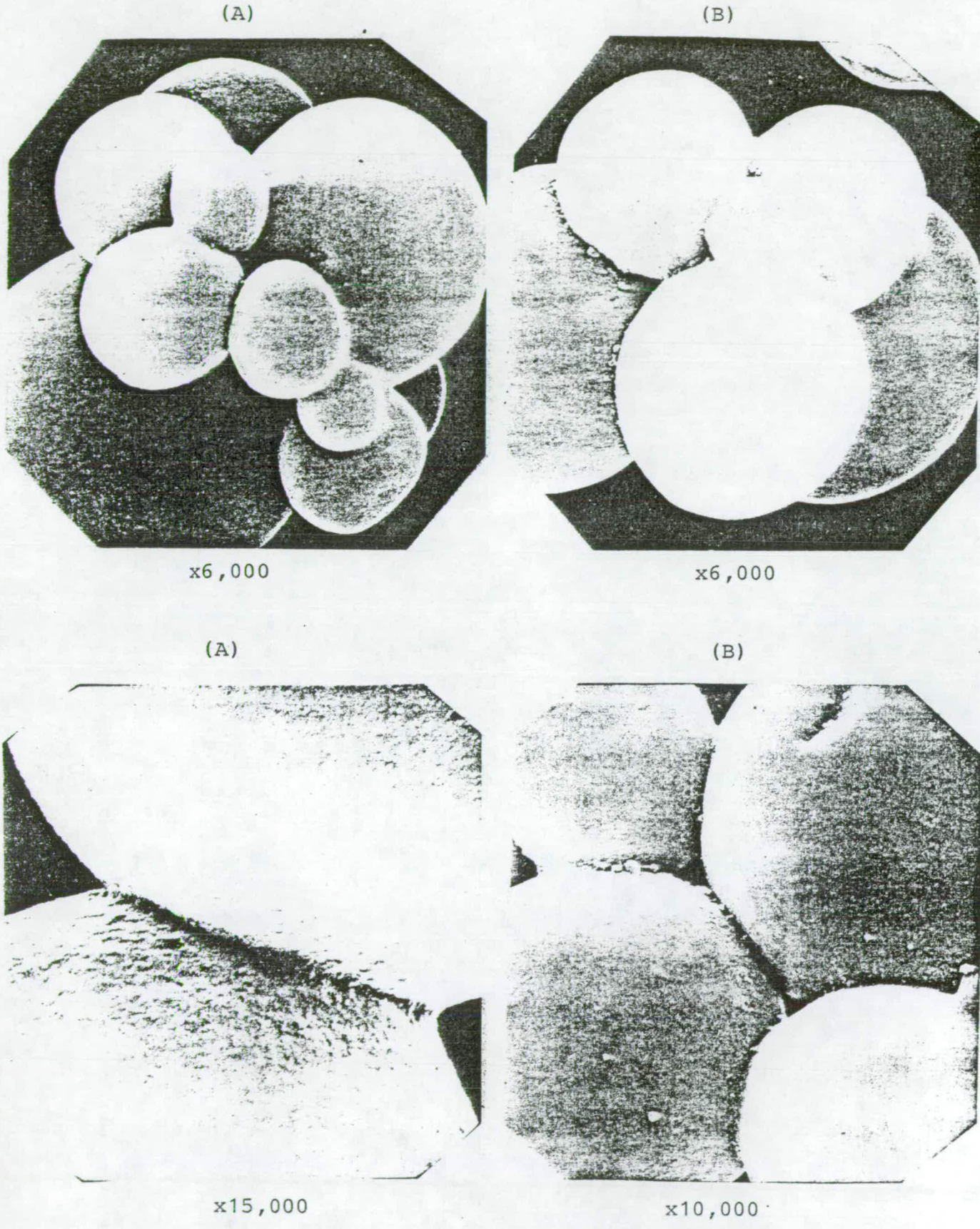

Figure 7.14 ODS-silica (nominally (A) 5-15μm and (B) 10-40μm), prepared as outlined in section R.3.1(iv) of the Reserved Chapter, as seen under an electron microscope.

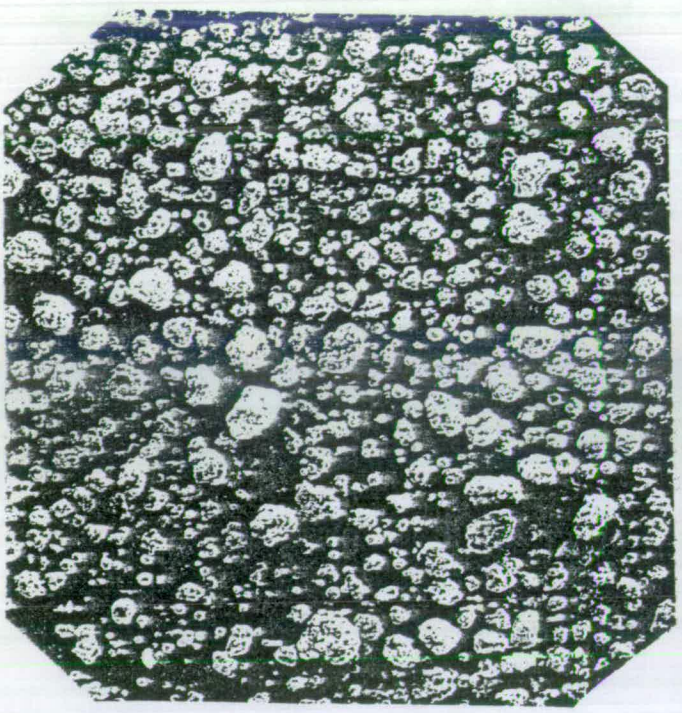

x100

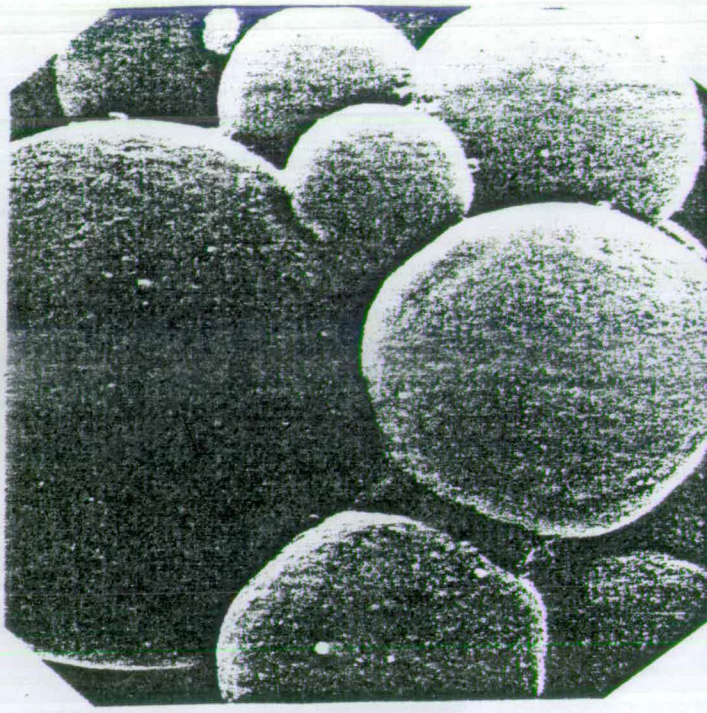

x6,000

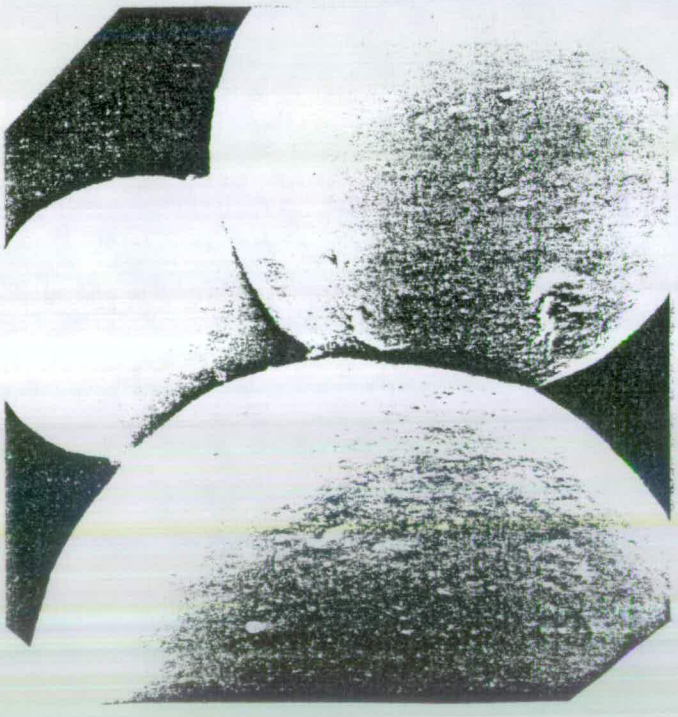

x6,000

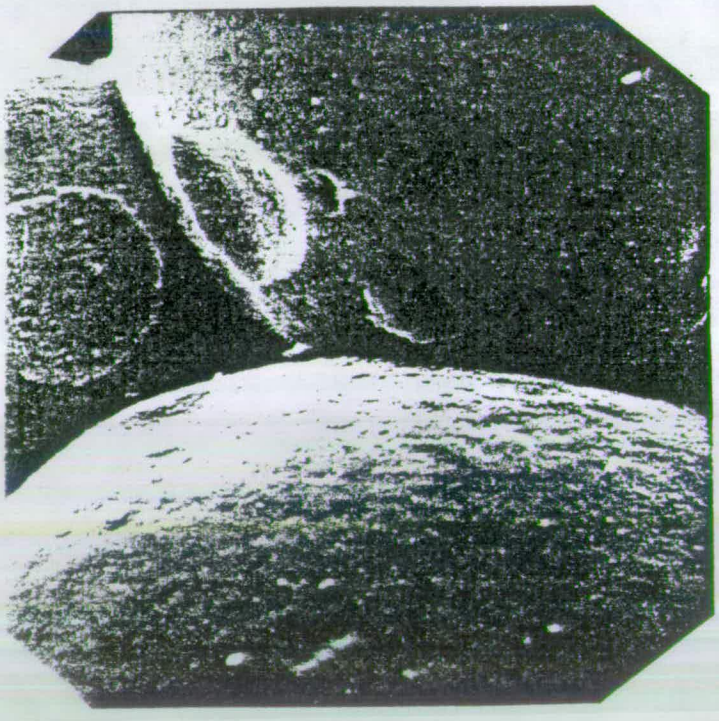

x10,000

Figure 7.15 ODS-silica (15-60μm nominally), prepared as outlined in section R.3.1(iv) of the Reserved Chapter, as seen under an electron microscope.

7.5 The Preparation and Bonding of Silica Gel

Silica gel particles of different sizes were prepared using a method which basically involved the emulsification of a silica containing solution, or sol, which was then hardened before the particles were separated and then dried using a spray drier. Experiments were then conducted to establish the effects of a number of variables on the particle size produced, such as the type of screen attachment on the mixer-emulsifier used and the stirring speed. The preparation and bonding of silica gel is discussed in more detail in a reserved section of this thesis.

Photographs of various silica gel particles made are shown in figures 7-12 to 7-15. The most noticeable difference between the particles which have been made and the more usual spherical particles is that the former appear to be fused together to produce "raspberry-like" clusters where smaller silica particles are fused together to produce a larger particle. This phenomenon has also been reported elsewhere.[22]

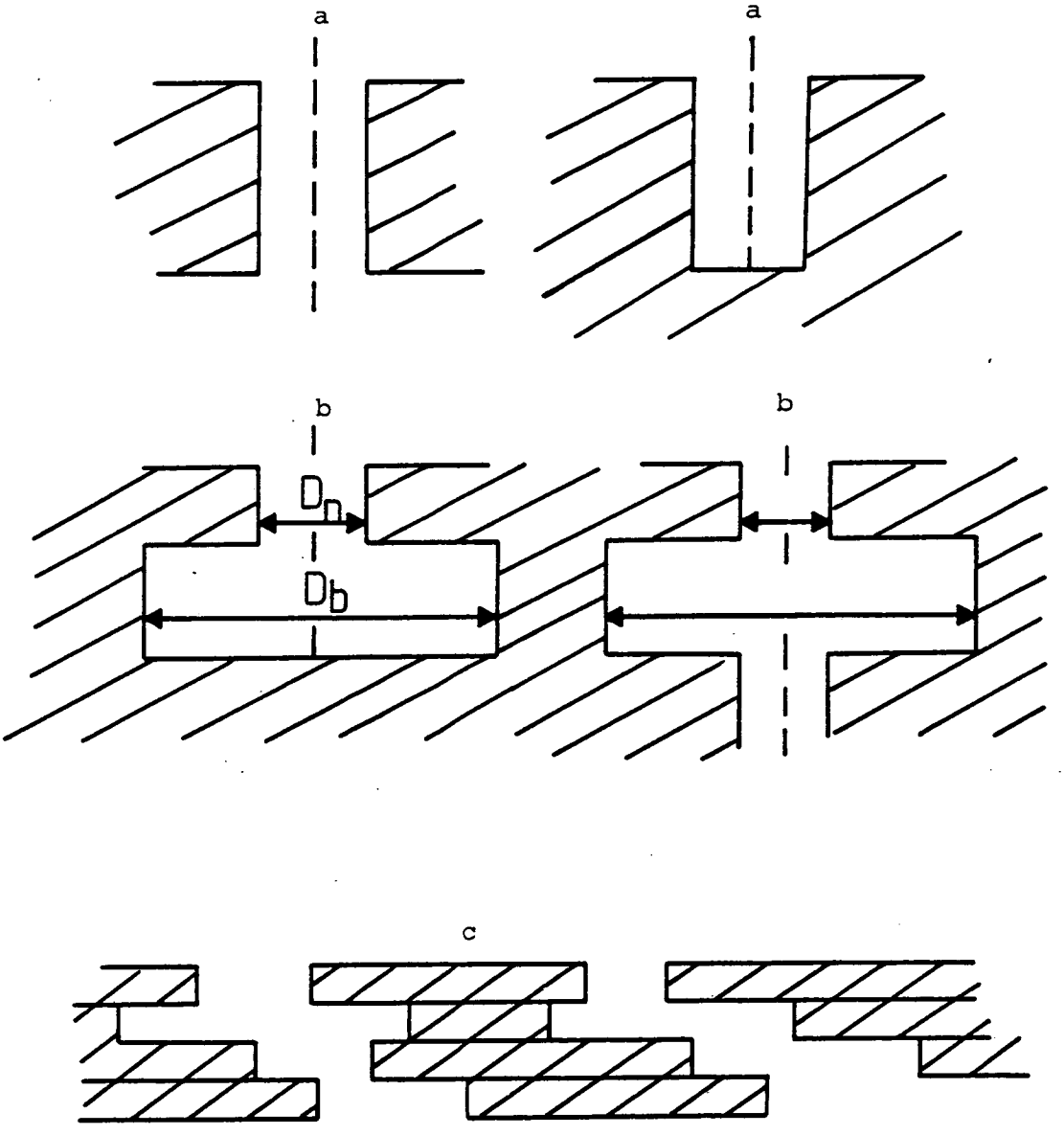

Figure 7.16 Pore models (a) cylindrical pores, circular in cross-section (b) "ink bottle" pores having a narrow neck and wide body (c) slit-shaped pores with parallel plates. (Reproduced from reference 23).

7.6 Characterization of the Surface of Silica Gel

Since the efficiency of column chromatography depends on the rate of mass transfer of solute molecules into and out of the pores of the stationary phase material, the nature of the surface of this stationary phase is important. Porous stationary phases can be characterized by three quantities, namely the mean pore diameter, D, the specific surface area, S, and the specific pore volume, Vp. The methods used to determine these quantities are based on the physisorption of gases or vapours and on the controlled penetration of fluids,[23] which is usually mercury.

7.6.1 Mean Pore Diameter, D.

According to the IUPAC[24] pores which are smaller than 2 nm in diameter are known as micropores and those which are greater than 50 nm are known as macropores while those with a diameter between 2 and 50 nm are known as mesopores. As porous silica is an amorphous solid, the pores are irregular in shape and cover a range of pore sizes. Because of this 3-dimensional array of irregularly shaped pores, it is difficult to determine the mean pore diameter, D. Approximate determinations of D can be made by using pore models as described in figure 7-16. A method of determining D without the use of models has been used by Brunauer *et al.*[25] where a hydraulic pore diameter D_h has been introduced such that

$$D_h = 2\,\frac{Vp}{S} \qquad (7\text{-}1)$$

where Vp is the specific pore volume and S is the specific surface area.

7.6.2 Measurement of the Specific Surface Area

The specific surface area, S, of a porous solid is equal to the sum of the internal surface areas, ie. the areas of the pore walls, and the external surface areas. For porous materials, the largest contribution to S is from the internal surface areas, and this contribution is much greater for micropores than it is for macropores. "A high specific surface area ($S>500m^2/g$) indicates the presence of very small pores, whereas a small value ($S<10m^2/g$) is characteristic of macropore samples".[23]

In determining S by physisorption, the quantity of gas adsorbed on the surface is measured as a function of the equilibrium partial pressure of the gas at constant temperature to give an adsorption isotherm. This temperature is that at which the gas is in the liquid state, which for nitrogen is 77K. The most widely used method to determine the surface area, and the one used in this thesis, is the Brunauer-Emmet-Teller (BET) method which uses nitrogen as the adsorbate. The aim of the BET method is to determine the monolayer capacity, Xm, of the adsorbate, in moles per gram of adsorbent, from the multilayer region of the adsorption isotherm. For monolayer coverage and assuming that (a) only a single adsorbate can bind to a single "site", and (b) the surface of the sample consists of a uniform array of sites, a simplified version of the BET equation is given by

$$\frac{P}{X_a P_o} = \frac{1}{CX_m} + \frac{1}{X_m} \quad (P/P_o) \qquad (7\text{-}2)$$

where X_a = amount adsorbed in moles per gram of adsorbent.

X_m = specific monolayer capacity in moles of adsorbate per gram of adsorbent,

P = equilibrium partial pressure of the adsorbate at temperature T,

P_o = saturation pressure of the adsorbate, and

C = constant which is $\propto \exp (\Delta H_{ads} - \Delta H_{liq})/RT$.

Thus X_m can be found by plotting $P/X_a P_o$ against the relative pressure P/P_o to give a straight line of gradient $1/X_m$ and intercept $1/CX_m$. The specific surface area, S, is then obtained using the equation

$$S_{BET}\ (m^2/g) = X_m A_m N\ 10^{-18} \qquad (7\text{-}3)$$

where A_m = the cross-sectional area of the adsorbate molecule, which for nitrogen is taken as $0.162 nm^2$/molecule,

and N = Avogadro's constant (6.02×10^{23} molecules/mole).

7.6.3 Specific Pore Volume, Vp

The amount of liquid which fills the total volume of pores per gram of adsorbent is known as the specific pore volume, Vp. Unlike the mean pore diameter, D, and the specific surface area, S, the measurement of Vp is not based on any models or assumptions.

The technique used to measure Vp is known as mercury intrusion or mercury porosimetry. Basically, a known weight of sample and some mercury are placed in a dilatometer, which consists of a small glass vessel and a capillary tube, and pressure is applied which forces the mercury into the pores of the sample. As the pressure is gradually increased, the small

Table 7.2 Results[†] of specific surface areas and specific pore volumes of the various stationary phases.

Stationary Phase	Nominal Size range/μm	S(m^2/g)	Vp (cm^3/g)
ODS-silica	"5-15"	133	0.507
ODS-silica	"10-40"	132	0.358
ODS-silica	"15-60"	178	0.387

[†] These results were obtained by Dr. H. Ceylan at the University of Edinburgh

Table 7. 3 Percentage carbon and hydrogen content for silica and ODS-silica

Stationary Phase	Nominal Size Range/μm	%C	%H
Silica gel	"5-15"	0.24	0.21
" "	"10-40"	0.17	0.19
" "	"15-60"	0.23	0.19
ODS-silica	" 5-15"	8.22	1.60
" "	"10-40"	7.89	1.52
" "	"15-60"	8.82	1.68

Table 7.4 Percentage coverage of the surface with octadecyl groups

Stationary Phase or group	C/H mole ratio	Mean C/H mole ratio	% Surface coverage
ODS-silica "5-15" µm	0.428		28.1%
ODS-silica "10-40" µm	0.433	0.433	26.9%
ODS-silica "15-60" µm	0.437		22.5%
$C_{18}H_{37}$-	0.486		
CH_3-	0.333		

changes in volume of the mercury are measured.

7.6.4 Results of Specific Surface Area and Specific Pore Volume for Stationary Phases.

The results of the specific surface area and specific pore volume for the stationary phases prepared and used in this thesis are given in table 7.2.

7.6.5 Carbon and Hydrogen Analysis on Silica and ODS-Silica

Of the three particle size ranges of silica which were obtained from batches 16-23, ie. nominally "5-15 µm", "10-40 µm" and "15-60 µm", half of each were bonded to produce ODS-silica by a method which is described in a reserved section of this thesis. Carbon and hydrogen analysis was carried out on both the silica gel and the ODS-silica. The results are shown in table 7.3.

7.6.6 Percentage Coverage of the Stationary Phase Surface with Octadecyl Groups

The percentage coverage of the surface of the stationary phase with octadecyl groups was calculated as follows. The data for "5-15 µm" ODS-silica was used in this example. The C/H mole ratio was calculated for all ODS-silica size ranges and the values obtained are given in table 7.4, along with those obtained for $C_{18}H_{37}$- and CH_3-groups.

$$\text{Mean C/H ratio} = 0.433$$

$$\equiv \begin{cases} 65\% & C_{18}H_{37}\text{-groups} \\ + & \\ 35\% & CH_3\text{-groups} \end{cases}$$

Assuming that there are four silanol groups per 1 nm^2, the number of silanols per gram of silica is given by

number of silanols = surface area x (4 silanols.nm^{-2})

number of silanols = $(133 \times 10^{18} nm^2 g^{-1}) \times (4 \text{ silanols}.nm^{-2})$

$= 532 \times 10^{18}$ silanols per gram silica

$= \frac{532 \times 10^{18}}{6.02 \times 10^{23}}$ moles silanols per gram silica

= 0.88 m.moles silanols per gram silica

A carbon content of 8.22% corresponds to 0.0822 g of carbon per gram of support,

$= \frac{0.0822}{12 \times 18} \times 0.65$ moles octadecyl groups per gram silica

= 0.247 m moles octadecyl groups per gram silica

$\therefore$ % surface coverage $= \frac{0.247}{0.88} \times 100$

$= \underline{\underline{28.1\%}}$

7.7 Fractionation of Silica Gel Particles by Sedimentation

Two methods of fractionating the silica gel particles were used, both of which were based on the following principle.

When a small sphere falls through a viscous fluid under the action of gravity, it eventually reaches a constant terminal velocity, u, which is given by Stokes Law as

$$u^{ST} = \frac{dp^{ST^2}(\rho_s - \rho_g)\ g}{18\quad \eta} \qquad (7\text{-}4)$$

where u^{ST} is the terminal velocity in $m.sec^{-1}$, and

dp^{ST} is the Stokes diameter of the sphere in m.

The Stokes diameter, dp^{ST} refers to spherical particles. However, for irregularly shaped particles, dp^{ST} corresponds to the diameter of a sphere with the terminal velocity of the particle under consideration.

ρ_s, ρ_g are the densities of the sphere and the fluid respectively in $kg.m^{-3}$,

g is the acceleration due to gravity in $m.sec^{-2}$ and

η is the coefficient of viscosity in $kg.m^{-1}.sec^{-1}$.

For a silica particle of 50% porosity falling through water,

$\rho_s = 1600\ kg.m^{-3}$

$\rho_g = 1000\ kg.m^{-3}$

and $\eta = 1.0 \times 10^{-3}\ kg.m^{-1}s^{-1}$

The density of a silica gel particle, ρ_s, is given by

$$\rho_s = \frac{\rho_{silica} \cdot V_{silica} + \rho_{water} \cdot V_{water}}{V_{silica} + V_{water}}$$

where V_{silica} is the volume of silica in a particle

and V_{water} is the volume of the pores in the particle.

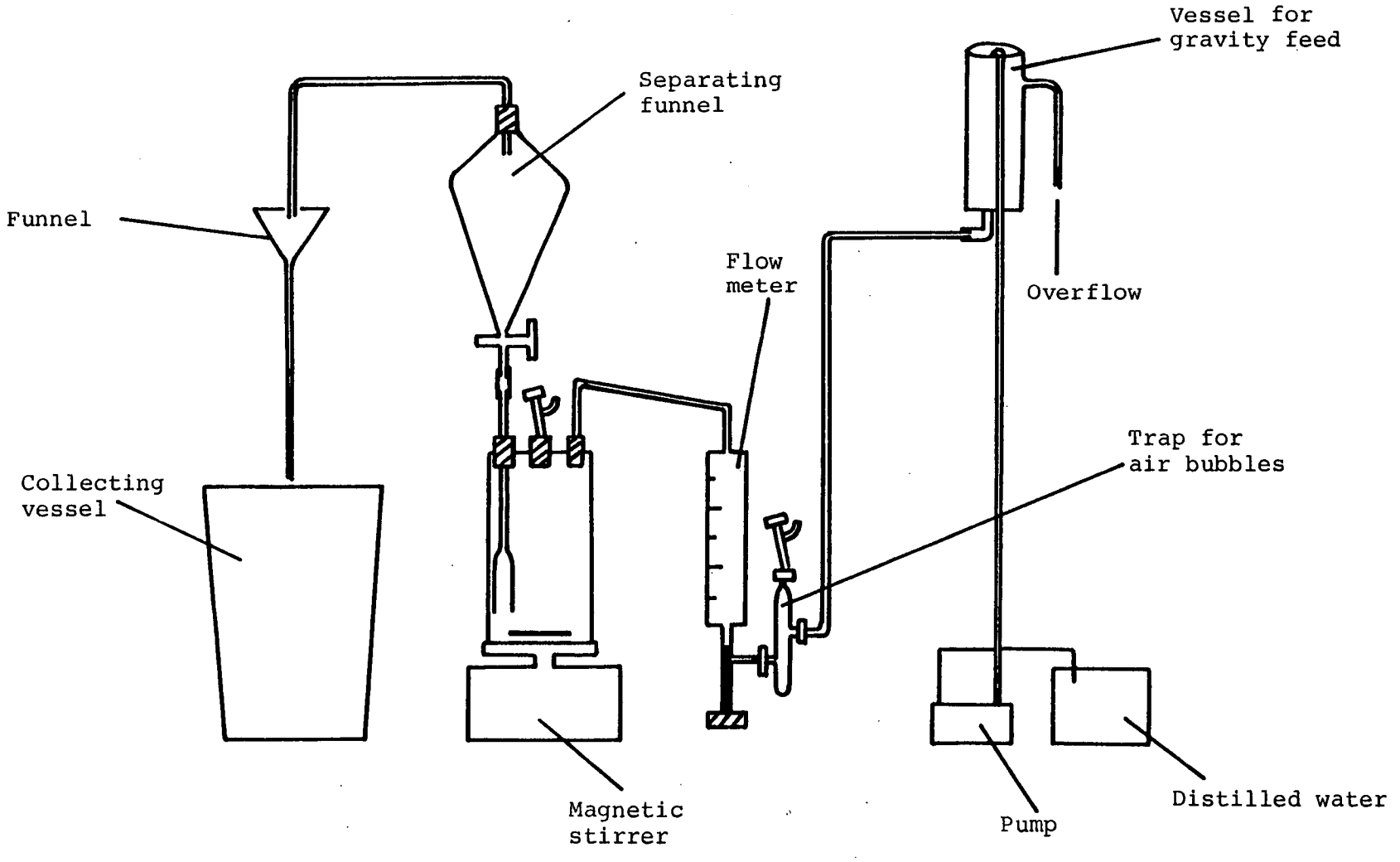

Figure 7.17 Apparatus used for the fractionation of silica using the upward flow technique.

Stokes Law can be simplified since for a given material $\left(\frac{\rho_s - \rho_g}{18\eta}\right) \cdot g$ will be constant, ie.

$$u^{ST} = (dp^{ST})^2 \times \text{constant} \qquad (7\text{-}5)$$

Inserting the above values into equation (7-4) gives, for a sphere of silica gel of 7 μm in diameter, a terminal velocity, u^{ST} in water of almost exactly 1 $mm.min^{-1}$. We can therefore express equation (7-5) as

$$u^{ST} \simeq \frac{1}{49} \times (dp^{ST})^2$$

$$\therefore \quad u^{ST}/_{mm.min^{-1}} \simeq 0.020 \; (dp^{ST}/\mu m)^2 \qquad (7\text{-}6)$$

Thus the terminal velocity, u^{ST}, can be calculated for any particle size, dp^{ST}.

7.7.1 Fractionation Using An Upward Flow Method

The first fractionation method by sedimentation uses the equipment illustrated in figure 7.17. This operates on the principle that if, for example, there is an upward flow of 1 $mm.min^{-1}$, then a sphere of 7 μm in diameter will remain stationary in the fluid suspension. Particles smaller than 7 μm will fall. As the funnel in which the fractionation takes place is conical in shape, the flow will be least at the widest part of the vessel and it is at this point that the separation into the different fractions will occur.

The flow rate required to keep a sphere stationary in suspension can be calculated by considering the volume of a narrow cylinder at the widest part of the separating funnel,

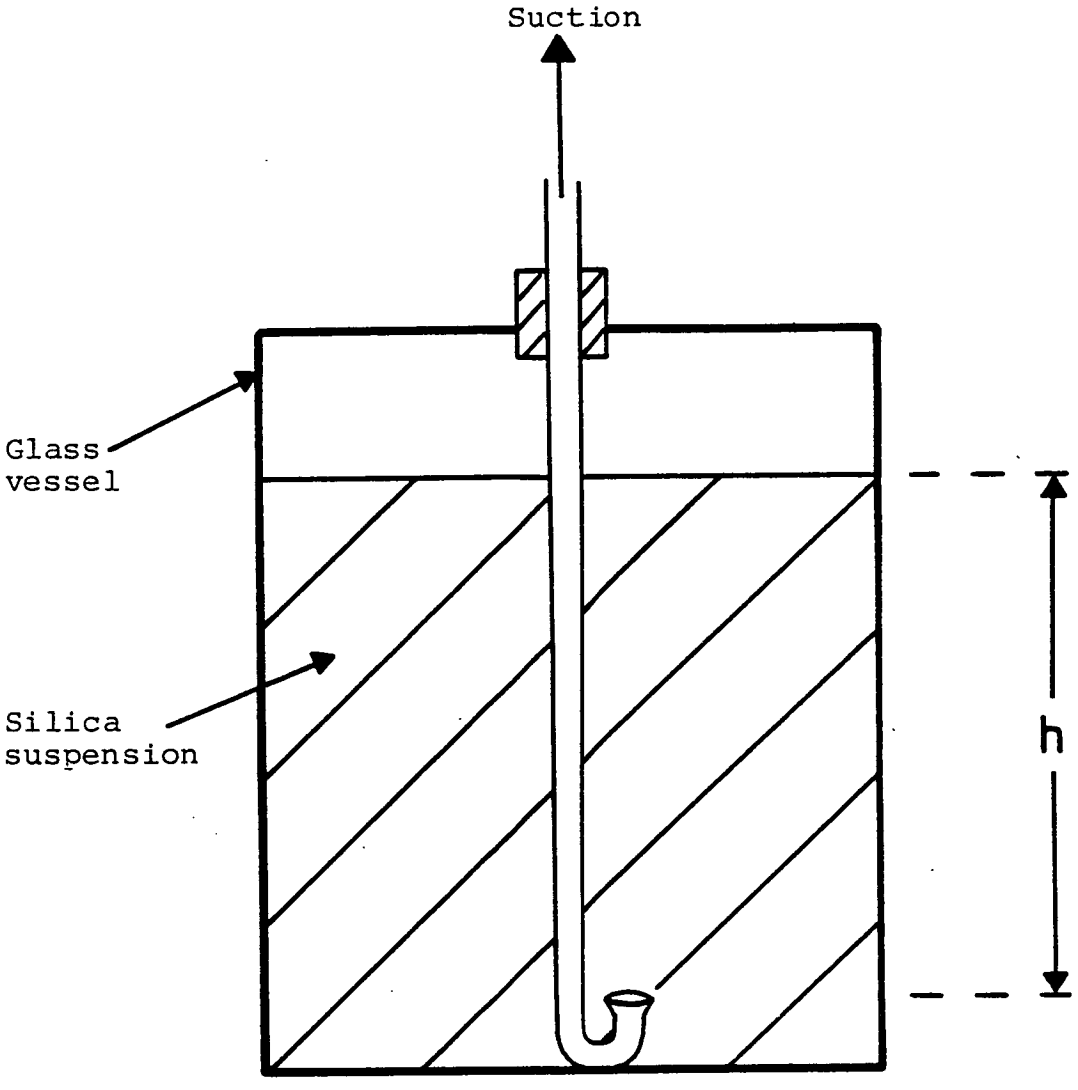

Figure 7.18 Apparatus used for fractionation by sedimentation and decantation.

and the simplified version of the Stokes equation. A flow rate in excess of the terminal velocity for a particular particle size would be required to push the particles upwards and over into a collecting vessel. This fractionation method was only used for batches 5 and 8 since very large volumes of distilled water were required and in view of the large amounts of silica required for preparative work this method proved impractical.

7.7.2. Sedimentation and Decantation

This is a much simpler method than the previous method, and the apparatus which was used is shown in figure 7-18.

The particles are suspended in water and are allowed to settle for a particular period of time which depends on the smallest particle size for a given size range. For a given height, h, the time t can be calculated according to the equation

$$u = \frac{h}{t} \qquad (7\text{-}7)$$

where u, the terminal velocity, is given by the Stokes equation (7-4)

By combining equations (7-4) and (7-7), we have

$$\frac{h}{t} = \frac{dp^2(\rho_s-\rho_g)\ g}{18\eta}$$

which can be rearranged to give

$$dp = \left(\frac{18\eta \quad h}{(\rho_s-\rho_g)g.t}\right)^{\frac{1}{2}} \qquad (7\text{-}8)$$

$$\text{or} \quad dp = \left(\frac{1 \quad h}{\text{constant}.t}\right)^{\frac{1}{2}} \qquad (7\text{-}9)$$

Thus for any desired particle size range, the time taken for those particles at either size limit to fall a certain distance can be evaluated.

The relationship as described in equation (7-4) strictly speaking only holds for the laminar flow region. Also, the velocity at which the particles settle is very much influenced by the concentration of particles dispersed in the fluid, especially if they are irregularly shaped. In suspensions which have a high concentration of particles, the interactions between the particles will alter the settling flow pattern and result in a different value for u than might otherwise be expected from equation 7-4. This effect is negligible for concentrations of below 1% (v/v) while above this concentration particles tend to settle en masse, with the small particles being carried down by the larger particles and to a lesser extent the larger particles not falling as fast as they might if the suspension was more dilute. Also, since the particles are in suspension, many of them will fall below the take off point before being syphoned off. As it is important to use particles of a narrow size range, it is therefore necessary to repeat the fractionation of each particle size range several times. In this thesis, the sedimentation step was carried out a total of 10 times in all cases.

A study on the feasibility of fractionation by sedimentation and decantation was carried out and is now described.

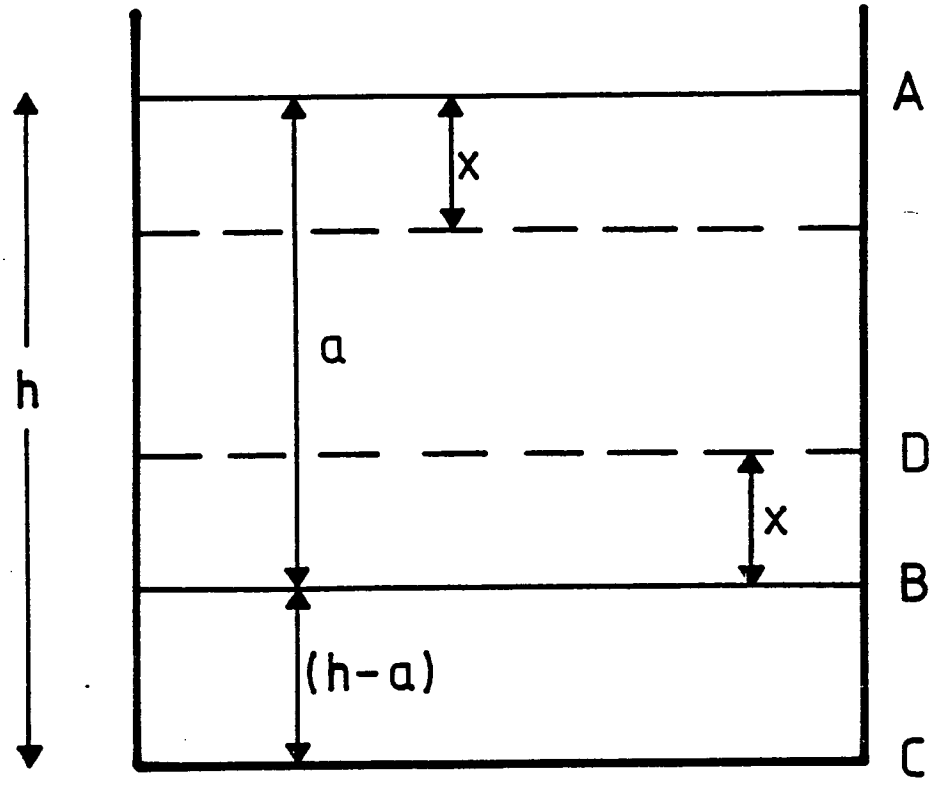

Figure 7.19 Schematic representation of sedimentation and decantation.

7.8 Feasibility of Fractionation by Sedimentation and Decantation

Consider the situation as illustrated in figure 7-19 where the silica particles are suspended in water. Initially, there will be a uniform distribution throughout all of the liquid.

Suppose a particle with a diameter equal to that of the cut-off particle diameter for a particular size range, ie. d_{cut}, takes a time, 't', to fall a distance, 'a', from point A to point B. Using equation (7-5) we can express this distance, a, as

$$a = d_{cut}^2 \cdot c \cdot t \qquad (7\text{-}10)$$

Similarly, after this same time, t, a particle of diameter, d, will only have fallen a distance, x, which can be expressed as

$$x = d^2 . c . t. \qquad (7\text{-}11)$$

By combining equations (7-10) and (7-11) we have

$$\frac{x}{a} = \frac{d^2}{d_{cut}^2} \qquad (7\text{-}12)$$

The fraction, F, of particles of diameter d which are removed by decantation after this time t, ie. the fraction contained in all of the liquid above the level B, and taking into consideration the fact that any particles of diameter d which were initially between level D and B will have fallen to below B during this time, is given by

$$F = \frac{a-x}{h} \qquad (7\text{-}13)$$

Table 7-5 Fraction of particles remaining after n sedimentations.

d/d_{cut}	F_1	F_2	F_3	F_4	F_5	F_6	F_7	F_8	F_9	F_{10}
0.1	0.21	0.04	9×10^{-3}	2×10^{-3}	4×10^{-4}	9×10^{-5}	2×10^{-6}	4.10^{-6}	9×10^{-7}	
0.2	0.23	0.05	1.2×10^{-2}	3×10^{-3}	6×10^{-4}	1×10^{-4}	3×10^{-5}	7.8×10^{-6}	2×10^{-6}	4×10^{-7}
0.3	0.27	0.07	2×10^{-2}	5×10^{-3}	1×10^{-3}	4×10^{-4}	1×10^{-4}	3×10^{-5}	8×10^{-6}	2×10^{-6}
0.4	0.33	0.11	3.6×10^{-2}	1.2×10^{-2}	4×10^{-3}	1×10^{-3}	4×10^{-4}	1×10^{-4}	5×10^{-5}	2×10^{-5}
0.5	0.40	0.16	6.4×10^{-2}	2.6×10^{-2}	1×10^{-2}	4×10^{-3}	2×10^{-3}	7×10^{-4}	3×10^{-4}	1×10^{-4}
0.6	0.49	0.24	1.2×10^{-1}	5.8×10^{-2}	3×10^{-2}	1.4×10^{-2}	7×10^{-3}	3×10^{-3}	2×10^{-3}	8×10^{-4}
0.7	0.59	0.35	2.1×10^{-1}	1.2×10^{-1}	7×10^{-2}	4×10^{-2}	2×10^{-2}	1.10^{-2}	9×10^{-3}	5×10^{-3}
0.8	0.71	0.50	3.6×10^{-1}	2.5×10^{-1}	1.8×10^{-1}	1.3×10^{-1}	9×10^{-2}	6.10^{-2}	5×10^{-2}	3×10^{-2}
0.9	0.85	0.72	6.1×10^{-1}	5.2×10^{-1}	4.4×10^{-1}	3.8×10^{-1}	0.32	0.27	0.23	0.20
1.0	∞									

which can also be written as

$$F = \frac{1-(x/a)}{h/a} \qquad (7\text{-}14)$$

By substituting equation (7-12) into equation (7-14), we have

$$F = \frac{1-(d/d_{cut})^2}{h/a} \qquad (7\text{-}15)$$

If y equals the fraction of the total volume removed, ie.

$$y = \frac{a}{h}$$

then we can write

$$F_1 = y\left\{1-(d/d_{cut})^2\right\} \qquad (7\text{-}16)$$

where F_1 is the fraction removed after 1 sedimentation.

Therefore, after n sedimentations, the fraction remaining will be

$$F_n \text{ (remaining)} = (1-F_1)^n$$

$$= \left[1-\left\{y\left[1-(d/d_{cut})^2\right]\right\}\right]^n \qquad (7\text{-}17)$$

If we take the ratio of a/h as being, say

$$\frac{a}{h} = y = \frac{4}{5}$$

then the values, which are listed in table 7.5, are obtained for the fraction of particles remaining after n sedimentations. The table shows that, for the narrower particle size ranges,

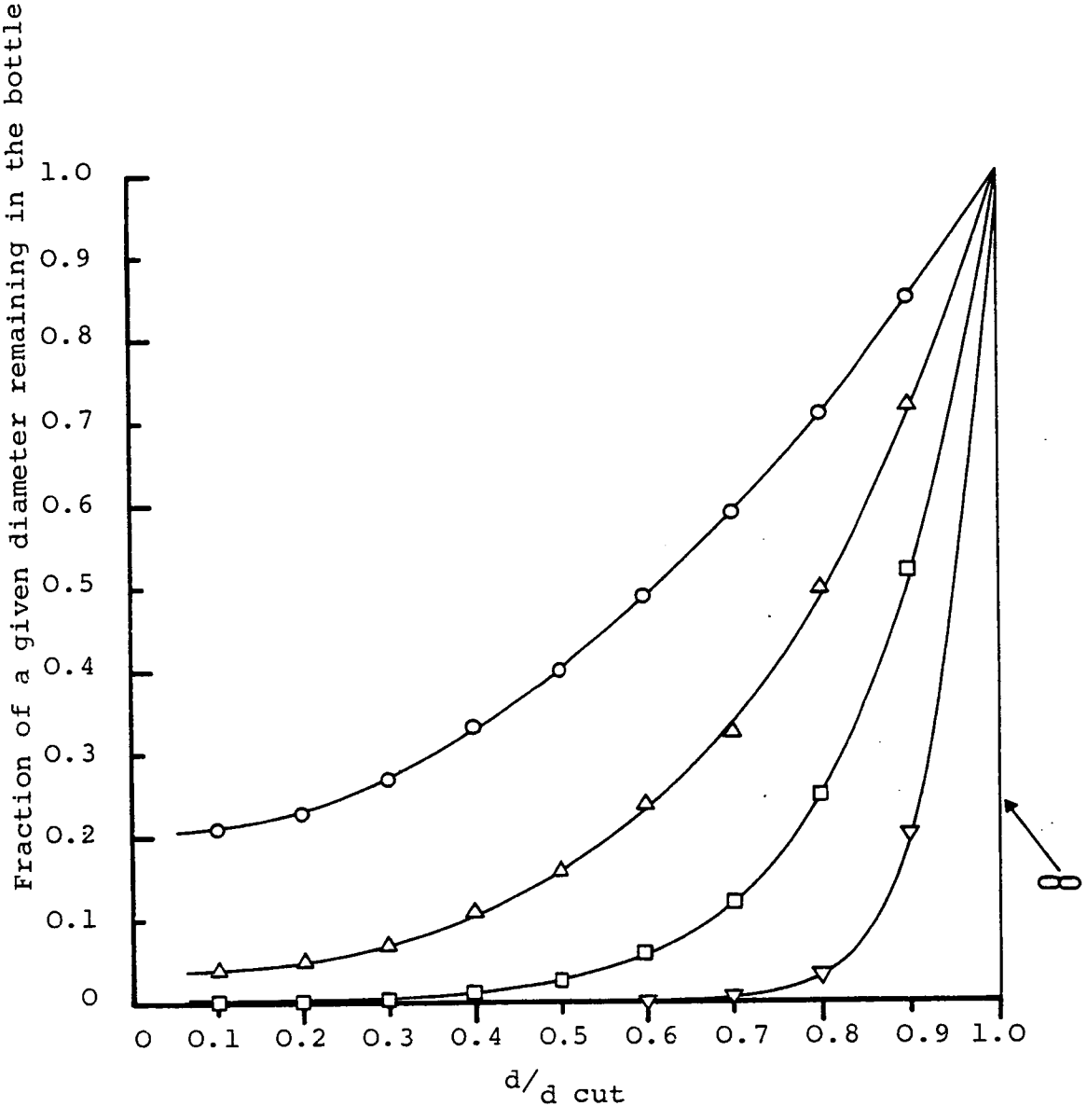

Figure 7.20 Sharpness of cut as a function of n, the number of sedimentation steps.

○ : n = 1

△ : n = 2

□ : n = 4

▽ : n = 10

i.e where d/d_{cut} is larger, a large number of sedimentation steps are required in order to achieve a sharp cut. This is shown clearly in figure 7-20 which plots the sharpness of cut as a function of n. After 10 fractionations, 90% or more of the particles are removed where the diameters are 0.86 or less than that of the desired cut.

REFERENCES

Chapter 7

1. L.R. Snyder; Sep.Sci., 1 (1966), 191.
2. C.G. Armistead, A.J. Tyler, F.H. Hamilton, S.A. Mitchell, and J.A. Hockey; J.Phys.Chem., 11 (1969), 3947.
3. J.H. De Boer and J.M. Vleeskens; Proc.Kon.Ned.Akad.Van Wetens, 1958, B61, 1.
4. F.H. Hambleton, J.A. Hockey, and A.J. Tyler; J.Catal., 13 (1969), 35.
5. R.K. Iler; "The Colloidal Chemistry of Silica and Silicates" 1955, New York: Cornell University Press.
6. J.H. De Boer, H. Hermans, and H.M. Vleeskens; Proc.Kon. Ned.Akad.Van Wetens, 1957, B60, 45.
7. J.H. De Boer, H. Hermans, and J.M. Vleeskens; Proc.Kon.Ned. Akad.Van Wetens, 1957, B60, 54.
8. J.H. De Boer, H. Hermans, and J.M. Vleeskens; Proc.Kon. Ned.Akad.Van Wetens, 1957, B60, 234.
9. J.H. Knox (Editor), "High Pressure Liquid Chromatography" Edinburgh University Press.
10. Z.El Rassi, C. Gonnet, and J.L. Rocca; J.Chromatogr., 125 (1976), 179.
11. G.A. Howard and A.J.P. Martin; Biochem.J., 56 (1950), 532.
12. I. Halasz and I.Sebastian; Angew.Chem., 81 (1969), 464.
13. A. Pryde; J.Chromatog.Sci., 12 (1974), 486.
14. E. Grushka (Editor), "Bonded Stationary Phases In Chromatography" Ann.Arbor Sci.Publ., Ann Arbor, Michigan 1974.
15. D.C. Locke J.Chromatog.Sci., 11 (1973), 120.

16. R.E. Majors; J.Chromatog.Sci., 18 (1980), 488.

17. G.B. Cox; J.Chromatog.Sci., 15 (1977), 385.

18. C. Horvath and W. Melander; J.Chromatog.Sci., 15 (1977), 393.

19. V. Rehak and E. Smolkova; Chromatographia, 9 (1976), 219.

20. C. Horvath in "Techniques in Liquid Chromatography" C.F. Simpson (Editor), Wiley 1982.

21. H. Hemetsberger, W. Maasfeld, and H. Ricken; Chromatographia, 9 (1976), 203.

22. B. Mattiasson, M. Ramstorp, K. Wideback, and G.Kronvall; J.Appl.Biochem., 2 (1980), 321.

23. K.K. Unger "Porous Silica" Journal of Chromatography Library, Vol.16, Elsevier, 1979.

24. IUPAC "Manual of Symbols and Terminology" Appendix 2, Part 1, Colloid and Surface Chemistry, Pure Appl.Chem., 31 (1972), 578.

25. S. Brunauer, R. Sh.Mikhail, and E.E. Bodov; J.Colloid. Interface Sci., 24 (1967), 451.

CHAPTER 8

EXPERIMENTS ON THE PROTOTYPE PREPARATIVE SYSTEM

Chapter 8. Experiments On The Prototype Preparative System

EXPERIMENTS ON THE PROTOTYPE PREPARATIVE SYSTEM

8.1 Introduction

Much of the work which has been done on preparative chromatography has concentrated on normal-phase preparative chromatography using silica gel as the stationary phase. This has the advantage in that it is cheaper than bonded phase materials and separated components are easily recovered at the end of the separation by evaporation of the organic mobile phase, usually under a nitrogen stream.

Work carried out by Done[1] and others involved studying the effects of increasing the sample load on column efficiency, sample capacity and resolution but failed in most cases to cover a wide range of injection volumes or sample concentrations. It was felt that a more complete study of both volume and concentration overloading was required in order to determine more fully the effect of overloading on the efficiency of the column and sample capacity. Also, since comparatively little work has been carried out on reversed phase preparative chromatography, and since Done[1] reported the possibility of reversed phase material having higher loading capacities, it was decided to carry out these loading experiments on chemically bonded material.

Finally, it was decided that there was room for improvement on existing preparative systems and so a new preparative column and loading system was designed, tested and then used for the loading experiments.

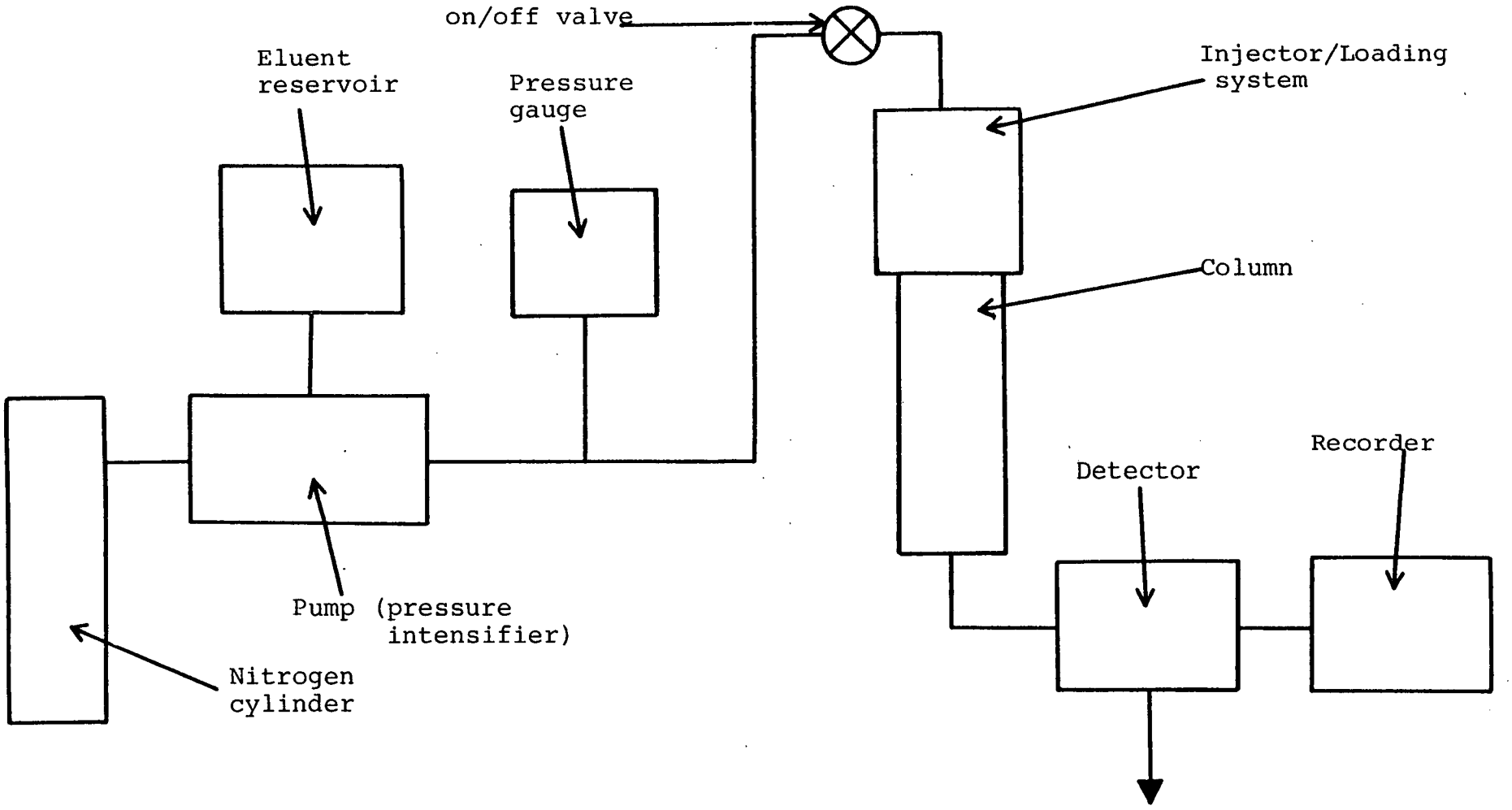

Figure 8.1 General features of the liquid chromatographic system.

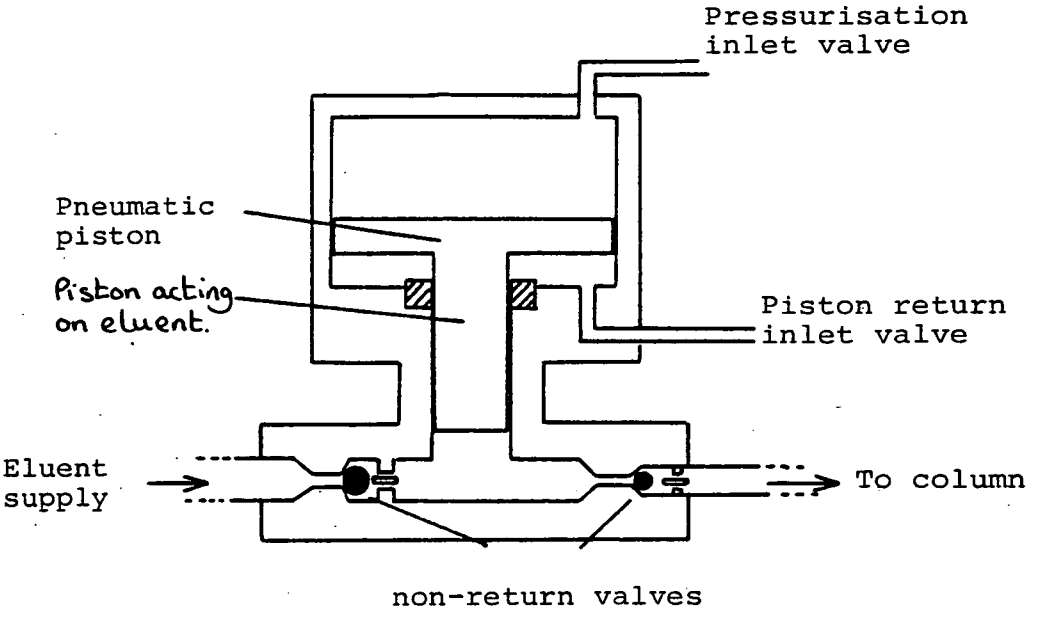

Figure 8.2 Diagram of a pneumatic pressure intensifier pump.

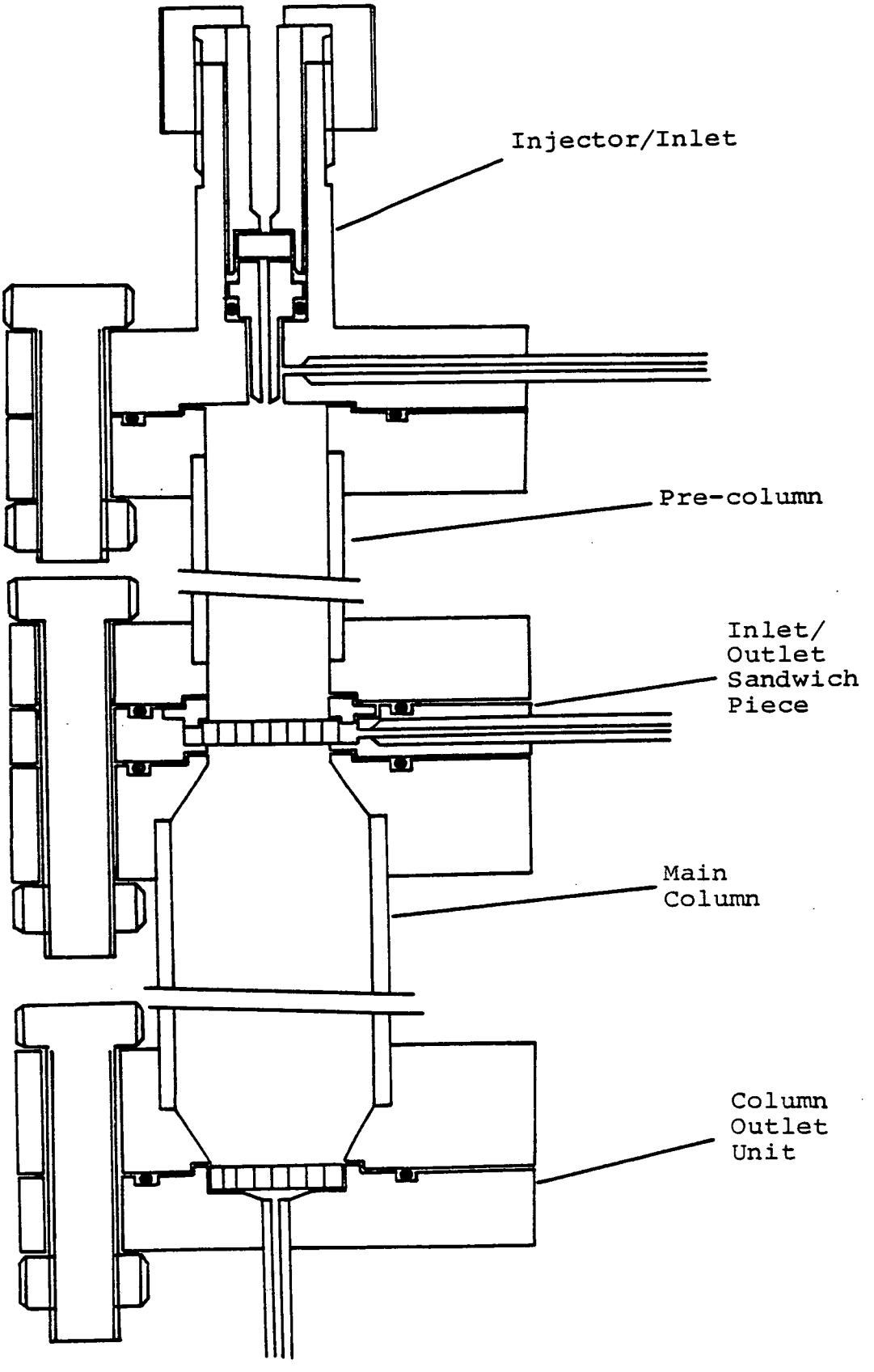

igure 8.3 General assembly of the various units for the preparative HPLC system.

8.2 Equipment and Experimental Techniques

A home-made chromatographic system was used throughout the experiments and the general features are illustrated in figure 8-1.

8.2.1 Pumping System

A Haskel Pneumatic Pressure Intensifier pump (Haskel Engineering Systems Ltd.) was used. This had a stroke capacity of 70 ml and was capable of delivering solvents at flow rates of up to 1ℓ/min or more. A diagram of this type of pump is shown in figure 8-2.

8.2.2 Pressure Gauge

A Bourdon manometer was used as a pressure gauge and was situated between the pump and the on/off valve used for the stop-flow injections.

8.2.3 Preparative-scale Column and Sample Loading System

The columns and sample loading system were designed in this department and were made by the Engineering Department, Unilever Research, Sharnbrook, Bedfordshire.

The essential features of the preparative column system are shown in figure 8-3 and consist of a number of axially connected units comprising of:

an injector/inlet unit,
a loading pre-column,
an inlet/outlet sandwich piece with frit,
a main column,
a column outlet.

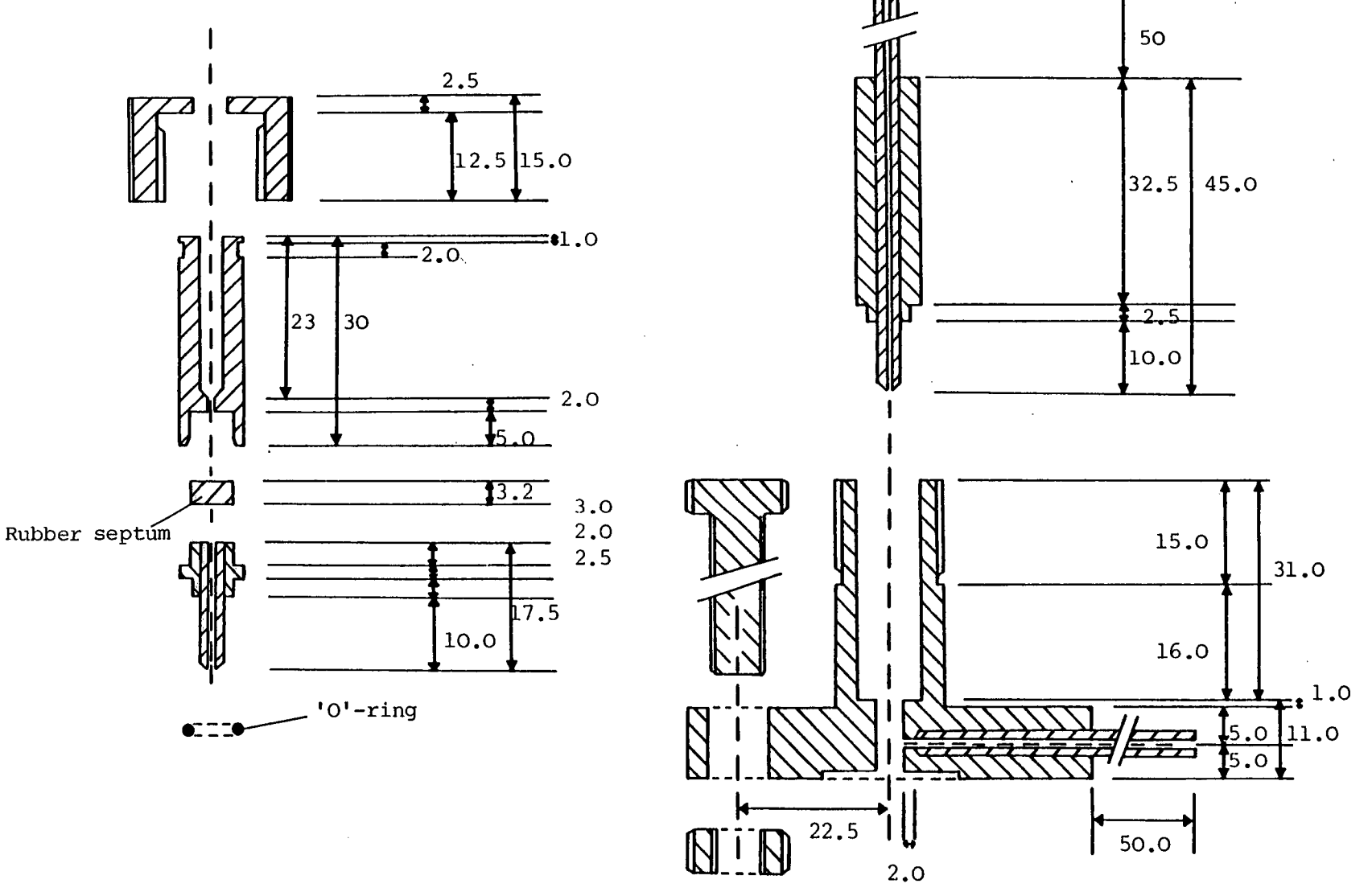

Figure 8.4 Injector/inlet for the preparative HPLC system (dimensions are in mm).

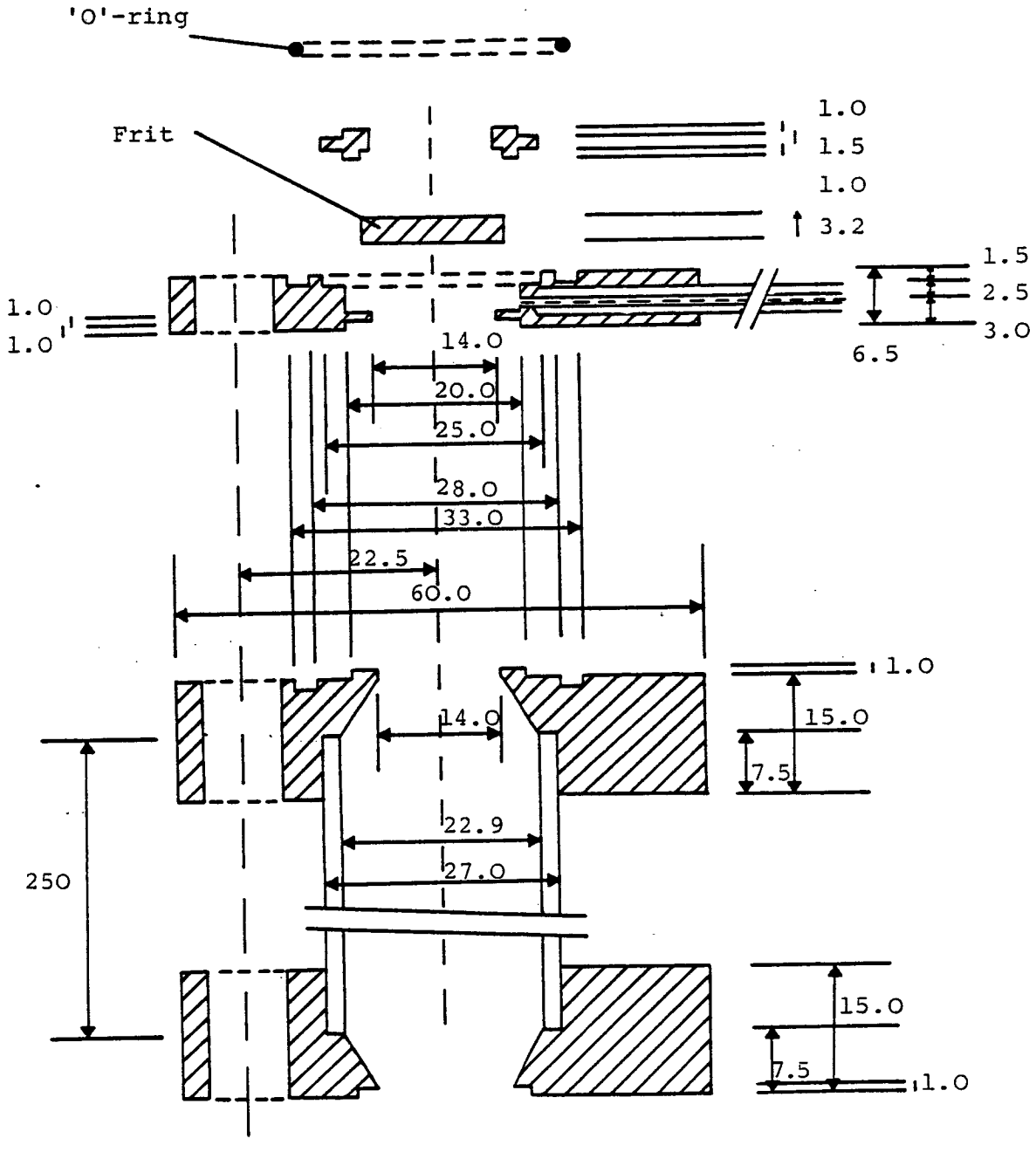

Figure 8.5 Sandwich piece unit and main column for the preparative HPLC system (dimensions are in mm).

The individual pieces have locating flanges which are sealed by "O" rings and held together by bolts as shown in figure 8-3. The flanges are designed so that all of the pieces are interchangeable thus making the system very versatile. The columns can be used either as loading pre-columns or as main columns. The unit can also be used as a slurry packing system. It is also possible to connect the injector head directly to the main column as well as connecting it to the loading pre-column which can in turn be connected either directly to the main column or via the sandwich piece. The peak dispersion caused by the various preparative system combinations was examined and will be discussed later in this chapter.

8.2.3.1 Injector

A diagram of the septum injector head used is also shown in figures 8-3 and 8-4. Injections were made either in the stop-flow or the on-stream mode using syringes from Hamilton (V.A. Howe, London), S.G.E. (V.A. Howe, London) or, in the case of large injection volumes, from Rockett.

8.2.3.2 Columns

All columns were made out of lengths of SS-316 grade stainless steel which had been honed inside to produce a mirror-like finish by Microfinnish Ltd. (Exeter Road, London, Great Britain). Several different columns were made. The larger diameter columns, 250mm x 22mm id. and 500mm x 22mmid, were made according to figure 8-5 which shows that the top and the bottom of the column are coned such that the diameter at the inlet (and outlet) is the same as that of the narrower columns,

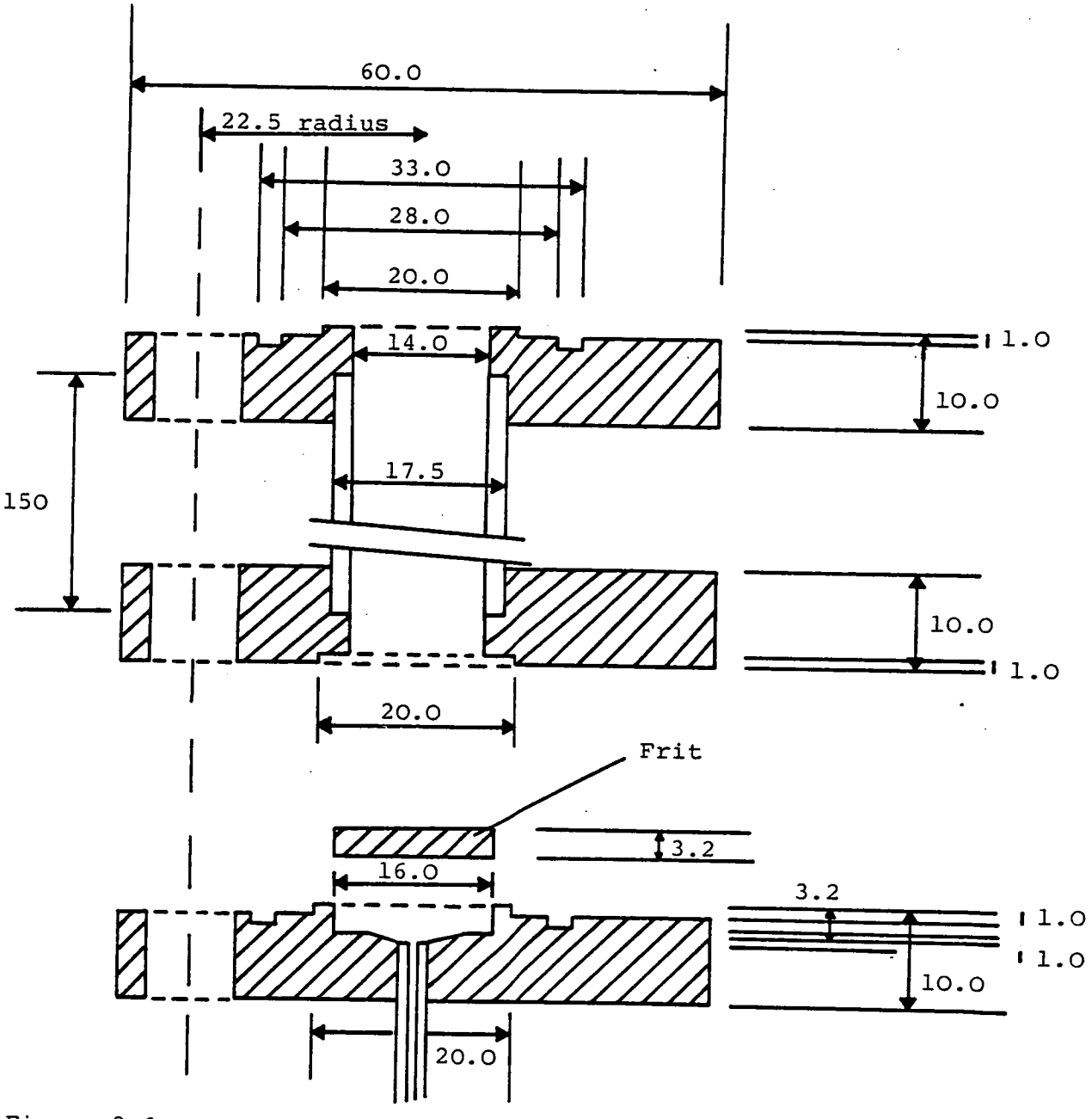

Figure 8.6 Pre-column and column outlet unit for the preparative HPLC system (dimensions in mm).

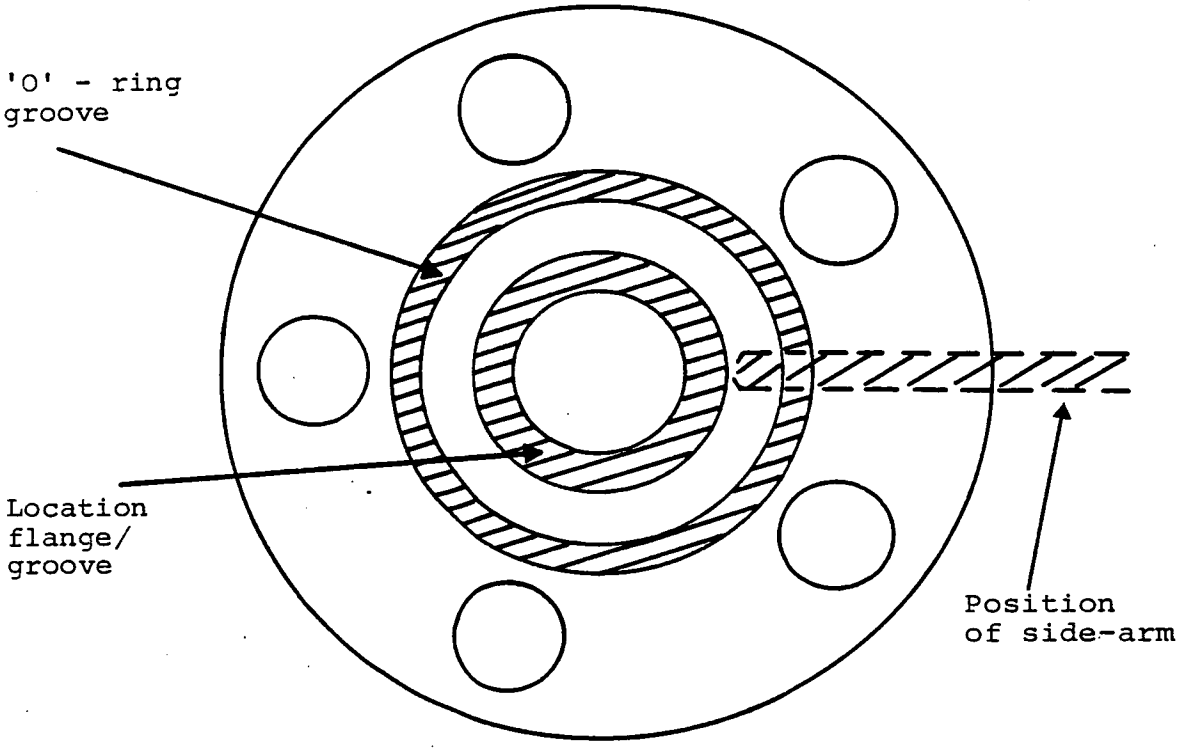

Figure 8.7 Top view of sandwich unit

150mm x 14mm id. and 250mm x 14mm id., which are illustrated in figure 8-6. The design of the narrower columns is similar to that of the wider columns except that the former are not coned at the ends.

Before being used, the insides of the columns were cleaned using concentrated R.B.S. surfactant and washed with water, carbon tetrachloride and finally acetone before being dried.

8.2.3.3 Sandwich Piece

The sandwich piece, as shown in figure 8-7, is used to connect the pre-column to the main column and its function is to assist in the loading of the main column as described in chapter 5. This consists of an annular outlet/inlet port with side-arm leading to waste via an on/off valve, and a frit which is inserted into the central location flange.

8.2.3.4 Column Outlet

The column outlet unit is described in figure 8-6 and consists of a flange with a frit situated in the central location flange.

A flow splitter was inserted between the column outlet and the inlet to the cell in the detector. This is necessary because the cell (8µl) cannot cope with large eluent flow rates. The flow splitter was a home made device constructed from a drilled through Swagelock T-piece such that the top and bottom were connected to the column terminator and cell inlet respectively and the sidearm was connected to a variable control valve leading to waste.

8.2.4 Detector

A Cecil 212 variable wavelength U.V. detector (Cecil Instruments, Cambridge, Great Britain), was used for all of the experimental work reported here. The detector used had an 8µl cell and required a flow splitter to be inserted between the column outlet and the detector when large flow rates were used.

The variable wavelength facility enabled the detector to be "backed off", when large sample masses were injected, to wavelengths where the absorbance of the solute was less. However, this type of detector has the disadvantage that the solute must have a U.V. absorbing chromophore. Another disadvantage is that while one component may absorb strongly at one wavelength, another may absorb weakly or not at all thereby giving a false impression of the relative amounts of the components in the sample.

8.2.5 Data Acquisition

The output from the detector was fed into a Servoscribe potentiometric chart recorder, type 501 (supplied by Belmont Instruments, Glasgow).

8.2.6 Connectors

All connectors on the high pressure side of the column system were made from stainless steel tubing while those on the low pressure side were made of PTFE. All unions were made by Swagelock (Crawford Fitting Company). The union connecting the column outlet and the detector cell inlet was drilled through

to prevent any dead-volume. The valves used were Whitey valves and were supplied by Glasgow Valve and Fitting Company.

8.2.7 Materials

The solvents used were HPLC grade methanol (Rathburn, Walkerburn, Scotland) and triply distilled water. All solvents were degassed prior to use.

The solutes used were acetone (A.R.grade), anisole, acetophenone and methyl benzoate, and solutions of these were made up in the eluent. The eluent used throughout these experiments was MeOH/H_2O 60:40 v/v. The stationary phase used in all columns was ODS-silica. Both the preparation and the bonding of the silica gel were carried out as described in chapter 7. The average particle size of the ODS-silica used in the preparative system was 19μm, while the particle size range of the glass beads which were used to pack the loading pre-column was 124-176μm.

8.2.8 Packing Techniques

8.2.8.1 Main Column

The 250mm x 22mm id. column, which was used as the main column, was packed with ODS-silica of 19μm in size using the rotate-bounce-tap method. This was carried out manually and consisted of adding small increments of material and then bouncing the column (the bottom terminator being protected by a rubber bung) at the rate of approximately 2-3 times per second while simultaneously rotating the column and tapping it on the side near the level of packing around 80-100 times,

followed by 20 seconds of gentle bouncing only. This was repeated until the column bed was about 2 cms below the top of the column whereupon the column was then bounced vertically for about 5 minutes. Glass beads (124-176μm) were then added directly on top of the ODS-silica and packed to the top of the column, again using the rotate-bounce-tap method.

The glass beads were found to be essential following early work with the injector head attached directly onto the main column when the packed bed was extended to the top of the column. In this situation a gauze had to be placed on top of the bed to protect the bed and to prevent blockage of the injector and therefore sample injection proved difficult and caused a peak 'ghosting' effect thought to be due to unswept areas at the top of the column. Due to the cone-shape of the top of the column, it was impossible to remove some of the packing, insert a guaze and top up with glass beads. The only alternative was to cease packing within 2 cm of the column top and add glass beads directly onto the bed.

Once packed, the column was equilibrated with eluent before use.

8.2.8.2 Loading Pre-column

The loading pre-column was packed with glass beads (124-176μm) and it had been noted that it was important to also ensure that the pre-column was well-packed in order to avoid any channelling. This was carried out by connecting the empty pre-column, via the sandwich piece, to the packed main column and placing the entire system on a home-made axially rotating device and tapping the pre-column gently on the side as it was being gradually filled.

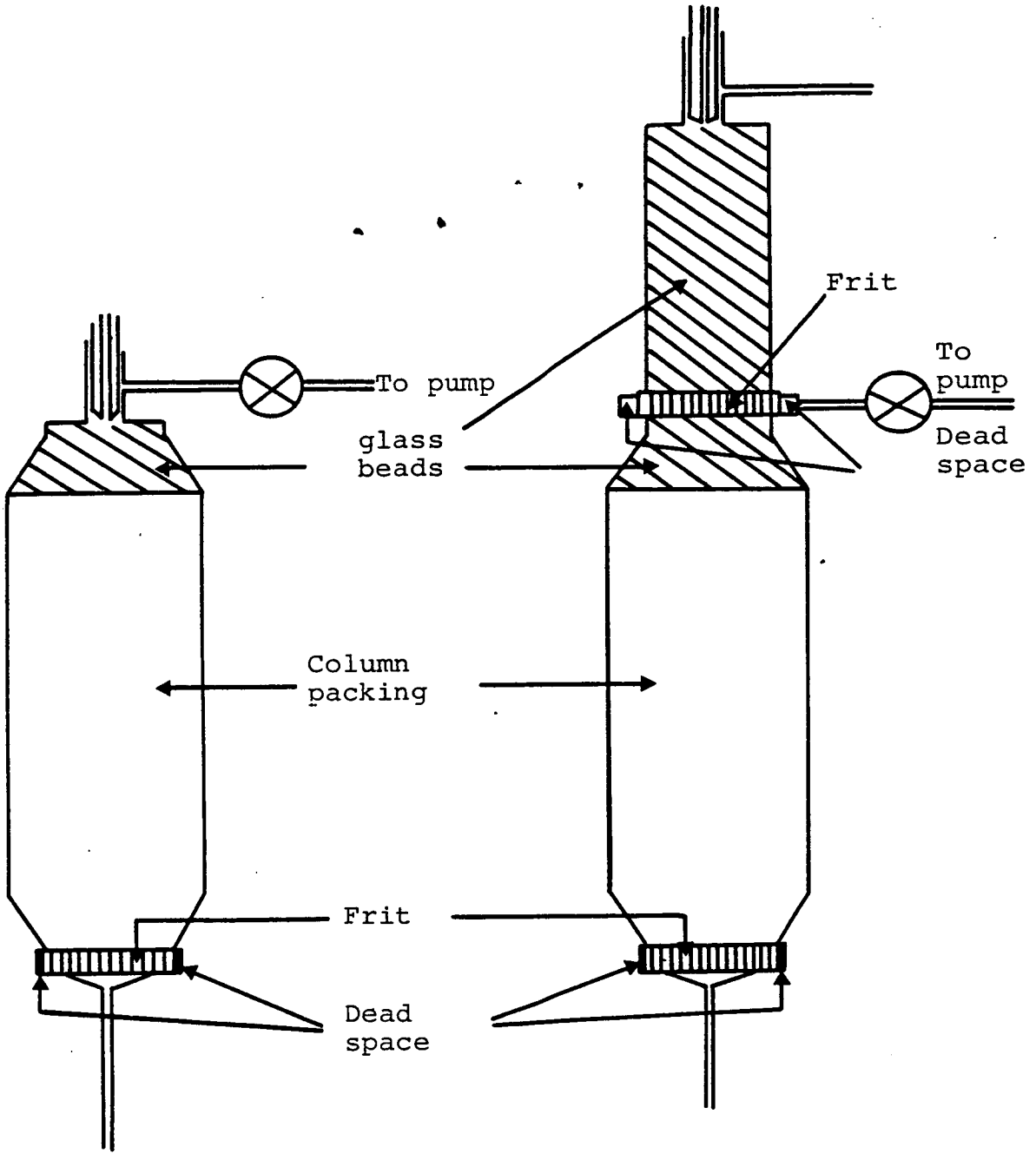

Figure 8.8

Regions of the column(s) which are accessible to eluent for (a) main column only and (b) pre-column, sandwich piece and main column.

8.2.9 Sample Loading with the Prototype Preparative System

Numerous different arrangements of the various components as described in figures 8-3 to 8-6 are possible due to the interchangeability of the different parts. The two main configurations which were used in this present work, and which are illustrated in figure 8-8, were (1) the injector connected directly to the main column followed by the end piece, and (2) the injector connected to the pre-column which was in turn connected to the main column and end piece assembly via the sandwich piece, but many other configurations can be envisaged. The choice of the component units assembled will depend on the volume of sample to be introduced onto the main column.

In order to test the column efficiency with an analytical size sample of a test mixture, the injector can be connected directly onto the top of a column. However, for large injection volumes this configuration is unsuitable since the high back pressure produced makes injection difficult and causes the syringes to leak.

For large sample volumes it is therefore better to use the loading pre-column connected via the sandwich piece, with the injector head connected to the top of the pre-column. To inject large sample volumes using this arrangement, the valve before the injector is closed and the valve on the side-arm of the sandwich piece is opened so enabling sample volumes up to the loading column dead volume to be injected against zero back pressure with an equivalent amount of eluent being displaced through the side-arm to waste. The valve on the side-arm is then closed and the valve in front of the injector opened. The eluent then washes the sample onto the main column.

8.3 Column Testing

The columns were tested using analytical-size samples to check that they were well-packed before any of the loading experiments were carried out.

The various combinations of injector, pre-column, sandwich piece and column end piece, which are described in detail in section 8.4.1, were tested to determine the contribution which each made to the extra-column band dispersion.

For an analytical-size injection of a solute onto a column, the chromatographic peak produced will be approximately Gaussian in shape and the number of plates, N, to which the column is equivalent can be calculated from

$$N = \left(\frac{t_R}{\sigma}\right)^2 \qquad (8\text{-}1)$$

where t_R is the retention time of the peak and σ is the standard deviation of the peak.

This equation can be expressed in terms of the peak width as

$$N = 16\left(\frac{t_R}{W_t}\right)^2, \quad \text{where } W_t = 4\sigma ;$$

$$N_{0.6} = 4\left(\frac{t_R}{W_{0.6}}\right)^2, \quad \text{where } W_{0.6} = 2\sigma ;$$

$$N_{\frac{1}{2}} = 5.54\left(\frac{t_R}{W_{\frac{1}{2}}}\right)^2, \quad \text{where } W_{\frac{1}{2}} = 2.35\sigma;$$

or $$N_{0.1} = 18.4\left(\frac{t_R}{W_{0.1}}\right)^2, \quad \text{where } W_{0.1} = 4.29\sigma.$$

N, $N_{0.6}$, $N_{\frac{1}{2}}$ and $N_{0.1}$ represent the plate height as determined at the peak base, 0.6 of the peak height, half of the peak height and 0.1 of the peak height respectively, and W_t, $W_{0.6}$, $W_{\frac{1}{2}}$ and $W_{0.1}$ are the corresponding peak widths. For Gaussian peaks all of the N-values would be identical, but in real chromatography they will generally differ somewhat.

The height equivalent to a theoretical plate, HETP or H, is given by

$$H = L/N \qquad (8\text{-}2)$$

$$= \frac{L}{16}\left(\frac{W_t}{t_R}\right)^2$$

$$= \frac{L}{4}\left(\frac{W_{0.6}}{t_R}\right)^2$$

$$= \frac{L}{5.54}\left(\frac{W_{\frac{1}{2}}}{t_R}\right)^2$$

$$= \frac{L}{18.4}\left(\frac{W_{0.1}}{t_R}\right)^2$$

The linear flow rate, U, is given by

$$U = \frac{L}{t_m} \qquad (8\text{-}3)$$

where t_m is the retention time for an unretained peak and is equal to

$$t_m = \frac{V_m}{\text{Flow}} \qquad (8\text{-}4)$$

It is more convenient to express the column parameters in terms of reduced parameters since this enables columns of different sizes packed with different materials to be compared easily. The reduced plate height, h, is calculated from

$$h = \frac{H}{d_p} \qquad (8\text{-}5)$$

$$= \frac{L}{16d_p}\left(\frac{W_t}{t_R}\right)^2$$

$$= \frac{L}{5.54d_p}\left(\frac{W_{\frac{1}{2}}}{t_R}\right)^2$$

$$= \frac{L}{18.4d_p}\left(\frac{W_{0.1}}{t_R}\right)^2$$

where d_p is the mean particle diameter.

The reduced velocity, ν, is given by

$$\nu = \frac{U.d_p}{D_m} \qquad (8\text{-}6)$$

where D_m is the diffusion coefficient of a solute molecule in the mobile phase. The values for the diffusion coefficient were not measured directly but were calculated from the Wilke-Chang equation, ie.

$$D_m = \frac{7.4.10T\sqrt{[\psi M_{eluent}]}}{\eta.V_{solute}^{0.6}} \qquad (8\text{-}7)$$

where D_m is in m^2s^{-1}, T is the temperature (°K), ψ is an eluent association factor (1 for non-polar solvents, 1.9 for methanol

and 2.6 for water), M_{eluent} is the molecular weight of the eluent (g), η is the eluent viscosity (mPas) and V_{solute} is the solute molar volume (ml).

The phase capacity ratio, k', is calculated from the equation

$$k' = \frac{t_R - t_m}{t_m} = \frac{V_R - V_m}{V_m} \qquad (8\text{-}8)$$

where t_R and t_m are the retention times of a retained and unretained solute, V_R and V_m are the corresponding retention volumes with

$$V_R = \frac{t_R}{\text{Chart speed}} \times \text{Volumetric flow} \qquad (8\text{-}9)$$

However, when dealing with the overloading experiments, allowances must be made in the calculations for the size of the injection volume. Therefore, a relative retention volume, $V_{R,Rel}$, is taken as being

$$V_{R,Rel} = V_R - \frac{V_{inj}}{2} \qquad (8\text{-}10)$$

where V_{inj} is the injection volume of the sample. Correspondingly, the relative phase capacity ratio, k'_{Rel}, is given as

$$k'_{Rel} = \frac{V_{R,Rel} - V_m}{V_m} \qquad (8\text{-}11)$$

The dimensionless column flow resistance parameter, ϕ, is calculated from the equation,

$$\Phi = \frac{\Delta\rho dp^2 t_m}{\eta L^2} \qquad (8\text{-}12)$$

where $\Delta\rho$ is the pressure drop (Nm^{-2}) across the column and η is the eluent viscosity (Nsm^{-2}).

The peak asymmetry factor, a_s, is calculated by

$$a_s = \frac{BC}{AB} \qquad (8\text{-}13)$$

where AB and BC are measured from the chromatographic peak as shown in figure 8-9.

8.4 Results

8.4.1 Extra-column Band Dispersion

While a well-packed column is essential for efficient chromatography, peak resolution may be lost if the extra-column fittings, ie. the injector, detector and connecting pieces, are either badly designed or badly assembled.

Theoretically, the peak dispersion due to the coupling of components each providing dispersion independently of the other components is given by

$$W_{total}^2 = W_v^2 + W_{inj}^2 + W_{con}^2 + W_{det}^2$$

$$= W_v^2 + W_{app}^2 \qquad (8\text{-}14)$$

where W_{total} is the total peak width as measured by the recorder, W_v is the peak width produced by the column itself, W_{inj} is the peak width produced by the injector, W_{con} is the peak width produced by the connecting pieces and W_{det} is the peak width produced by the detector. W_{app} is the peak width produced by all of the apparatus other than the column and is equal to $(W_{inj}^2 + W_{con}^2 + W_{det}^2)^{\frac{1}{2}}$.

Having designed a new preparative chromatographic column system, it was therefore important to determine the extra-column dispersion produced. It is assumed that the above applies in the present situation but it is difficult to obtain any experimental evidence on this point.

The dispersion produced by the various permutations of injector head, pre-columns, sandwich piece and end piece were measured by connecting particular combinations directly to the detector ie. omitting the packed column, and injecting an

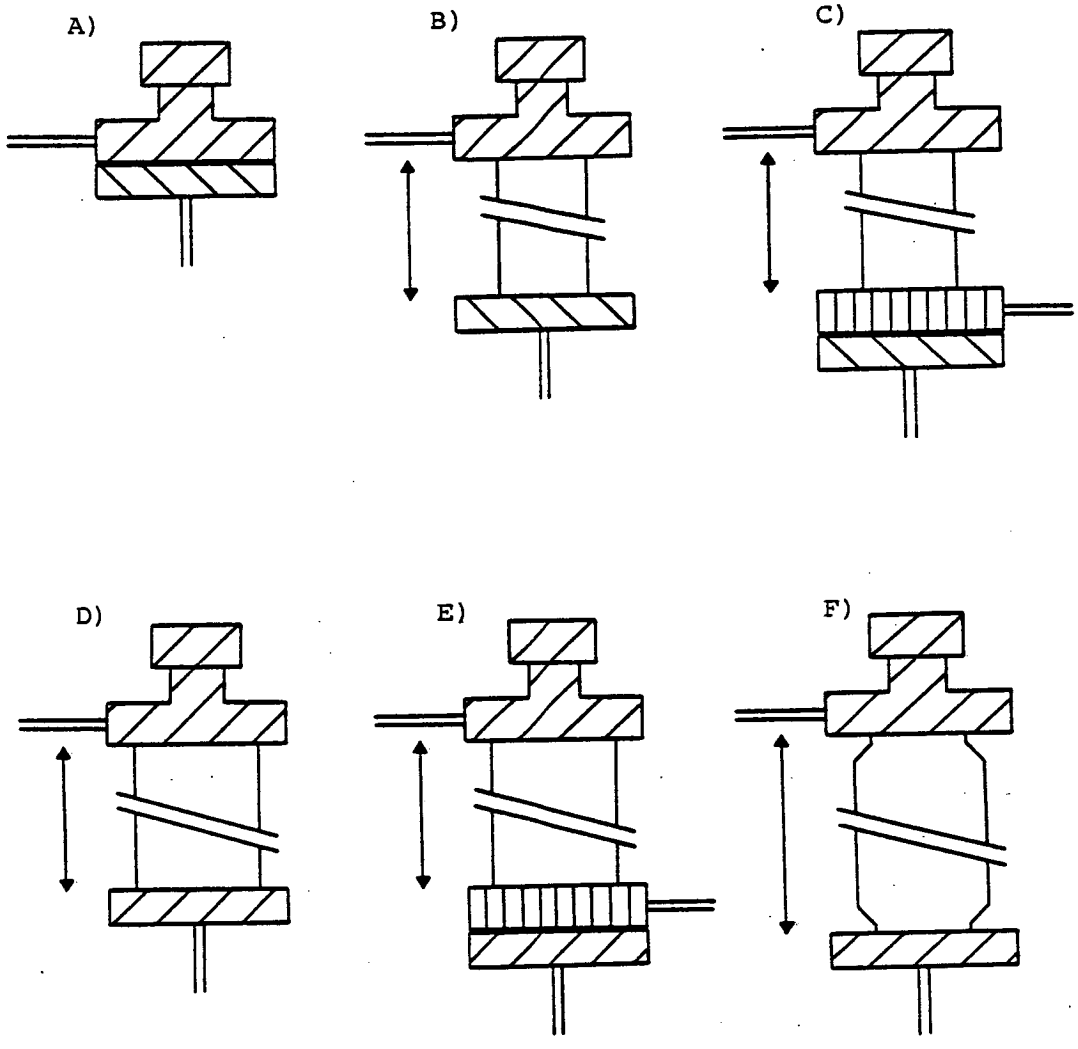

Figure 8.10 Schematic representation of various combinations of apparatus whose dispersion was measured.

A) Injector/End piece.

B) Injector/Pre-column (150mm x 14mmid)/End piece

C) Injector/Pre-column (150mm x 14mmid)Sandwich piece/End piece.

D) Injector/Pre-column (150mm x 22mmid)/End piece.

E) Injector/Pre-column (150mm x 22mmid)/Sandwich piece/End piece.

F) Injector/Main column (250mm x22mmid) /End piece.

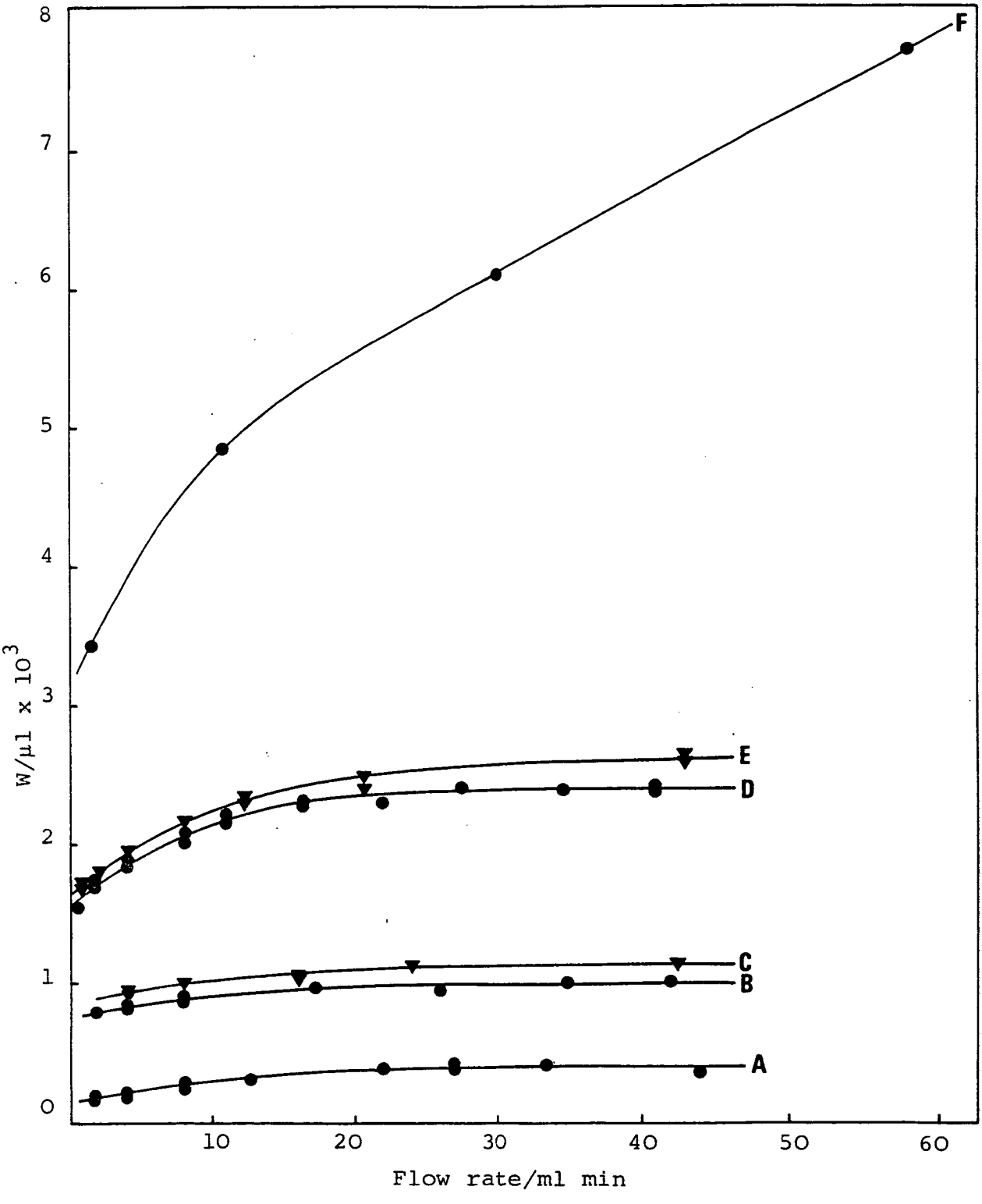

Figure 8.11 Dispersion produced by the various combinations of apparatus (A-F as illustrated in figure 8.10) given as the peak width, W, against the eluent flow rate.

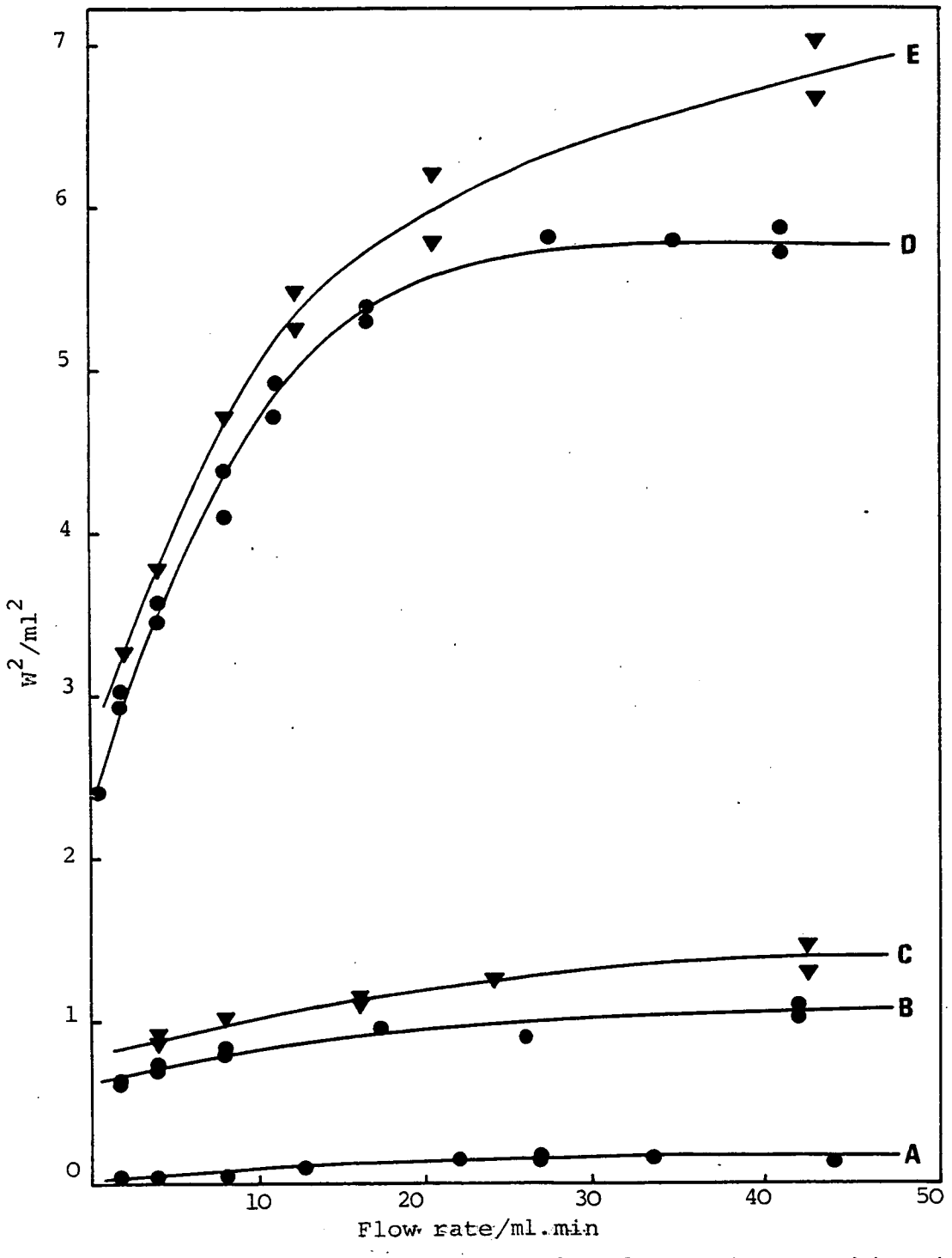

Figure 8.12 The dispersion results for various combinations of apparatus (A-E as illustrated in figure 8.10) given as the square of the peak width, W^2, against the eluent flow rate.

analytical size sample into the system. These were compared to the dispersion produced by the main column only. The various combinations of apparatus which were investigated are illustrated schematically in figure 8-10 and were as follows:

A) Injector/End piece

B) Injector/Pre-column /End piece
150mm x 14mm id.

C) Injector/Pre-column /Sandwich piece/End piece
150mm x 14mm id.

D) Injector/Pre-column /End piece
150mm x 22mm id.

E) Injector/Pre-column /Sandwich piece/End piece
150mm x 22mm id.

F) Injector/Main column /End piece
250mm x 22mm id.

The loading pre-columns were packed with glass beads and the main column with ODS-silica as described in section 8.2.5.

The dispersion was measured by connecting the above combinations directly to a U.V. detector and injecting 5µl of 1% w/v acetone.

The dispersion results obtained are shown in figure 8-11 as the peak base width against the flow rate and in figure 8-12 as (peak base width)^2 against the flow rate. The graphs show that the dispersion produced by the injector head/end piece, W_A^2, is small.

The dispersion produced by the sandwich piece, $(W_{sandwich})^2$, is also small, but it should be noted that $(W_E^2-W_D^2)$ is much

greater than $(W_C^2-W_B^2)$ particularly above a flow rate of about 20 ml min^{-1}, which is contrary to what one might expect from equation 8-14.

The introduction of a pre-column into the system causes the dispersion to increase, as one would expect, due to the band being able to spread out within the pre-column. The results also show that the peak dispersion is greater for the wider column and that the extra dispersion is proportional to the increase in the cross-sectional area which again is as expected. At lower flow rates, the dispersion increases more rapidly for the wider pre-column than for the narrower pre-column although at higher flow rates there is little increase in the dispersion and the curve flattens out.

Finally, the dispersion produced by the inclusion of the main column (250mm x 22mmid.) packed with stationary phase into the system to give the injector head/main column/end piece configuration is given in figure 8.11. This shows that the dispersion produced by the main column is substantially greater than the dispersion produced by the pre-columns, the injector head or the sandwich and end pieces.

In conclusion, these results have shown that the extra-column dispersion of the prototype preparative system, as produced by the various different components, is small in comparison to that produced by the main column and that therefore the system is well designed.

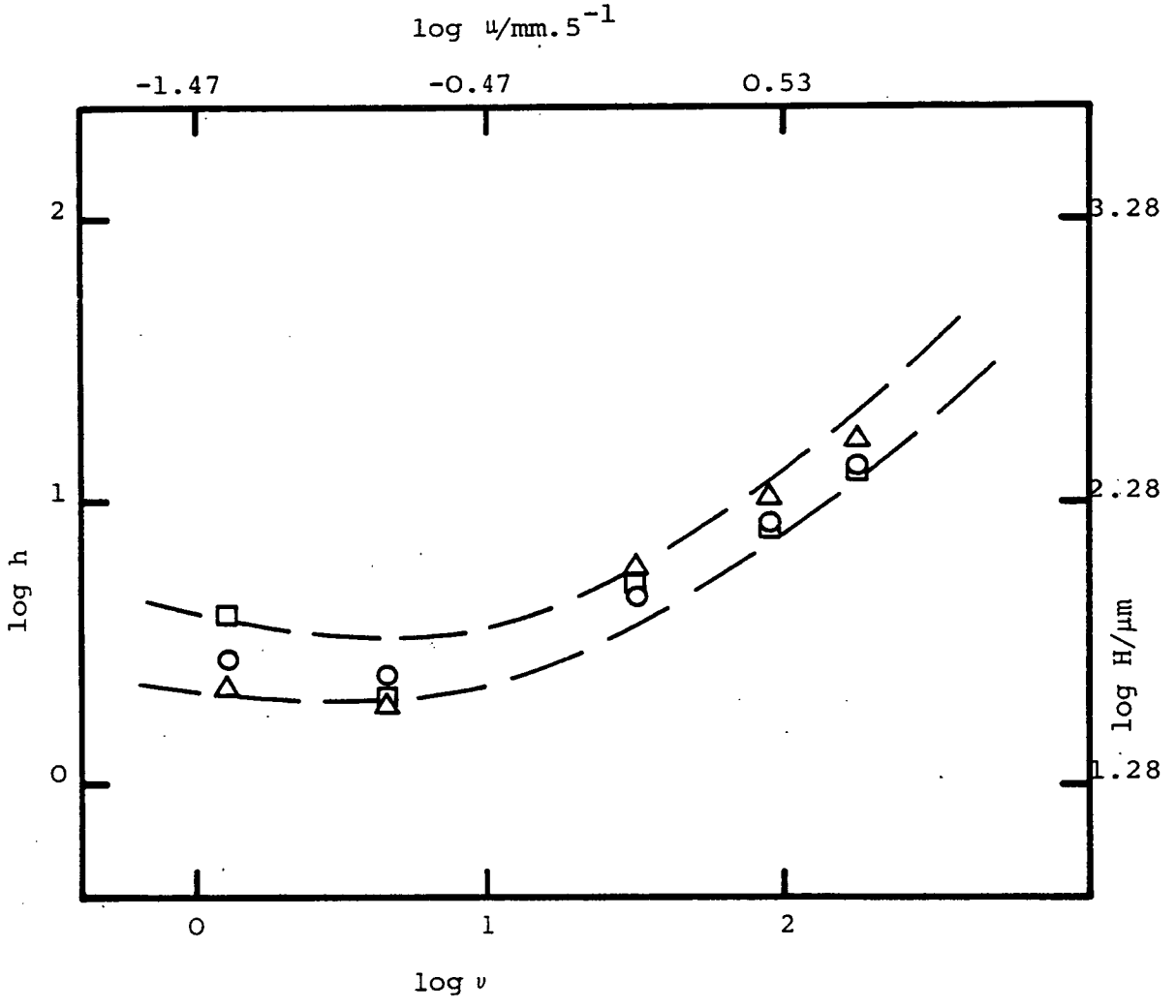

Figure 8.13 Relationship between column efficiency and eluent flow rate for the main column only (configuration F in figure 8.12).

- ○ Acetone, k' = 0.50
- △ Phenol, k' = 1.03
- □ Anisole, k' = 3.94

Table 8-1 Summary of Column Characteristics

Column Dimensions	250 x 22mm id.
Length of Packed Bed	230mm
Stationary Phase	ODS-Silica
Amount of Stationary Phase	64.7 g
Average Particle Size, dp	19 μm
Surface Area (m^2g^{-1})	178 m^2g^{-1}
Pore Volume (cm^3g^{-1})	0.387 cm^3g^{-1}
h_{min}	1.9 at ν = 4.5
ϕ	1118

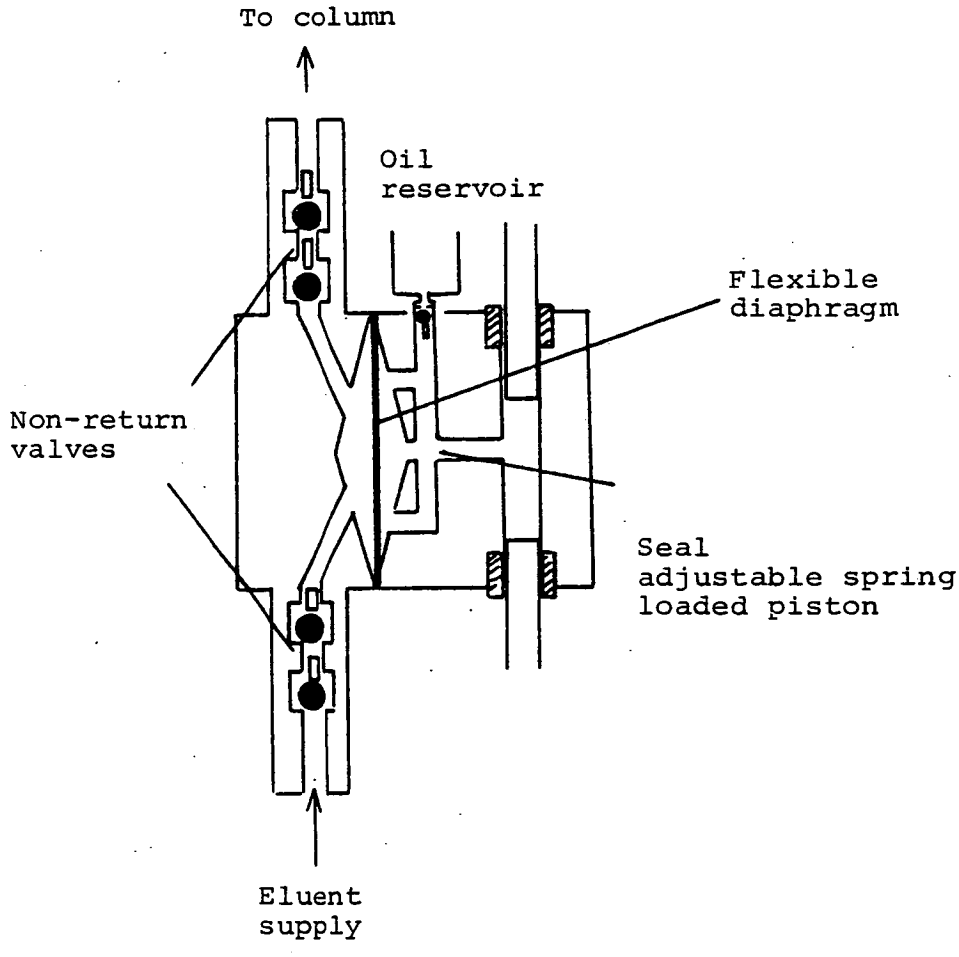

Figure 8.14 Diagram of a diaphragm pump

8.4.2 Testing of the Column Efficiency

The main column (250mm x 22mm id.) was packed using the method described in section 8.2.5 and the column efficiency was determined as described in section 8.3. The results, plotted both in the reduced form as log $h_{0.5}$ against log ν and in the absolute form as log $H_{0.5}/\mu m$ against log $U/mm.s^{-1}$, are given in figure 8-13 and show that the column is very well-packed, having a minimum h value of 1.9 at a reduced velocity, ν, of 4.5. It is generally found[2] that, for well-packed columns, h_{min} is between 2 and 5 at a value of ν of between 2 and 10. The reason for h_{min} for this column being so low may be that, because the internal diameter of the column is large, the sample does not experience any wall effects whatsoever.

The important characteristics of this column are summarised in table 8.1.

8.4.3 Investigation into the use of a Second Eluent Pump

Investigations were carried out to see whether the peak volume and peak shape were affected by introducing a secondary flow through the side-arm of the sandwich piece during the chromatographic run. This was achieved by connecting an Orlita (constant flow) pump similar to the type illustrated in figure 8-14, to the side-arm of the sandwich piece and using it in conjunction with a Haskel pump which provided the main eluent flow. The Orlita pump delivered a flow rate of 4.9 ml/min, while the overall flow rate was 50 ml/min.

Various volumes (1-5 ml) of 1% w/v acetone were injected

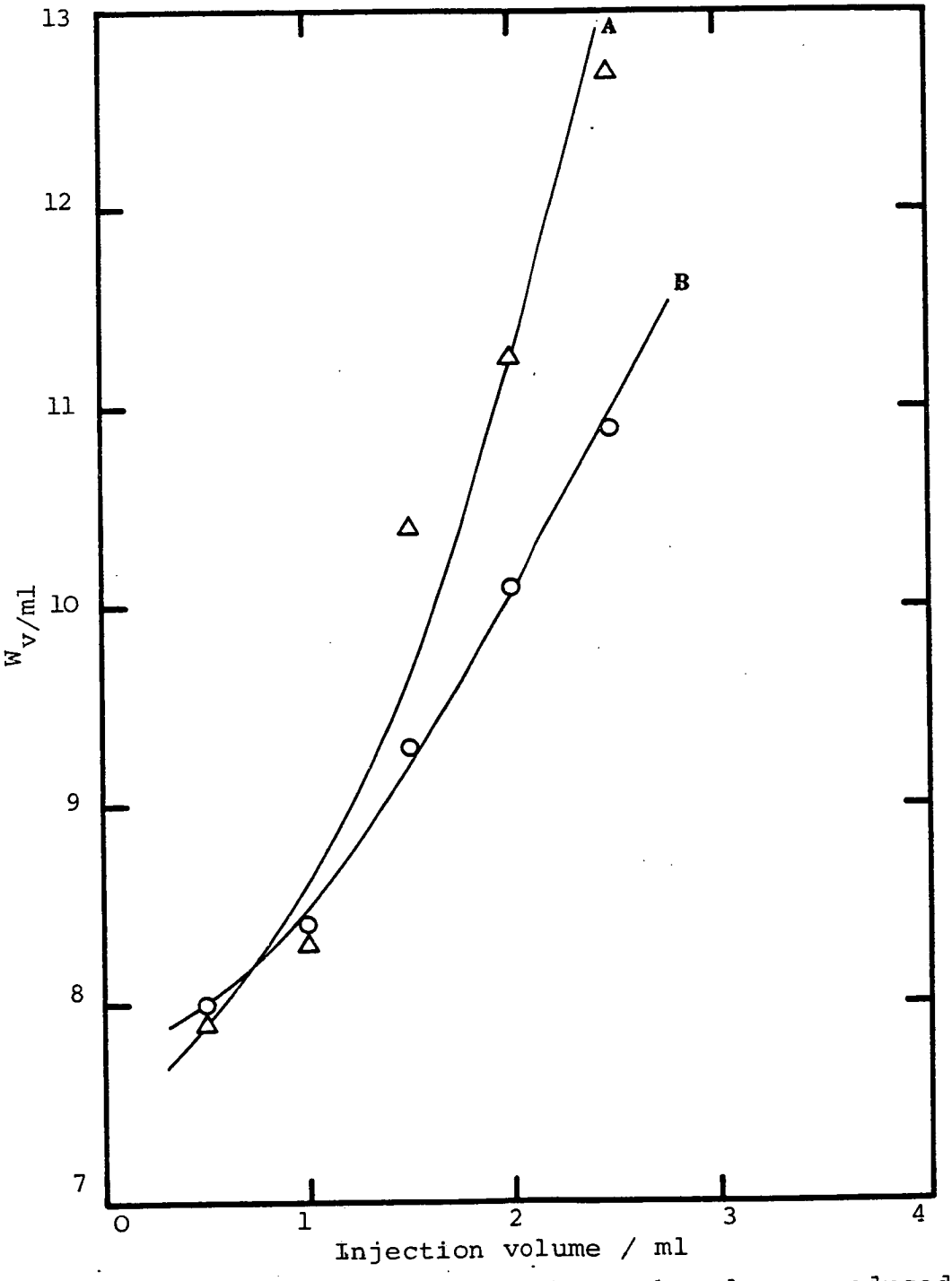

Figure 8.15 Comparison of the peak volume produced A) with and B) without secondary flow through the sandwich piece side-arm.

into the pre-column as follows. The valve between the Haskel pump and the injector head was closed and the valve in the side-arm was opened to allow these injections to be made easily by displacing the equivalent volume of eluent from the pre-column. When the secondary flow was to be used, the side-arm was then connected to the Orlita pump which was then switched on before the valve to the Haskel pump was opened. Where no secondary flow was used, the valve on the side-arm was closed after injection and the valve to the Haskel pump was then opened to commence chromatography.

The results obtained are given in figure 8-15 as the peak volume, W_v, against the injection volume. These indicate that, for injection volumes smaller than 1 ml there was very little difference in the peak volume and it was noted that the peaks were fairly symmetrical with only slight peak tailing. However, for injection volumes greater than 1 ml, results indicate that the peak volume is significantly larger when using a 10% secondary flow through the side-arm of the sandwich piece. It was also noted that the peaks became more tailed when the secondary flow was used whereas the peak shape remained fairly symmetrical when no secondary flow was used. This is the opposite to what was expected. One possible explanation is that the flow from the side-arm through the annular part of the sandwich piece is uneven.

The conclusion, therefore, is that it is best to use the sandwich piece without introducing a secondary flow through the side-arm.

8.4.4 Loading Experiments

8.4.4.1 Introduction

Experiments were carried out in order to observe the extent to which the efficiency of the particular system is affected as the sample load is increased and to optimise a number of parameters, such as

(1) the method of sample introduction,

(2) sample concentration,

(3) sample volume, and

(4) eluent flow rate.

The two different methods of sample introduction which were investigated were the direct injection method and injection via a loading pre-column. For the direct injection experiments the various units were assembled as follows:

injector head | main column 250mm x 22mm id | end piece,

while for the experiments using a loading pre-column the system assembled was as follows:

injector head | pre-column 150mm x 14mm id | sandwich piece | main column 250mm x 14 mm id | end piece.

The above two configurations are illustrated schematically in figure 8-8. The actual procedure for loading the main column via the pre-column is discussed more fully in section 8-2.9.

The concentrations of the solutes used were 0.1%, 1%, 10% w/v acetone and 0.1%, 1%, 2% w/v anisole. These solutions were made up in the eluent which throughout the experiments was methanol/distilled water 60:40 v/v.

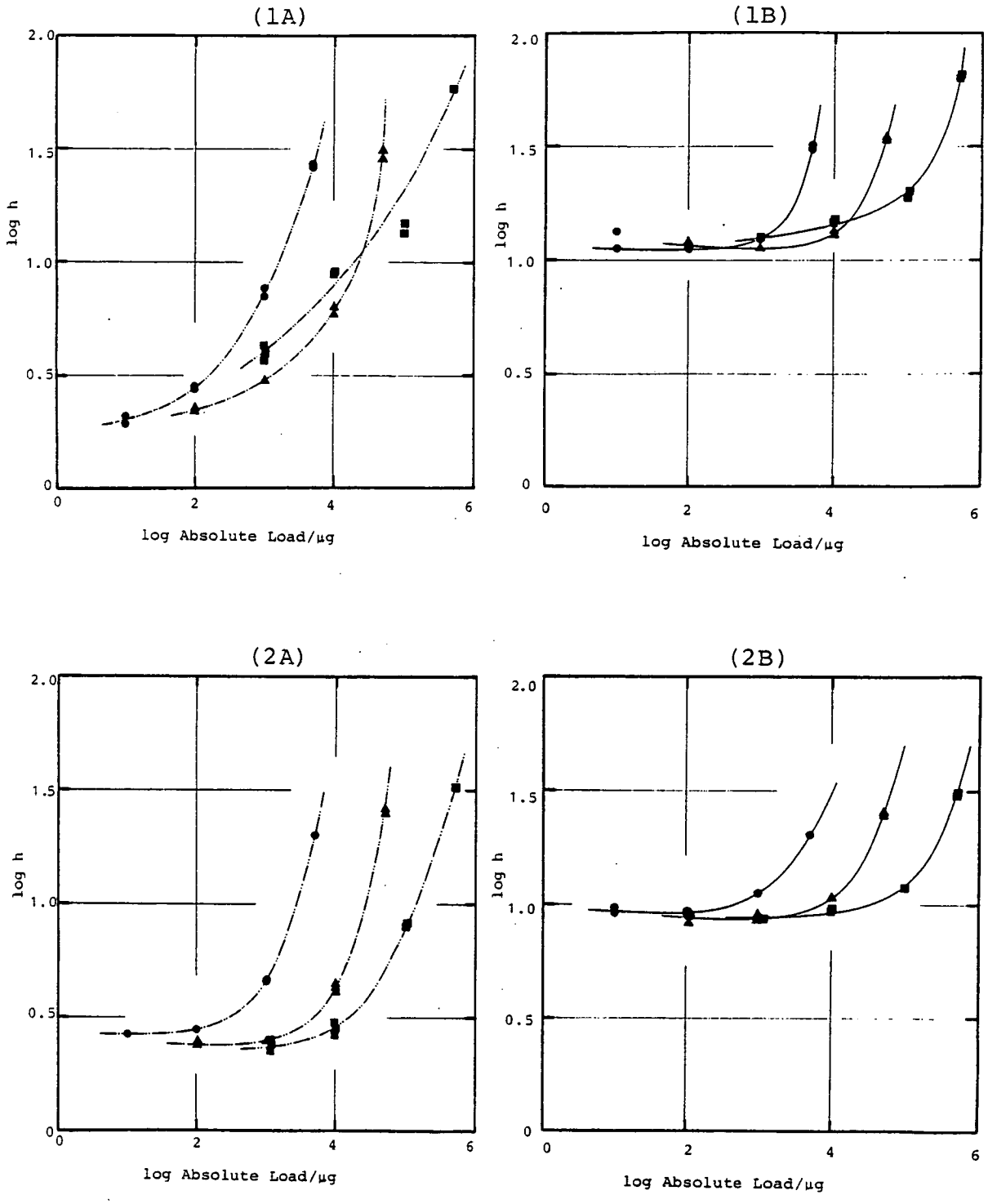

Figure 8.16 Reduced plate height, h, versus Absolute Load at constant concentration for acetone (k' ~ 0.6) at various solute concentrations using different sample loading methods.

1A, 1B: Direct injection method at low and high eluent flow rates respectively.

2A, 2B: Loading pre-column method at low and high eluent flow rates respectively.

●— , ▲— , ■— represent sample concentrations of 0.1%, 1% and 10% (w/v) respectively.

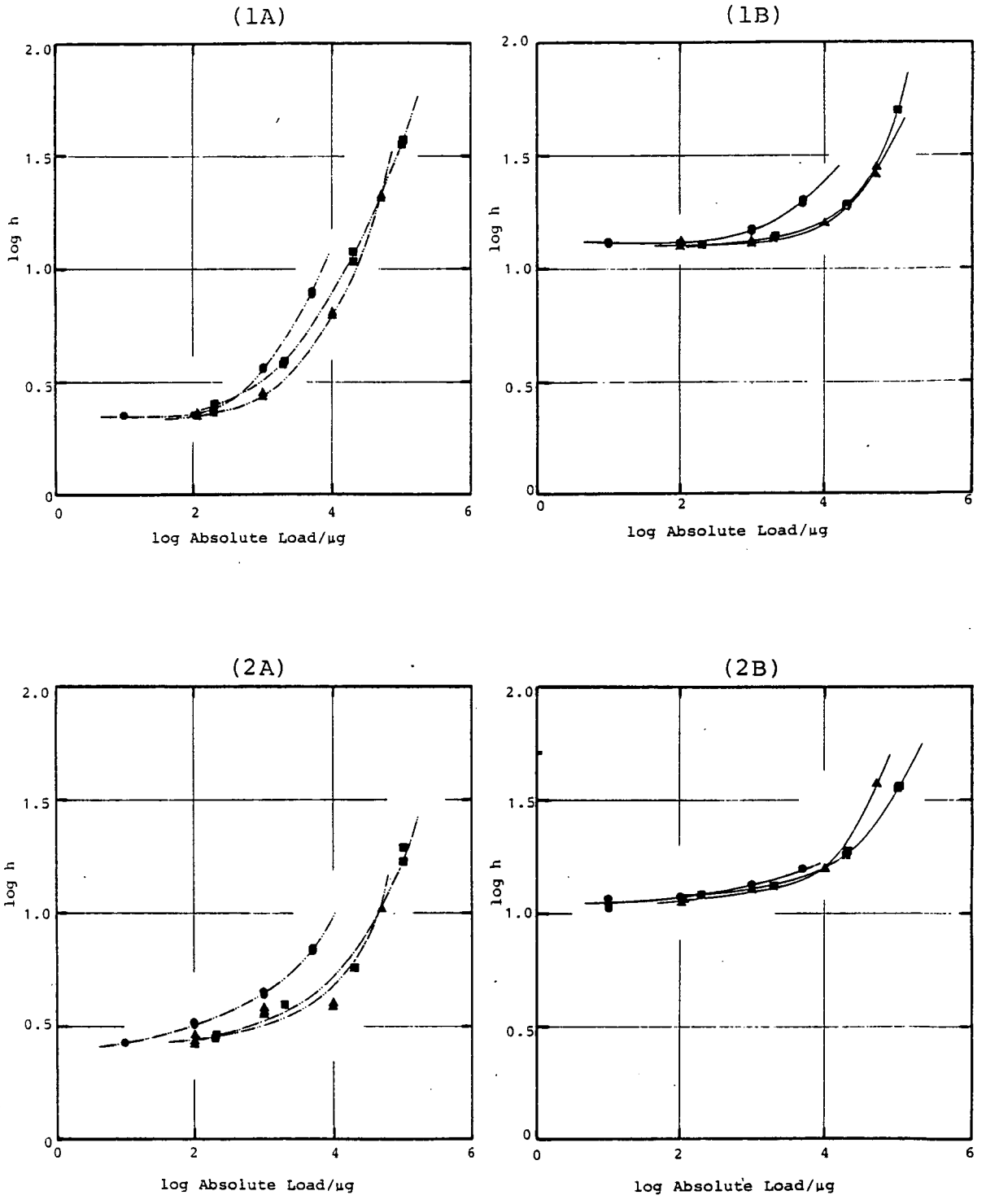

Figure 8.17 Reduced plate height, h, versus Absolute Load at constant concentration for anisole (k' ~ 3.5) at various solute concentrations using different sample loading methods.

1A, 1B: Direct injection method at low and high eluent flow rates respectively.

2A, 2B: Loading pre-column method at low and high eluent flow rates respectively.

●— , ▲— , ■— represent sample concentrations of 0.1% 1% and 2% (w/v) respectively.

The injection volumes in which the solutes were introduced into the column ranged from 10µl, 100µl, 1ml to 5ml and were injected in the stop-flow mode.

Finally, the various loading experiments were all carried out at two different flow rates. These were a low flow rate of $U \sim 4 ml min^{-1}$, or $\nu=3$, and a high flow rate of $U \sim 50 ml min^{-1}$, or $\nu=42$.

The results obtained, which were calculated as described in section 8-3, can be presented in various ways eg.
(1) log h against log Absolute Load at constant concentration
(2) log h against log Absolute Load at constant volume.

8.4.4.2 Data Plotted As log h Against log Absolute Load At Constant Concentration

The data obtained for acetone and for anisole using both injection systems and at both eluent flow rates are given in figures 8-16 and 8-17 respectively as log h against log Absolute Load.

The information obtained from these graphs can be interpreted in several different ways.

(1) The Effect Of Increasing The Sample Load

All graphs show the same feature ie. that as the load is increased the peaks become wider and the column efficiency drops. This is as expected since at low sample loads the column is operating in the linear part of the distribution isotherm while at high loads the column is operating in the non-linear part of the distribution isotherm.

(2) The Comparison Between The Two Injection Systems

In most cases, results show that it is best to use a pre-column and this improvement is particularly noticeable when high loads and high flow rates are used, which is as expected.

The only situation where the direct injection system gives slightly better results is where the main column is operated close to optimum conditions with respect to sample load (up to $\sim$100µg) and eluent flow rate (ν of 2-5), which again is to be expected.

(3) Effect Of Introducing The Same Sample Loads At Different Concentrations

At low levels of sample loads there appears to be little difference as to what concentration of sample solution is used for both acetone and anisole. At high sample loads it appears that for acetone, which is only slightly retained (k'=0.6), it is better to use lower volumes of a higher concentration (eg. 1ml of 10% w/v) than a higher volume of a lower concentration (eg. 5ml of 1% w/v). Thus, for slightly retained solutes at high sample loads, volume overloading is more serious than concentration overloading. For anisole, which is more retained (k'=3.5), there appears to be little difference between the results obtained for the 1% and 2% solutions. Volume over-loading is seen to occur with the 0.1% anisole solution, except for when the high flow rate was used with the loading pre-column/main column system when results were similar to those obtained with the 1% and 2% solutions.

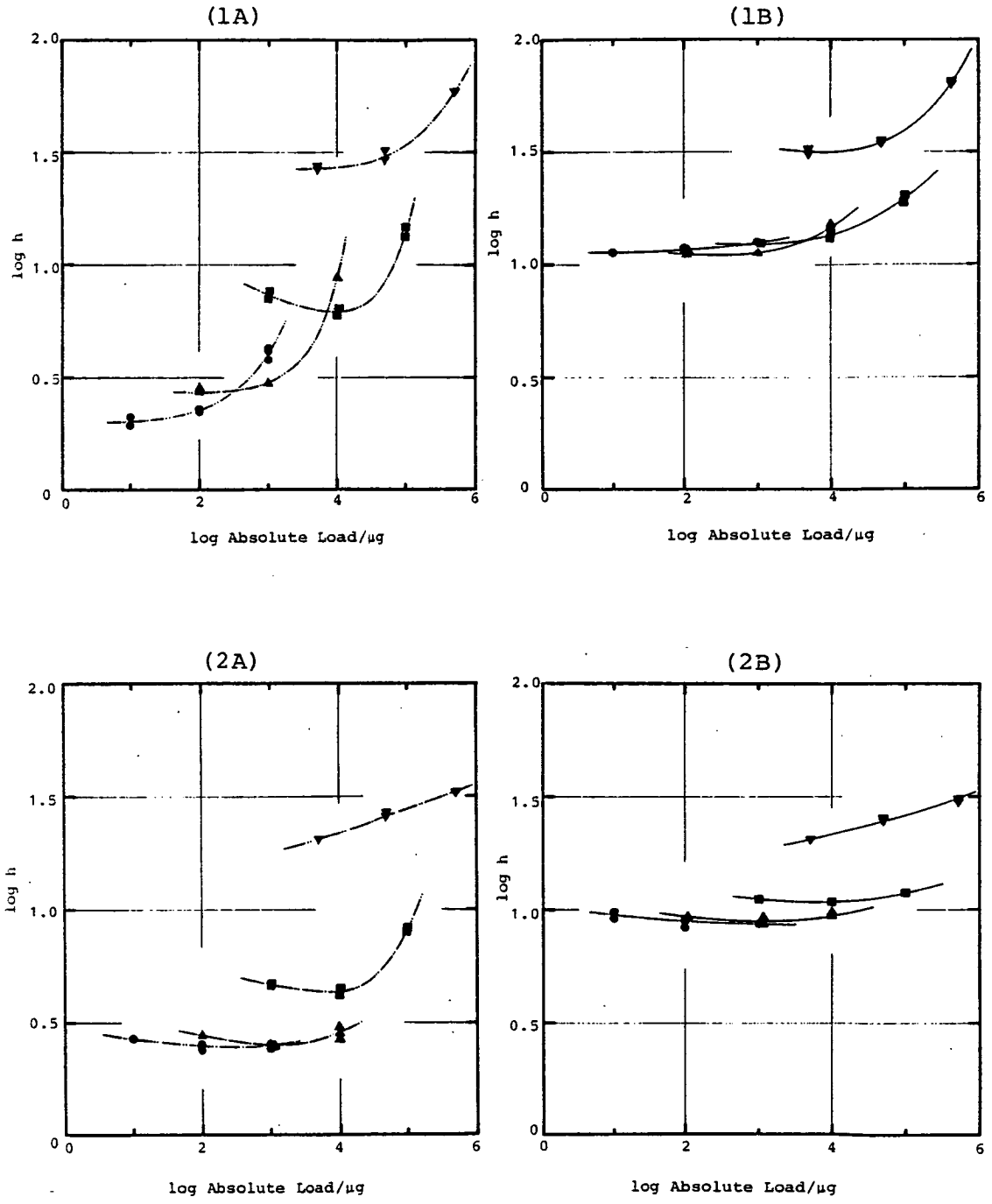

Figure 8.18 Reduced plate height, h, versus Absolute Load for acetone at constant volume using different sample loading methods.

1A, 1B: Direct injection method at low and high eluent flow rates respectively.

2A, 2B: Loading pre-column method at low and high eluent flow rates respectively.

●—, ▲—, ■—, ▼— represent injection volumns of 10, 10^2, 10^3 and 5 x 10^3 µl respectively.

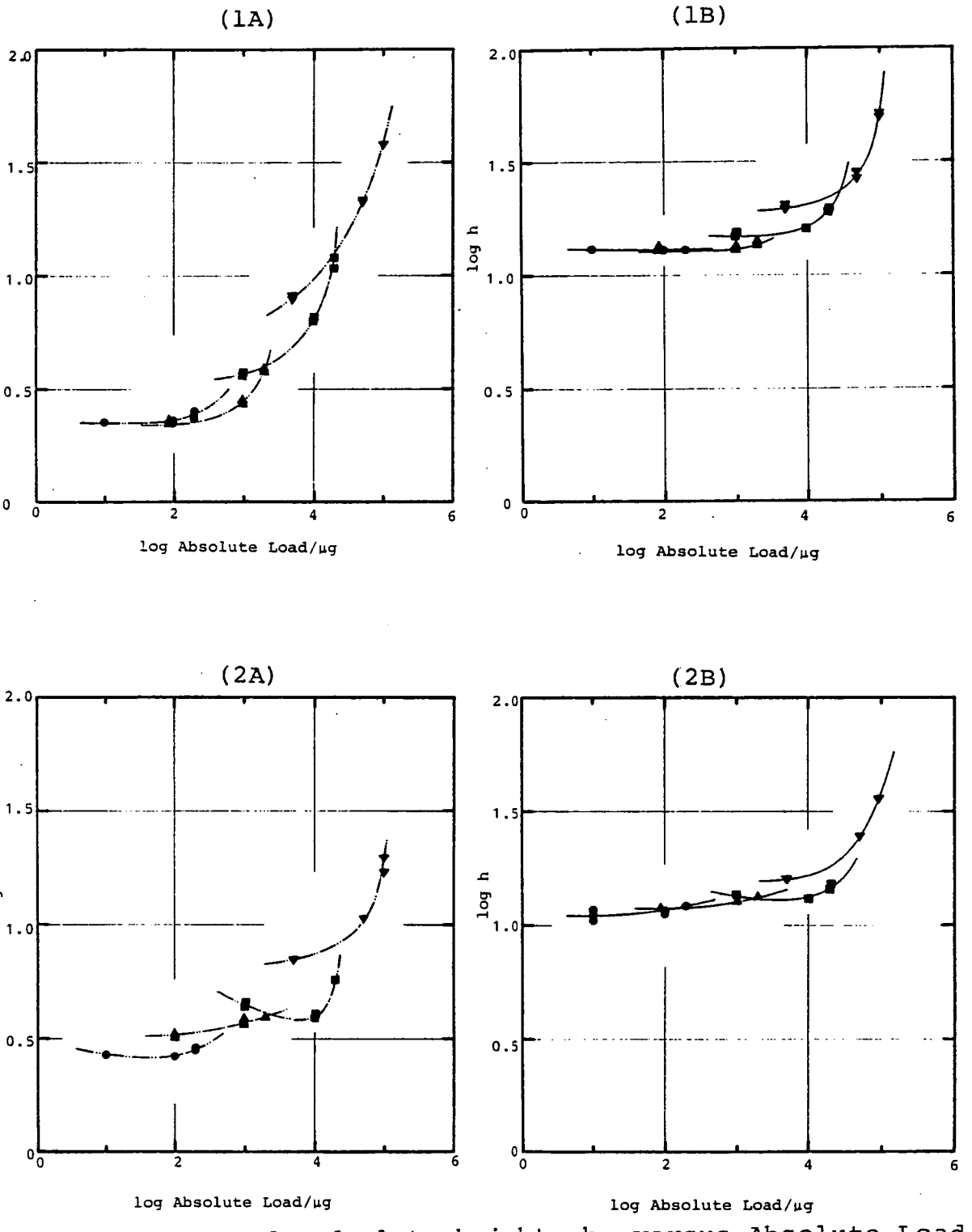

Figure 8.19 Reduced plate height, h, versus Absolute Load for anisole at constant volume using different sample loading methods.

1A, 1B : Direct injection method at low and high eluent flow rates respectively.

2A, 2B : Loading pre-column method at low and high eluent flow rates respectively.

●—, ▲—, ■—, ▼— represent injection volumes of 10, 10^2, 10^3 and 5 x 10^3 µl respectively.

(4) The Effect Of Eluent Flow Rates

When small sample loads are injected into both of the column systems, the column efficiency is much greater for low flow rates than for high flow rates. As the sample load is increased, the efficiency decreases much more quickly for the low flow rates ie. the curves are steeper than those obtained for the higher flow rates till eventually, at high sample loads, there is little difference in the column efficiency produced by the low and high flow rates. This implies that sample throughput, ie. the amount of material separated per unit time, can be increased by using high sample loads at high eluent flow rates.

8.4.4.3 Data Plotted As log h Against log Total Load At Constant Volume

An alternative way of representing the data is to plot log h against log Total Load for constant injection volumes as illustrated in figure 8-18 for acetone and figure 8-19 for anisole. Once again there are several different ways of considering the graphs produced.

(1) The Effect Of Increasing The Sample Load

For most of the load range covered by the data, ie. up to $\sim 10^5 \mu g$ of sample, the best column efficiency obtained when increasing the sample load is achieved by increasing the injection volume, which in turn suggests that there is an optimum sample concentration as was observed in section 8.4.4.2. This is illustrated by an envelope which can be drawn through the

optimum points on each curve. For most of the load range covered here, results suggest that a 1% solution is the optimum sample concentration.

Figure 8-18 indicates that for acetone, which is slightly retained, volume overloading is a more serious problem than it is for anisole as shown by the 5ml curve. This was also observed in section 8.4.4.**2** (**3**).

(2) Comparison Between The Two Injection Systems

In almost all cases, a higher column efficiency is obtained when a loading pre-column is used. The direct injection method is slightly better for low loads at low eluent flow rates. This is in agreement with the observations made in 8.4.4.**2**(**2**).

(3) The Effect Of Introducing The Same Sample Loads At Different Concentrations

In theory, small volumes of high sample concentrations can lead to poor column efficiency due to concentration overloading but the results shown in figures 8-18 and 8-19 show that this is not a serious problem in this case. On the other hand, it is noticeable, especially for acetone, that very large volumes of low concentrations do not give the best results as this causes volume overloading which is a serious problem. This again suggests that it is best, over most of the range of sample loads covered here, to use a moderate sample concentration eg. 1% w/v. However, at very high sample loads, eg. $>10^5\mu g$, it appears that it is possibly better to use a higher sample concentration eg. 10% w/v, since the volume of a 1% w/v solution required to deliver such a load would once again lead to volume overloading.

(4) The Effect Of Eluent Flow Rates

The effect of the eluent flow rate on the column efficiency is noticeable in figures 8-18 and 8-19. While the efficiency produced at low load levels is far greater for low flow rates than for high flow rates, there is very little difference between the efficiencies produced by the two flow rates at high load levels. This was also observed in 8.4.4.2(4).

(5) Conclusions

The results presented in the form of log h against log Total Load at constant volume suggest that, in order to obtain the best column efficiency when increasing the sample load, it is best to keep the sample concentration constant and to increase the sample volume. It also appears that, over most of the sample load range covered in this present work, a 1% w/v concentration is best.

Results also show that there are no disadvantages in using the pre-column. Indeed, when high sample loads are used there are significant improvements on the column efficiency. Another important advantage of using the pre-column is that it is much easier to introduce the sample via the loading pre-column/sandwich piece/main column arrangement when large sample volumes are to be introduced since the valve on the side-arm of the sandwich piece can be opened during injection to facilitate the introduction of the sample onto the main column as described earlier in this chapter.

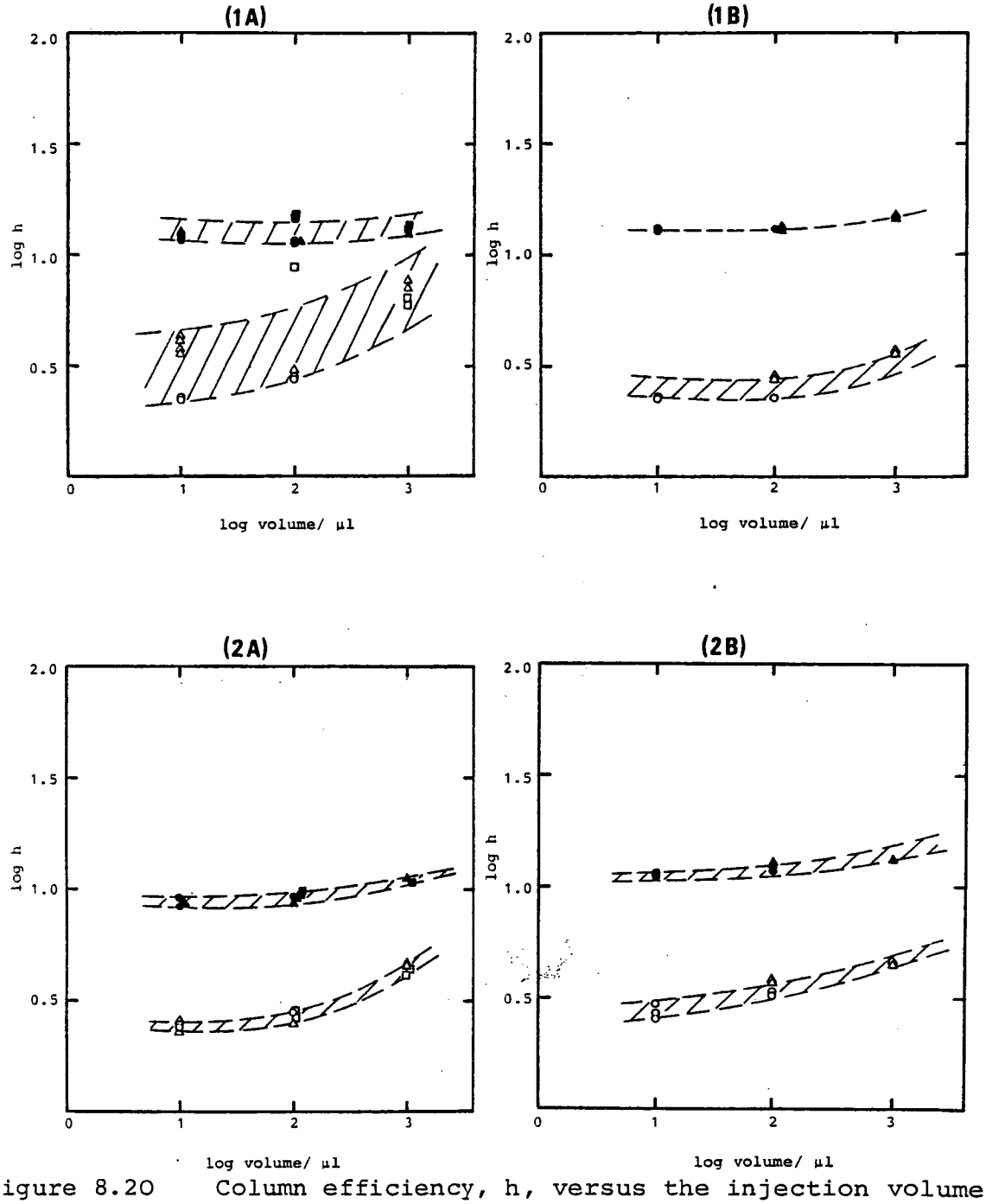

Figure 8.20 Column efficiency, h, versus the injection volume for acetone (1A, 2A) and anisole (1B, 2B) using the two different sample loading methods. 1A, 1B: Direct injection method. 2A, 2B: Loading pre-column method.

○—.△—.□— represents a total load of 10^2, 10^3 and 10^4 µg respectively at low eluent flow rate.

●—.▲—.■— represents a total load of 10^2, 10^3 and 10^4 µg respectively at high eluent flow rate.

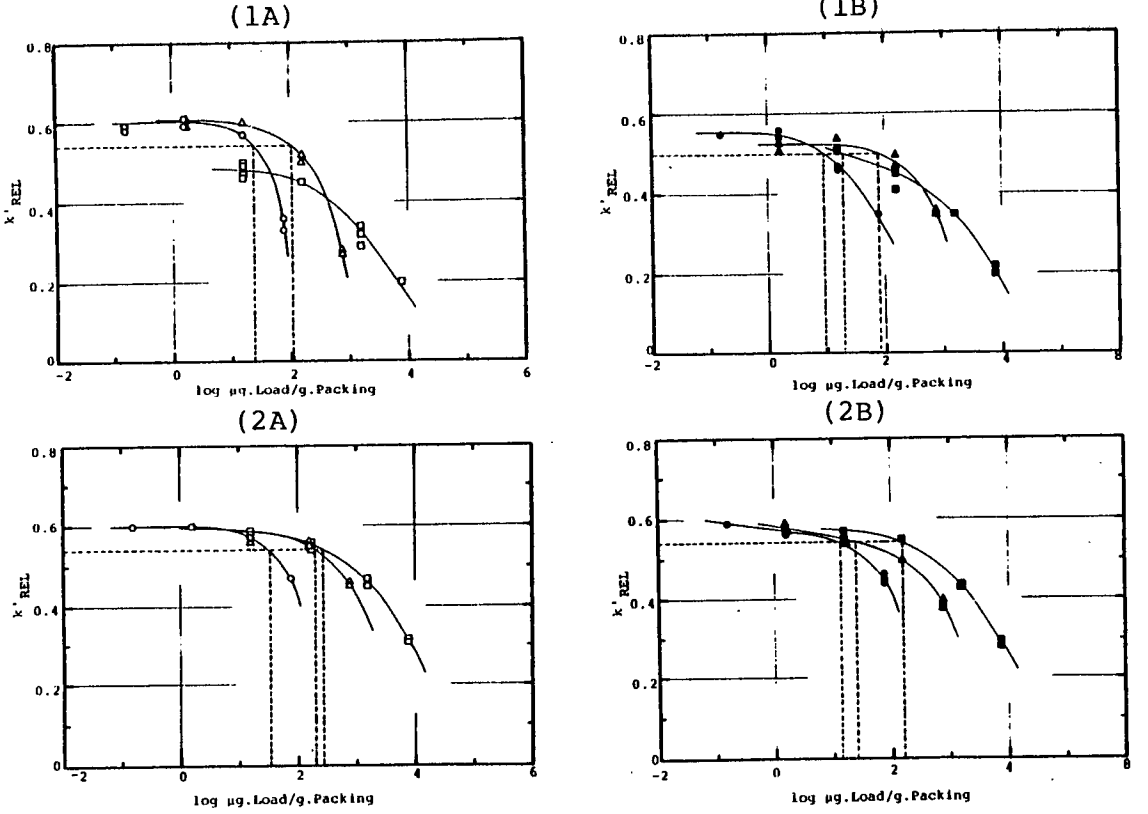

Figure 8.21 The relative phase capacity ratio, k'_{REL}, versus log Specific Load for acetone at various solute concentrations using different sample loading methods.

1A, 1B : Direct injection method at low and high eluent flow rates respectively.

2B, 2B : Loading pre-column method at low and high eluent flow rates respectively.

●—, ▲—, ■— represent sample concentrations of 0.1%, 1% and 10% ($^{W}/V$) respectively.

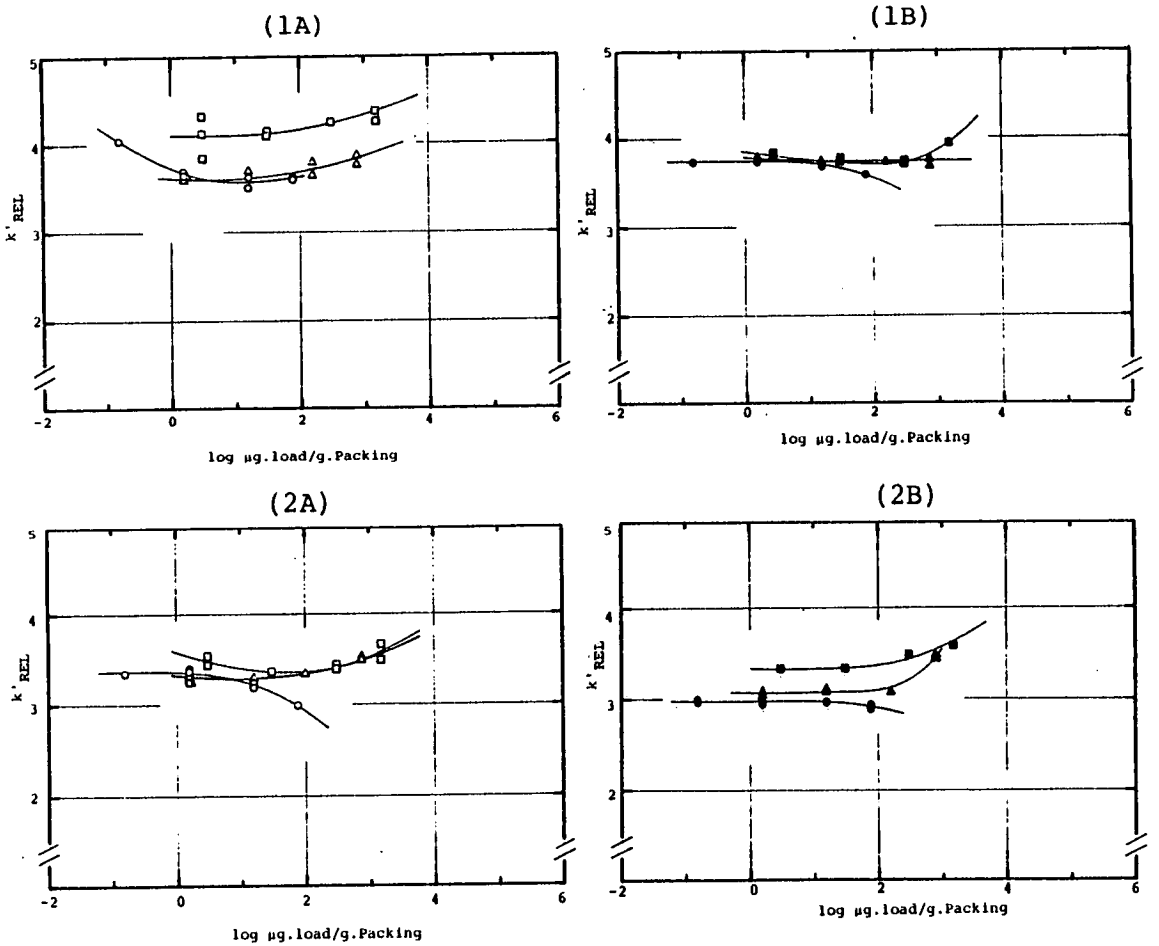

Figure 8.22 The relative phase capacity ratio, k'_{REL}, versus log Specific Load for anisole at various solute concentrations using different sample loading methods

1A, 1B : Direct injection method at low and high eluent flow rates respectively.

2B, 2B : Loading pre-column method at low and high eluent flow rates respectively.

●—, ▲—, ■— represent sample concentrations of 0.1%, 1% and 2% ($^{W}/V$) respectively.

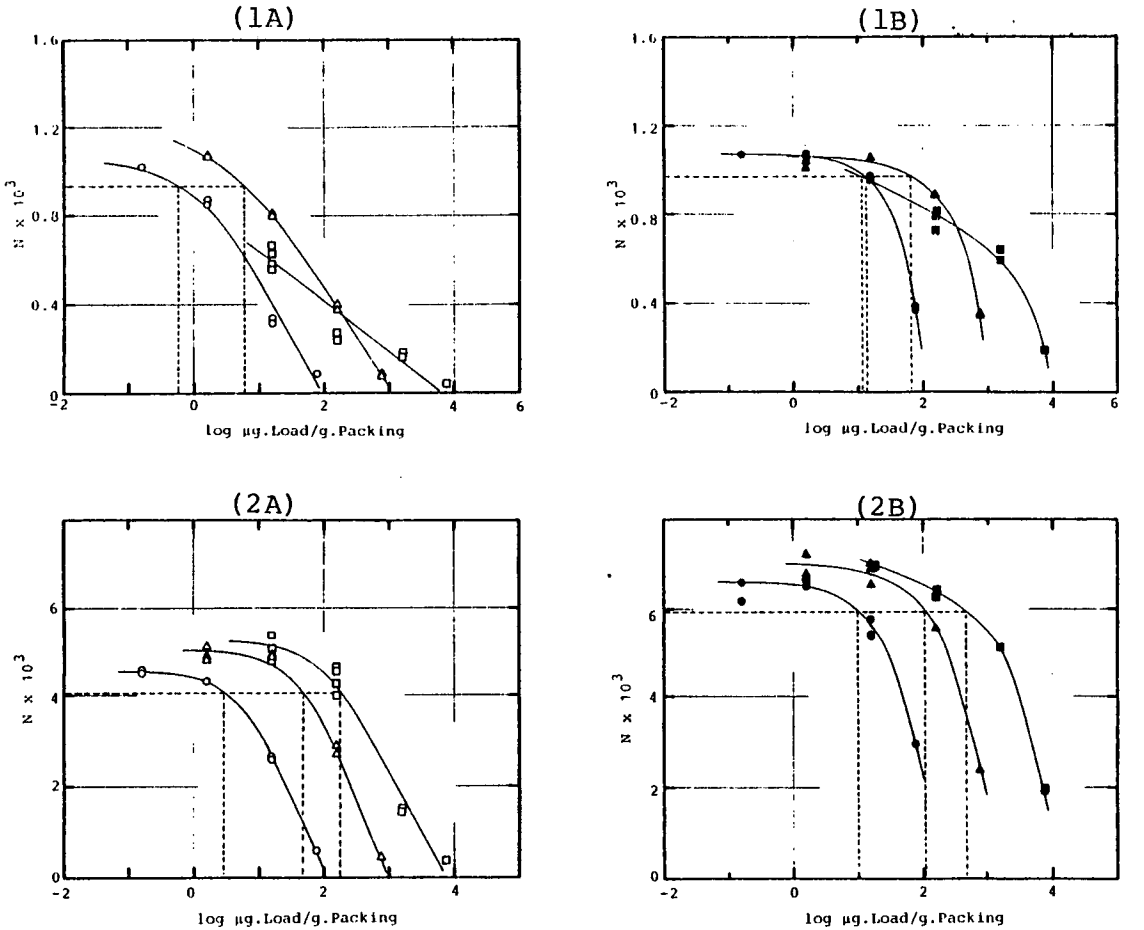

Figure 8.23 Column plate number, N, versus log Specific Load for acetone at various solute concentrations using different sample loading methods.

1A, 1B: Direct injection method at low and high eluent flow rates respectively

2A, 2B: Loading pre-column method at low and high eluent flow rates respectively

●——, ▲——, ■—— represent sample concentrations of 0.1%, 1% and 10% (w/v) respectively

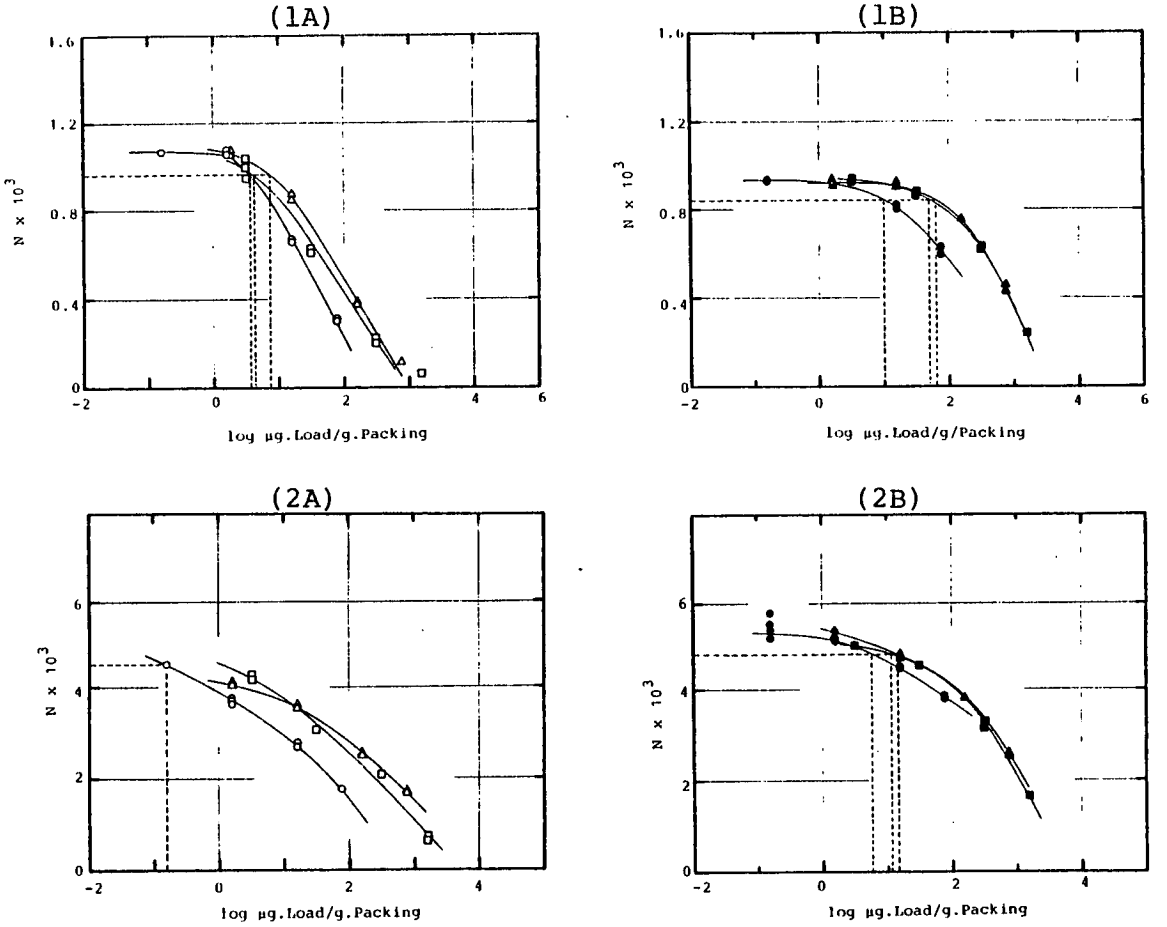

Figure 8.24 Column plate number, N, versus log Specific Load for anisole at various solute concentration using different sample loading methods.

1A, 1B : Direct injection method at low and high eluent flow rates respectively.

2B, 2B : Loading pre-column method at low and high eluent flow rates respectively.

●—, ▲—, ■— represent sample concentrations of 0.1%, 1% and 2% ($^{W}/V$) respectively.

8.4.4.4 Data Plotted As log h Against log Volume At Constant Load

The curves produced when plotting the data as log h against log Volume at constant load for both the direct injection method, ie. using the main column only, and for the loading pre-column method are similar as shown in figure 8-20. As the eluent flow is increased so the curves flatten out, as expected.

8.4.4.5 Linear Capacity Limit, $\theta_{0.1}$

It has previously been mentioned in chapter 6 that the linear capacity may be defined either in terms of a 10% reduction in k' from its original value at low load levels, $\theta_{0.1}^{k'}$, or in terms of a 10% reduction in N from its original value at low load levels, $\theta_{0.1}^{N}$

The results for both injection methods plotted as k' against log Specific Load are given in figures 8-21 and 8-22 while figures 8-23 and 8-24 show the results plotted as N against log Specific Load.

(1) Comparison Between The Two Injection Systems

In general, the linear sample capacity limit is increased when the loading pre-column is used. This is to be expected since there is a greater possibility of localized overloading occurring at the top of the bed when the direct injection method is used.

(2) The Difference Between $\theta_{0.1}^{k'}$ and $\theta_{0.1}^{N}$

In general, the same trends are observed for $\theta_{0.1}^{N}$ as for $\theta_{0.1}^{k'}$. However, for anisole, a variety of effects appear to be

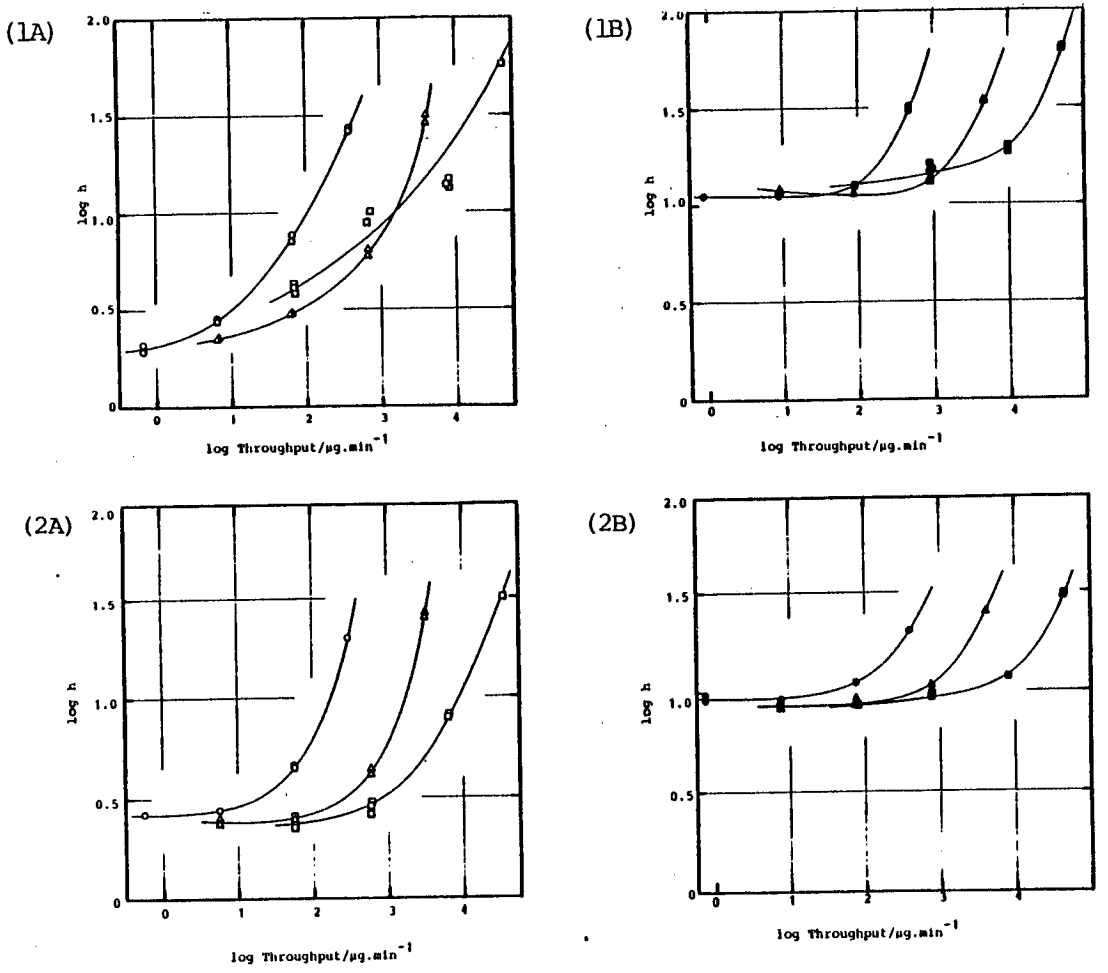

Figure 8.25 Reduced plate height, h, versus sample throughput for acetone at various concentrations using different sample loading methods.

1A, 1B: Direct injection method at low and high eluent flow rates respectively

2A, 2B: Loading pre-column method at low and high eluent flow rates respectively

●—— , ▲—— , ■—— represent concentrations of 0.1%, 1% and 10% (w/v) respectively

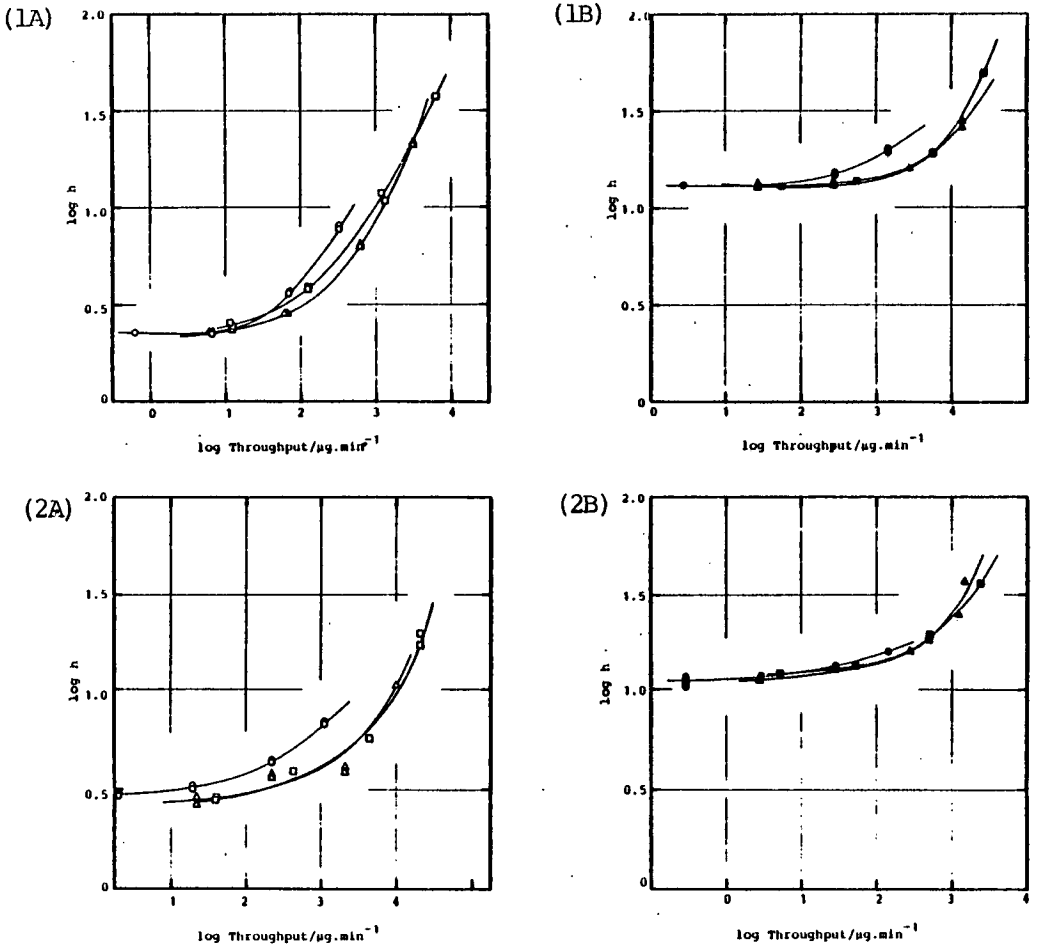

Figure 8.26 Reduced plate height, h, versus sample throughput for anisole at various concentrations using different sample loading methods.

1A, 1B : Direct injection method at low and high eluent flow rates respectively.

2A, 2B : Loading pre-column method at low and high eluent flow rates respectively.

●—.▲—.■— represent concentrations of 0.1%, 1% and 2% ($^{W}/V$) respectively.

involved and in this case it is impossible to define the linear sample capacity in terms of a reduction in k', although it is possible to establish $\theta^{N}_{0.1}$.

The values obtained for $\theta^{N}_{0.1}$ are in general approximately a factor of ten times smaller than those obtained for $\theta^{k'}_{0.1}$, which has been observed by other workers.

(3) The Effect Of Sample Concentration

At low eluent flow rates, a higher linear capacity can be obtained, in the case of the direct injection method, by increasing the sample concentration from 0.1% to 1% w/v since volume overloading occurs at high injection volumes. By using the loading pre-column, $\theta^{k'}_{0.1}$ is increased at both the 0.1% and 1% w/v concentration levels and can be further improved by increasing the sample concentration to 10% w/v, although this increase is only marginal.

When high eluent flow rates are used, it appears that the linear capacity limits obtained using the different concentrations decrease, although this decrease is only marginal in the case of the 10% w/v solution.

8.4.4.6 The Effect Of Sample Concentration And Eluent Flow Rate On Sample Throughput

Sample throughput has already been defined in section 6.4 as the amount of material of specific purity collected per unit time.

Figures 8-25 and 8-26 show the data plotted for acetone and anisole respectively as log h against log Throughput ($\mu g.min^{-1}$).

(1) The Effect Of Sample Concentration And Eluent Flow Rate

For acetone using the direct injection method, we see that for most values of h, throughput is greater when a 1% w/v solution is used. At high flow rates, where the curves flatten out, one can increase the throughput by increasing the concentration to 10% w/v without losing too much efficiency. When the sample is loaded onto the column using the pre-column, then for any particular column efficiency at both low and high eluent flow rates, the highest throughput is obtained using the 10% w/v concentration.

For anisole when using the direct injection method, there is little difference between the throughput obtained using the 1% and 2% w/v solutions although the 1% w/v solution is marginally better at both low and high eluent flow rates. When the loading pre-column is used again there is virtually no difference in the throughput obtained when using either the 1% or the 2% concentration.

(2) Comparison Between The Different Injection Systems

If we consider the two modes of sample introduction then we can see that at low eluent flow rates, if we require a high efficiency, then the best throughput is obtained using the direct injection method. However, if it is not necessary to have such a high column efficiency then the best throughput is obtained using the loading pre-column. At high eluent flow rates, there is virtually no difference between the throughput obtained using either sample loading method.

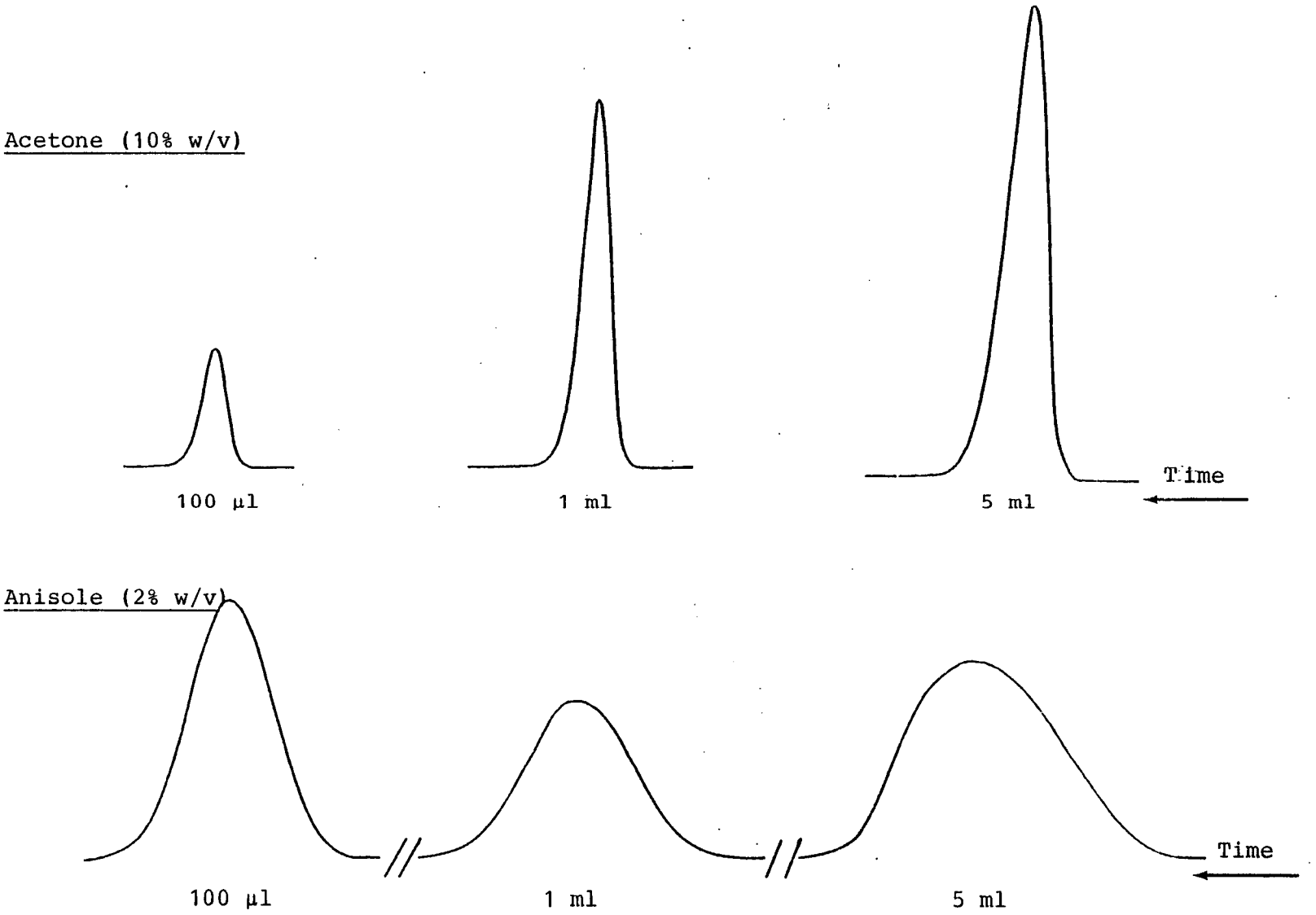

Figure 8.27 Representative chromatograms showing the peak shape produced by the different injection volumes. Column 250mm x 22mm id + loading pre-column; flow rate 50 ml/min; Chart speed 120 mm/min (Acetone, k' = 0.6) and 30 mm/min (anisole, k' = 3).

8.4.4.7 Typical Chromatograms

Typical chromatograms obtained during the loading experiments are shown in figure 8-27 and it is noticeable that even when the column is overloaded the peak shape is still fairly close to Gaussian in shape, as observed by Wall[3], and not square-topped.

8.5 Summary Of Conclusions

1) The best geometry of column units is that which connects the loading pre-column via the sandwich piece to the main column, with no flow through the side-arm of the sandwich piece.
2) The optimum all round concentration is a 1% w/v solution.
3) When increasing the sample load, it is best to keep the concentration constant and increase the injection volume.
4) The sample linear capacity is greater when the sample is loaded via the pre-column.
5) It may be more useful to define the linear sample capacity in terms of a 10% reduction in N from its original value at low load levels since it is not always possible to do so in terms of k'.

References

Chapter 8

1. J.N. Done; J.Chromatogr. 125 (1976) 43.

2. J.H. Knox, G. Laird and P. Raven; J.Chromatogr. 122 (1976) 129.

3. R.A. Wall; J.Liq.Chromatog. 2 (1979) 775.

CHAPTER 9

EXPERIMENTS ON ISOCHRONIC COLUMNS

Chapter 9. Experiments On Isochronic Columns

EXPERIMENTS ON ISOCHRONIC COLUMNS

9.1 Introduction

A set of columns was constructed such that the internal diameters were the same but the column lengths were different. These columns were then packed such that the particle diameter, dp, of the stationary phase material used was roughly proportional to the column length, L, ie.

$$dp \propto L, \text{ approximately.}$$

The term *"isochronic"* has been coined to describe such a set of packed columns since the elution time of any solute will be the same with all such columns if the pressure drop, Δp, remains the same since

$$\Delta p = \frac{\phi' \eta}{t_m} \left(\frac{L}{dp}\right)^2$$

where ϕ' is the column resistance proportionality factor (which is typically between 500 and 1,000), η is the eluent viscosity, L is the column length, t_m is the elution time of an unretained solute and dp is the particle diameter.

In addition the efficiency of each column should deteriorate in a similar way when overloading occurs as measured on the basis of microgram of sample per gram of packing material.

When using these columns for relatively large-scale separations, therefore, two things have to be taken into consideration. As the column length increases then for the same Δp, the flow rate, U, increases and therefore so too does the reduced velocity, ν. When using analytical size samples these

Table 9.1 Values of the reduced lengths, $L/_{dp}$, of the various columns

Column dimensions/mm	Particle size/μm	$L/_{dp} \times 10^3$
93 x 7 id	10.64	8.74
134 x 7 id	15.75	8.49
247 x 7 id	19.00	13.00

Table 9.2 Conditions for the loading experiments

Column/mm	Vm/ml	t_m*/sec	ν	Average flow rate/ml.min^{-1}	Average Δp/psi	Average linear flow rate, U,/ cm.sec^{-1}	$U/_{dp}$
93x7	1.34	82	3.44	0.98	210	0.11	0.01
		27	11.19	3.0	610	0.35	0.03
		9	32.93	8.83	1930	1.02	0.09
134x7	1.94	78	8.20	1.49	150	0.17	0.01
		26	25.05	4.55	490	0.52	0.03
		9	70.08	12.73	1350	1.47	0.09
247x7	3.57	120	11.82	1.78	200	0.21	0.01
		42	34.26	5.16	600	0.60	0.03
		15	95.60	14.40	1900	1.66	0.09

* t_m measured using potassium nitrate.

longer columns produce fewer plates. However, as the longer columns contain more stationary phase material, larger samples can be loaded onto these columns before the effects of overloading appear. The original aim, therefore, was to carry out a series of loading experiments on columns which had the same reduced length such that for a given Δp, the retention time t_R for a solute to be eluted from each of the columns would be the same. However, in order to correct a fault in the manufacture of the original columns, the end of each column had to be cut off and a new end fitting made and as a result it was not possible to produce columns with precisely the same reduced length. The actual reduced lengths which were obtained for the various columns are given in table 9.1.

It was therefore decided to carry out the experiments at three different flow rates such that the ratio of the linear flow velocity, U, to the particle diameter, dp, ie. $^{U}/_{dp}$, was constant, in order to mimic a true isochronic set as closely as possible. In this way

$$\text{since} \quad \frac{U}{dp} = \text{constant}$$

$$\text{and} \quad \nu = \frac{Udp}{D_m}$$

$$\text{then} \quad \nu \propto dp^2.$$

Table 9.2 shows the actual conditions used for the loading experiments and it can be seen that the ratios of $^{U}/_{dp}$ actually used were

$$1 : 3 : 9$$

The loading experiments were carried out using a test mixture

containing 1% w/v each of acetone, acetophenone and methyl benzoate made up in the eluent, which was MeOH/H_2O 60:40 v/v. The volumes of sample injected were 10µl, 25µl, 100µl, 250µl and 1 ml. Initially, detection was at 254nm, but as the load injected increased the absorbance wavelength was backed off as necessary.

9.2 Equipment

A home-made chromatographic system was used throughout the experiments and the general features of such a system are illustrated in figure 8-1.

9.2.1 Pumping System

A Haskel Pneumatic Pressure Intensifier pump (Haskel Engineering Systems Ltd., England) was used which had a stroke capacity of 70ml and which was capable of delivering solvents at flow rates of up to 1ℓ min^{-1} or more. A diagram of this type of pump is shown in figure 8-2.

9.2.2 Pressure Gauge

A Bourdon manometer was used as a pressure gauge and was situated between the pump and the on/off valve used for stop-flow injections.

9.2.3 Columns

The columns used were made to a design similar to those

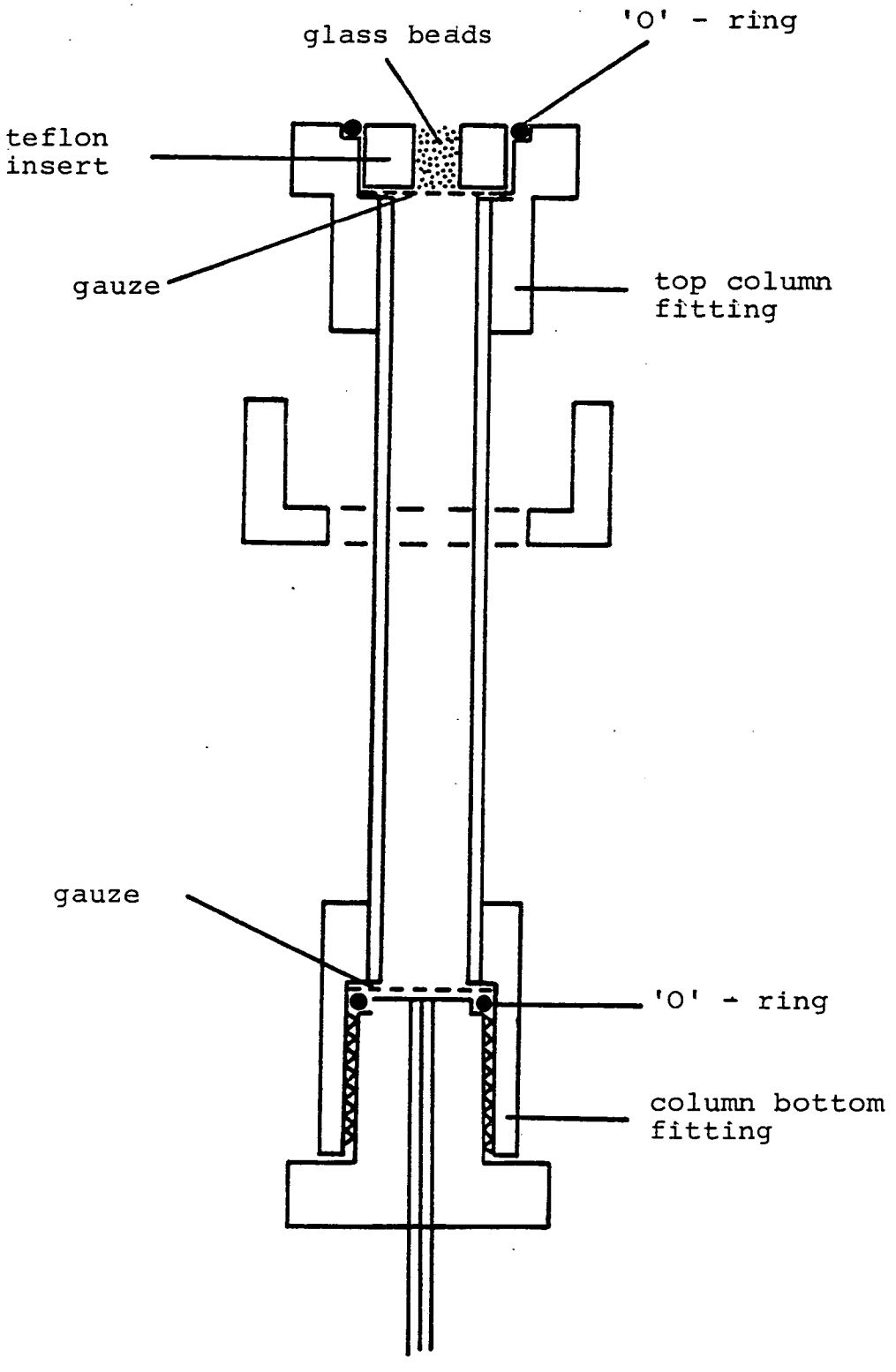

Figure 9.1 Column fittings

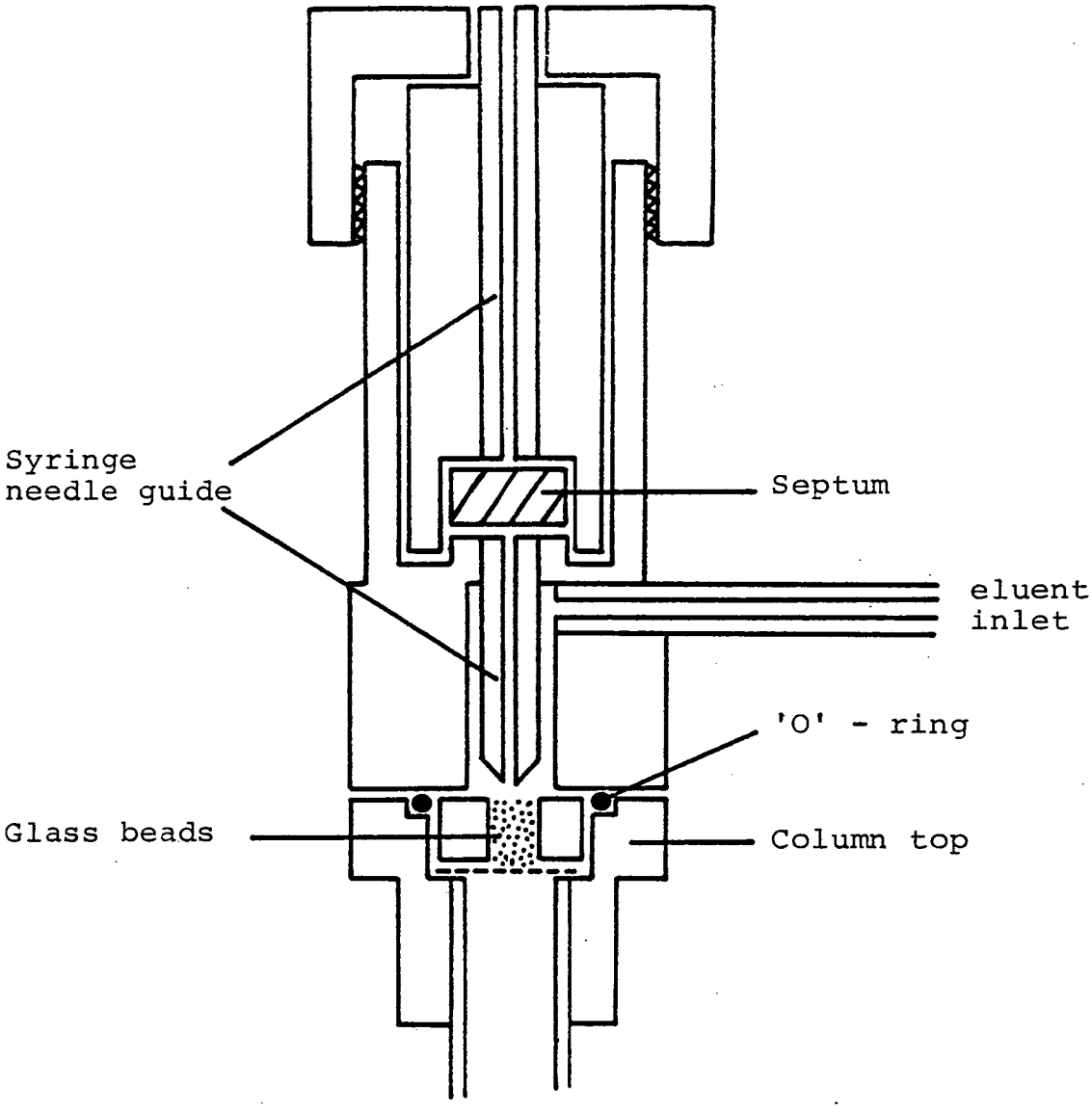

Figure 9.2 Column injector head

marketed by Shandon (Runcorn, England) and are illustrated in figure 9-1. The columns, whose dimensions were 93mm x 7mm id, 134mm x 7mm id and 247mm x 7mm id, were made in this department of SS 316 stainless steel and were honed on the inside to a smooth finish.

9.2.4 Injector

The injector head was also made in this department to a design similar to that used by Shandon and is illustrated in figure 9-2. This type of injector introduces the sample by syringe into a curtain-flow of eluent.

9.2.5 Detector

A Cecil 212 variable wavelength detector (Cecil Instruments, Cambridge, Great Britain) was used which contained an 8µl cell.

9.2.6 Connectors

All connecting tubing was made from stainless steel tubing. The unions which were used were made by Swagelock and the one which was used to connect the column outlet to the detector cell inlet was drilled through to prevent any dead-volume.

The on/off valves used were Whitey valves (supplied by the Glasgow Valve and Fitting Company).

9.2.7 Syringes

Both Hamilton and S.G.E. syringes were used throughout the experiments.

9.2.8 Materials

The solvents used were HPLC grade methanol (Rathburn, Walkerburn, Scotland) and triply distilled water. All solvents were degassed prior to use.

The solutes used were acetone (A.R. grade), acetophenone and methyl benzoate, and solutions of these were made up in the eluent.

The stationary phase used in all of the columns was ODS-silica. Both the preparation and the bonding of the silica gel were carried out as described in Chapter 7 and in a reserved section of this thesis. The mean particle size diameter used in these experiments was 10.68μm, 15.78μm, and 19.00μm.

9.3 Packing of the Isochronic Columns

All of the columns used in these experiments were packed using a Shandon packing machine (Runcorn, England) using an upward slurry packing method as described in more depth in Chapter 5. The 93mm x 7mm id. column was packed with 10.64μm ODS-Silica, the 134mm x 7mm id. column was packed with 15.75μm material and the 247mm x 7mm id. column was packed with 19μm material.

The 93mm x 7mm, and the 134mm x 7mm columns were both packed by slurrying the stationary phase in IPA and packing upwards at a pressure of 7,000 psi with IPA as the following solvent. Once 70-120ml had passed through the columns were then inverted and another 40-60ml IPA were pumped through. Finally, some methanol was passed through the column. The pump was then switched off and the column left to stand before

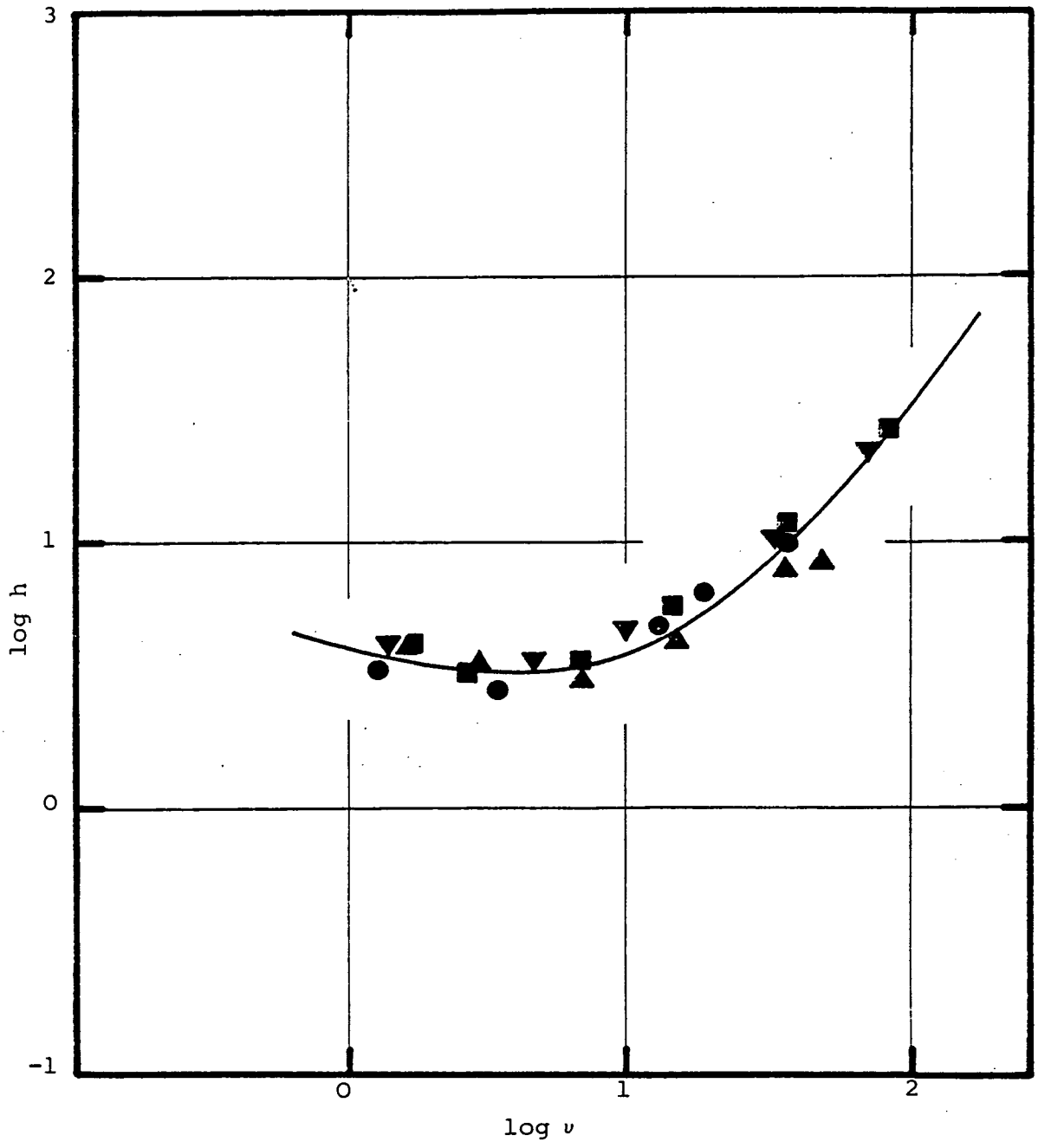

Figure 9.3 The variation of column efficiency with eluent velocity for various columns using acetophenone as the solute.

- ●—— Column 93mmx7mmid; ODS-silica, dp = 10.64μm
- ▲—— Column 134mmx7mmid; ODS-silica, dp = 15.78μm
- ■—— Column 247mmx7mmid; ODS-silica, dp = 19.00μm
- ▼—— Column 134mmx7mmid; ODS-silica, dp = 18.13μm

Table 9.3 Summary of the characteristics of the various packed columns

Column Dimensions /min	Type of Particles	dp/μm [b]	Weight of Packing Material/g	V_m/ml	Surface Area As/m^2g^{-1}	Pore Volume $/cm^3g^{-1}$	Maximum Efficiency	ϕ_{AV}	Impedience E	Packing Technique
93x7id	'Raspberries' [a]	10.64	2.75	1.34	133.09	0.5071	h=2.8 at ν=3.5	929	7283	Upward slurry
134x7id	'Raspberries'	15.78	3.80	1.94	131.89	0.3576	h=3.6 at ν=4.7	677	8774	Upward slurry
247.7id	'Raspberries'	19.00	6.20	3.57	178.06	0.3872	h=3.2 at ν=3.6	578	5919	Balanced density
134x7id	Spherical	18.13	3.02	1.94	185.44	0.7996	h=3.0 at ν=6.3	904	8136	Balanced density

[a] Particles consisted of smaller particles fused together.

[b] Taken as the arithmetic mean diameter.

being disconnected. The 247mm x 7mm id column was packed using a balanced density slurry since this column was packed with larger particles (19μm). The material was slurried in a mixture of methyl iodide/IPA such that the particles remained in suspension. 0.01% w/v of sodium acetate was also added to help dissipate any electrokinetic charge that may be built up during the packing. The column was then packed in the same way as the other two columns.

9.4 Results

9.4.1 Column Testing

The columns were packed as described in Section 9.3, equilibrated with eluent and then tested to determine the efficiency. This was measured using MeOH/H_2O 60:40 v/v as the eluent and a test mixture containing acetone, phenol, p-cresol, 2,5-xylenol and anisole made up in the eluent.

The data obtained were plotted in the form of log h against log ν, and graphs produced for each column are shown in figure 9-3. These show that all of the columns were well-packed, having values of h between 2.8 and 3.6 at values of ν between 3.5 and 6.3. The columns therefore conform to the general idea that with analytical size samples there is a unique h-value for a unique ν-value which is independent of the particle size, dp. The characteristics of the various columns are summarized in table 9-3.

Table 9.4 Table of conditions and identification of figures

Description of Graph	Column/mm	ν	Acetone	Acetophenone	Methyl Benzoate	Comments
log h vs log	All columns	-	-	9.3	-	
log h vs log Absolute Load	93x7id	L,M,H[a]	9.4A	9.5A	9.6A	For 1 column at each flow rates
	134x7id	"	9.4B	9.5B	9.6B	
	247x7id	"	9.4C	9.5C	9.6C	
log vs log Absolute Load	All columns	L	9.7A	9.8A	9.9A	For each column at 1 flow rate
		M	9.7B	9.8B	9.9B	
		H	9.7C	9.8C	9.9C	
log h vs log ν at constant load	All columns	-	9.10A	9.10B	9.10C	At low and high sample loads
log h vs log throughput	All columns	L	9.11A	9.12A	9.13A	For each column at 1 flow rate
		M	9.11B	9.12B	9.13B	
		H	9.11C	9.12C	9.13C	
log h vs log throughput	93x7id	L,M,H	9.14A	9.15A	9.16A	For 1 column at each flow rate
	134x7id	"	9.14B	9.15B	9.16B	
	247x7id	"	9.14C	9.15C	9.16C	
log N vs log Specific Load	93x7id	L,M.H		9.17A		For 1 column at each flow rate
	134x7id	"	-	9.17B	-	
	247x7id	"		9.17C		
k'_{REL} vs log Specific Load	93x7id	L,M,H	9.18	9.18	9.18	For 1 column and each solute at each flow rate
	247x7id	"	9.19	9.19	9.19	
log N vs log Specific Load	All columns	L	9.20A	9.20B	9.20C	For columns of similar efficiency

'a' : Low, Medium and High flow rates respectively (See Table 9.2)

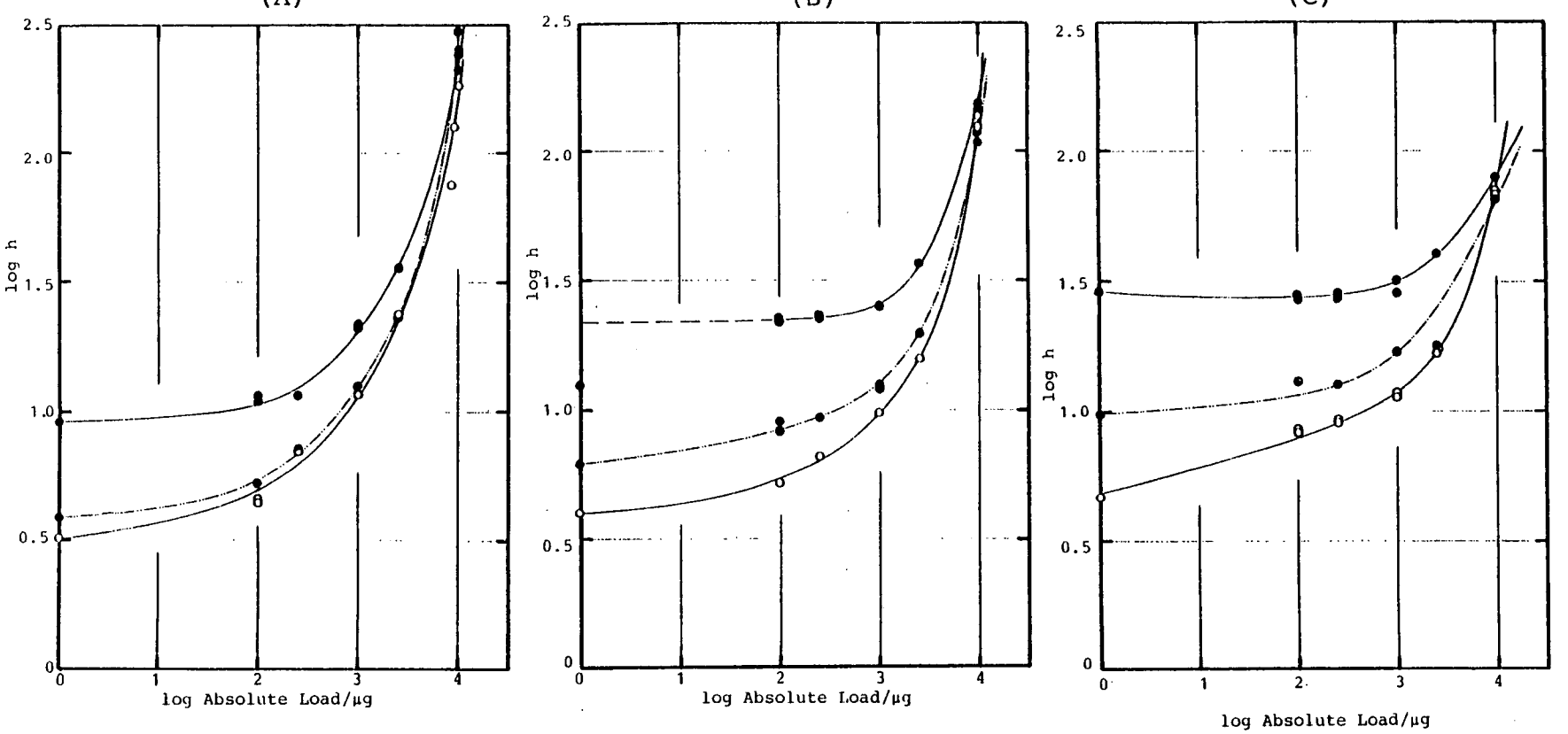

Figure 9.4 Log h against log Absolute Load for acetone at low, medium and high eluent flow rates using columns (A) 93mmx7mm id, (B) 134mmx7mm id and (C) 247mmx7mm id.

○——, ●—··, ●—— represent $^{u}/_{dp}$ ratios of 0.07, 0.21 and 0.59 respectively.

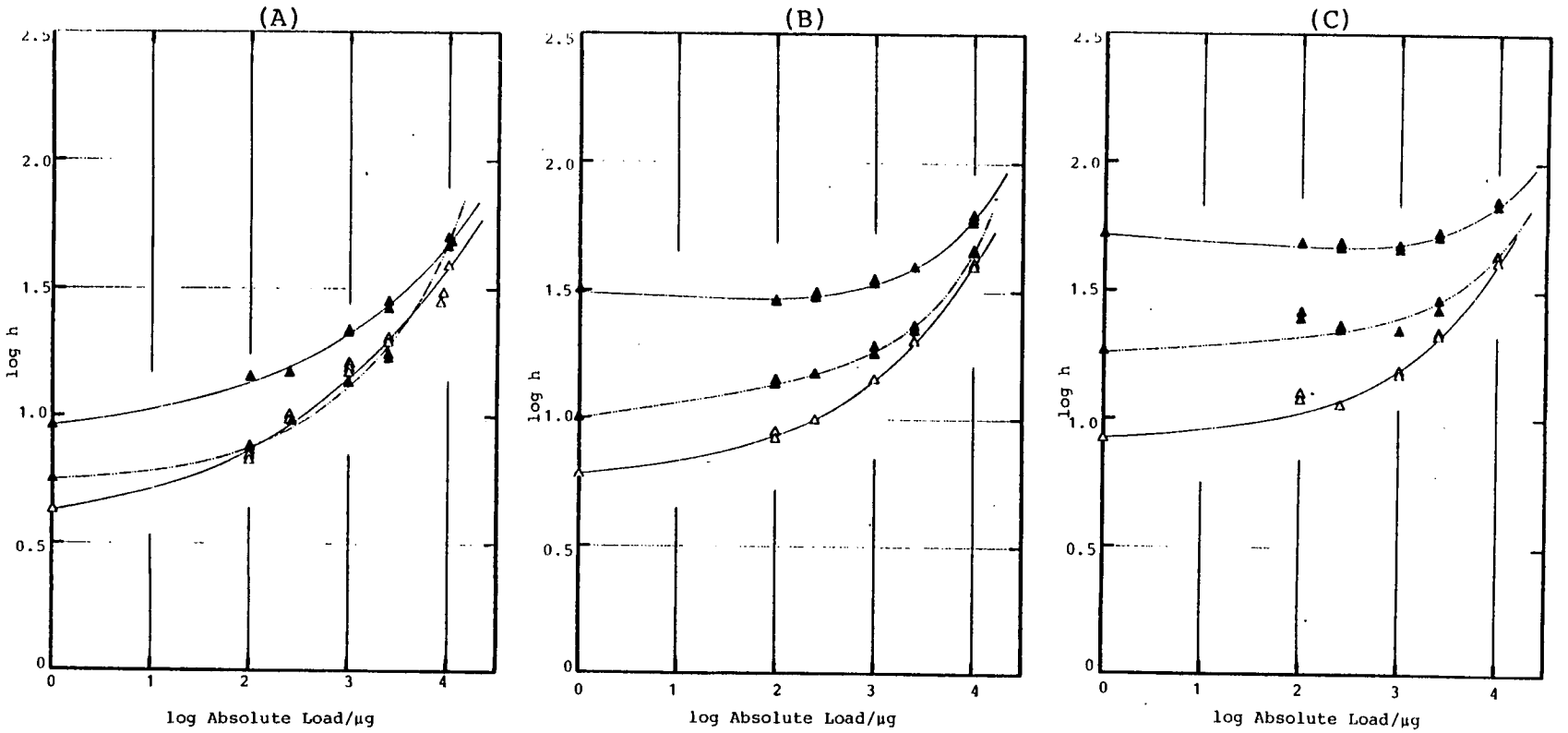

Figure 9.5 Log h against log Absolute Load for acetophenone at low, medium and high eluent flow rates using columns (A) 93mmx7mm id, (B) 134mmx7mm id, and (C) 247mmx7mm id.

△— , ▲··· , ▲— represent $^{u}/_{dp}$ ratios of 0.07, 0.21 and 0.59 respectively.

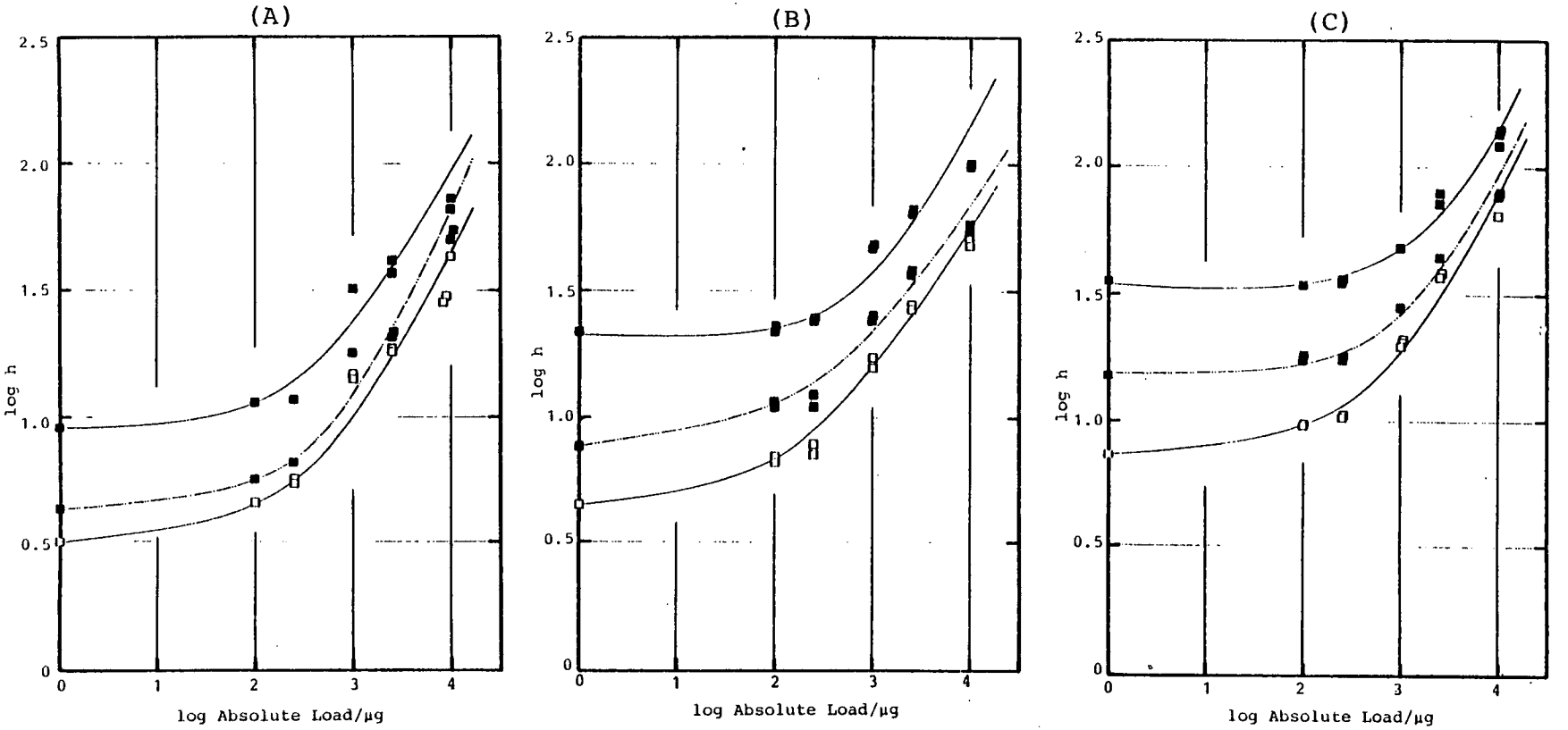

Figure 9.6 Log h against log Absolute Load for methyl benzoate at low, medium and high eluent flow rates using columns (A) 93mmx7mm id, (B) 134mmx7mm id and (C) 247mmx7mm id.

□—— , ■—·· , ■—— represent $^{u}/_{dp}$ ratios of 0.07, 0.21 and 0.59 respectively.

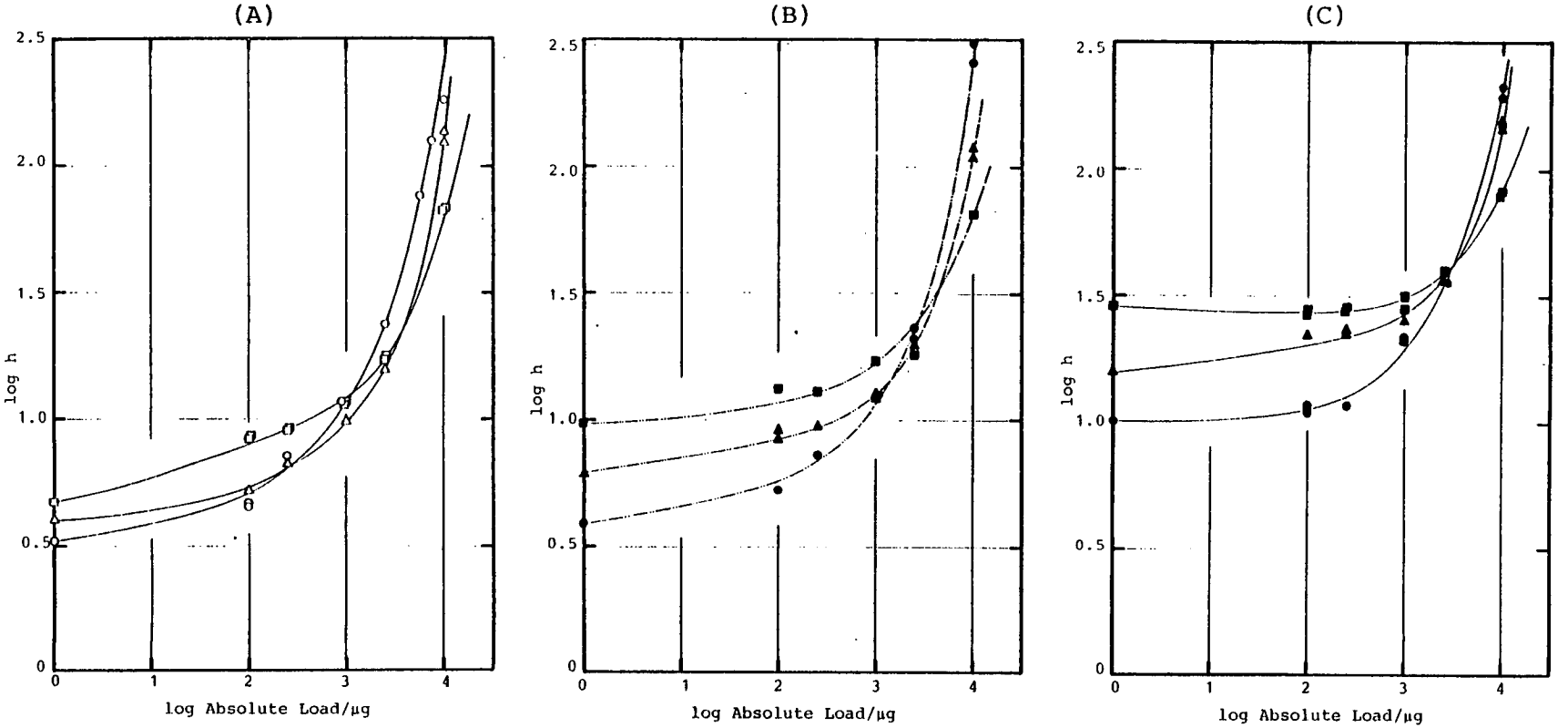

Figure 9.7 Log h against log Absolute Load for acetone using different columns at different eluent flow rates.

(A) ○—— , △—— , □—— represent columns 93mmx7mm id, 134mmx7mm id and 247mmx7mm id respectively at $^{u}/_{dp}$ = 0.07

(B) ●—·· , ▲—·· , ■—·· represent columns 93mmx7mm id, 134mmx7mm id and 247mmx7mm id respectively at $^{u}/_{dp}$ = 0.21

(C) ●—— , ▲—— , ■—— represent columns 93mmx7mm id, 134mmx7mm id and 247mmx7mm id respectively at $^{u}/_{dp}$ = 0.59

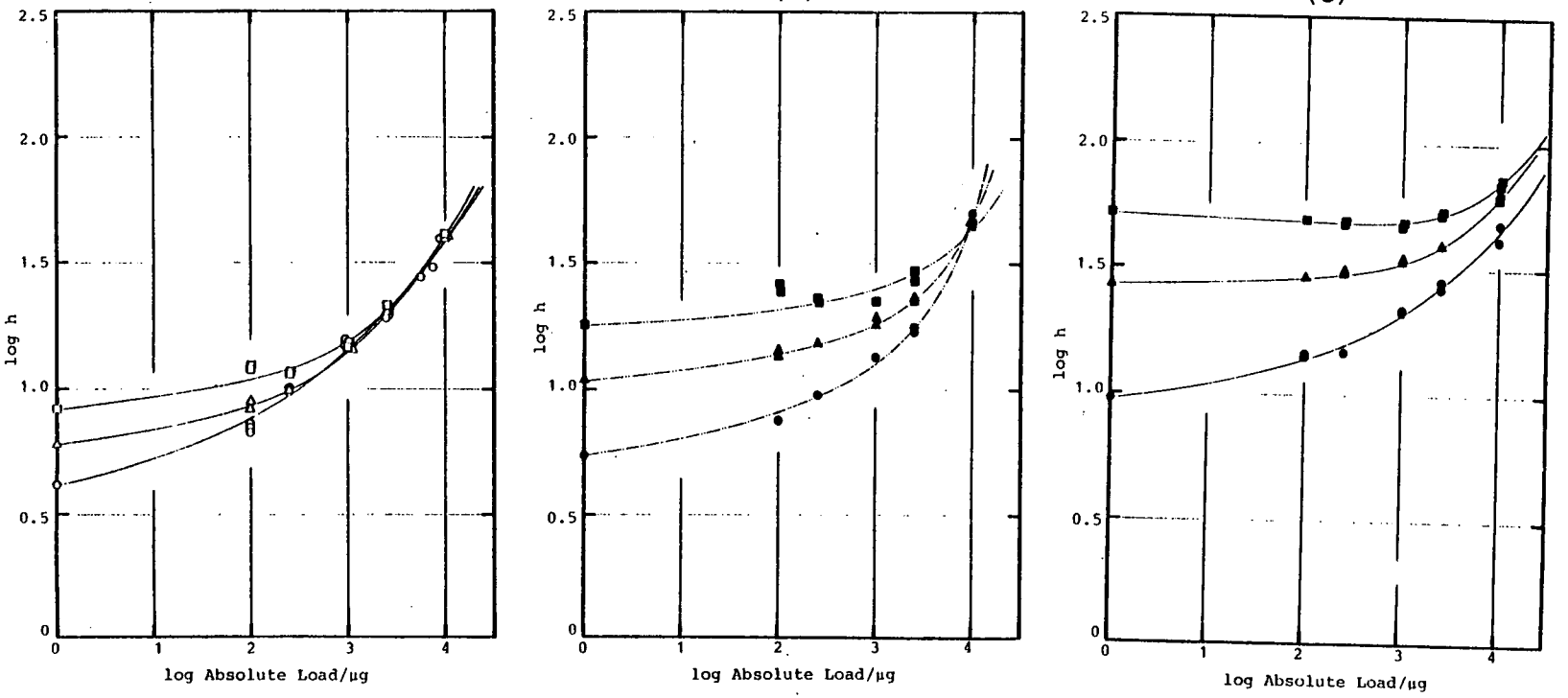

Figure 9.8 Log h against log Absolute Load for acetophenone using different columns at different eluent flow rates.

(A) ○—— , △—— , □—— represent columns 93mmx7mm id, 134mmx7mm id and 247mmx7mm id respectively at $u/dp = 0.07$

(B) ●—·· , ▲—·· , ■—·· represent columns 93mmx7mm id, 134mmx7mm id and 247mmx7mm id respectively at $u/dp = 0.21$

(C) ●—— , ▲—— , ■—— represent columns 93mmx7mm id, 134mmx7mm id and 247mmx7mm id respectively at $u/dp = 0.59$

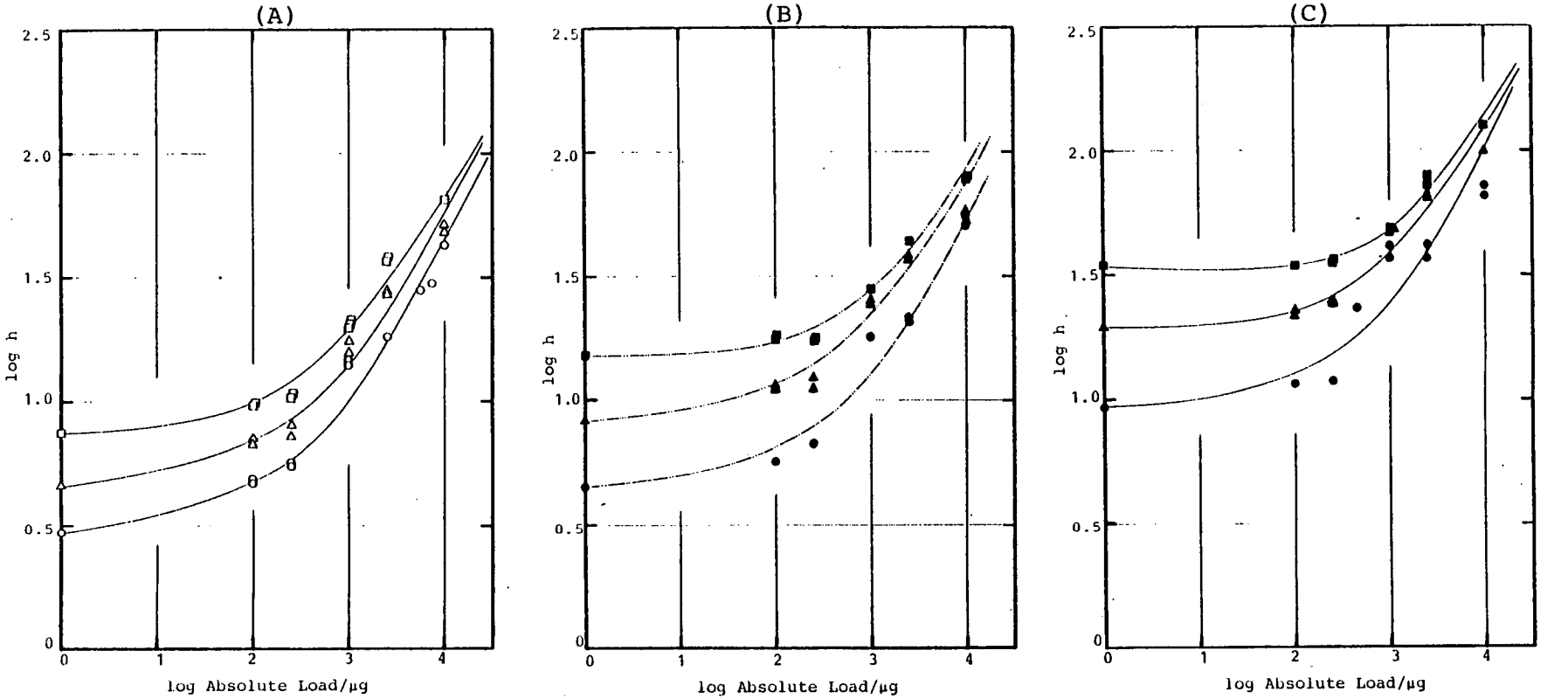

Figure 9.9 Log h against log Absolute for methyl benzoate using different columns and different columns and different eluent flow rates.

(A) ○— , △— , □— represent columns 93mmx7mm id, 134mmx7mm id and 247mmx7mm id respectively at $^{u}/_{dp}$ = 0.07

(B) ●··· , ▲··· , ■··· represent columns 93mmx7mm id, 134mmx7mm id and 247mmx7mm id respectively at $^{u}/_{dp}$ = 0.21

(C) ●— , ▲— , ■— represent columns 93mmx7mm id, 134mmx7mm id and 247mmx7mm id respectively at $^{u}/_{dp}$ = 0.59

9.4.2 Loading Experiments

Following the results obtained from the preparative columns as described in Chapter 8, which suggest that it is best to use a 1% w/v solution, the sample concentration used throughout the experiments on the isochronic columns was 1% w/v.

The results obtained can be presented in a number of ways to illustrate the various aspects of increasing the sample load. Table 9-4 shows the conditions and identification of the figures which illustrate the results obtained. The data presented in these figures is complex and can be looked at in several different ways.

9.4.2.1 The Effect of Sample Load On Column Efficiency

The results plotted as log h against log Absolute Load for each solute with each column at different flow rates are shown in figures 9-4 to 9-6 inclusive while figures 9-7 to 9-9 inclusive show the results plotted as log h against log Absolute Load for each solute at a particular flow rate using the different columns. All of these graphs show that at low sample loads and low eluent flow rates column efficiency is high. Under such conditions, the peak broadening is due to kinetic factors.

As the load is increased, the efficiency starts to drop as peak broadening is now the result of thermodynamic as well as kinetic factors. At high sample loads, the column efficiency decreases considerably as the effects of sample overloading, ie. the thermodynamic factors, overshadow the kinetic dispersion. This effect of overloading is most noticeable for acetone using the shortest column.

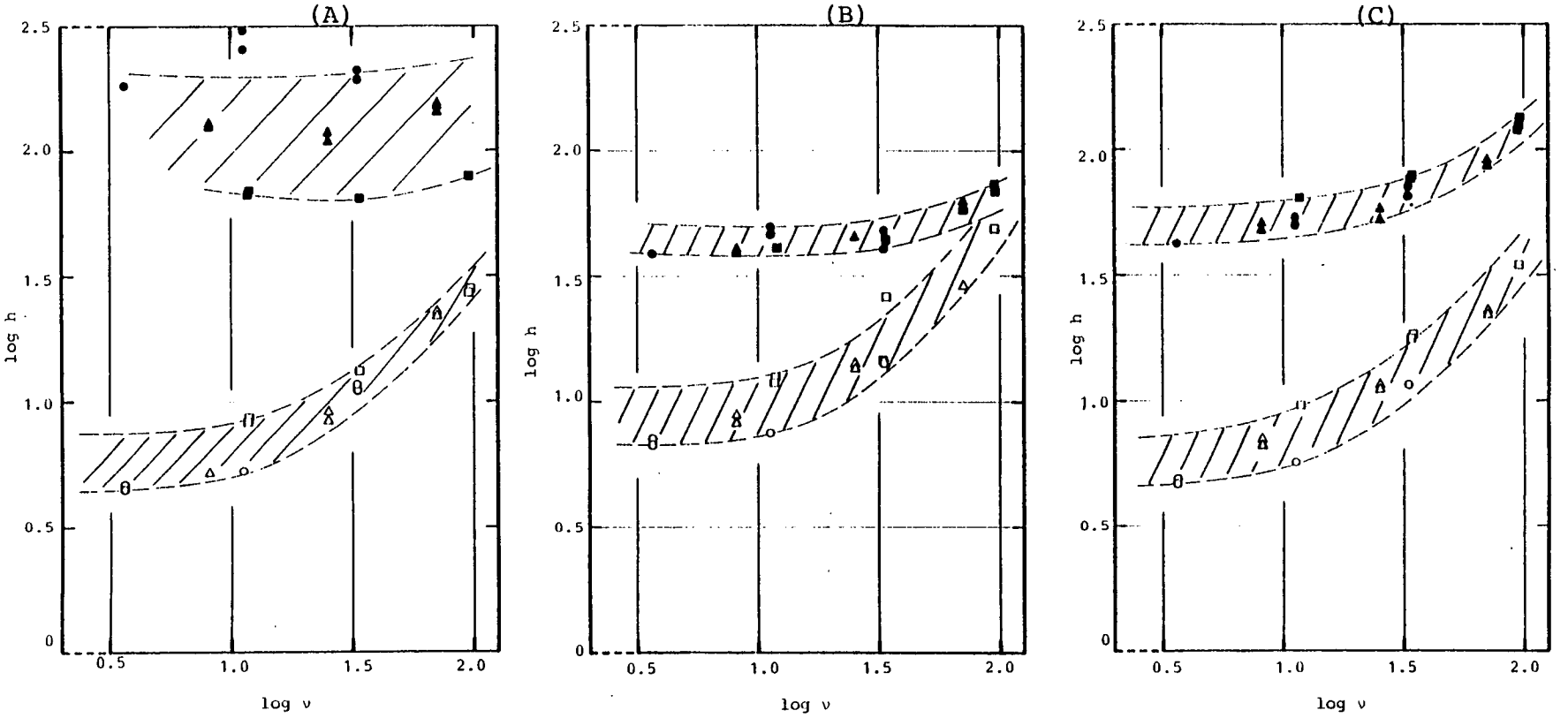

Figure 9.10 Log h against log ν at low and high sample leads for (A) acetone and (B) acetophenone and (C) methyl benzoate using different columns.

○—— , △—— , □—— represents a load of $10^2\mu$g using columns 93mmx7mm id, 134mmx7mm id, and 247mmx7mm id respectively

●—— , ▲—— , ■—— represents a load of $10^4\mu$g using columns 93mmx7mm id, 134mmx7mm id, and 247mmx7mm id respectively

In general, there is still some advantage at high sample loads in operating at low reduced velocities but it takes a longer time to collect a particular amount of sample, ie. throughput is less at low reduced velocities, than if higher reduced velocities are used, as we shall see later from figures 9-14 to 9-16 inclusive.

9.4.2.2 Difference In Efficiency Between Short And Long Columns

In general, as we go from short to long columns we can see from figures 9-7 to 9-9 inclusive that the efficiency for a given low load is higher for the shorter column since, for a given $U/_{dp}$ ratio, the reduced velocity is much lower for the shorter column and therefore it is operating closer to the optimum conditions. However, at high sample loads, the kinetic dispersion effects become insignificant as the column is now operating in the overload region and there appears, in general, to be little or no difference between the length of the isochronic column used. However, for acetone, which is only slightly retained, it does appear that the longer columns are better for high loads at all eluent flow rates. For the more retained solutes there is no evidence that it is better to work with longer columns at low flow rates while at higher flow rates there appears a slight advantage in using shorter columns.

Figure 9-10 illustrates more clearly the efficiencies produced by the various columns with respect to the reduced eluent velocity and sample load. For lower loads (eg. $10^2\mu g$) the graphs show that, for each solute, it is best to use the shortest column when operating at low reduced velocities. For

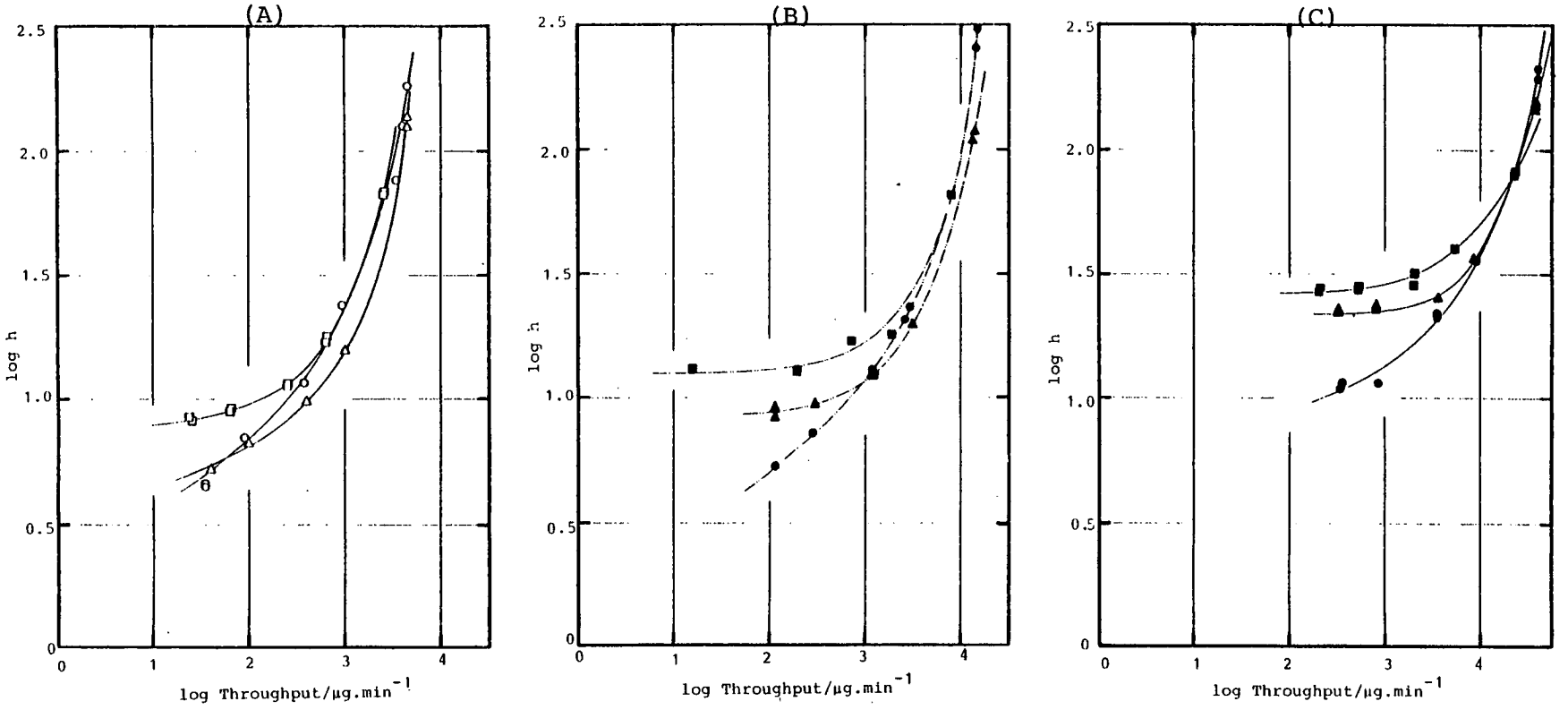

Figure 9.11 Log h against log Throughput (absolute load per unit time) for acetone using different columns at different eluent flow rates.

○—— , △—— , □—— represent columns 93mmx7mm id, 134mmx7mm id and 247mmx7mm id respectively at $u/dp = 0.07$

●—·· , ▲—·· , ■—·· represent columns 93mmx7mm id, 134mmx7mm id and 247mmx7mm id respectively at $u/dp = 0.21$

●—— , ▲—— , ■—— represent columns 93mmx7mm id, 134mmx7mm id and 247mmx7mm id respectively at $u/dp = 0.59$

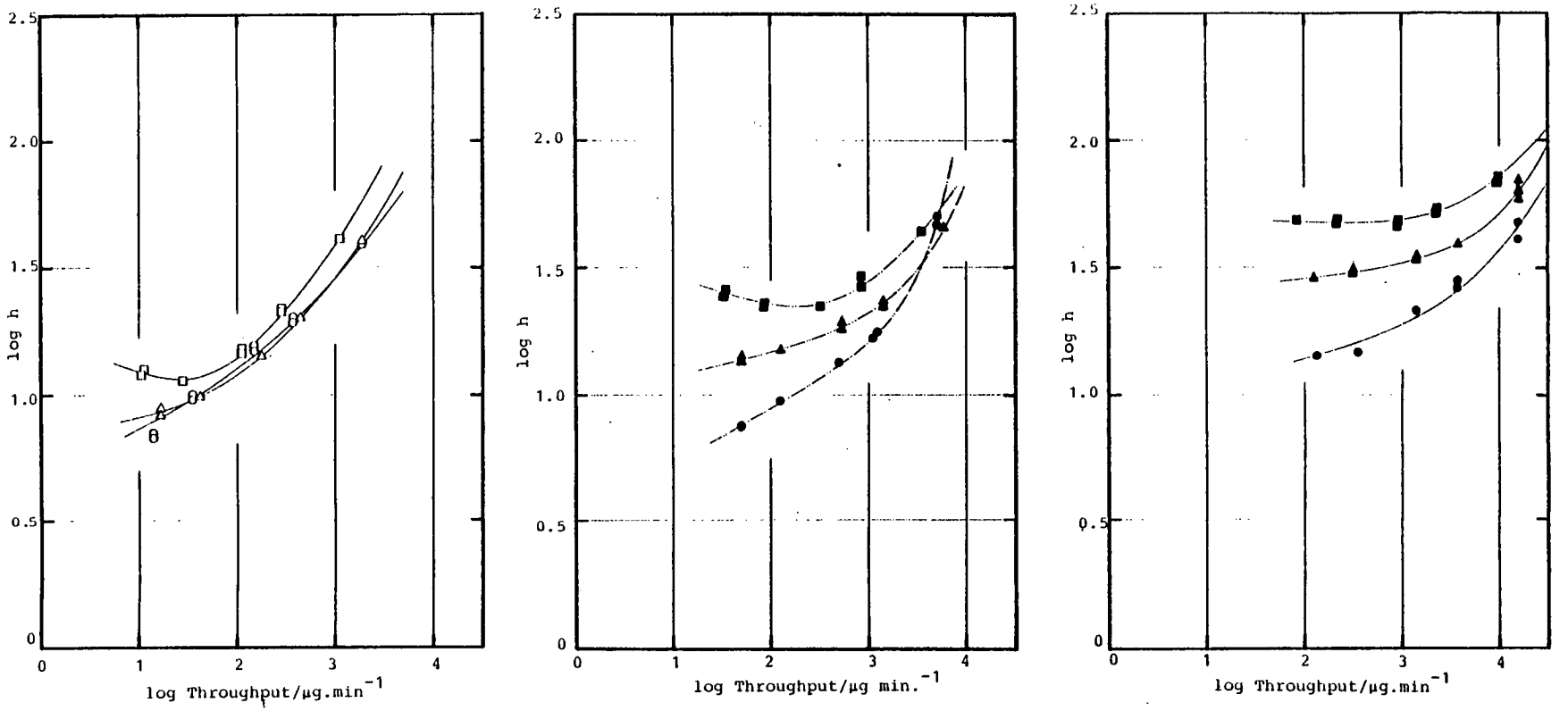

Figure 9.12 Log h against log Throughput (absolute load per unit time) for acetophenone using different columns at different eluent flow rates.

○—— , △—— , □—— represent columns 93mmx7mm id, 134mmx7mm id and 247mmx7mm id respectively at $^{u}/dp$ = 0.07

●···· , ▲···· , ■···· represent columns 93mmx7mm id, 134mmx7mm id and 247mmx7mm id respectively at $^{u}/dp$ = 0.21

●—— , ▲—— , ■—— represent columns 93mmx7mm id, 134mmx7mm id and 247mmx7mm id respectively at $^{u}/dp$ = 0.59

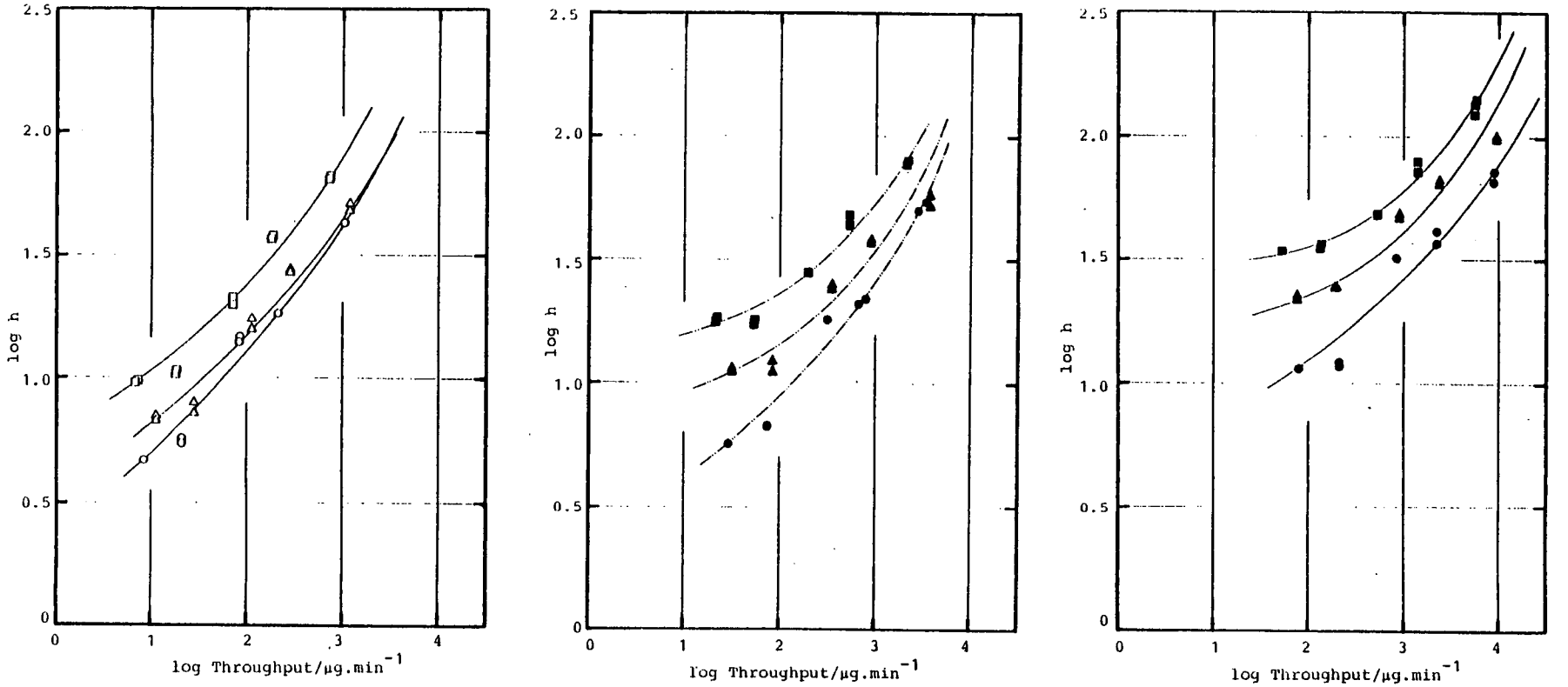

Figure 9.13 Log h against log Throughput for methyl benzoate using different columns at different eluent flow rates.

○— , △— , □— represent columns 93mmx7mm id, 134mmx7mm id and 247mmx7mm id respectively at $^{u}/dp$ = 0.07

●··· , ▲··· , ■··· represent columns 93mmx7mm id, 134mmx7mm id and 247mmx7mm id respectively at $^{u}/dp$ = 0.21

●— , ▲— , ■— represent columns 93mmx7mm id, 134mmx7mm id and 247mmx7mm id respectively at $^{u}/dp$ = 0.59

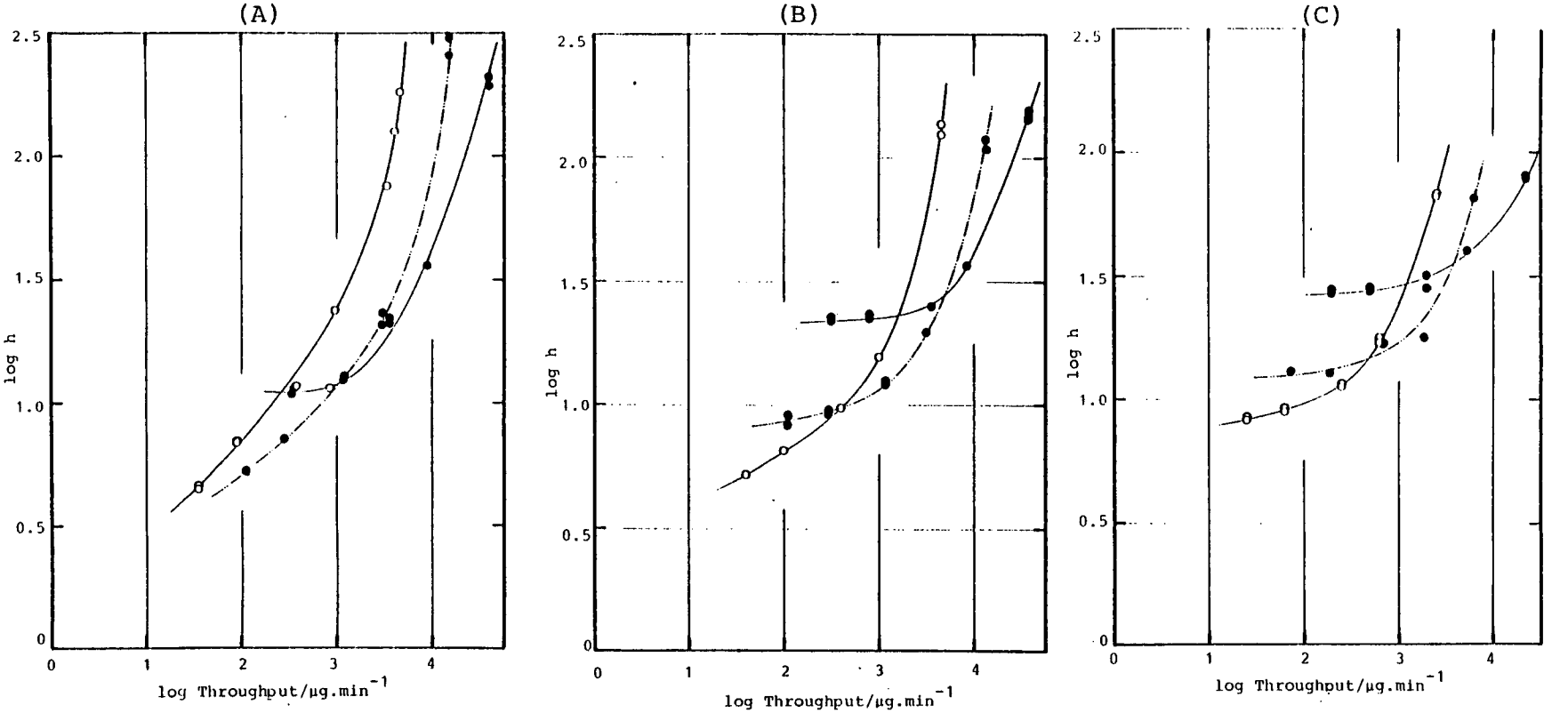

Figure 9.14 Log h against log Throughput for acetone at low, medium and high eluent flow using columns (A) 93mmx7mm id, (B) 134mmx7mm id and (C) 247mmx7mm id.
○—— , ●—·· , ●—— represent u/dp ratios of 0.07, 0.21 and 0.59 respectively.

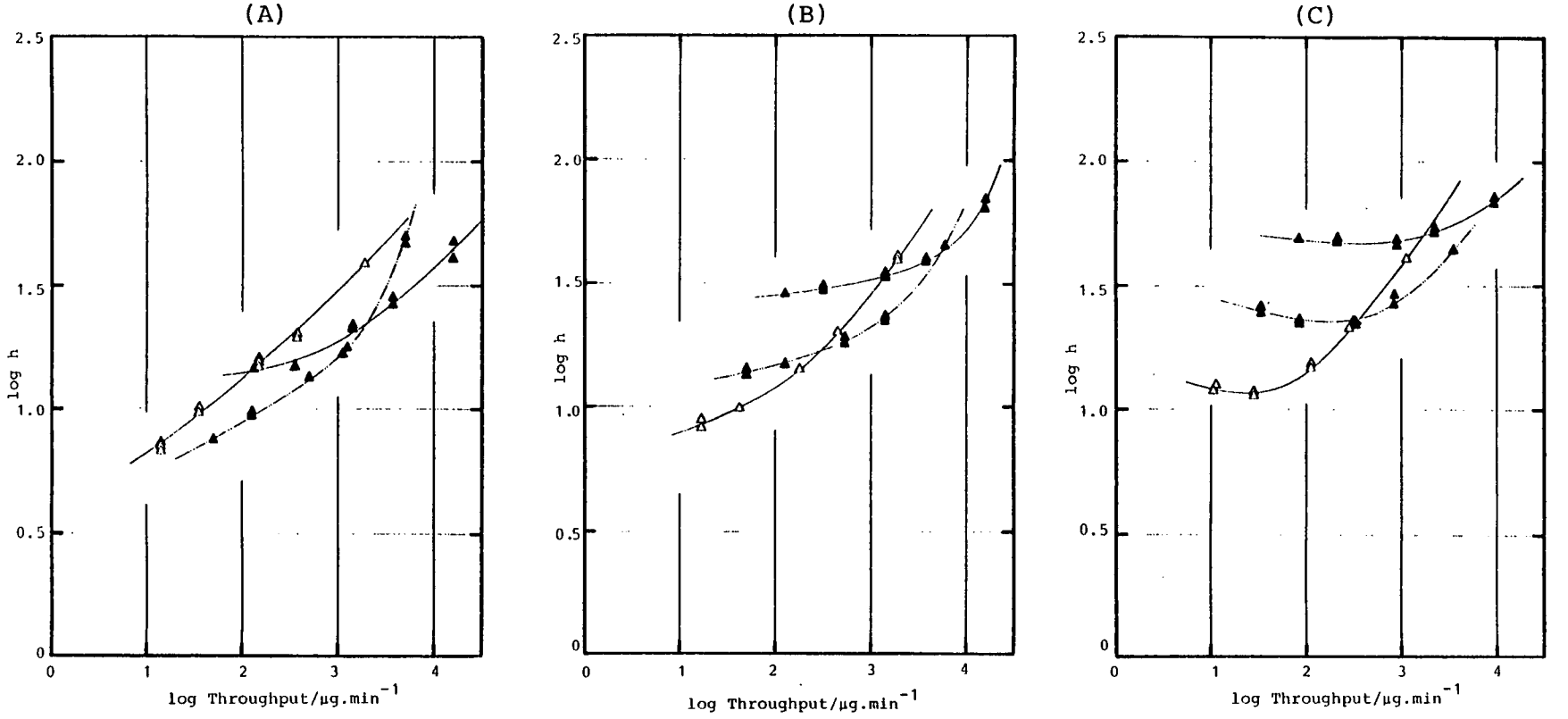

Figure 9.15 Log h against log Throughput for acetophenone at low, medium and high eluent flow rates using columns (A) 93mmx7mm id, (B) 134mmx7mm id and (C) 247mmx7mm id.

△——, ▲—··—, ▲—— represent $^{u}/_{dp}$ ratios of 0.07, 0.21 and 0.59 respectively.

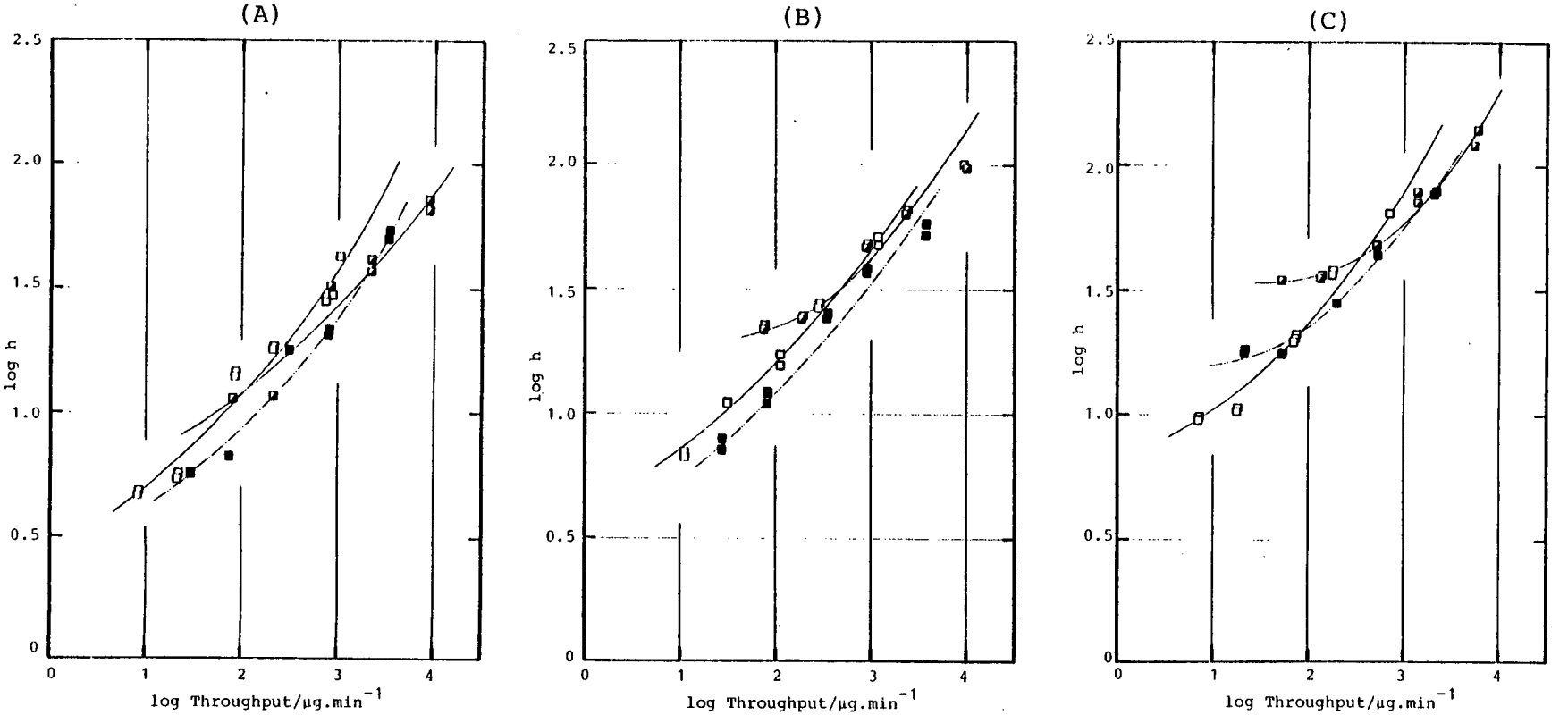

Figure 9.16 Log h against log Throughput for methyl benzoate at low, medium and high eluent flow rates using columns (A) 93mmx7mm id, (B) 134mmx7mm id and (C) 247mmx7mm id.

□—— , ■—··· , ◪—— represent $^{u}/_{dp}$ ratios of 0.07, 0.21 and 0.59 respectively.

the more retained solutes at high reduced velocities it does appear that the optimum column length is increasing in that the second longest column (ℓ = 134mm) is now the optimum column while for acetone it is best to use the longest column (ℓ = 247mm). For higher sample loads (eg. 10^4μg) it appears that, for acetone, the longest column is best for all reduced velocities. However, for acetophenone and methyl benzoate there appears to be little difference in the columns used at high reduced velocities while the shorter columns still appear to be slightly better at the low reduced velocities. This is not exactly what one might have expected as in general there appears to be no advantage in using longer columns packed with larger particles for separations in this load range.

9.4.2.3 The Effect Of Flow Rate And Column Length On Throughput And Column Efficiency

For a particular required column efficiency, it can be seen from figures 9-11 to 9-16 inclusive that if a high column efficiency is required then, for acetone and acetophenone, the best throughput is in general achieved using the short column although if a high column efficiency is not required then there is little difference in the throughput obtained using the different columns. However, for methyl benzoate, the most retained solute, it appears that the short column is best all round.

In general, as the eluent flow rate is increased, then it becomes more noticeable, particularly when high column efficiencies are required, that the short column produces the best throughput, although for acetone there is little difference obtained by each column when low column efficiencies suffice.

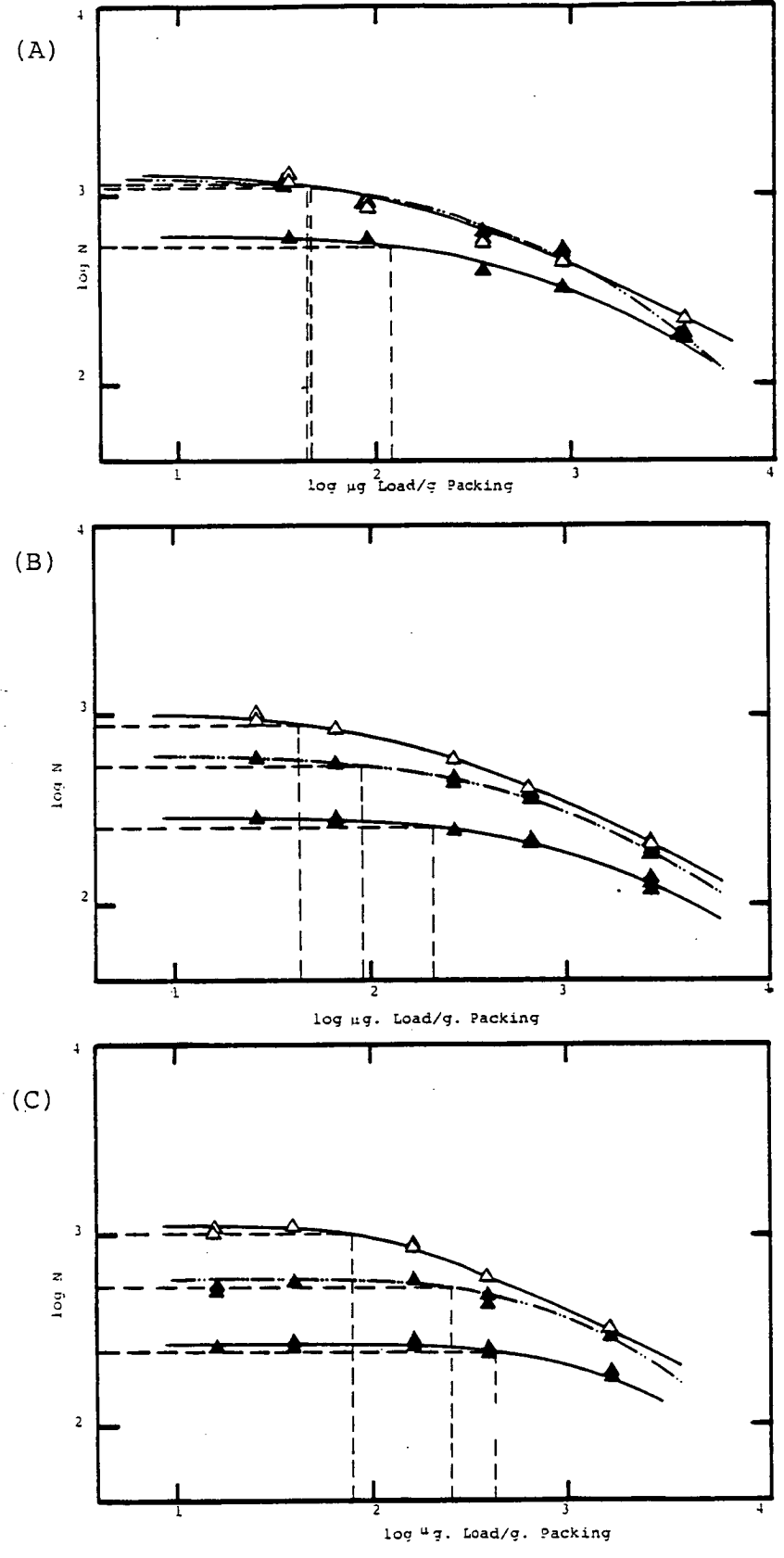

Figure 9.17 Column plate number, N, versus Specific Load for acetophenone at different eluent flow rates using columns (A) 93mmx7mm id, (B) 134mmx7mm id and (C) 247mmx7mm id.

△—— , ▲—··· , ▲—— represent u/d_p ratios of 0.07, 0.21 and 0.59.

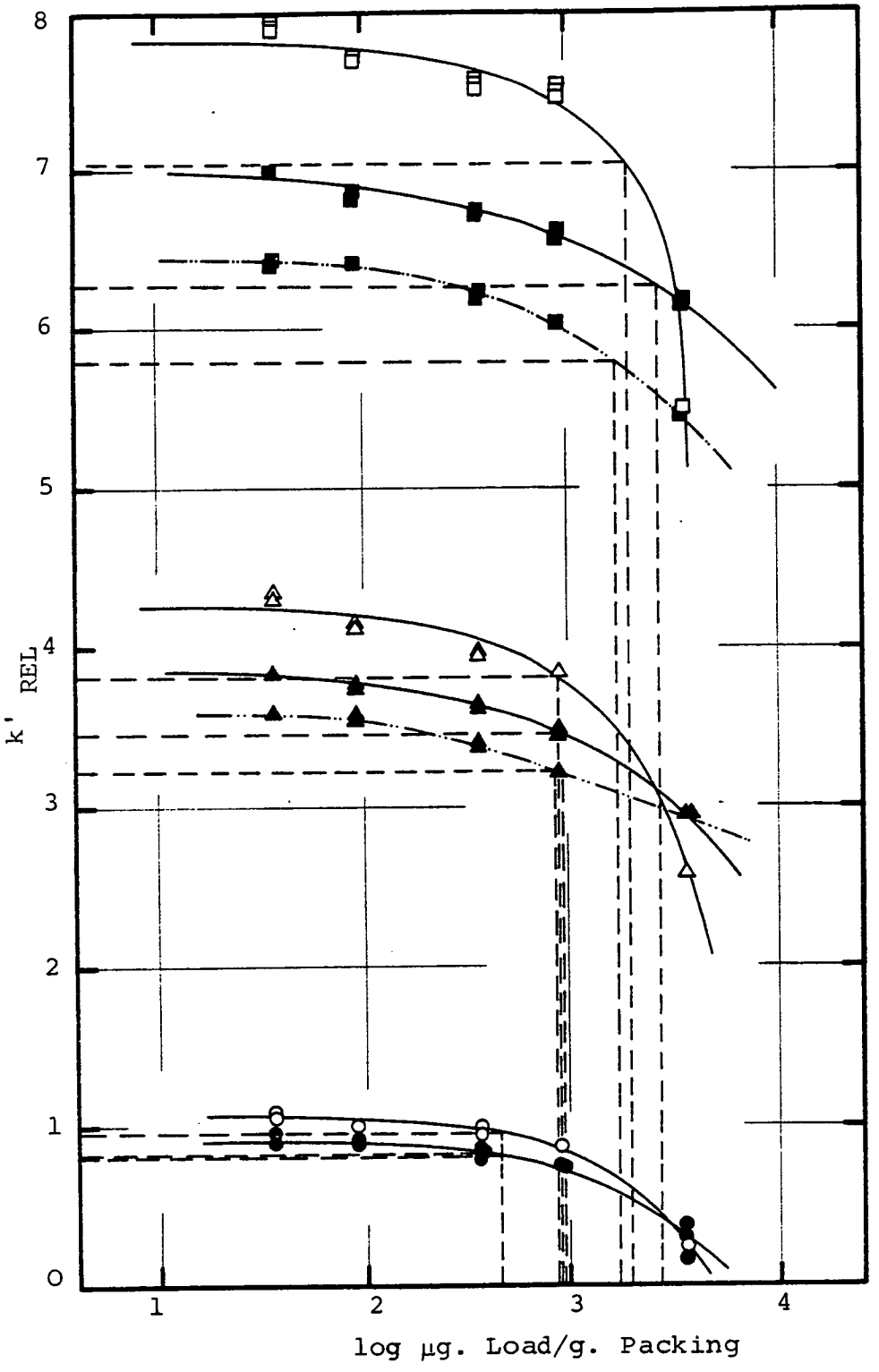

Figure 9.18 Relative phase capacity ratio, k'_{REL}, versus Specific Load for 3 solutes at 3 eluent flow rates using column 93mm x 7mm id.

○—.△—.□— represent acetone, acetophenone and methyl benzoate respectively.

○—.●—··.●— represent $u/_{dp}$ ratios of 0.07, 0.21 and 0.59 respectively.

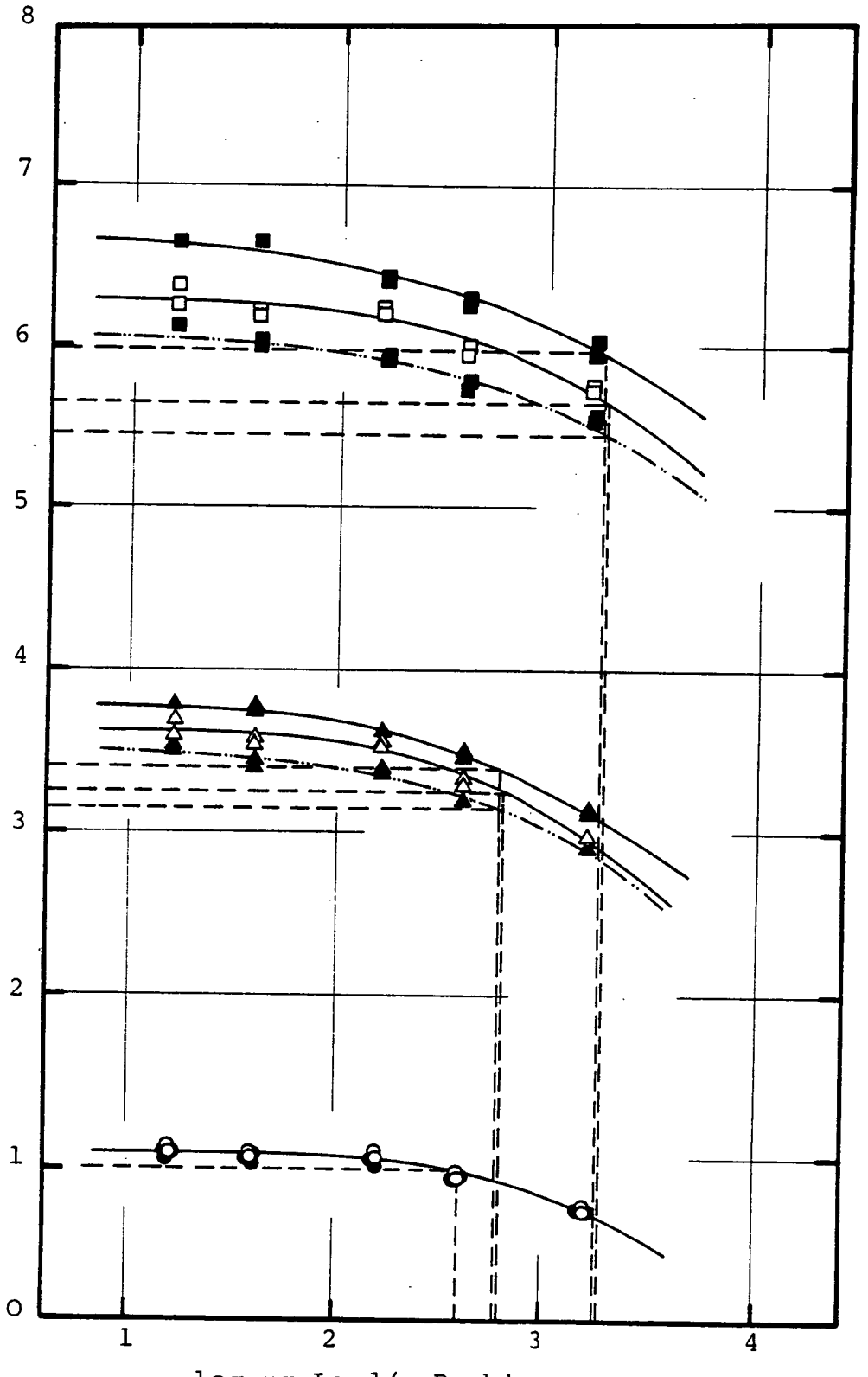

Figure 9.19 Relative phase capacity ratio, k'_{REL}, versus Specific Load for 3 solutes at 3 eluent flow rates for column 247mmx7mm id.

○—, △—, □— represent acetone, acetophenone and methyl benzoate respectively

○—, ●—, ●— represent u/dp ratios of 0.07, 0.21 and 0.59 respectively

Figures 9-14 to 9-16 inclusive show that in general, for columns operating at reasonably high efficiencies, throughput can be increased by increasing the flow rate to a certain optimum value, while increasing the flow rate beyond this value results in a decrease in throughput.

9.4.2.4 The Effect Of Column Efficiency And Flow Rate On The Linear Sample Capacity, $\theta_{0.1}$

Using the decrease in N as the basis for the definition of the linear sample capacity, ie. $\theta^{N}_{0.1}$, it can be seen from graph 9-17 that the loadability appears to increase with increasing eluent flow rate ie. with decreasing plate number, N. This observation was also made by De Jong[1] who found that the curves produced for a column operating at different eluent flow rates converged to form a borderline, and indeed the curves produced in figure 9-17 are also tending to converge.

However, if we consider the same data plotted in terms of the relative phase capacity ratio, k'_{REL}, against log specific load then from figures 9-18 and 9-19 it appears that in general there is little or no difference in the loadability with increasing eluent flow rate nor therefore with decreasing plate number.

The difference in the results obtained is due to the fact that k' is purely a thermodynamic effect while N is a combination of both thermodynamic and kinetic effects and one would expect therefore that increasing the eluent velocity would influence $\theta^{N}_{0.1}$. The results also show that the column overload limit, as determined by the linear sample capacity, $\theta_{0.1}$, depends on how

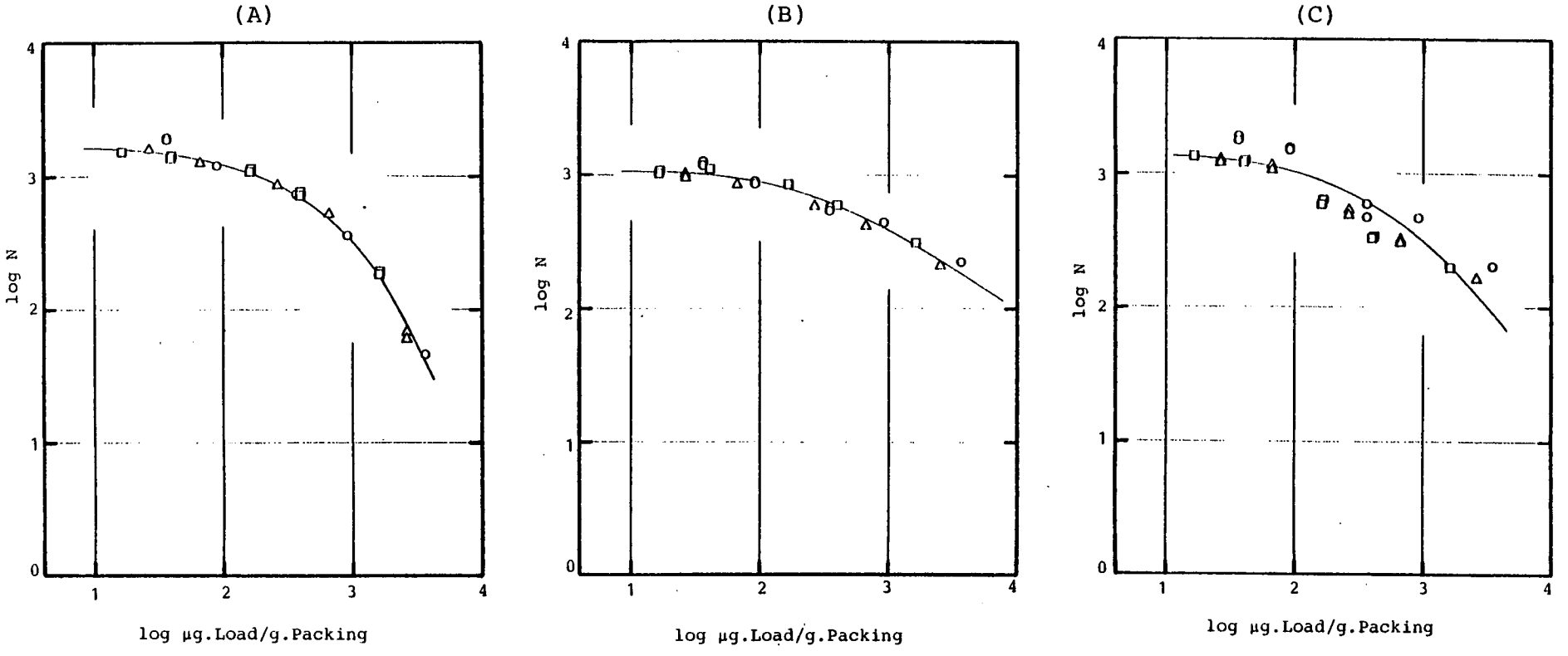

Figure 9.20 Log N against log Specific Load for columns of approximately equal column efficiency for (A) acetone (B) acetophenone and (C) methyl benzoate at low eluent flow rates ($u/dp = 0.07$).

○—— , △—— , □—— represent columns 93mmx7mm id, 134mmx7mm id and 247mmx7mm id respectively.

Table 9.5 k' values for the different solutes with the different columns

	Column Dimensions/mm		
	93x7id	134x7id	247x7id
Acetone	1.1	1.0	1.0
Acetophenone	4.3	3.5	3.6
Methyl Benzoate	7.8	6.0	6.3

it is defined ie. whether based on a reduction in k' or a reduction in N.

9.4.2.5 Linear Capacity Of Columns Of Equal Efficiency

For columns of different lengths packed with different particle sizes but producing similar numbers of plates, figure 9-20 shows that the data plotted as log N against log Specific Load for the different columns with a particular solute lie on the same curve. This shows that the best measure of overload is the specific load injected, ie. the weight of sample per weight of packing material. Furthermore, these curves which are produced for solutes with different k' values, as given in table 9.5, are nearly identical suggesting that there is some universal relationship between column efficiency and total sample load and that, to a first approximation, there is a particular specific load above which overload, with respect to plate number, occurs.

9.5 Summary of Conclusions

The results of these experiments show that, contrary to what was expected, it is better in terms of sample throughput to use the SHORT column packed with SMALL particles, as illustrated by figures 9-11 to 9-13 inclusive. This has the added advantage that the solute elutes from the column in a more concentrated form and thus makes recovery of the solute easier. From such graphs of log h against log throughput, then if a certain number of plates is required one can determine what the maximum throughput will be for that particular separation.

Increasing the sample throughput beyond this value, for example by increasing the flow rate as illustrated in figures 9-14 to 9-16 inclusive is possible only at the expense of resolution between adjacently eluting solutes.

If we compare the results obtained for the 247mmx7mm id. column plotted in terms of log h against log throughput with the corresponding results for the preparative-scale column, 250mm x 22mm id., (length of packed bed equal to 230mm) packed with the same material and operating at comparable eluent flow rates (see Chapter 8), we find that the maximum throughput obtainable for a particular number of plates is greater for the WIDER column.

The results also show that there is no advantage in using large particles, except for the cost and pressure requirements and practicallity of packing the columns, and that therefore IT IS BEST TO USE SHORT, WIDE COLUMNS PACKED WITH SMALL PARTICLES IN THE RANGE 10-20µm, providing that the k' of the sample is greater than, say, 1.

RESERVED CHAPTER

THE PREPARATION OF SILICA GEL PARTICLES

Reserved Chapter. The Preparation Of Silica Gel Particles

Table R.1 Typical Properties of Ludox Colloidal Silica

Properties	Grades HS-40%	HS-30%
Stabilising Counter ion	Sodium	Sodium
Particle Charge	Negative	Negative
Av.particle diameter, nm	12	12
Specific surface area, m^2/g	230	230
Silica (as SiO_2), wt.%	40	30
pH (25 C, 77 F)	9.7	9.8
Titratable alkali (as Na_2O),wt.%	0.41	0.32
SiO_2/Na_2O (by wt.)	95	95
Chlorides (as NaCl), wt.%	0.01	0.01
Sulphates (as Na_2SO_4),wt.%	0.05	0.04
Viscosity (25C,77F), CP, (mPa.S)	20	5
Wt.per gallon (25C,77F), lb	10.8	10.1
Specific Gravity (25C,77F)	1.31	1.21

THE PREPARATION OF SILICA GEL PARTICLES

R.1 Introduction

The method which was used involves the acidification of a silica sol which consists of discrete uniform spherical colloidal particles of silica dispersed in an alkaline medium of around pH 9. This gives the silica surface a negative charge and results in a stable colloidal suspension due to the mutual repulsion of the particles.

There are various silica sols which are commercially available, for example †Syton (from Monsanto) and †Ludox (from Du Pont). The silica sol used throughout this work was Ludox HS-30%, the characteristics of which, as given by Du Pont, are given in table R-1.

The sol can be gelled by the addition of acid to give a pH of between 5 and 6. At this pH, the colloidal suspension will collapse to produce silica particles, the gelling time of which is controlled by the amount of acid added. In practice, this was carried out by the addition of conc.HCl mixed with an equal volume of water.

In order to obtain spherical silica particles, the newly acidified silica sol was immediately emulsified in an immiscible non-polar liquid using a Silverson variable speed emulsifier in the presence of a surfactant. Throughout this work, the non-polar liquid used was 100-120 petroleum-ether and the surfactant used was Span 80. Surfactant molecules consist of

---

† Trade names

a long chain non-polar part and a polar part. The polar part of the surfactant is attracted to the charged silica particles as the droplets are formed during the emulsification and the non-polar part sticks outwards into the non-polar liquid, thus keeping the newly formed silica particles apart and in the organic phase until they harden. The size of the silica gel particles is determined by the viscosity of the silica sol and the speed of the rotor used in the emulsification. The time required for gelling to occur depends on the temperature, the pH and the concentration of both the sodium silicate solution and the acid, and has to be carefully controlled. In practice, tests were carried out each time prior to the preparation of the silica gel to determine the amount of acid required to achieve a given gelling time, which in this case was around 20 minutes.

R.2 Experimental

R.2.1 Quantities used for the Various Batches

Batches 1-9, 13

1)	600 ml	100-120 Petroleum-ether
	20 ml	Span 80
2)	200 ml	Ludox
	†5 ml	50% v/v HCl

Batch 12 Preparation of chipped material

1)	200 ml	Ludox
	†5.4 ml	50% v/v HCl
2)	600 ml	100-120 Petroleum-ether

Batches 14-23

1)	1.5 ℓ	100-120 Petroleum-ether
	40 ml	Span 80
2)	0.5 ℓ	Ludox
	†12.5 ml	50% v/v HCl

† The volume of acid required to produce a gelling time of 20 minutes was established each time.

R.2.2 Method used in the Preparation of Batches 1-4

All of the above batches were made using an electric drill which had a special rotor attachment, comprising of a 45 mm impeller and a 200 mm shaft. This had a fixed speed of 2,400 RPM.

The acid was added to the silica sol and a small sample removed to act as a control for the gelling process. The rest of the acidified silica sol was added to the already mixed petroleum-ether and span 80. This was immediately followed by vigorous mixing for 5 minutes with the electric rotor. Stirring of the emulsion was then continued using a magnetic stirrer until the control acidified silica sol had gelled. At this stage the temperature of the emulsion was raised to around 60°C and the mixture was left stirring for an hour. The emulsion was then poured into 1.5 ℓ acetone + 10% v/v H_2O. The silica was allowed to settle for about an hour before the supernatant was removed and discarded. The silica was then washed 6 times with acetone (500 ml) then twice with methylene chloride before drying in a rotary evaporator till free-flowing. The silica was then heated in a vacuum oven at 120°C for 24 hours to remove the physically adsorbed water and then heated in an oven at 450°C for 16 hours.

Rehydration was not carried out as the particles produced were mainly in the size range 64 μm - 149 μm as measured through an ordinary microscope and were therefore larger than was desired.

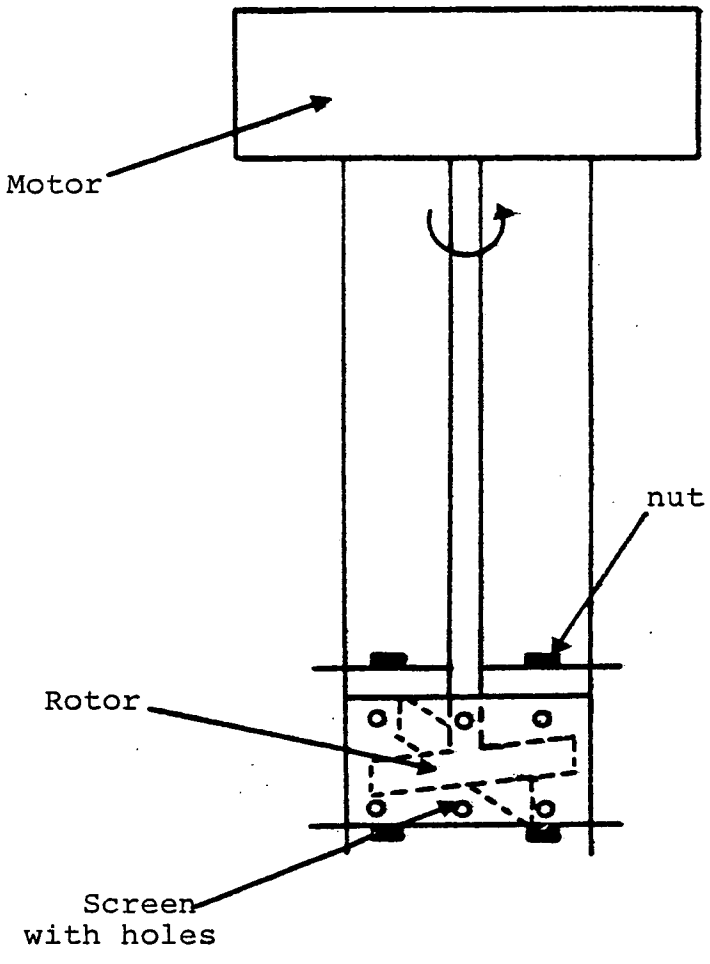

Figure R1. Schematic representation of the Silverson mixer emulsifier.

Table R-2 Conditions used for the preparation of the various batches of silica gel.

Batch	Duration of emulsification/ min	Screen	Rotor Clearance/ mm	Speed† Setting	Average RPM (where measured)
5	5	6x10mm id holes	0.32	90°	
6	"	2 mm id holes	"	"	
7	"	1 mm id holes	"	"	
8	"	square holes 3 mm across	"	"	
9	"	1 mm id holes	"	110°	
13	"	"	"	90°	
14	"	"	1.31	90°	4143
15	10	"	"	70°	3507
16	"	"	"	70°	
17	"	"	"	90°	
18	"	"	"	90°	
19	"	"	"	70°	
21	"	"	"	70°	
22	"	"	"	70°	
23	"	"	"	70°	

† Arbitrary scale, 0 → 180° (slow → fast)

R.2.3 Methods used in the Preparation of Batches 5-9 and 13-23

Batches 5-9 and 13-23 inclusive were made using a heavy duty Silverson mixer emulsifier, model number L2R (Silverson Machines Ltd., Chesham, Bucks) which is illustrated in figure R-1. This emulsifier has a variable speed setting and a series of different screen attachments. The stainless steel rotor has a 200 mm shaft and a 45 mm impeller.

A number of different screens were examined to determine the particle size ranges which each produced (Batches 5-8) and the results of these experiments are given in section R3.

For batches 14-23, the rotor head was machined to give a greater clearance between the rotor and the screen in an attempt to produce larger particles and again the results are given in section R3.

The rotor speed was measured at random using a Digital Phototach (Power Instruments). Unfortunately this broke down after being used for batch 16 and the average RPM was not measured for later batches.

The method used in the preparation of batches 9,13-23 was similar to that used in the preparation of batches 1-4, and the conditions which were used for the various batches are summarized in table R-2. The silica sol and the petroleum-ether/Span 80 mixture were heated in a water bath to 32°C. The sol was then acidified by the addition of 50% v/v HCl and, after removal of a small control sample, was added to the petroleum-ether/span mixture in a plastic beaker. This was then emulsified using the Silverson mixer emulsifier using conditions

as laid out in table R-2.

The emulsion was then transferred to another water bath set at 60°C and stirred with a Gallenkamp Variable Speed Stirrer set at speed 3 until the temperature of the emulsion reached 60°C and the control sample had gone brittle-hard. This took approximately 1 hour.

The next stage varied depending on whether the silica gel was to be dried using (a) a rotary evaporator, or (b) a spray dryer.

(a) Rotary evaporator

For batches 5-13, the emulsion was allowed to cool slightly before being poured onto 1.5 ℓ acetone containing 10% v/v water. The silica was then allowed to settle and the supernatant removed before washing the silica gel 6 times with acetone (500 ml) and twice with methylene chloride. The silica was then dried in a rotary evaporator till free-flowing before being dried in a vacuum oven at 120°C for 24 hours followed by a further 16 hours at 450°C. The batches were then hydrated by boiling in distilled water containing 0.01% v/v of 50% v/v HCl for 2 hours taking care to keep the silica dispersed in the water. After settling, the water was removed and the silica washed twice with acetone (500 ml) and then twice with methylene dichloride (500 ml) before being dried on a rotary evaporator. The silica gel was then fractionated as described in chapter 7.

(b) Spray Drier

For batches 14-23, the emulsion was removed from the 60°C water bath and added to an equal volume of 10% acetic acid solution. The supernatant formed on settling was removed and

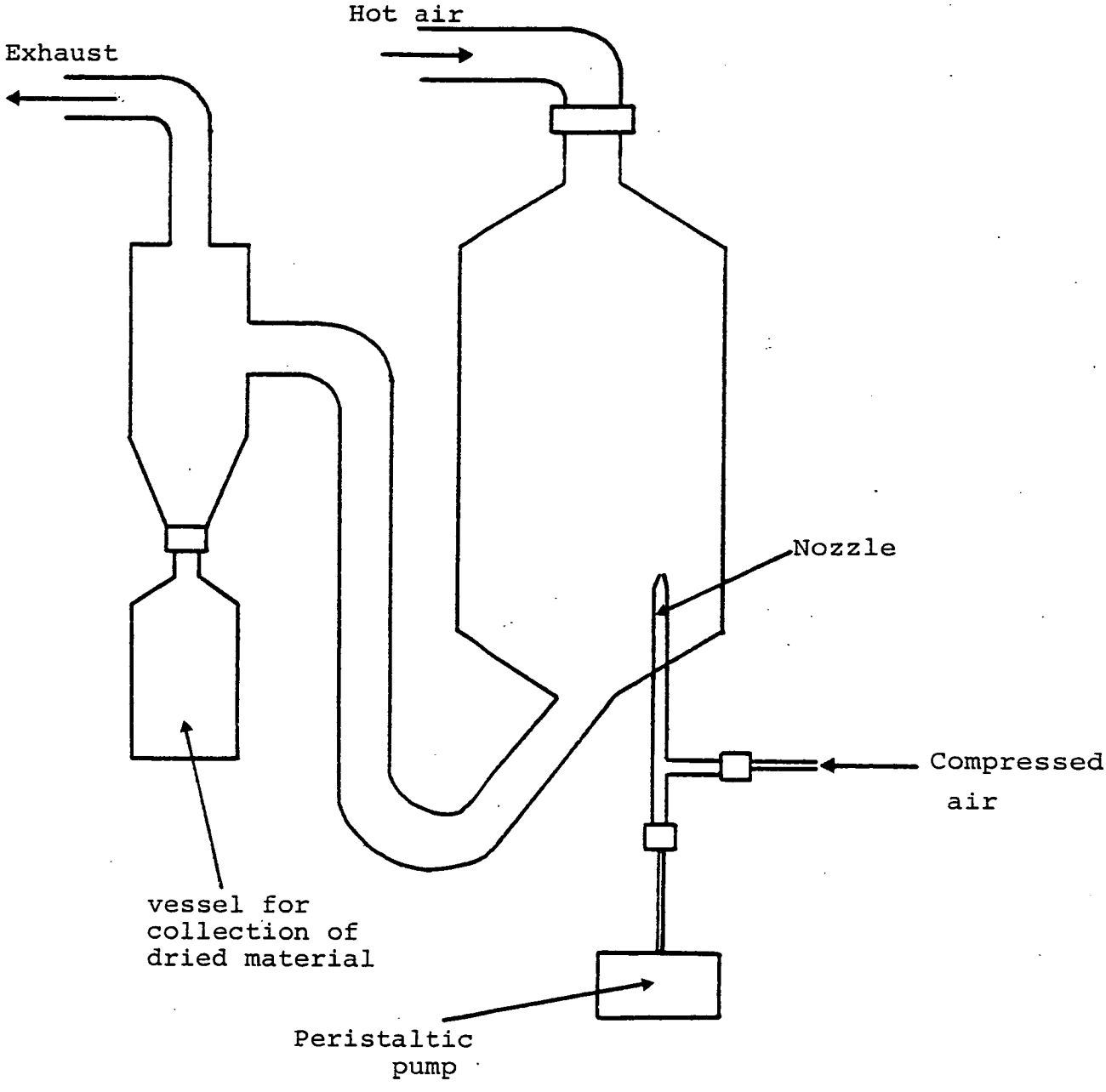

Figure R.2 Schematic representation of the spray drier.

the silica was washed thoroughly with distilled water until the smell of acetic acid had disappeared and no "debris" was left floating in or on the water. This took around eight x 1 litre H_2O washings. The silica was then resuspended in distilled water (1:3 v/v) and was then dried using a spray drier, before being fired at 450°C for 16 hours as before.

The silica was then hydrated by boiling in distilled water containing 0.01% v/v of 50% v/v HCl for 2 hours, keeping it in suspension by means of a Gallenkamp variable speed stirrer (set at 3).

The spray drier which was used (Lab Plant Ltd., Huddersfield, England) dries the silica gel particles from a suspension in water, the particles being kept in suspension using a magnetic stirrer. A diagram of the apparatus is shown in figure R-2.

The jet with the largest nozzle (0.5mm) was used and the silica suspension was pumped through using a peristaltic pump at the rate of 4 ml/min.

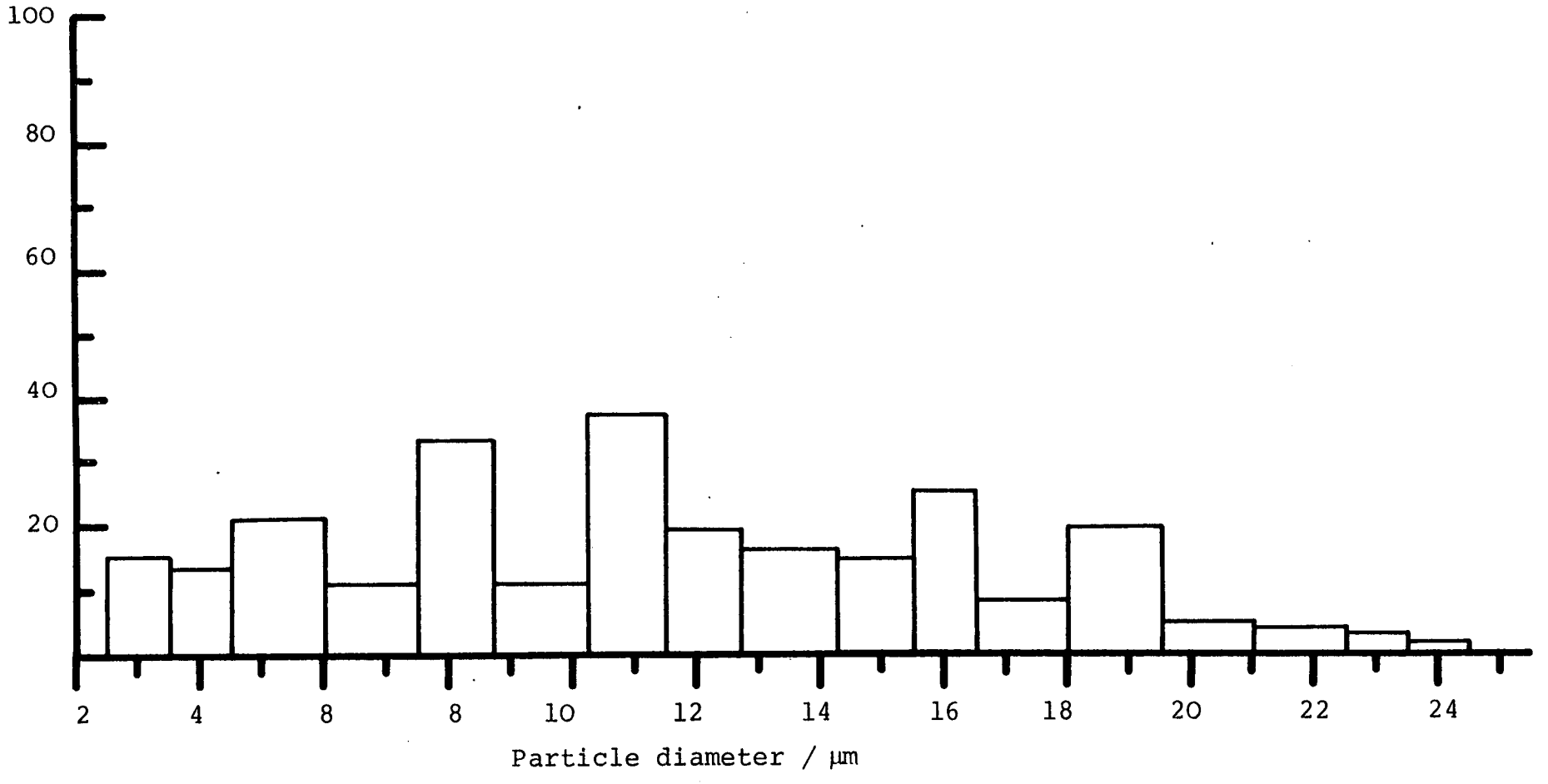

Figure R.3 Histogram showing the relative number of particles within a given particle size range for Batch 5. Arithmetic mean diameter = 12 μm. Standard deviation = 5.2μm.

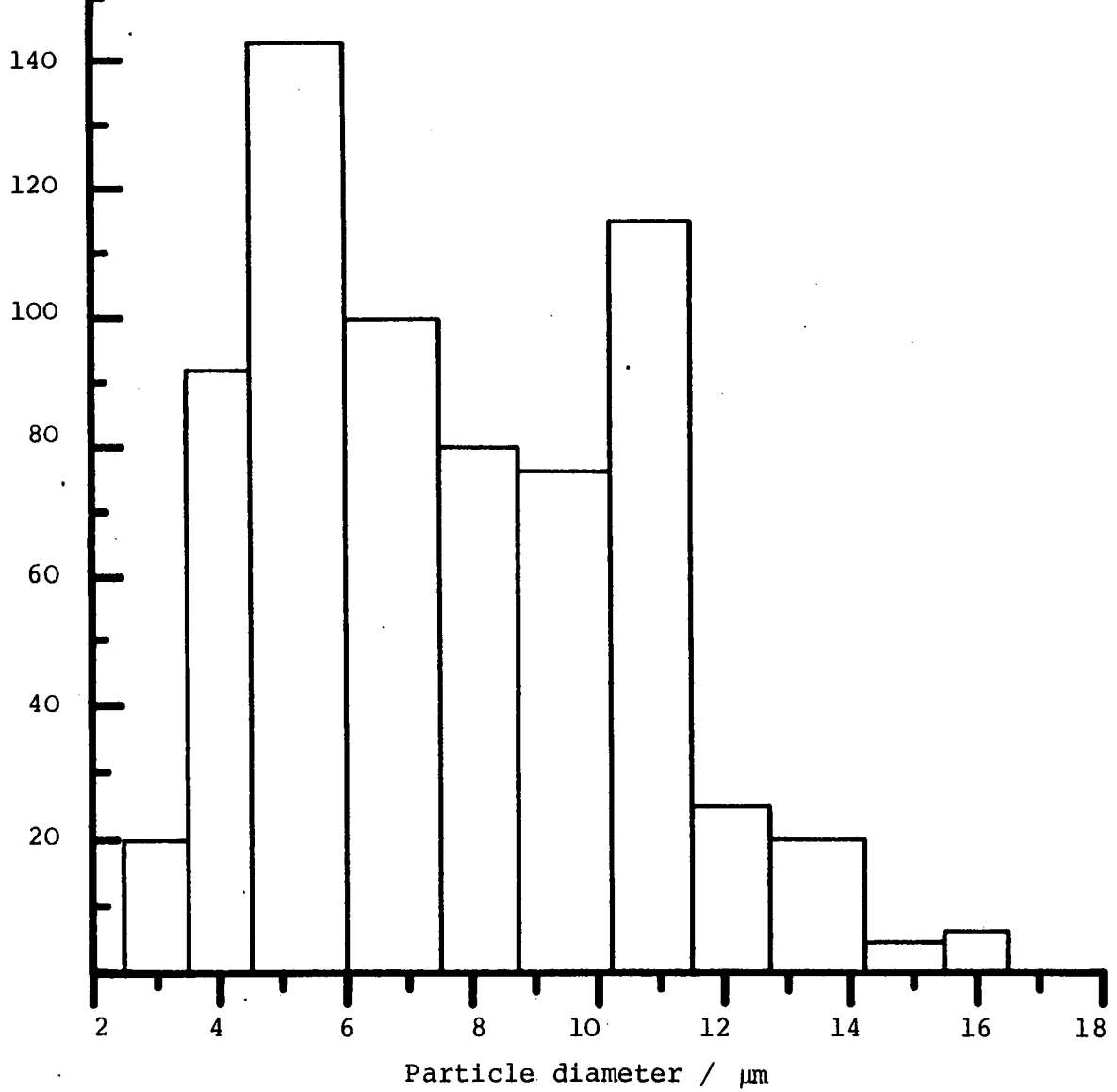

Figure R.4 Histogram showing the relative number of particles within a given particle size range for Batch 6. Arithmetic mean diameter = 8 μm. Standard deviation = 3 μm.

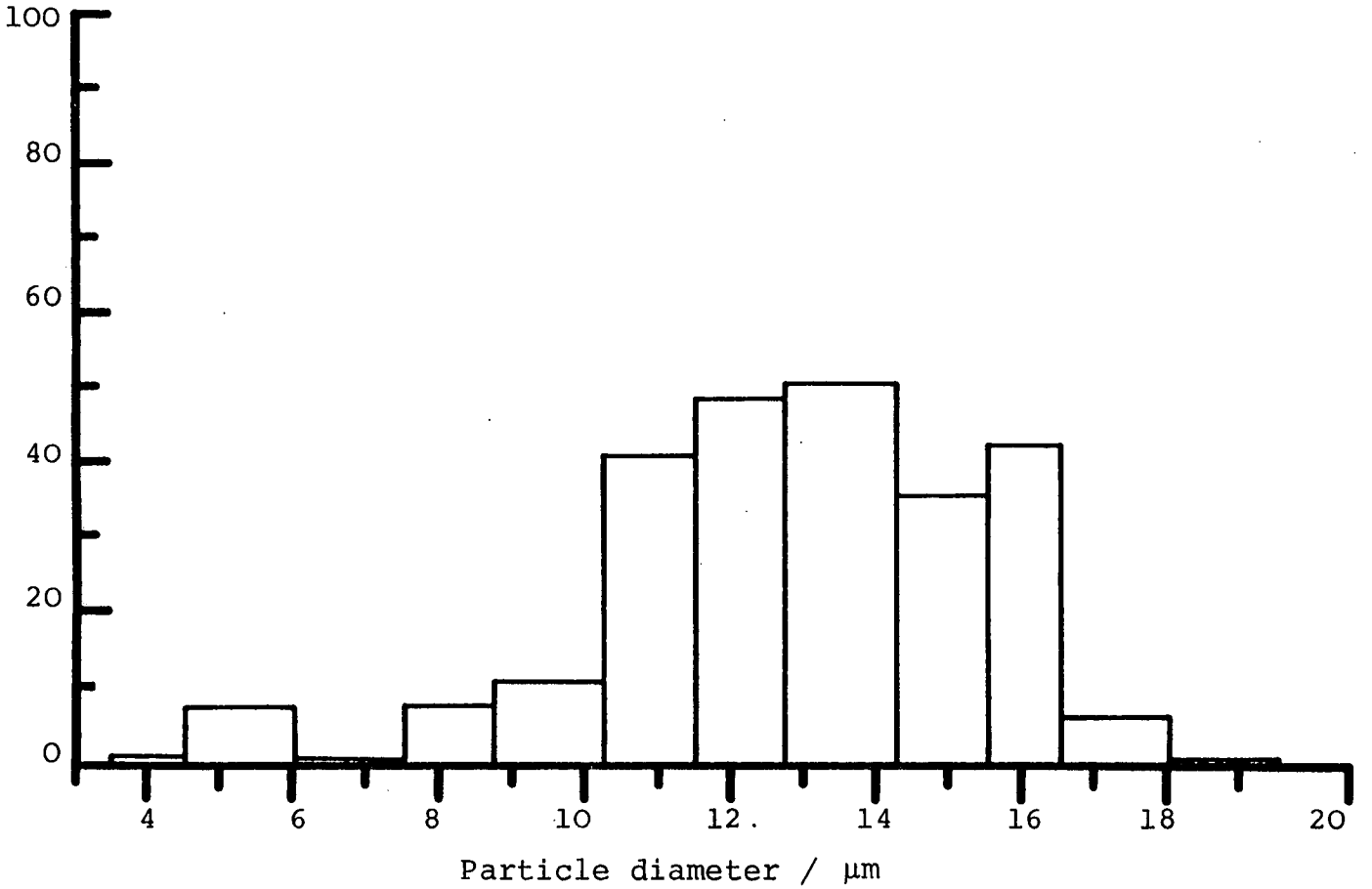

Figure R.5 Histogram showing the relative number of particles within a given particle size range for Batch 7. Arithmetic mean = 13 μm. Standard deviation = 2.5 μm.

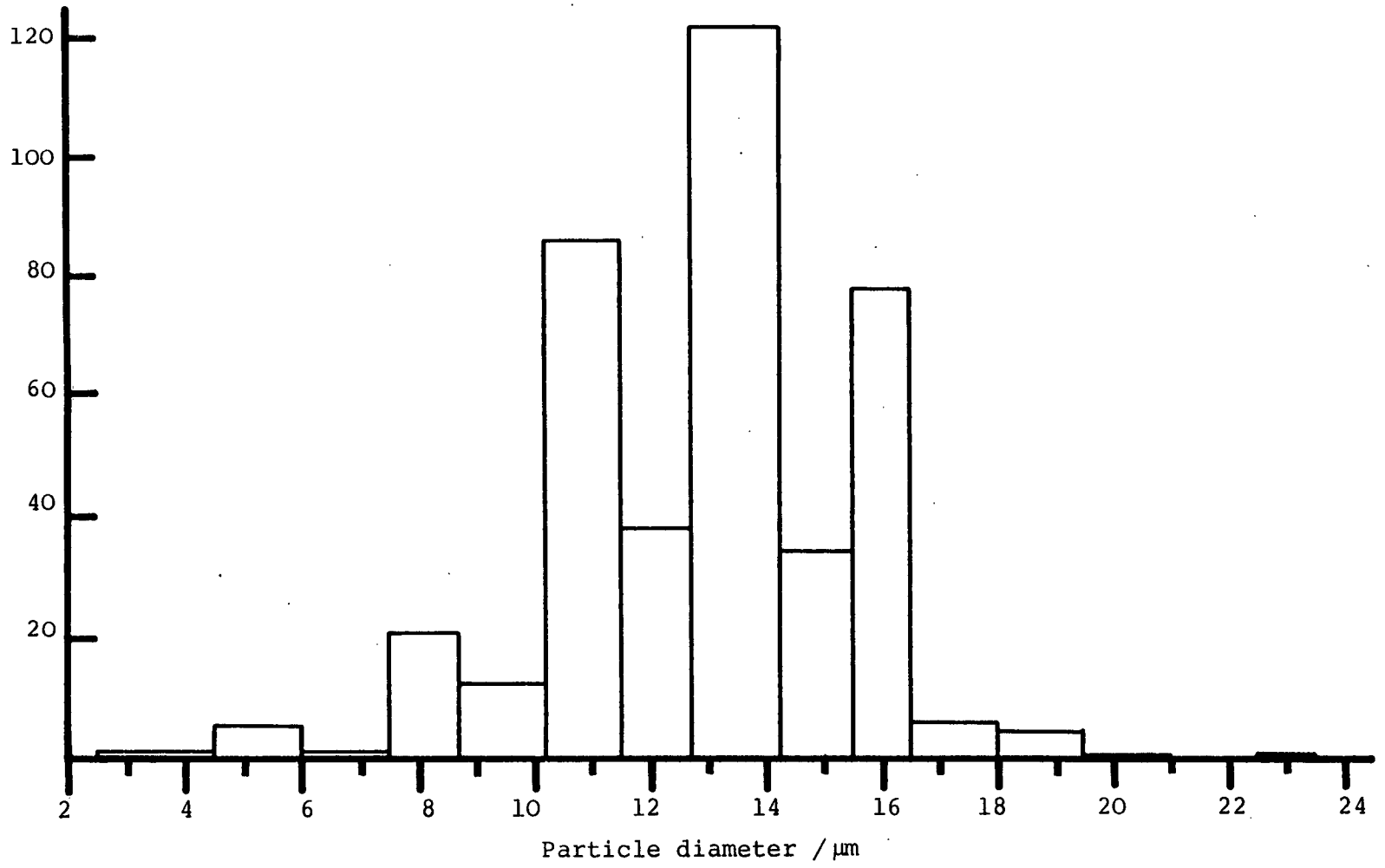

Figure R.6 Histogram showing the relative numbers of particles within a given particle size ranges for Batch 8. Arithmetic mean = 13μm. Standard deviation = 2.6 μm.

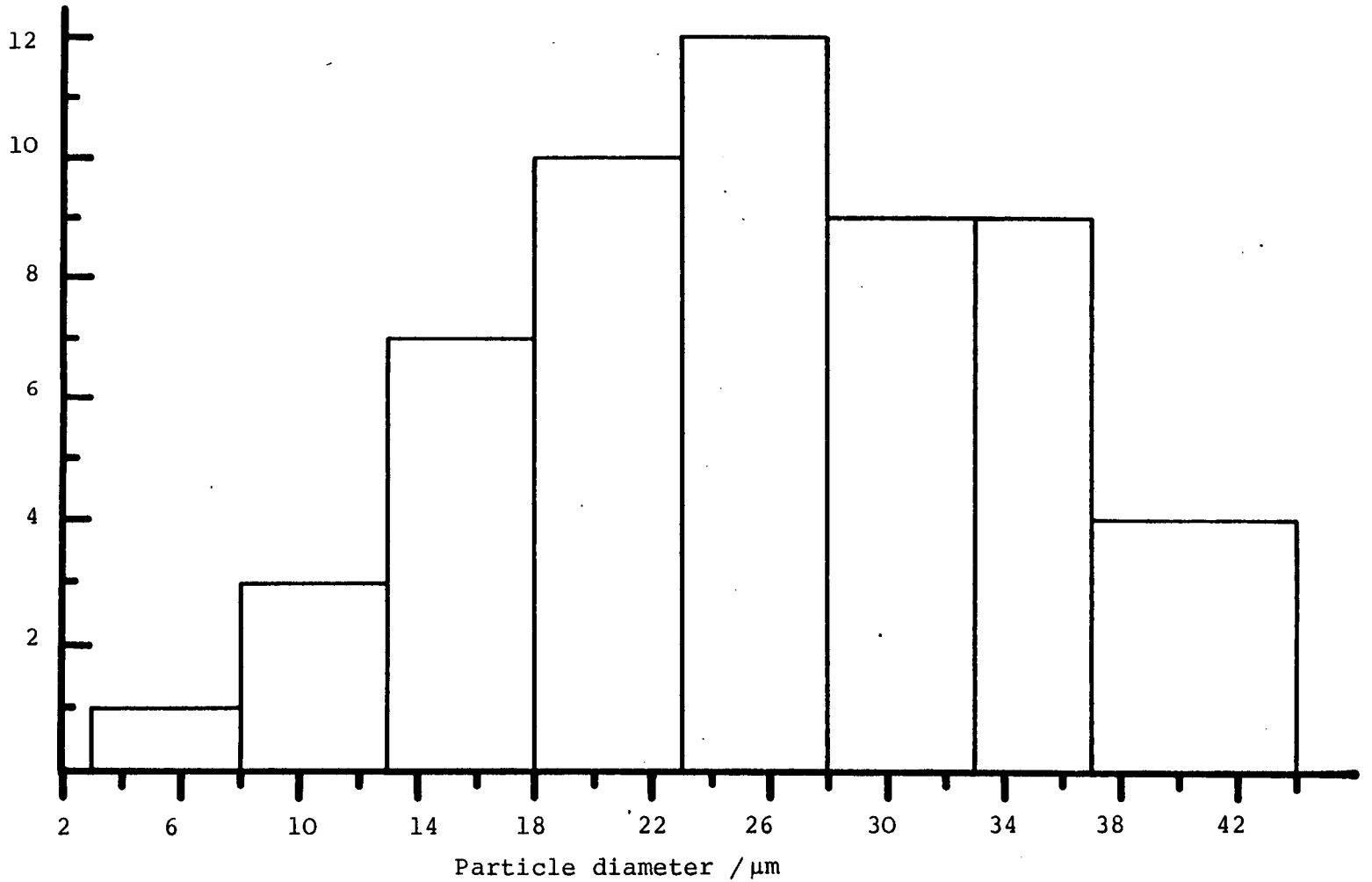

Figure R.7 Histogram showing the relative amounts in a given particle size range for Batch 14. Arithmetic mean diameter = 25.6 μm. Standard deviation = 8.5 μm.

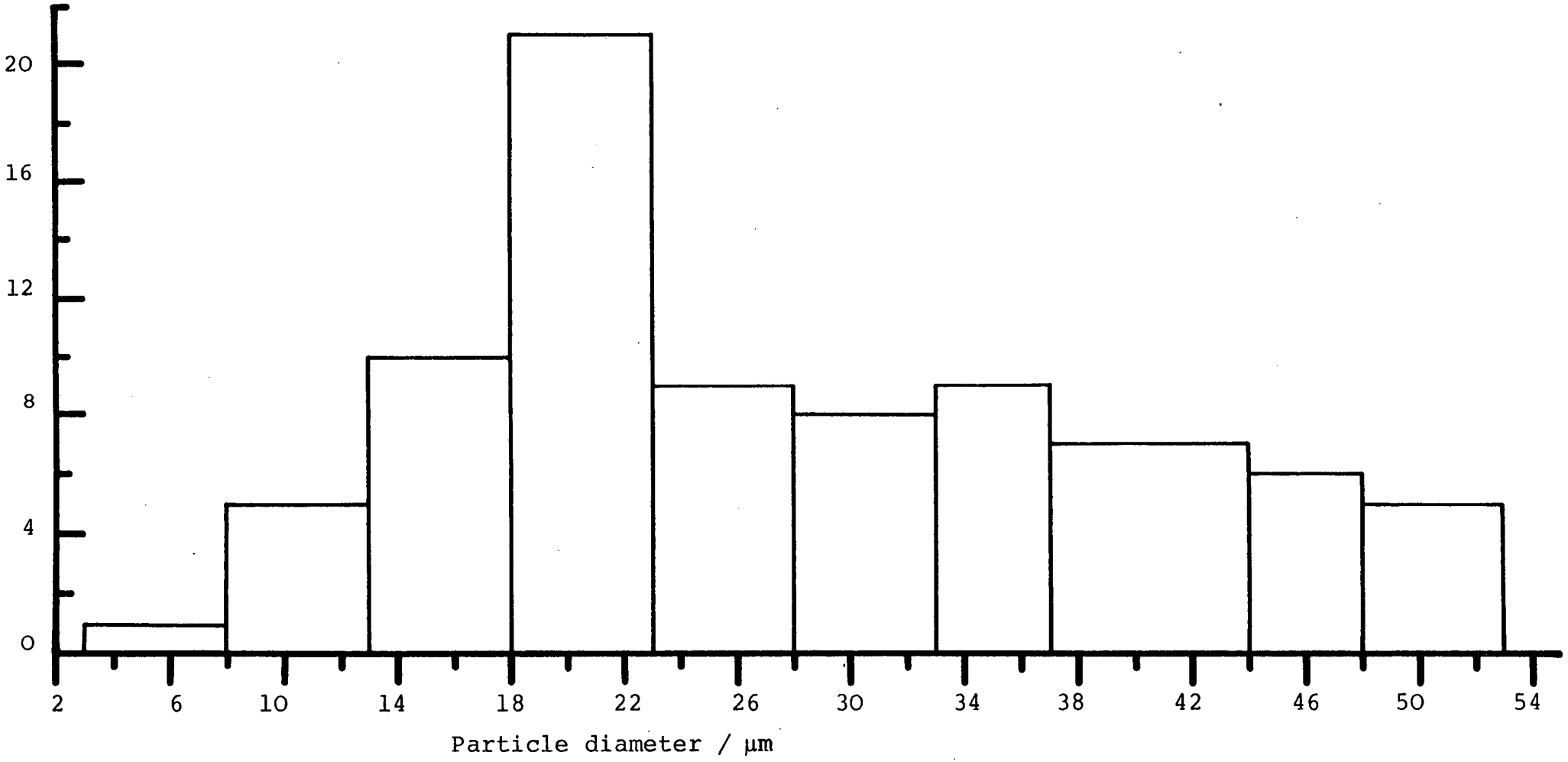

Figure R.8 Approximate relative amounts in the different particle size ranges. Arithmetic mean = 27.7 µm. Standard deviation = 11.6 µm.

R.3 Results

R.3.1 Particle Sizes and Ranges of the Various Batches Produced

(i) Batches 1-4

These batches were the only ones which were emulsified using a stainless steel rotor attached to a fixed speed drill and produced particles in the range 64-137 μm as measured through an ordinary microscope.

(ii) Batches 5-8

The conditions were exactly the same for all of the batches except that different screens were used as detailed in table R-2. Photographs of samples of each batch were taken through an electron microscope and the measurements were taken from these photographs and the photograph of a grid.

The results of the particle size determination of batches 5,6,7 and 8 have been plotted in the form of a histogram as shown in figures R-3, R-4, R-5 and R-6 respectively.

(iii) Batches 14 and 15

For these batches, the screen with the 1 mm holes was used. However, the rotor clearance was increased from 0.32 mm, as it was for batches 5-8, to 1.31 mm. Also, two different speed settings were used as given in table R-3. The relative amounts in the different particle size ranges were based on the approximate volumes of silica gel obtained. The results are plotted in the form of a histogram and are given in figures R-7 and R-8 for batches 14 and 15 respectively.

(iv) Batches 16-19 and 21-23

Batches 16 and 19 were combined prior to fractionation as were batches 17 and 18, and batches 21-23.

Batches 16, 19, 21-23 were made using the same conditions as for batch 15, and it was therefore assumed that the particle size ranges produced would be the same as for batch 15. During fractionation of these batches two cuts were made to produce fractions with particle size ranges of 5-15 μm and 15-60 μm.

Batches 17 and 18 were made under the same conditions as batch 14 and it was therefore assumed that the range of particle sizes produced was the same as for batch 14. Fractionation of batches (17+18) was carried out to produce one cut of 10-40 μm.

R.3.2 Summary of Results and Conclusions

The results obtained are summarized in the following tables.

R.3.2.1

Table R-3 Particle Size Ranges Obtained using Different Screens

Batch	Screen	Arithmetic Mean/μm	S.D./ μm	% Range of dp/μm	Chips & Fines
5	6x10mm id.holes	12	5.2	95% 1.2-22.4	Chips & fines
6	2mm id.holes	8	3.0	95% 2-14	Some fines
7	1mm id.holes	13	2.4	95% 8.2-17.8	None
8	Square holes, 3mm across	13	2.6	95% 7.8-18.2	Chips & fines

It appears that the size of the holes in the screen has little effect on the actual size of the particles produced but it does influence whether chipped or very fine particles are produced. From the results obtained, it appears that the best screen to use is the one with 1 mm id holes.

R.3.2.2

Table R-4 Particle Size Ranges Obtained using Different Rotor Clearance

Batch	Rotor Clearance/mm	Arithmetic Mean/μm	SD/μm	% Range of dp/μm
7	0.32	13	2.4	95% 8.2-17.8
14	1.31	25.6	8.5	95% 8.6-42.6

The above results indicate using a larger rotor clearance produces larger particles and a wider size range.

R.3.2.3

Table R-5 Particle Size Ranges Obtained using Different Rotor Speeds

Batch	Average Speed/RPM	Arithmetic Mean/μm	SD/μm	% Range of dp/μm
14	4143	25.6	8.5	95% 8.6-42.6
15	3507	27.7	11.6	95% 4.5-50.9

These results show that a slower rotor speed produces slightly larger particles and a wider size range.

R.3.2.4 Conclusions

The conclusions reached as a result of the above experiments are that it is best to use the screen with the 1 mm holes and a rotor clearance of 1.31 mm in order to produce large particles (mean dp $\sim$ 25 μm) with few fines or chipped particles, and that the mean particle size can be slightly increased by operating at a slower rotor speed.

Table R-6 Particle Sizes of Various Fractions of Batches 16-23 as measured using a Quantimet.

Average particle size diameter	"5-15"μm	"10-40"μm	"15-60"μm	"Av.16"μm*
Geometric Mean Diameter/μm	10.52	15.75	17.83	17.86
Arithmetic Mean Diameter/μm	10.64	15.78	19.00	18.13
Mean Area Diameter/μm	11.09	16.31	20.17	18.58
Mean Volume Diameter/μm	11.61	16.97	21.39	19.28
Total Number Counted	1056	1055	1493	527
Standard Deviation	3.11	4.12	6.78	2.78

* These particles were fractionated using the apparatus as described in figure 7-18.

R.4 Particle Size Determination of the Various Fractions using a Quantimet

The particle sizes of the various silica fractions of batches 16-23 were measured using a Quantimet, belonging to Unilever, Sharnbrook, Beds.

The results for fractions which were nominally "5-15 μm", "10-40 μm" and "15-60 μm" are given in Table R-6. The different particle diameter averages which are derived are obtained by considering different aspects of the particle eg.

(i) Geometric Mean Diameter $= (d_1 \times d_2 \times \ldots\ldots d_N)^{1/N}$

(ii) Arithmetic Mean Diameter $= (d_1 + d_2 + \ldots\ldots d_N)/N$

(iii) Mean area Diameter $= \left\{(d_1^2 + d_2^2 + \ldots\ldots d_N^2)/N\right\}^{\frac{1}{2}}$

(iv) Mean volume Diameter $= \left\{(d_1^3 + d_2^3 + \ldots\ldots d_N^3)/N\right\}^{\frac{1}{3}}$

The Geometric mean diameter emphasises the small particle diameters and this emphasis decreases from categories (i)→(iv), with the mean volume diameter emphasising the large particles.

For the calculations used in this thesis, the arithmetic mean diameter has been used.

R.5 Chemical Bonding of Silica Gel

The following method was used to convert the silica gel to an octadecyl-bonded reversed phase material.

(i) Bonding Stage

The silica was first dried in a 3-necked flask for 4 hours at 150°C under vacuum. 1 ℓ of dry solvent, decalin/xylene 3:1 v/v, was then added followed by 50 ml ODTCS (octadecyltrichlorosilane) and this was stirred under reflux at 140°C in an oil bath for 16 hours with nitrogen just bubbling through the system. The nitrogen was left bubbling through the mixture until it cooled down. The bonded material was then washed as follows:

4 x 500 ml hexane
3 x 500 ml acetone
1 x 500 ml 50% aqueous acetone
2 x 500 ml acetone
2 x 500 ml methylene chloride.

The ODS-silica was then placed in a wide necked bottle and left to dry in the air.

(ii) Capping Stage

In order to remove surface silanol groups, the bonded material was 'capped' with trimethylchlorosilane as follows.

After the bonding stage, the silica was placed in a 3-necked flask and dried at 120°C for 4 hours under vacuum. To the bonded silica was added 1 litre of dry toluene, 10 ml pyridine and finally 100 ml trimethylchlorosilane (TMS). The

pyridine reacts with the hydrochloric acid to ensure that the equilibrium is towards the side of the product. The reaction mixture was then refluxed under nitrogen at around 140°C in an oil bath for 16 hours, allowed to cool and then washed as for the bonding stage. The ODS-silica was finally bottled and left to dry in the atmosphere. Before being used, it was dried in an oven at 120°C under vacuum for 4 hours.